



ASSESSING THE PERFORMANCE, BIOSOLIDS DYNAMICS AND MICROBIAL  
PROFILES OF MOVING BED BIOFILM REACTORS TREATING  
WASTEWATERS FROM PESTICIDE AND PULP & PAPER INDUSTRIES

Maurício Carvalho Matheus

Tese de Doutorado apresentada ao Programa de Pós-graduação em Engenharia Química, COPPE, da Universidade Federal do Rio de Janeiro, como parte dos requisitos necessários à obtenção do título de Doutor em Engenharia Química.

Orientadores: João Paulo Bassin

Márcia Walquíria de Carvalho

Dezotti

Maria Piculell

Rio de Janeiro

Novembro de 2020

ASSESSING THE PERFORMANCE, BIOSOLIDS DYNAMICS AND MICROBIAL  
PROFILES OF MOVING BED BIOFILM REACTORS TREATING  
WASTEWATERS FROM PESTICIDE AND PULP & PAPER INDUSTRIES

Maurício Carvalho Matheus

TESE SUBMETIDA AO CORPO DOCENTE DO INSTITUTO ALBERTO LUIZ  
COIMBRA DE PÓS-GRADUAÇÃO E PESQUISA DE ENGENHARIA DA  
UNIVERSIDADE FEDERAL DO RIO DE JANEIRO COMO PARTE DOS  
REQUISITOS NECESSÁRIOS PARA A OBTENÇÃO DO GRAU DE DOUTOR EM  
CIÊNCIAS EM ENGENHARIA QUÍMICA.

Orientadores: João Paulo Bassin

Márcia Walquíria de Carvalho Dezotti

Maria Piculell

Aprovada por: Prof. Tito Livio Moitinho Alves

Prof<sup>a</sup>. Isabelli Dias Bassin

Prof. Geraldo Andre Thurler Fontoura

Prof<sup>a</sup>. Claudia Regina Xavier

RIO DE JANEIRO, RJ - BRASIL

NOVEMBRO DE 2020

Matheus, Maurício Carvalho

ASSESSING THE PERFORMANCE, BIOSOLIDS DYNAMICS AND MICROBIAL PROFILES OF MOVING BED BIOFILM REACTORS TREATING WASTEWATERS FROM PESTICIDE AND PULP & PAPER INDUSTRIES / Maurício Carvalho Matheus. – Rio de Janeiro: UFRJ/COPPE, 2020.

XXVIII, 234 p.: il.; 29,7 cm.

Orientadores: João Paulo Bassin

Márcia Walquíria de Carvalho Dezotti

Maria Piculell

Tese (doutorado) – UFRJ/ COPPE/ Programa de Engenharia Química, 2020.

Referências Bibliográficas: p. 180-199

1. Moving Bed Biofilm Reactor MBBR. 2. Pesticide formulation wastewater. 3. Pulp and paper wastewater. I. Bassin, João Paulo *et al.* II. Universidade Federal do Rio de Janeiro, COPPE, Programa de Engenharia Química. III. Título.

## AGRADECIMENTOS

Primeiramente, gostaria de elucidar alguns pontos sobre os agradecimentos:

- Se, eventualmente, você não viu seu nome aqui e ficou chateado: não fique, por favor. Provavelmente eu estava muito preocupado com as outras 258 páginas desta tese. Fica aqui meu muito obrigado a você! ;
- Não deu para ser sucinto demais, é uma jornada longa e muita gente para agradecer;
- Não ligue para a ordem, seja entre parágrafos ou nomes;
- Não pretendi ser formal demais por aqui. :)

Minha mãe e meu pai, se eu tive competência e resiliência para traçar o caminho que escolhi e chegar no momento de defender meu doutorado, saibam que vocês foram alicerces para isso. Pela minha formação, por todo apoio incondicional e por aturarem todo o sacrifício que tive que fazer, sem nunca deixar de acreditar em mim, meu muito obrigado. Amo muito vocês! E meu irmão e cunhada (e meu sobrinho) que, tenho certeza, em todo momento desejam meu sucesso e vibram pelas minhas vitórias. Obrigado por acreditarem em mim. Amo vocês!

João e Márcia, meus orientadores e amigos que me guiaram ao longo dessa jornada, essa conquista também é de vocês. Sei o quão desgastante a vida docente pode ser, ainda mais em um programa de excelência como o PEQ, e, apesar disso, vocês se fizeram sempre presentes. Seja com a orientação técnico-científica, seja com conselhos e ombros amigos para superar os tantos percalços que aconteceram dentro e fora do laboratório. Obrigado por todas as oportunidades apresentadas e por confiarem tanto na minha capacidade. Que essa defesa seja apenas um marco na parceria com vocês e que ela se perpetue, rendendo muitos frutos futuros.

Tainá, você foi a maior incentivadora desse período final de doutorado, de muita escrita e “não aguento mais!”. Obrigado por ser parte da força motriz diária na conclusão desse trabalho e me apoiar em momentos de dificuldade. Eu sei que você já chegou no ponto de desejar tanto o fim dessa tese quanto eu. Pois bem, chegou! Te amo! Você é sol!  
P.s.: obrigado por me fazer comprar o mouse novo no dia do Madero!

From October 2018 to October 2019, I experienced one of the most remarkable periods of my life so far, by moving to Sweden to work within AnoxKaldnes laboratories as part of this doctorate. Shoutouts to Maria Piculell and Maria Ekenberg that kindly guided me through developing the best possible experiments with their experience and intelligence, also taking time for some (many?) friendly conversations. Sofia, thanks for helping to make this exchange possible. Same goes for my dear friend Fernando. Special thanks to people that made the day-by-day in the lab or in the office more pleasant (don't mind the order!): Stig, Ali, Fabian, Linn, Esther, Per, Alex, Xin, Can, Pia, Andrea, Eva, Luca Quadri. And, of course, you guys were a gift and deserve at least a sentence just for you: Henrique, Luca (the Prince) and Maytham (aka Tomate).

You ladies were not part of the AnoxKaldnes routine, however, I'm so glad that I have met you and appreciate all the support and good times we shared in Sweden (and Rome): dzięki, Ewelina i Ewa! Patrz na praca doktorska.

Thamires, independentemente de você chegar a ler isso ou não, seria muito injusto com o significado da palavra gratidão não agradecer a você. Seu apoio foi essencial nos anos iniciais dessa trajetória. Sou grato por todo o tempo me incentivando e ajudando a alcançar meus objetivos. De coração, obrigado.

Mais da metade do trabalho experimental que deu origem a esta tese foi feito na minha "casa científica": o Laboratório de Controle de Poluição de Águas, o LabPol. Conheci muita gente maravilhosa por lá, desde os alunos de IC até os pós-graduandos e técnicos. Por vocês tenho muito carinho e desejo muito sucesso (não liguem para a ordem, cada um sabe a intensidade do agradecimento): Morgana, Francine, Doralice, Paula, Ana Paula, Natália, Haline, Reynel, Gustavo, Fernanda, Cyntia, Renato, Ricardo, Bruna, Kalina, Robson, Sandra, Andressa, André, Paixão, Rafael, Renato, Alan, Bruna, Jéssica, Bianca, Suellen. Foi nesse ambiente que também tive a sorte de orientar duas admiráveis pessoas, graduandos de engenharia química. Bruno e Giselle, agradeço aos dois por tudo e tenho muito carinho por vocês.

Ao pessoal do PEQ e seus demais professores, presto meus agradecimentos por fazerem deste programa uma referência de qualidade e excelência, do qual me orgulho tanto de fazer parte e que estará para sempre carimbado na minha vida profissional. Também agradeço aos demais servidores e funcionários terceirizados que são parte das engrenagens da Universidade. Aos amigos pós-graduandos contemporâneos, da minha ou outras turmas, um grande abraço a todos vocês. Em especial para Mellyssa, Marcel,

Ariane, Thiago Miceli, Roberta, Henrique e Daniel. Estarei sempre torcendo por suas vitórias.

Igualmente ao orgulho do PEQ, sinto pela UFF. A melhor engenharia química sem dúvida me ajudou a abrir as portas do PEQ, não apenas pelo renome, mas pelo efetivo bom preparo. Agradeço aos professores - em especial, Ana Carla, Rosenir, Jorge e Hugo - e aos amigos da graduação. Um abraço apertado especialmente para Matouk, Marcus Vinícius, Pedro Paulo, Guilherme, Nadine e Thathiana.

Ao pessoal do colégio, grandes amigos do Plínio Leite para a vida: Luís “Primu” Alberto, Tatiane, Tamara, Kaio, Bernardo, e ~~Dun~~ Marco Filipe. Amo vocês e agradeço a amizade desde que eu nem sabia que ia fazer engenharia química. Tive muitos professores maravilhosos no Plínio e sou grato a todos, mas queria agradecer a dois por quem tenho grande admiração: Chiquinho e Vladimir (olha o professor de português aparecendo na tese de doutorado do engenheiro químico).

Pessoal do Voltaire, engraçado como em somente um ano foram construídas amizades que se mantêm por tanto tempo, independente de períodos mais ou menos afastados. Certamente é a intensidade e a tensão do vestibular, né? Priscila, Thamiris, Patrícia, Tatiane, André, Daniel, Luiz “Drummond”, Gustavo, Grael, Bia, e os “agregados” Thamires, Bruna e Pedro. Obrigado por serem parte da minha vida, amo vocês. No pré-vestibular também tive professores que me impulsionaram muito. Sou grato especialmente ao Léo Allen.

Aos amigos da infância até os cabelos brancos que ainda virão (ou já vieram): Nelson, Vinícius, Guga. Tenho certeza se a gente não tivesse jogado tanto D&D e videogame eu não teria a mesma capacidade cognitiva para desenvolver uma tese de doutorado e nem um inglês bom o suficiente para escrevê-la nesse idioma. Obrigado pela continua parceria, amo vocês!

À indústria de formulação de pesticidas que forneceu o efluente para o desenvolvimento deste trabalho, nas pessoas do Ricardo e do Geraldo, agradeço pelas colaborações científicas que permitem ganhos objetivos e subjetivos para todas as partes envolvidas. Que essa mentalidade de interação indústria-academia permaneça e se expanda para outras empresas e setores. Deixo também um “obrigado” aos funcionários da empresa que sempre com tanta gentileza me receberam lá, ou trouxeram as amostras até o laboratório.

Expresso minha gratidão também ao Roberto Júnio Pedroso Dias, do Laboratório de Protozoologia da Universidade Federal de Juiz de Fora, por ter contribuído na identificação dos microrganismos observados por microscopia.

Aos membros da banca, Isabelli, Tito, Geraldo e Claudia, que gentilmente aceitaram dispende de tempo para ler este extenso documento, avaliar a qualidade do trabalho e contribuir com seus conhecimentos e experiências. Muito obrigado!

Para fechar com uma brincadeira, com fundos de verdade, parafraseio Annita no Rock in Rio 2019, à despeito de gosto musical: "Quero muito agradecer a todos vocês porque vocês me colocaram aqui hoje. Se eu fosse contar para vocês tudo o que aconteceu na minha história até eu chegar neste momento, talvez vocês nem acreditassem. Às vezes, nem eu acredito. De verdade, hoje eu só quero agradecer. A gente que é ~~artista~~ doutorando tem sempre que agradecer a todo mundo para ninguém poder falar que a gente não é humilde. Mas hoje eu queria muito agradecer a mim porque eu não desisti. Vocês sabem que eu sempre agradeço a vocês [público] e hoje passou um filme na minha cabeça. Quero muito agradecer a mim."

Resumo da Tese apresentada à COPPE/UFRJ como parte dos requisitos necessários para a obtenção do grau de Doutor em Ciências (D.Sc.)

AVALIAÇÃO DE DESEMPENHO, DINÂMICA DE BIOSÓLIDOS E MICROBIOTA  
EM REATORES DE LEITO MÓVEL COM BIOFILME NO TRATAMENTO DE  
EFLUENTES DE INDÚSTRIAS DE PESTICIDA E CELULOSE E PAPEL

Maurício Carvalho Matheus

Novembro/2020

Orientadores: João Paulo Bassin

Márcia Walquíria de Carvalho Dezotti

Maria Piculell

Programa: Engenharia Química

Alta carga orgânica e variabilidade sazonal são exemplos de desafios inerentes a águas residuárias industriais, requisitando tecnologias robustas de tratamento. Para tal, o reator de leito móvel com biofilme (MBBR) tem abrangente aplicação e potencial, de forma que avanços em sua operação tem grande relevância. Nesse sentido, dois estudos laboratoriais independentes foram conduzidos com MBBRs alimentados com efluentes reais de indústrias de pesticida e de celulose e papel. Parâmetros-chave como o tempo de retenção hidráulica (TRH), fração de enchimento e disponibilidade de nutrientes foram analisados frente à remoção de matéria orgânica e de nitrogênio amoniacal, à utilização de nutrientes e à dinâmica da biomassa aderida e suspensa. O tratamento de efluente de pesticidas com o MBBR mostrou-se viável com TRH de 6 h e fração de enchimento de 50% (a 250 m<sup>2</sup>/m<sup>3</sup>), enquadrando os parâmetros de descarte nos limites legais. Com o efluente da indústria de celulose, a utilização de uma área específica efetiva de biofilme 3 vezes maior permitiu um volume 33% menor sem alteração de desempenho. A dosagem de nutrientes (necessária para este tipo de efluente) mínima foi de 100:0,70:0,14 (DQO:N:P), obtida quando se limitou a disponibilidade de nitrogênio com o maior TRH aplicado (4,9 h). O sequenciamento de DNA revelou que a escassez de nutrientes foi o fator dominante para a composição da comunidade microbiana, seguida pelo TRH.

Abstract of Thesis presented to COPPE/UFRJ as a partial fulfillment of the requirements for the degree of Doctor of Science (D.Sc.)

ASSESSING THE PERFORMANCE, BIOSOLIDS DYNAMICS AND MICROBIAL  
PROFILES OF MOVING BED BIOFILM REACTORS TREATING  
WASTEWATERS FROM PESTICIDE AND PULP & PAPER INDUSTRIES

Maurício Carvalho Matheus

November/2020

Advisors: João Paulo Bassin

Márcia Walquíria de Carvalho Dezotti

Maria Piculell

Department: Chemical Engineering

High organic load and seasonal quality variation are examples of challenges inherent to industrial wastewaters, requiring robust technologies for its treatment. For such, the moving bed biofilm reactor (MBBR) has wide applicability and potential, so that operational optimizations might have extensive relevance. In this context, two independent lab-scale studies were conducted with the MBBRs fed with pesticide and pulp and paper (P&P) industrial wastewaters. Key parameters – as the hydraulic retention time (HRT), carrier filling degree, and nutrients availability – were assessed in relation to the removal of organic matter and ammoniacal nitrogen, the nutrients utilization, and the dynamics of attached and suspended biomass. The treatment of the pesticide wastewater by the MBBR was shown to be feasible with 6 h HRT and 50% filling ratio ( $250 \text{ m}^2/\text{m}^3$ ), placing the discharge parameters below the legal limits. With the P&P wastewater, using threefold higher effective specific surface area allowed to preserve the performance in 33% smaller reactor. The minimal nutrients dosage needed for this sort of wastewater was 100:0.70:0.14 (COD:N:P), achieved when nitrogen availability was limited at the higher tested HRT (4.9 h). DNA sequencing revealed that nutrients scarcity was the major factor shaping the microbial profile, followed by HRT.

# LIST OF CONTENTS

<b>1.</b>	<b>INTRODUCTION AND OBJECTIVES.....</b>	<b>1</b>
1.1.	Objectives and Strategies.....	7
<b>2.</b>	<b>LITERATURE REVIEW.....</b>	<b>10</b>
2.1.	Wastewater Characterization and Treatment.....	10
2.2.	Secondary Wastewater Treatment.....	13
2.2.1.	<i>Microbial Metabolism.....</i>	<i>13</i>
2.2.2.	<i>Classification of Biological Processes.....</i>	<i>17</i>
2.2.3.	<i>Aerobic Biological Organic Matter Removal.....</i>	<i>20</i>
2.2.4.	<i>Biological Nitrogen Removal.....</i>	<i>22</i>
2.2.5.	<i>Forms of Microbial Growth in Biological Treatment.....</i>	<i>27</i>
2.2.6.	<i>Microorganisms and Ecology in Biological Wastewater Treatment.....</i>	<i>32</i>
2.3.	Moving Bed Biofilm Reactor (MBBR).....	40
2.3.1.	<i>MBBR Features.....</i>	<i>43</i>
2.3.2.	<i>Biofilm Carriers.....</i>	<i>46</i>
2.3.3.	<i>Aeration System.....</i>	<i>49</i>
2.3.4.	<i>BAS Configuration.....</i>	<i>51</i>
2.4.	Brazilian Legislation on the Disposal of Industrial Wastewaters.....	53
2.5.	Pesticides: Industry, Wastewater, and its Treatment.....	56
2.5.1.	<i>Pesticide Industry.....</i>	<i>59</i>
2.5.2.	<i>Pesticide Industries Wastewater.....</i>	<i>60</i>
2.5.3.	<i>Treatment of Industrial Pesticide Wastewaters.....</i>	<i>61</i>
2.5.4.	<i>Local Pesticide Formulation Industry.....</i>	<i>68</i>
2.6.	Pulp and Paper: Industry, Wastewater, and its Treatment.....	70
2.6.1.	<i>Pulp and Paper Industry.....</i>	<i>72</i>
2.6.2.	<i>Pulp and Paper Industries Wastewater.....</i>	<i>76</i>

2.6.3.	<i>Treatment of Industrial Pulp and Paper Wastewaters</i>	78
2.6.4.	<i>Södra Cell Värö Pulp and Paper Industry</i>	82
<b>3.</b>	<b>METHODS AND EXPERIMENTAL SETUPS</b>	<b>84</b>
3.1.	Pesticide Wastewater Research	85
3.1.1.	<i>Receipt and Storage of Wastewaters</i>	85
3.1.2.	<i>Pretreatment with Powdered Activated Carbon (PAC) Adsorption</i>	88
3.1.3.	<i>MBBR System Setup</i>	90
3.1.4.	<i>MBBR Startup and Inoculum</i>	92
3.1.5.	<i>MBBR Operational Phases</i>	93
3.1.6.	<i>MBBR Monitored Parameters</i>	94
3.1.7.	<i>Biofilm Batch Trials for Nitrification and Organic Matter Removal</i>	95
3.2.	Pulp and Paper Wastewater Research	96
3.2.1.	<i>Receipt and Storage of Wastewater</i>	96
3.2.2.	<i>MBBRs Experimental Setup</i>	97
3.2.3.	<i>Operational Phases</i>	99
3.2.4.	<i>Monitored Parameters</i>	100
3.2.5.	<i>Kincannon-Stover Kinetic Model</i>	101
3.2.6.	<i>Batch Trials with Biomass Fractions for COD Removal</i>	102
<b>4.</b>	<b>PESTICIDE RESEARCH: RESULTS AND DISCUSSION</b>	<b>104</b>
4.1.	MBBR General Aspects	104
4.1.1.	<i>Visual Observations</i>	106
4.1.2.	<i>pH</i>	109
4.2.	Organic Matter Removal	110
4.3.	Nitrogen Removal	115
4.3.1.	<i>Removal Mechanism and Nitrogen Species Distribution</i>	115
4.3.2.	<i>Nitrification Performance</i>	117
4.3.3.	<i>Assessment of Nitrifying Community (AOB and NOB) by FISH</i>	120

4.4.	Biofilm Batch Trials .....	122
4.5.	Suspended Solids Assessment .....	128
4.6.	Biofilm Microscopy .....	130
<b>5.</b>	<b>P&amp;P RESEARCH: RESULTS AND DISCUSSION.....</b>	<b>133</b>
5.1.	General Aspects .....	133
5.2.	COD Removal.....	138
5.3.	Solids Production.....	142
5.4.	Efficiency of Nutrients Utilization for COD Removal.....	144
5.5.	Activity Batch Trials with Attached and Suspended Biomass .....	148
5.6.	Assessment of Biofilm Bacterial Profile .....	153
5.7.	Microscopy of Suspended and Attached Biomass.....	168
<b>6.</b>	<b>CONCLUSIONS .....</b>	<b>173</b>
6.1.	Conclusions of the Pesticide Research .....	173
6.2.	Conclusions of the P&P Research .....	175
<b>7.</b>	<b>SUGGESTIONS AND ADVICES FOR FUTURE WORKS .....</b>	<b>178</b>
7.1.	Suggestions Arising from the Pesticide Research .....	178
7.2.	Suggestions Arising from the P&P Research .....	179
<b>8.</b>	<b>REFERENCES.....</b>	<b>180</b>
<b>A.</b>	<b>APPENDIX: ANALYTICAL METHODS.....</b>	<b>200</b>
A.1.	Chemical Oxygen Demand (COD).....	202
A.2.	Dissolved Organic Carbon (DOC).....	203
A.3.	Total Nitrogen (TN).....	203
A.4.	Total Ammoniacal Nitrogen (TAN) .....	204
A.5.	Nitrite (NO <sub>2</sub> <sup>-</sup> ) .....	205
A.6.	Nitrate (NO <sub>3</sub> <sup>-</sup> ).....	206
A.7.	Nitrous Oxide Gas (N <sub>2</sub> O).....	207
A.8.	Phosphate (PO <sub>4</sub> <sup>3-</sup> ).....	207

A.9.	Suspended Solids (TSS, VSS and FSS).....	207
A.10.	Attached Solids (TAS, VAS and FAS).....	208
A.11.	Turbidity.....	209
A.12.	pH.....	209
A.13.	Temperature .....	210
A.14.	Dissolved Oxygen (DO).....	210
A.15.	Optical Microscopy (Biomass).....	210
A.16.	Optical Stereomicroscopy (Carriers).....	211
A.17.	Fluorescence <i>in situ</i> hybridization (FISH) .....	211
A.18.	DNA Screening .....	215
A.19.	Microtoxicity to <i>Vibrio fischeri</i> .....	218
<b>B.</b>	<b>APPENDIX: CALCULATION PROCEDURES .....</b>	<b>219</b>
B.1.	Removal Efficiencies .....	219
B.2.	Total, Particulate and Soluble Concentrations.....	219
B.3.	Hydraulic Retention Time (HRT).....	220
B.4.	Theoretical Chemical Oxygen Demand.....	220
B.5.	Nitrogen Mass Balance in Liquid Phase.....	220
B.6.	Ammoniacal Nitrogen Distribution .....	221
B.7.	Fraction of Nitrogen Assimilated .....	221
B.8.	Volumetric and Surface Loading Rates (VLR and SLR) .....	222
B.9.	Quantity and Concentration of Attached Biomass .....	223
B.10.	Heterotrophic Cell Yield .....	224
B.11.	Apparent and Maximum Substrate Removal Rates .....	224
B.12.	Statistical Methods .....	226
<b>I.</b>	<b>ANNEX: DNASENSE REPORT .....</b>	<b>228</b>

## LIST OF FIGURES

Figure 2.1 – Representation of the metabolism of living organisms, composed of catabolic and anabolic processes. Source: adapted from (HENZE, VAN LOOSDRECHT, <i>et al.</i> , 2008).....	14
Figure 2.2 – Four trophic types of organisms according to metabolic characteristics. ..	15
Figure 2.3 – Transformations taking place in biological treatment, as a function of electron acceptor and redox potential. Source: adapted from (VON SPERLING, 2007b).....	17
Figure 2.4 – Classification of secondary wastewater treatment processes with respect to the type of biomass growth and examples of technologies. Source: adapted from (MARA, HORAN, 2003).....	19
Figure 2.5 – Reactions within the biological nitrogen cycle. ON states for organic nitrogen. Source: (GRADY, DAIGGER, <i>et al.</i> , 2011).....	23
Figure 2.6 – Basic structure of a microbial floc. Source: adapted from (HORAN, 1990 apud VON SPERLING, 2007b).....	28
Figure 2.7 – Microbial flocs with scarcity (a) and abundance (b) of filaments. Source: (BASSIN, DEZOTTI, 2008).....	28
Figure 2.8 – Stages of biofilm formation. Source: (LEWANDOWSKI, BOLTZ, 2011). .....	29
Figure 2.9 – Propagation of biofilm and its mechanisms. Source: (LEWANDOWSKI, BOLTZ, 2011). .....	29
Figure 2.10 – Schematic view of biofilm structure and diffusion of substrates and products in and out of the microbial film. Source: (MARA, HORAN, 2003). .....	31
Figure 2.11 – Representation of the effect of the biofilm thickness on the substrate concentration ( $S$ ) gradient towards the support medium. Source: adapted from (VON SPERLING, 2007b). .....	32
Figure 2.12 – Relative abundance over time of microbial groups in aerobic sewage treatment. Source: (BASSIN, DEZOTTI, 2008, CANLER, PERRET, <i>et al.</i> , 2011). .....	34

Figure 2.13 – Succession over time of relative abundance of microbial groups in a biofilm. Source: adapted from (IWAI & KITAO, 1994 apud MARA, HORAN, 2003). .....	34
Figure 2.14 – Typical moving bed biofilm reactor setup, with the biofilm carriers kept in suspension whether by (a) aeration (aerobic MBBRs) or (b) mechanical stirring (anoxic or anaerobic MBBRs). Source: adapted from (BASSIN, DEZOTTI, 2018, RUSTEN, EIKEBROKK, <i>et al.</i> , 2006). .....	41
Figure 2.15 – Extent of hydrolysis of particulate organic COD to soluble COD as a function of the soluble biodegradable organic surface load. Source: adapted from (HELNESS AND SJØVOLD, 2001 apud ØDEGAARD, 2019).....	42
Figure 2.16 – Representation of the reduction of biofilm contact perimeter, therefore of the area, when the biofilm thickens. Source: adapted from (WEF, 2010).....	46
Figure 2.17 – The Z carrier Z400, in reference to the 400µm height of the grid. Source: photo by Alan Werker (PICULELL, 2016). .....	48
Figure 2.18 – Biofilm carriers (Kaldnes K1) with clogged voids due to poor mixing within the reactor. Source: lab-scale MBBR from pesticide research. ....	49
Figure 2.19 – Dependence of the nitrification rate with the ammonium concentration for some DO levels in an MBBR. Source: (RUSTEN, EIKEBROKK, <i>et al.</i> , 2006, RUSTEN, HEM, <i>et al.</i> , 1995, VAN HAANDEL, VAN DER LUBBE, 2012).....	51
Figure 2.20 – Biofilm-Activated Sludge (BAS) configuration: a high loaded MBBR followed by a low loaded activated sludge reactor. Source: adapted from (VAN HAANDEL, VAN DER LUBBE, 2012). .....	52
Figure 2.21 – Main Brazilian policies, associated systems and organs originating norms and usage grants related to the disposal of industrial wastewaters. ....	54
Figure 2.22 – Shape of a generic (a) softwood tree and a (b) hardwood tree. Source: (BAJPAI, 2018). .....	71
Figure 2.23 – Main processing steps employed by the pulp and paper making industries. ....	72
Figure 2.24 – Percentage distribution of 206 published studies, listed in a literature review (ZODI, LOUVET, <i>et al.</i> , 2011), by type of treatment investigated over P&P	

wastewaters: biological (B), chemical (C), mechanical (M), or a combination of those. .....	79
Figure 3.1 – Operational strategy summary of the pesticide (a) and P&P (b) researches. .....	84
Figure 3.2 – Industrial raw pesticide wastewater containers received on May 25, 2016. .....	86
Figure 3.3 – Timeline of the receipt of IPT and S lots, with received volume in parentheses and respective day of MBBR operation timeline next to the vertical dashed line. Day 0 is highlighted in black text balloon.....	87
Figure 3.4 – Lab-scale system for reproducing the real scale adsorption onto powdered activated carbon. ....	89
Figure 3.5 –Experimental setup schematic diagram. P1 to P7 denote the operational phases 1 to 7, described in section 3.1.5.....	91
Figure 3.6 – The operating lab-scale MBBR system.....	92
Figure 3.7 – MBBR in operation during the startup phase.....	92
Figure 3.8 - Experimental setup schematic diagram (identical for both MBBRs, out of scale).....	98
Figure 3.9 – The lab-scale MBBR system experimental set-up, with reactors A and B highlighted. ....	98
Figure 4.1 – Timeline of MBBR operation, with time range (in days) for each operational phase and wastewater lots given in parentheses as (start-end). Dilution of pesticide or sanitary wastewater with water is also specified, as percentage of IPT or S, whenever applicable. “NO DATA” correspond to periods with minimal monitoring, as explained in section 3.1.5. ....	105
Figure 4.2 – MBBR system showing scum formation during the inadequate IPT dilution (days 100 to 115, Figure 4.1).....	107
Figure 4.3 – Appearance of inlet (left) and outlet (right) streams of the MBBR. Phase, pesticide wastewater lot, sanitary wastewater lot, and day of operation are given in the upper left corner of each image. ....	108
Figure 4.4 – Stereomicroscopy micrographs of the biofilm carriers in phase 7.....	108

Figure 4.5 – MBBR inlet and outlet pH during phases 1 and 2 (a) and phases 3 to 7 (b). Text balloons identify changes in pesticide wastewater lot. Upper and lower discharge limits are given by dotted horizontal lines. Time, x-axis, is out of scale. ....	109
Figure 4.6 – MBBR inlet and outlet COD and removal percentage during phases 1 and 2 (a) and phases 3 to 7 (b). Text balloons identify changes in pesticide wastewater lot. The discharge limit is given by the dotted horizontal line. Time, x-axis, is out of scale. .....	111
Figure 4.7 – Mean value of outlet sCOD and removal of sCOD in relation to influent IR sCOD (phases 4 to 7). ....	113
Figure 4.8 – Relative distribution of inorganic nitrogen species in the MBBR effluent for various operating days. Vertical dashed lines depict phases transitions. Time is out of scale .....	116
Figure 4.9 – MBBR inlet and outlet TAN concentrations and removal percentage during phases 1 and 2 (a) and phases 3 to 7 (b). Text balloons identify changes in pesticide wastewater lot. Time, x- axis, is out of scale. ....	118
Figure 4.10 – Relative abundance of AOB and NOB in relation to the total bacterial community at the end of phases 2 to 7, as determined by FISH analysis.....	120
Figure 4.11 - sCOD (black circles) and TAN (white triangles) over time for batch trials, from phases 1 to 7 (P1 to P7). The data points with red outline were used to calculate the maximum removal rates.....	123
Figure 4.12 – MBBR influent and effluent suspended solids distribution during (a) phases 1 to 3 and (b) phases 4 to 7. Sum of VSS and FSS corresponds to TSS. Text balloons identify changes of pesticide wastewater lot. Time, x-axis, is out of scale. ....	128
Figure 4.13 – Micrographs taken at the end of phases 2 to 7, with magnifications of 100 or 400x. Letters indicate identified organisms: (a) Rotifera; (b) Nematoda; (c) Ciliophora ( <i>Epistylis sp.</i> ); (d) shelled amoebae; (e) flagellate; (f) Ciliophora ( <i>Vorticella sp.</i> ); (g) Ciliophora. Yellow color refers to uncertain identifications.....	132
Figure 5.1 – Timeline of the MBBRs operation, with duration the of each phase and wastewater lot specified, in days, as (start-end). Remarks are described in Table 5.1. .....	133
Figure 5.2 – Stereomicroscopy of the carriers from reactors A (left) and B (right).....	135

Figure 5.3 – Stereomicroscopy of carriers from reactor A (left) and B (right) with maximum backlight intensity.....	136
Figure 5.4 – (a) Darkening and loss of reactor B’s biofilm on day 241, (b) during the freezing event in the feed tank. ....	137
Figure 5.5 – Inlet and outlet sCOD for both reactors and their respective sCOD removal percentages during the whole operation. Changes of pulp & paper wastewater lot and transition between operating phases are identified by text balloons and vertical dashed lines, respectively.....	139
Figure 5.6 - Plot of data from reactor B according to the linearized Kincannon-Stover model ( $n = 20$ ) (see section 3.2.5). ....	141
Figure 5.7 - Average ratio of sCOD removed over consumed P (a) or N (b) for both reactors and each operational phase. Error bars show standard deviation. Text labels above columns refer to nutrients availability condition.....	145
Figure 5.8 – sCOD over time for biofilm and planktonic batch trials for reactors A and B, from phases 1 to 5. Red outlined data points were used for linear regressions. ....	149
Figure 5.9 – (a) Biofilm maximum and apparent sCOD surface removal rates, and surface concentration of VAS; and (b) planktonic maximum and apparent (suspended solids only) specific removal rates, and percentage of suspended solids over total biosolids ( $f_{SS/TS}$ ), in phases 1 to 6, for reactors A and B. Maximum rates are not available for phase 6. ....	151
Figure 5.10 – Distribution of unique and shared OTUs (accounting all phases) amongst reactors A and B and the BioChip P, and the relative abundance of each group of OTUs in each operational phase (P1 to P6), expressed as a percentage of the total reads. ....	156
Figure 5.11 – Non-metric multidimensional scaling (NMDS) analysis based on the Bray-Curtis distance (BRAY, CURTIS, 1957) of 13 samples and 374 OTUs. Prior to the analysis, OTUs with no more than 0.1% relative abundance in any sample have been removed. The label at each point identifies the biofilm source (A, B, or Chip from the full-scale) in each phase (1 to 6). Heatmap in the lower-left corner show the relative Euclidean distances between each pair of samples within the NMDS plot.....	158

Figure 5.12 – Relative abundance of the 10 most common phyla amongst the 13 samples, for each operational phase and each reactor. Nutrients (N or P), whether in excess or limited, are indicated below each phase. ....	160
Figure 5.13 – Relative abundance of the 15 most common classes amongst the 13 samples, for each operational phase and each reactor. Nutrients (N or P), whether in excess or limited, are indicated below each phase. Superscript number refers to the phylum that each class belongs to, according to the rank in Figure 5.12. ....	162
Figure 5.14 – Biofilm micrographs taken at the end of each phase and reactor (magnifications of 100 or 200x). Identified organisms are indicated: (a) Ciliophora ( <i>Vorticella sp.</i> ); (b) Ciliophora ( <i>Peritrichia</i> ); (c) flagellate; (d) Ciliophora; (e) Ciliophora ( <i>Epistylis sp.</i> ). Yellow color refers to uncertain identifications. ....	169
Figure 5.15 –Micrographs of suspended biomass of each reactor at the end of each phase (except phases 3 and 6) (magnifications of 100 or 200x). Identified organisms are indicated: (a) Ciliophora; (b) Ciliophora ( <i>Peritrichia</i> ); (c) Nematoda. Yellow color refers to uncertain identifications. ....	170
Figure A.1 – Biofilm extraction (a) and biofilm carriers after (bottom) and before (middle) cleaning with the interdental brush (top). ....	208
Figure A.2 – Immobilized samples in each slide during FISH procedure, showing triplicates for each phase (P2 to P7), for each combination of probes targeting AOB and NOB. <sup>a</sup> AOB, NOB and EUB stands for the oligonucleotide hybridization probe blends (Table A.2), while the fluorescent labels are denoted by 488 (Alexa Fluor 488 - green) and 594 (Alexa Fluor 594 - red). ....	213
Figure A.3 – Example of images taken during NOB evaluation where (a) is the area of the red labeled hybridized total bacteria (EUB), (b) is the area of the green labeled NOB. ....	215
Figure A.4 – Biofilm extraction (a), settling (b), and storage (c) for subsequent DNA screening. ....	216

## LIST OF TABLES

Table 2.1 – Some of the most important parameters and constituents for characterization of wastewaters. Source: adapted from (VON SPERLING, 2007a).....	11
Table 2.2 – Classes of wastewater treatment by level. Source: adapted from (METCALF & EDDY, TCHOBANOGLOUS, <i>et al.</i> , 2014, VON SPERLING, 2007a).....	12
Table 2.3 – Trophic classification of various microbial groups organisms. Source: (HENZE, VAN LOOSDRECHT, <i>et al.</i> , 2008).....	16
Table 2.4 – Classification of biological processes with respect to the electron acceptor used in the metabolism of the microorganisms. Source: adapted from (METCALF & EDDY, TCHOBANOGLOUS, <i>et al.</i> , 2003). .....	18
Table 2.5 – Classification of biological processes in relation to their functionality. Source: adapted from (METCALF & EDDY, TCHOBANOGLOUS, <i>et al.</i> , 2003). .....	20
Table 2.6 – Example of bacterial genera found in biological reactors with respect to their metabolic function and their morphologic growth type. Source: adapted from (BENTO, HOFFMANN, 2007). .....	36
Table 2.7 – Groups of organisms composing the microfauna in activated sludges systems. Source: adapted from (BASSIN, DEZOTTI, 2008). .....	37
Table 2.8 – Most frequent genera found in activated sludges for various organisms groups of the microfauna. Source: adapted from (BASSIN, DEZOTTI, 2008).....	38
Table 2.9 – Treatment conditions related to the presence or predominance of certain groups of organisms in the biomass. Source: adapted from (BASSIN, DEZOTTI, 2008).....	39
Table 2.10 – MBBR overall features and benefits in comparison to activated sludge and other biofilm reactors.....	44
Table 2.11 – Several examples of commercial MBBR carriers from AnoxKaldnes and their main characteristics. Source: adapted from (BASSIN, DEZOTTI, 2018, MORGAN-SAGASTUME, 2018).....	47

Table 2.12 – Classification of pesticides according to the kind of plague and action. Source: adapted from (SILVA, COSTA, 2012). .....	57
Table 2.13 – Pesticides classification with respect to the danger to health as defined by the WHO. Source: adapted from (WORLD HEALTH ORGANIZATION, 2010)... 58	
Table 2.14 – Toxicological classification of pesticides according to the Brazilian ordinance n° 03 (SNVS, Ministry of Health). Source: (BRASIL, 1992)..... 58	
Table 2.15 – Main techniques applied in the management and treatment of wastewaters in pesticide manufacture and formulation industries. Source: adapted from (ATKINS, 1972, WANG, YUNG-TSE, <i>et al.</i> , 2006)..... 62	
Table 2.16 – Literature review of researches assessing the treatment of pesticide wastewaters..... 65	
Table 2.17 – Nominal values for flow rate, COD and TAN concentrations for the different waste streams of the pesticide formulation industry..... 70	
Table 2.18 – Approximate elemental composition of wood materials. Source: adapted from (BAJPAI, 2018, GOYAL, 2020b). .....	71
Table 2.19 – Typical composition of hard and softwood, based on North American species, by classes of compounds. Source: adapted from (BAJPAI, 2018). .....	72
Table 2.20 – Summary of the most commonly applied pulping processes. Source: adapted from (BAJPAI, 2018, WANG, YUNG-TSE, <i>et al.</i> , 2006). .....	74
Table 2.21 – Description of some of the most common pulp bleaching stages. Source: adapted from (GOYAL, 2020a).....	75
Table 2.22 – Main best available technologies guidelines, from the European Integrated Pollution and Prevention Control and the International Finance Corporation, for minimizing wastewater load in bleaching kraft pulp mills. Source: adapted from (CABRERA, 2017, WANG, YUNG-TSE, <i>et al.</i> , 2006). .....	78
Table 2.23 – Summary of the MBBR stage operational characteristics of studies evaluating the BAS process over the treatment of P&P wastewater. ....	81
Table 3.1 – Definition of the acronyms used for the identification of each waste stream and differentiation from one collected lot to another. ....	85

Table 3.2 – Characteristics of each IPT lot and the IR lot in terms of physicochemical parameters (average values are shown). .....	87
Table 3.3 – Characteristics of each S lot and the related average of physicochemical parameters.....	88
Table 3.4 – COD results and treatment conditions for each batch adsorption on PAC. 90	
Table 3.5 – MBBR operational phases and their characteristics throughout the pesticide wastewater study.....	94
Table 3.6 – Monitored parameters and their approximate analysis frequencies. ....	95
Table 3.7 – Experimental conditions during the batch trials.....	96
Table 3.8 - Average characteristics of the different wastewater lots, at the time of collection at the industry. “Start” and “End” refers to the operational timescale of the MBBRs. ....	97
Table 3.9 – P&P research operational phases and its characteristics, duration, and number <i>n</i> of analysis dates.....	99
Table 3.10 – Monitored parameters and their approximate analysis frequencies. ....	100
Table 4.1 – Summary of MBBR average inlet and outlet monitored parameters in each operational phase. ....	106
Table 4.2 – MBBR influent and effluent sCOD/DOC ratio for operational phases 1 to 3. ....	114
Table 4.3 - Biofilm quantification, fraction of suspended solids in the MBBR ( $f_{SS/TS}$ ), apparent specific removal rates and maximum specific removal rates for each phase. ....	125
Table 5.1 – Remarkable time spans throughout MBBRs operation with potential impact on results interpretation. ....	134
Table 5.2 – Summary of MBBR influent and effluent monitored parameters on each operational phase. ....	138
Table 5.3 – Average suspended solids concentration, percentage of volatile suspended solids relative to total suspended solids, and sludge yield at each operational phase, for both reactors. Standard deviation within brackets and one-way ANOVA statistics (F and p values), comparing reactors A and B, are also listed. ....	143

Table 5.4 – Number of OTUs assigned at various taxonomical levels and amount of corresponding unique taxa. ....	154
Table 5.5 - Richness and alpha diversity indices for the 13 biofilm samples. Linear color scale goes from white to grey with increasing values for every index. ....	155
Table 5.6 - Relative abundance of the 40 most abundant genera amongst all the 13 biofilm samples from each reactor (A or B) and phase (1 to 6). Square root color scale goes from white to red with raising abundance. Superscript number refers to the phylum that each genus belongs to, according to the rank in Figure 5.12. ....	164
Table A.1 – Methods employed for each analysis performed during the experimental investigations. ....	201
Table A.2 – Oligonucleotide probes utilized and target microbial groups. ....	214

## SYMBOLS

$a$	Carrier specific surface area [area/volume]
$A$	Total area for biofilm development [area]
$C$	Concentration of a certain substance/substrate [mass/volume]
$LD_{50}$	Median Lethal Dose
$ED_{50}$	Median Effective Dose
$f$	Carriers filling degree or filling ratio [dimensionless]
$f_e$	Fraction of substrate directed to catabolism
$f_s$	Fraction of substrate directed to anabolism
$f_{SS/TS}$	Ratio of suspended solids to the sum of suspended and attached solids
$HRT$	Hydraulic retention time [time]
$K_B$	Saturation constant from the Kincannon-Stover kinetic model
$n$	Number of carriers contained in the MBBR
$[TKN]$	Total kjeldahl nitrogen concentration [mass N/volume]
$[TAN]$	Total ammoniacal nitrogen concentration [mass N/volume]
$[N_{NH_3}]$	Concentration of nitrogen in free ammonia [mass N/volume]
$[N_{NO_2^-}]$	Concentration of nitrogen in nitrite [mass N/volume]
$[N_{NO_3^-}]$	Concentration of nitrogen in nitrate [mass N/volume]
$[N_{org}]$	Concentration of organic nitrogen [mass N/volume]
$[TN]$	Total nitrogen concentration [mass N/volume]
$p$ (prefix)	Particulate portion of a parameter
$pH$	Power of hydrogen [dimensionless]
$q$	Specific substrate removal rate [mass/(mass·time)]
$Q$	Flow rate [volume/time]
$r$	Volumetric substrate removal rate [mass/(volume·time)]
$s$	Surface substrate removal rate [mass/(area·time)]
$s$ (prefix)	Soluble portion of a parameter
$SLR$	Surface loading rate [mass/(area·time)]
$t$	Time
$t$ (prefix)	Sum of particulate and dissolved portions of a parameter

$T$	Temperature
$TAS$	Total attached solids
$U_{max}$	Maximum substrate removal rate (from Kincannon-Stover kinetic model)
$V$	Volume
$VAS$	Volatile attached solids
$[VSS]$	Volatile suspended solids concentration [mass/volume]
$VLR$	Volumetric loading rate [mass/(volume.time)]
$Y_H$	Heterotrophic cell yield [mass COD <sub>vss</sub> /mass COD]
$Y_{Hv}$	Heterotrophic cell yield [mass VSS/mass COD]

### **GREEK LETTERS**

$\eta$	Removal efficiency
--------	--------------------

### **SUPERSCRIPTS**

*	Maximum (removal rate)
---	------------------------

### **SUBSCRIPTS**

$i$	Influent
$e$	Effluent
$S$	Surface concentration (of attached solids)
$T$	Total amount (of attached solids)
$V$	Volumetric concentration (of attached solids)

## ABBREVIATIONS

ABNT	<i>Associação Brasileira de Normas Técnicas</i> (Brazilian Association of Technical Norms)
ADP	<u>A</u> denosine <u>D</u> iphosphate
ANA	<i>Agência Nacional de Águas</i> (Water National Agency)
Anammox	<u>A</u> naerobic <u>A</u> mmonium <u>O</u> xidation
AOB	<u>A</u> mmonia- <u>O</u> xidizing <u>B</u> acteria
AOP	<u>A</u> dvanced <u>O</u> xidation <u>P</u> rocesses
AOX	Chlorinated organics
AS	<u>A</u> ctivated <u>S</u> ludge
ATP	<u>A</u> denosine <u>T</u> riphosphate
BAS	<u>B</u> iofilm- <u>A</u> ctivated <u>S</u> ludge
BOD	<u>B</u> iological <u>O</u> xygen <u>D</u> emand
BRL	<u>B</u> razilian <u>R</u> eal (currency)
CTMP	<u>C</u> hemi- <u>T</u> hermo <u>m</u> echanical <u>P</u> ulp
COD	<u>C</u> hemical <u>O</u> xygen <u>D</u> emand
CONAMA	<i>Conselho Nacional do Meio Ambiente</i> (National Environment Counsel)
CSTR	<u>C</u> ompletely <u>S</u> tirred <u>T</u> ank <u>R</u> eactor
DDT	<u>D</u> ichloro <u>d</u> iphenyl <u>t</u> richloroethane
DNA	<u>D</u> eoxyribo <u>n</u> ucleic <u>A</u> cid
DO	<u>D</u> issolved <u>O</u> xygen
DOC	<u>D</u> issolved <u>O</u> rganic <u>C</u> arbon
ECF	<u>E</u> lemental <u>C</u> hlorine <u>F</u> ree
ED <sub>50</sub>	Median <u>E</u> ffective <u>D</u> ose
EGSB	<u>E</u> xpanded <u>G</u> ranular <u>S</u> ludge <u>B</u> ed
EPS	<u>E</u> xtracellular <u>P</u> olymeric <u>S</u> ubstances
FAS	<u>F</u> ixed <u>A</u> ttached <u>S</u> olids
FISH	<u>F</u> luorescent <i>in situ</i> <u>h</u> ybridization
FSS	<u>F</u> ixed <u>S</u> suspended <u>S</u> olids
GAC	<u>G</u> ranular <u>A</u> ctivated <u>C</u> arbon
HDPE	<u>H</u> igh <u>D</u> ensity <u>P</u> oly <u>e</u> thylene

HRT	<u>H</u> ydraulic <u>R</u> etention <u>T</u> ime
IBR	<u>I</u> mmobilized <u>B</u> iomass <u>R</u> eactor
IC	<u>I</u> norganic <u>C</u> arbon
IFAS	<u>I</u> ntegrated Fixed-Film <u>A</u> ctivated <u>S</u> ludge
INEA	<i>Instituto Estadual do Ambiente</i> (Environment State Institute)
IPT	<u>I</u> ndustrial <u>P</u> retreated (pesticide formulation wastewater)
IR	<u>I</u> ndustrial <u>R</u> aw (pesticide formulation wastewater)
LD <sub>50</sub>	Median <u>L</u> ethal <u>D</u> ose
MBBR	<u>M</u> oving <u>B</u> ed <u>B</u> iofilm <u>R</u> eactor
MBR	<u>M</u> embrane <u>B</u> ioreactor
MF	<u>M</u> icro <u>f</u> iltration
MWEUV	<u>M</u> icrowave <u>E</u> lectrodeless <u>U</u> ltraviolet
NA	<u>N</u> ot <u>A</u> vailable
NMDS	<u>N</u> on-Metric <u>M</u> ultidimensional <u>S</u> caling
NOB	<u>N</u> itrite- <u>O</u> xidizing <u>B</u> acteria
NSSC	<u>N</u> eutral <u>S</u> ulfite <u>S</u> emi- <u>C</u> hemical (pulping technology)
NTNU	<i>Norges Teknisk-Naturvitenskaplige Universitet</i> (Norwegian University of Science and Technology)
NTU	<u>N</u> ephelometric <u>T</u> urbidity <u>U</u> nits
OTU	<u>O</u> perational <u>T</u> axonomic <u>U</u> nit
p	<u>P</u> articulate (prefix)
PBS	<u>P</u> hosphate <u>B</u> uffered <u>S</u> aline
P&P	<u>P</u> ulp and <u>P</u> aper
PS	<u>P</u> ersulfate
PX	Operational <u>P</u> hase <u>X</u> (where X is 1, 2, 3, ...)
PAC	<u>P</u> owdered <u>A</u> ctivated <u>C</u> arbon
PERH	<i>Política Estadual de Recursos Hídricos</i> (State Policy for Water Resources)
PNMA	<i>Política Nacional do Meio Ambiente</i> (National Environment Policy)
PNRH	<i>Política Nacional de Recursos Hídricos</i> (National Policy for Water Resources)
RJ	<u>R</u> io de <u>J</u> aneiro
rRNA	<u>R</u> ibosomal <u>R</u> ibonucleic <u>A</u> cid
RO	<u>R</u> everse <u>O</u> smosis

s	<u>S</u> oluble (prefix)
S	<u>S</u> anitary wastewater (pesticide research)
SBR	<u>S</u> equencing <u>B</u> atch <u>R</u> eactor
SEGRHI	<i><u>S</u>istema <u>E</u>stadual de <u>G</u>erenciamento de <u>R</u>ecursos <u>H</u>ídricos</i> (State System of Water Resources Management)
SINGREH	<i><u>S</u>istema <u>N</u>acional de <u>G</u>erenciamento de <u>R</u>ecursos <u>H</u>ídricos</i> (National System of Water Resources Management)
SISNAMA	<i><u>S</u>istema <u>N</u>acional do <u>M</u>eio <u>A</u>mbiente</i> (National Environment System)
SLR	<u>S</u> urface <u>L</u> oading <u>R</u> ate
SNVS	<i><u>S</u>ecretaria <u>N</u>acional de <u>V</u>igilância <u>S</u>anitária</i> (National Secretary of Sanitary Surveillance)
SRT	<u>S</u> ludge <u>R</u> etention <u>T</u> ime
t	<u>T</u> otal (prefix)
TAN	<u>T</u> otal <u>A</u> mmoniocal <u>N</u> itrogen
TAS	<u>T</u> otal <u>A</u> ttached <u>S</u> olids
TC	<u>T</u> otal <u>C</u> arbon
TCF	<u>T</u> otal <u>C</u> hlorine <u>F</u> ree
TKN	<u>T</u> otal <u>K</u> jeldahl <u>N</u> itrogen
TMP	<u>T</u> hermomechanical <u>P</u> ulping
TN	<u>T</u> otal <u>N</u> itrogen
TOC	<u>T</u> otal <u>O</u> rganic <u>C</u> arbon
TP	<u>T</u> otal <u>P</u> hosphorous
TS	<u>T</u> otal <u>S</u> olids (attached and suspended)
TSS	<u>T</u> otal <u>S</u> suspended <u>S</u> olids
UASB	<u>U</u> pflow <u>A</u> naerobic <u>S</u> ludge <u>B</u> lanket
UFF	<i><u>U</u>niversidade <u>F</u>ederal <u>F</u>luminense</i> (Federal Fluminense University)
UV	<u>U</u> ltraviolet
VAS	<u>V</u> olatile <u>A</u> ttached <u>S</u> olids
VFA	<u>V</u> olatile <u>F</u> atty <u>A</u> cids
VLR	<u>V</u> olumetric <u>L</u> oading <u>R</u> ate
VRR	<u>V</u> olumetric <u>R</u> emoval <u>R</u> ate
VS	<u>V</u> olatile <u>S</u> olids (attached and suspended)
VSS	<u>V</u> olatile <u>S</u> suspended <u>S</u> olids
WHO	<u>W</u> orld <u>H</u> ealth <u>O</u> rganization

## 1. INTRODUCTION AND OBJECTIVES

In 2007, more than 11,300 readers of the British Medical Journal elected the development and expansion of basic sanitation as the greatest medical advance since 1840, ahead of antibiotics, anesthesia, vaccines and the discovery of the DNA structure (FERRIMAN, 2007). The seriousness of water pollution is exemplified by estimations from the World Health Organization: around 842,000 deaths per year happen due to unsafe water supplies (WORLD HEALTH ORGANIZATION, 2014). In Brazil, it is estimated that for 1 BRL invested in sanitation, 4 BRL are saved in public health (FUNASA, 2004). Those are potent demonstrations of the huge importance of water pollution control, amongst other basic sanitation actions, for preserving public health and the environment for the present and future generations. No wonder, the 6<sup>th</sup> item of the United Nations Sustainable Development Goals urges for universal access to clean water and sanitation by 2030, with its target 6.3 aiming to

improve water quality by reducing pollution, eliminating dumping and minimizing release of hazardous chemicals and materials, halving the proportion of untreated wastewater and substantially increasing recycling and safe reuse globally (UN, 2016).

Pollutant streams - whether industrial, agricultural, or domestic - are diverse in flow rate and composition, depending intrinsically on their sources. Several factors imply in this variability, such as life habits, level of regional development, strictness of regional norms regulating wastewater disposal, type and seasonality of industrial or agricultural production, etc. (HENZE, VAN LOOSDRECHT, *et al.*, 2008, VON SPERLING, 2007a). Several parameters may translate the pollution in measurable terms, being some of the most important: organic matter content, nitrogen in its various forms, phosphorous, suspended solids, turbidity, color, oil and grease, acidity/alkalinity, temperature, and toxicity. Minimizing the environmental impact by properly treating the wastewaters is an ethical and legal responsibility of public Power and commercial organizations. The major challenge consists of allying socio-environmental and economic sustainability.

Biological technologies often appear as one of the most cost-effective options for the treatment of wastewaters, regardless of the kind of source. These treatment processes rely on suspended and/or attached growth of microbial biomass, in form of biofilms in the latter case. The microbial community established in the bioreactor is able to reduce the polluting load of a certain wastewater by metabolizing pollutant compounds to less harmful forms. Despite requiring more intensive aeration, the biofilm growth format makes the biomass more resistant to load shocks, and the sludge age independent from hydraulic retention time, often dismissing the need of a sludge recycle line. Ultimately, a superior sludge age can be implemented, causing greater overall performance and specialization of the biomass to degrade otherwise persistent substances. Biofilm reactors tend to be more resistant to fluctuations in organic load, toxicity and pH (ØDEGAARD, 2006, VAN HAANDEL, VAN DER LUBBE, 2012, VON SPERLING, 2007c).

One particular biofilm technology in evidence is the moving bed biofilm reactor (MBBR), which is intended to combine the best features of suspended and attached growth processes, providing a robust, compact, easy-to-operate, and efficient wastewater treatment solution. In this kind of reactor, the biofilm grows on the protected surface of plastic carriers that freely move throughout a reactor completely mixed by aeration (for aerobic reactors) or mechanical mixing (for anoxic/anaerobic reactors). The MBBR carriers have specific surface area usually ranging from 200 to 1200 m<sup>2</sup>/m<sup>3</sup> of dry bed, and generally have density close to that of the water. In addition to the attributes common to any biofilm reactor, the MBBR excels for providing very low head loss, great use of the entire reactional volume, minimization of clogging issues, and capacity to stand as an easy upgrade option from existing activated sludge (AS) systems (BASSIN, DEZOTTI, 2018, ØDEGAARD, 2019).

The compactness, robustness and biomass specialization features turn the MBBR into an especially attractive option for the treatment of industrial wastewaters, as these are particularly liable to seasonal oscillations in quality and quantity that come alongside the production changes. High flow rates, as in the pulp and paper (P&P) industry, are common, as well as vast concentrations of chemical residues that are potentially toxic, recalcitrant and bioaccumulative. This is the case of the industrial segment producing pesticides, substances that are used as the main measure for crop protection from harmful living organisms. They are known to be damaging to the human health and the environment, posing a risk even at concentrations as low as µg/L or ng/L (AFFAM,

CHAUDHURI, *et al.*, 2016, FIROUZSALARI, SHAKERKHATIBI, *et al.*, 2019, LIU, ZHAO, *et al.*, 2010, LUO, GUO, *et al.*, 2014).

Pesticide production and application stands as one of the main industrial activities to the present day, producing approximately 150 million tons of wastewater every year (XIONG, CHENG, *et al.*, 2011). Nonetheless, the use of those substances is made necessary so that agricultural productivity may follow the growing food consumption consequent to the increasing world population and changes in eating habits (NATIONAL RESEARCH COUNCIL, 2000, OERKE, DEHNE, 2004). Intensive agriculture techniques, also employed for raising productivity, are commonly used instead of traditional cultivation, which may increase the pesticides usage up to 200 times (MALATO, BLANCO, *et al.*, 2000).

Pesticide industries can be classified as manufacture - where the technical grade active ingredients are synthesized - or formulation - where the technical grade pesticides are mixed with other ingredients to make the final commercial pesticide product (WANG, YUNG-TSE, *et al.*, 2004). The formulation industry has the washing of lines and equipment as the main source of wastewater. As the formulated pesticide frequently changes, the residual water has great variability regarding composition. Various organic groups are normally found in this kind of wastewater as well as conventional pollutants such as easily degradable organic matter, oil, ammonia and inorganic salts (WANG, YUNG-TSE, *et al.*, 2004).

The toxicity and high persistent organic load of this kind of waste streams are challenges for the application of biological treatment technologies. Consequently, their association with physicochemical pretreatment steps and/or the mix of the pesticide-containing wastewater with sanitary sewage (which additionally provides nutrients) are common approaches used to improve the industrial wastewater biodegradability and lower its toxicity (WANG, YUNG-TSE, *et al.*, 2004).

Few studies assessed the performance of the MBBR as a biological treatment for pesticide wastewaters (BACHMANN PINTO, MIGUEL DE SOUZA, *et al.*, 2018, CAO, FONTOURA, *et al.*, 2016, CHEN, SUN, *et al.*, 2007). As this kind of wastewater may present great quality variations, it is important to build up a more solid base of knowledge regarding the treatment of this complex matrix. This implies the need for a greater number of applied researches on this topic. Although the toxicity and low biodegradability of pesticide wastewaters have been highlighted in previous investigations, so far none investigated the exposure of a biological process to increasing

loads of real raw pesticide formulation wastewater.

Another industrial segment consisting of one of the most polluting and water-intensive is the P&P sector (CABRERA, 2017, THOMPSON, SWAIN, *et al.*, 2001, VIRKUTYTE, 2017). Taking into account only the European and U.S. markets, the P&P segment generated approximately 2.5 billion m<sup>3</sup> of wastewater in 2015, which represented around 42% of the total industrial wastewater production in those regions (URIOOC, 2015). Numbers like those stress how impactful to the environment the P&P industry can be and the importance of correct and efficient wastewater management and treatment to reduce the impact of the final effluent in receiving water bodies (KARRASCH, PARRA, *et al.*, 2006).

P&P mills turn the raw material - mostly wood - into different types of paper products by the following general steps: wood debarking and chipping; pulping; bleaching; and paper making. Each step comprises a series of operations and may differ noticeably from one industry to another, with the pulping and bleaching stages generating the majority of the liquid wastes. Pulping consists of mechanical and/or chemical breakdown of the wood chips to facilitate cellulose and hemicellulose fiber separation, while bleaching involves the whitening of the cellulosic pulp by removing residual lignin by means of chemical agents such as chlorine, chlorine dioxide, hydrogen peroxide, sodium peroxide, oxygen, ozone, etc. (DOBLE, KUMAR, 2005, WANG, YUNG-TSE, *et al.*, 2006).

The quality of the wastewater from P&P industry depends on the type of raw material processed, on the chosen pulping and bleaching technologies, and also on the amount of water used and effluent recirculated in the process (POKHREL, VIRARAGHAVAN, 2004). Overall, the liquid waste streams are primarily composed of degradation products of carbohydrates, lignin and wood extractives, containing high chemical oxygen demand (COD), biological oxygen demand (BOD) and concentration of chlorinated chemicals (in case of non-chlorine-free bleaching) (ZODI, LOUVET, *et al.*, 2011). The BOD to COD ratio, often used to express the biodegradability of aqueous matrices, is usually within the range 0.05 to 0.5, reflecting the significant presence of recalcitrant compounds. High total suspended solids (TSS) content is also common as a result of the wood preparation and pulp screening stages. Dark brown color of the residual water is attributed to lignin and its degradation products (WANG, YUNG-TSE, *et al.*, 2006). The lack of nutrients (nitrogen (N) and phosphorous (P)) is another point of concern regarding this type of wastewater (SLADE, ELLIS, 2004). For implementing

biological treatment, this limitation should be overcome without over supplementation of N and P, which could raise their effluent concentrations and dosing costs.

The main challenges faced in the treatment of P&P wastewaters are not only reducing organic matter and suspended solids contents, but also color and chlorinated organics, especially when the bleaching technology is not chlorine-free. Primary treatment is commonly done by mechanical processes such as sedimentation, flotation, or filtration, providing an effluent lower in solids content for the secondary treatment. Although the characteristics of the P&P wastewater may hinder the application of biological treatment, this condition can be attenuated with the use of adapted microbial cultures. Previous studies showed that the use of microorganisms pre-acclimated to P&P wastewater may render high BOD reduction as compared to those achieved with non-adapted biomass (ORDAZ-DÍAZ, ROJAS-CONTRERAS, *et al.*, 2014, ZODI, LOUVET, *et al.*, 2011). Biological processes face the additional challenge of abating the high organic loads, typically found in P&P wastewaters, while producing biosolids with good separability. To circumvent the operating obstacles, the Biofilm-Activated Sludge (BAS) process, consisting of a high loaded MBBR as pre-treatment of a conventional activated sludge reactor, is commonly applied for the treatment of P&P wastewater. Indeed, the BAS technology has been effectively applied to treat such waste streams (DALENTOFT, THULIN, 1997), with multiple reports of pilot and full-scale plants around the world (MALMQVIST, WELANDER, *et al.*, 2007, REVILLA, GALÁN, *et al.*, 2018a, VILLAMAR, JARPA, *et al.*, 2009).

In a BAS system, the upfront MBBR step is intended to remove 30-60 % of the incoming soluble COD (sCOD), protecting the AS step from load variations. This strategy helps to prevent issues associated with filamentous bacterial growth in the AS tank, which could result in poor settling sludge and deterioration of effluent quality. Harder to degrade COD fractions and suspended biomass exiting the MBBR are then degraded in the lower loaded AS, reducing the sludge production in comparison with a standalone AS system. By lacking readily degradable COD, the effluent of the MBBR stimulates the development of slow-growing organisms in the AS reactor that can consume the difficult-to-degrade organics, thereby constituting a significant fraction of the biomass. Such process configuration yields better compactness and COD removal efficiency than a single AS reactor at similar sludge age (MALMQVIST, BERGGREN, *et al.*, 2004, VAN HAANDEL, VAN DER LUBBE, 2012).

In addition to the above-mentioned possibilities with BAS, it has also been shown that the BAS configuration can improve the efficiency of nutrient usage. First reported in a research work from 2002, BAS operation under nutrient restriction was found to prevent excessive amounts of N and P in the outlet stream, while further lowering the sludge production and improving its separability (WELANDER, OLSSON, *et al.*, 2002). The limitation of nutrients stimulates microorganisms to produce more extracellular polymeric substances (EPS) in the MBBR, especially when P is limited, as a means of consuming the organic carbon without production of new cells. High EPS production is generally related to slimy biomass formation (JENKINS, RICHARD, *et al.*, 2004), but this EPS-rich biomass is readily degraded in the following AS step, recycling nutrients to the process and lessening the sliminess of the final effluent sludge (SLADE, ELLIS, 2004).

Several studies have been conducted with the BAS system for treating P&P wastewater, at varying operating conditions (DALENTOFT, THULIN, 1997, MALMQVIST, BERGGREN, *et al.*, 2004, MALMQVIST, WELANDER, *et al.*, 2007, RANKIN, AERT, *et al.*, 2007, REVILLA, GALÁN, *et al.*, 2018a, WELANDER, OLSSON, *et al.*, 2002). However, all of these studies were conducted at a relatively low effective specific surface area in the reactor (i.e. carrier area by carrier fill), ranging between 60 (MALMQVIST, BERGGREN, *et al.*, 2004) and 223 m<sup>2</sup>/ reactor m<sup>3</sup> (DALENTOFT, THULIN, 1997). With the evolvement of new MBBR carriers with higher protected area, the MBBR stage of the BAS process could easily be designed with up to at least 600 m<sup>2</sup>/m<sup>3</sup> using carriers with high surface area at high carrier filling fraction, substantially improving the compactness of the BAS process.

The carrier filling ratio alone was shown to be a major factor influencing the structure of the microbial community and the performance of MBBRs (CALDERÓN, MARTÍN-PASCUAL, *et al.*, 2012). Also, although the MBBR is a biofilm-based process, it has been demonstrated that the suspended biomass within these systems may also play a relevant role in the overall treatment performance (LIMA, DEZOTTI, *et al.*, 2016), and that this contribution relies on the operating HRT (PICULELL, WELANDER, *et al.*, 2014). The characteristics of the effluent biomass of the MBBR may be particularly relevant in a BAS system since the hydrolysis and degradation of these solids are crucial steps in the downstream AS stage. Thus, for the BAS application in P&P wastewater treatment, the selection between a small MBBR with high specific surface area (as to

favor biofilm growth) or a larger one (higher HRT) with lower specific surface area (as to favor suspended biomass) needs further evaluation.

These subjects have not been addressed in earlier literature assessing the BAS application (DALENTOFT, THULIN, 1997, MALMQVIST, BERGGREN, *et al.*, 2004, MALMQVIST, WELANDER, *et al.*, 2007, RANKIN, AERT, *et al.*, 2007, REVILLA, GALÁN, *et al.*, 2018a, WELANDER, OLSSON, *et al.*, 2002). Also, no in-depth discussion was given about how nutrients availability affects the efficiency of nutrients utilization for substrate removal, essential knowledge for optimizing consumption and minimizing the discharge of N and P.

### **1.1. Objectives and Strategies**

Despite being a well-developed technology vastly applied to industrial wastewaters, it is noticed that there is still great room for expanding the knowledge on the MBBR. This is especially true considering that any industrial wastewater has particularities that result in distinct challenges, as previously mentioned. A deeper understanding on how operational parameters relate to overall performance, biosolids dynamics, and microbial community activity and diversity could bring advantages both to the industry - that might be able to design and operate MBBRs more optimally, saving footprint, energy and resources – and to the environment – as the effluent quality would potentially improve.

Therefore, this doctorate thesis aimed at gaining further insights on the effects of operational parameters on the performance of the MBBR technology applied for the treatment of complex industrial matrices. Independent experimental lab-scale investigations were set up with MBBRs treating real wastewaters from a Brazilian pesticide formulation industry and a Swedish P&P mill.

For the pesticide wastewater, the bioreactor was evaluated in terms of organic matter removal and nitrification. The robustness of the process was evaluated under different HRTs, and diverse qualities and proportions of the industrial pesticide wastewater - either pretreated or raw - mixed with sanitary sewage. The exposure of the bioreactor to increasing proportions of the raw pesticide wastewater is a unique feature of this study, particularly considering that nitrification is seldom evaluated for pesticide wastewaters and nitrifying bacteria are inherently more sensitive to the toxicity posed by a wide range of chemical compounds. Additionally, the bench-scale experiments served

to evaluate if the MBBR constitutes an efficient treatment alternative, and as a design basis for a full-scale MBBR to substitute the full-scale AS plant in the industrial site that provided the wastewater. The strategy involved the study of the system:

- With reference to local discharge legal restrictions;
- Under superior organic matter and nitrogen loads than the normally observed in the existing treatment plant, evaluating the robustness of the assessed treatment;
- For distinct hydraulic residence times;
- When fed with different lots of pretreated pesticide wastewater, with special attention to the accumulation of persistent organics in the effluent and/or in the biofilm;
- For various proportions of raw pesticide wastewater instead of the pretreated one.

The study with the P&P wastewater aimed to address how high loaded MBBRs, with distinct effective specific surface areas and HRTs, responded to nutrient limitation during the treatment of P&P wastewater. Organic matter removal, efficiency of nutrients utilization, and biosolids dynamics were monitored over time. Batch tests with isolated suspended biomass and biofilm were performed to separately evaluate the activity of each biomass fraction, while data from reactor continuous operation was fitted to the Kincannon-Stover kinetic model for assessing both the maximum substrate utilization rate and the wastewater biodegradability. DNA sequencing of biofilm samples was also performed to track changes in microbial communities resulting from the shifts in operational conditions. The following topics were addressed in this study:

- The effect of different carriers filling ratios;
- The importance of different hydraulic retention times and organic loading rates;
- How limitation of nitrogen and phosphorous impact the biological treatment in comparison with excess of nutrients;
- The possible influence of the temporal variation of the wastewater quality.

The content of this work is presented as fluid as possible, trying to minimize divisions between the topics related to the pesticide and P&P studies, and making the two independent experimental investigations part of the same umbrella. However, content separation was unavoidable as the bench-scale experiments were independent and had

remarkable differences from each other. Thereby, the MBBR operation with the wastewater from pesticide formulation industry will be regarded as “pesticide research”, whereas the operation with pulp and paper wastewater will be designated as “P&P research”.

## 2. LITERATURE REVIEW

For the contextualization of this work, this chapter presents a brief literature review on the fundamental topics and concepts linked to the research projects executed during this doctoral thesis, emphasizing the biological wastewater treatment and the moving bed biofilm reactor. An overview is also taken of specific notions about the pesticide and pulp and paper industries and of the literature regarding the treatment of their wastewaters.

### 2.1. Wastewater Characterization and Treatment

An immense variety of characteristics and individual compounds could be evaluated for a certain wastewater but would not necessarily be meaningful for another wastewater source. In this sense, it is common to characterize the polluting potential of wastewaters by groups of physical, chemical, and biological parameters, as well as key individual constituents that possess clear significance. Some of such parameters and constituents that were explored in the experimental progress of this work are defined in Table 2.1. A few other worth-mentioning characteristics include oils and grease, conductivity, metals, chloride, color, odor, flavor, radioactivity, particular organic substances, etc. These are better described elsewhere (METCALF & EDDY, TCHOBANOGLOUS, *et al.*, 2014).

Table 2.1 – Some of the most important parameters and constituents for characterization of wastewaters. Source: adapted from (VON SPERLING, 2007a).

<i>Parameters or constituents</i>	<i>Comment</i>
<i>Total solids (TS)</i>	Sum of total suspended and dissolved solids.
<i>Dissolved solids</i>	Residual solids left after evaporation.
<i>Total suspended solids (TSS)</i>	Solids retainable by filtration.
<i>Volatile suspended solids (VSS)</i>	Organic fraction of the TSS.
<i>Fixed suspended solids (FSS)</i>	Mineral residue of the TSS.
<i>Turbidity</i>	Measure of light scattering caused by TSS.
<i>Carbonaceous organic matter</i>	Liable or not to biological oxidation.
<i>Biological oxygen demand (BOD)</i>	Oxygen demanded for biological stabilization of organic matter (usually 5 days, 20°C).
<i>Chemical oxygen demand (COD)</i>	Equivalent oxygen demanded for chemical stabilization of organic matter (+ oxidizable inorganics)
<i>Total organic carbon (TOC)</i>	Direct measure of the carbonaceous organic matter.
<i>Total nitrogen (TN)</i>	Sum of all nitrogen forms.
<i>Total ammoniacal nitrogen (TAN)</i>	Sum of ammonia and ammonium, product of decomposition of organic nitrogen.
<i>Nitrite (NO<sub>2</sub><sup>-</sup>)</i>	Intermediary product of ammonia oxidation.
<i>Nitrate (NO<sub>3</sub><sup>-</sup>)</i>	Final product of ammonia oxidation.
<i>Organic nitrogen</i>	Nitrogen contained in organic compounds.
<i>Total phosphorous (TP)</i>	Sum of phosphorous forms.
<i>Inorganic phosphorous (PO<sub>4</sub><sup>3-</sup>)</i>	Orthophosphates and polyphosphates.
<i>Organic phosphorous</i>	Phosphorous contained in organic compounds.
<i>Dissolved oxygen (DO)</i>	Relates to microbial profile and metabolism.
<i>Temperature</i>	Relates to microbial profile and reactions/transfer rates.
<i>pH</i>	Relates to microbial profile and activity in bioreactors.
<i>Toxicity</i>	Chronic or acute toxic effects on living organisms.
<i>Microorganisms</i>	Relatable to pathogenicity and bioreactor conditions.

Many parameters may be divided into soluble (s, prefix) and particulate (p, prefix) fractions, as is the case for BOD, COD, TOC, TN, TP, etc. For those, particulate refers to their portion within the suspended solids. The counterpart is usually designated as soluble or dissolved, being part of the dissolved solids. Thus, the total (t, prefix) of a certain constituent is the sum of the particulate and dissolved portions (VON SPERLING, 2007a). In addition, each of these fractions may be characterized as biodegradable or inert, with the biodegradability being easy/rapid or slow/hard, depending on the chemical

nature of the substance and organisms acting on its metabolization (VON SPERLING, 2007b).

Instances of adverse effects to water bodies receiving polluted streams include (but are not limited to) oxygen depletion, eutrophication, toxicity, bioaccumulation, aesthetic worsening, risk for recreation, and loss of potability/usability (HENZE, VAN LOOSDRECHT, *et al.*, 2008, VON SPERLING, 2007a). In order to prevent these damages to water bodies and respect legal thresholds defined by environmental organs, wastewater treatment plants employ one or more physical, chemical, and biological processes to minimize the polluting load. Such treatment facilities are generally designed to treat municipal sewage or locally treat industrial wastewaters. The stages within the treatment plant can be categorized with respect to the level of treatment achieved: preliminary, primary, secondary or tertiary (METCALF & EDDY, TCHOBANOGLOUS, *et al.*, 2003, VON SPERLING, 2007a). Table 2.2 briefly explains each class of treatment.

Table 2.2 – Classes of wastewater treatment by level. Source: adapted from (METCALF & EDDY, TCHOBANOGLOUS, *et al.*, 2014, VON SPERLING, 2007a).

<b>Level</b>	<b>Removal of</b>
<i>Preliminary</i>	Coarse solids and grease that may cause maintenance or operational problems in the treatment operations, processes, and auxiliary systems.
<i>Primary</i>	Settleable suspended solids and associated organic matter.
<i>Secondary</i>	Biodegradable organic matter (in solution or suspension) and nutrients (nitrogen and/or phosphorous) by biological mechanisms, and suspended solids. Disinfection is sometimes included in the definition of conventional secondary treatment.
<i>Tertiary</i>	Nutrients, pathogens (disinfection), non-biodegradable substances, metals, inorganic dissolved solids, and residual suspended solids.

As this doctoral work focuses on a particular biological treatment technology, the MBBR, only the secondary treatment level is further detailed. The reader is advised to search in the available literature for studying other treatment levels (DEZOTTI, 2008, HENZE, VAN LOOSDRECHT, *et al.*, 2008, METCALF & EDDY, TCHOBANOGLOUS, *et al.*, 2014, VAN HAANDEL, VAN DER LUBBE, 2012, VON SPERLING, 2007a).

## 2.2. Secondary Wastewater Treatment

Comprised of biological processes, the secondary treatment acts by removing biodegradable organic and inorganic substrates via metabolization performed by microorganisms, mostly bacteria, inside a controlled reactional volume. This biological stabilization of pollutant substances generally transforms them into more stable products with lower polluting potential. In this process, organic matter is mineralized<sup>1</sup> or converted to inert substances (VON SPERLING, 2007a). At some level, the biological processes mimic the natural depuration of biodegradable compounds that happens in water bodies (BASSIN, DEZOTTI, 2008). By controlling ambient conditions - such as temperature, pH, hydraulics, DO, etc. - to boost microbial activity, it is possible to obtain much higher biological degradation rates than those occurring naturally in the environment. Therefore, secondary treatment takes advantage of this feature. In this context, it is essential to understand the basic aspects of microbial metabolism when discussing secondary treatment technologies.

### 2.2.1. Microbial Metabolism

Metabolism refers to the entirety of the chemical reactions taking place in a living cell or organism. Catabolic reactions (dissimilation) transform energy sources into utilizable energy for cell functions - as locomotion and transport - or for anabolic reactions (assimilation), that uses energy to convert simpler molecules into complex ones for cell growth and maintenance (HENZE, VAN LOOSDRECHT, *et al.*, 2008, VON SPERLING, 2007b). Figure 2.1 summarizes the catabolism and anabolism. The catabolic processes include the transport of electrons from a donor substance to an acceptor one as a driving force for the transformation of adenosine diphosphate (ADP) into adenosine

---

<sup>1</sup> Mineralization of organic compounds refers to their conversion to inorganic substances, mainly CO<sub>2</sub> and H<sub>2</sub>O.

triphosphate (ATP), the most important energy-transfer compound in cells (GRAY, 2004, MARA, HORAN, 2003).

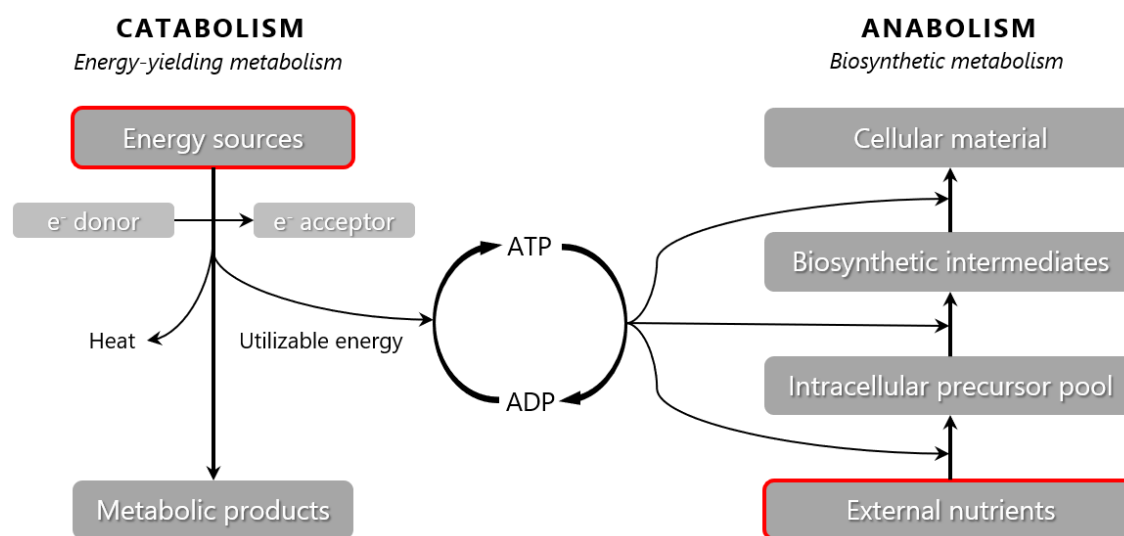


Figure 2.1 – Representation of the metabolism of living organisms, composed of catabolic and anabolic processes. Source: adapted from (HENZE, VAN LOOSDRECHT, *et al.*, 2008).

As highlighted in red frames in Figure 2.1, there are two major inputs from the environment necessary for the organisms to perform their metabolic functions: energy sources and external nutrients. With regards to the latter, in secondary treatment reactors, it is important to consider the chemical composition of the bacterial cells, suggested by some authors as  $C_5H_7NO_2$ , or  $C_{60}H_{87}O_{23}N_{12}P$ , in dry basis (HENZE, VAN LOOSDRECHT, *et al.*, 2008, METCALF & EDDY, TCHOBANOGLOUS, *et al.*, 2014). That represents around 53% of carbon, the major nutritional requirement for anabolism. From the cell composition, the average nutritional needs to convert substrates into cell material, in terms of BOD:N:P proportion, is approximately 100:5:1. Other macroelements used by microorganisms are O, H, N, P and S. In contrast, some elements are needed in smaller quantities (K, Ca, Mg, Na, Cl and Fe), or even trace amounts (Mn, Zn, Co, Mo, Ni, Cu, etc.) (MARA, HORAN, 2003).

Given the considerations above, organisms are grouped according to their carbon source, energy source, and electron donor (METCALF & EDDY, TCHOBANOGLOUS, *et al.*, 2014). In this context, four trophic types of organisms may be described, as represented in Figure 2.2 (MARA, HORAN, 2003).

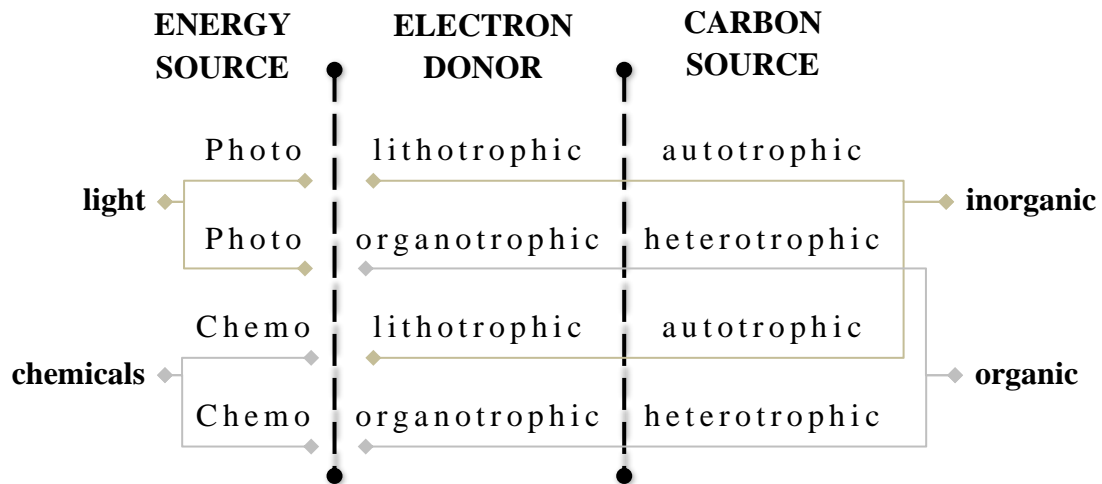


Figure 2.2 – Four trophic types of organisms according to metabolic characteristics.

Additionally, organisms may also be classified with regards to the origin and quality of the electron acceptor. Those who utilize external electron acceptors are said to have a respiratory metabolism, whereas fermentative metabolism is the term employed when internal electron acceptors are used. The respiration may be aerobic, anoxic or anaerobic. That means that the electron acceptor is, respectively, oxygen, nitrate, or other oxidized compounds. Some organisms are facultative and can use more than one type of electron acceptor, depending on the availability (VON SPERLING, 2007b). Denitrifying microorganisms fall within this category, as they may perform aerobic or anoxic heterotrophic metabolism. Several microbial groups are shown in Table 2.3, where the components of their metabolism are detailed.

Table 2.3 – Trophic classification of various microbial groups organisms. Source: (HENZE, VAN LOOSDRECHT, *et al.*, 2008).

Energy source					
<i>Electron donor</i>			Electron acceptor	Typical products	Carbon source
Trophic group	Microbial group	Type of e <sup>-</sup> donor			
Chemo-					-
<i>organotroph</i>	Aerobic heterotrophs	Organic	O <sub>2</sub>	CO <sub>2</sub> , H <sub>2</sub> O	Organic
	Denitrifiers	Organic	NO <sub>3</sub> <sup>-</sup> , NO <sub>2</sub> <sup>-</sup>	N <sub>2</sub> , CO <sub>2</sub> , H <sub>2</sub> O	Organic
	Fermenting organisms	Organic	Organic	VFA	Organic
	Iron reducers	Organic	Fe (III)	Fe (II)	Organic
	Sulphate reducers	Acetate	SO <sub>4</sub> <sup>2-</sup>	H <sub>2</sub> S	Acetate
	Methanogens (acetoclastic)	Acetate	Acetate	CH <sub>4</sub>	Acetate
<i>lithotroph</i>	Nitrifiers: AOB	NH <sub>4</sub> <sup>+</sup>	O <sub>2</sub>	NO <sub>2</sub> <sup>-</sup>	CO <sub>2</sub>
	Nitrifiers: NOB	NO <sub>2</sub> <sup>-</sup>	O <sub>2</sub>	NO <sub>3</sub> <sup>-</sup>	CO <sub>2</sub>
	Anammox bacteria	NH <sub>4</sub> <sup>+</sup>	NO <sub>2</sub> <sup>-</sup>	N <sub>2</sub>	CO <sub>2</sub>
	Denitrifiers	H <sub>2</sub>	NO <sub>3</sub> <sup>-</sup> , NO <sub>2</sub> <sup>-</sup>	N <sub>2</sub> , H <sub>2</sub> O	CO <sub>2</sub>
	Denitrifiers	S	NO <sub>3</sub> <sup>-</sup> , NO <sub>2</sub> <sup>-</sup>	N <sub>2</sub> , SO <sub>4</sub> <sup>2-</sup> , H <sub>2</sub> O	CO <sub>2</sub>
	Iron oxidizers	Fe (II)	O <sub>2</sub>	Fe (III)	CO <sub>2</sub>
	Sulphate reducers	H <sub>2</sub>	SO <sub>4</sub> <sup>2-</sup>	H <sub>2</sub> S, H <sub>2</sub> O	CO <sub>2</sub>
	Sulphate oxidizers	H <sub>2</sub> S, S, S <sub>2</sub> O <sub>3</sub> <sup>2-</sup>	O <sub>2</sub>	SO <sub>4</sub> <sup>2-</sup>	CO <sub>2</sub>
	Aerobic hydrogentrophs	H <sub>2</sub>	O <sub>2</sub>	H <sub>2</sub> O	CO <sub>2</sub>
	Methanogens (hydrogenotrophic)	H <sub>2</sub>	CO <sub>2</sub>	CH <sub>4</sub>	CO <sub>2</sub>
Photo-					-
<i>lithotroph</i>	Algae, plants	H <sub>2</sub> O	CO <sub>2</sub>	O <sub>2</sub>	CO <sub>2</sub>
	Photosynthetic bacteria	H <sub>2</sub> S	CO <sub>2</sub>	S	CO <sub>2</sub>

AOB, ammonia-oxidizing bacteria; Anammox, anaerobic ammonium oxidation; NOB, nitrite-oxidizing bacteria; VFA, volatile fatty acids

Given that the objective of the biological treatment processes is reducing pollutant loads through metabolic action of microorganisms, some of the groups listed in Table 2.3 are of particular relevance. For biological organic matter removal, aerobic, anoxic (denitrifiers) and anaerobic (fermenting) heterotrophic microorganisms are highlighted. In turn, biological nitrogen removal is performed mostly by the sequential actions of aerobic autotrophic nitrifiers and the anoxic heterotrophic denitrifiers, or by the autotrophic anammox process. The sequence of transformations that will take place in a bioreactor depends on the oxidation state of the electron acceptors and the redox potential of the electron transfer reaction, once the correct substrates and operating conditions (temperature, pH, dissolved oxygen, etc.) are ensured, as shown in Figure 2.3. Greater

redox potential forms more ATP, providing more favorable energetic metabolism (GRAY, 2004).

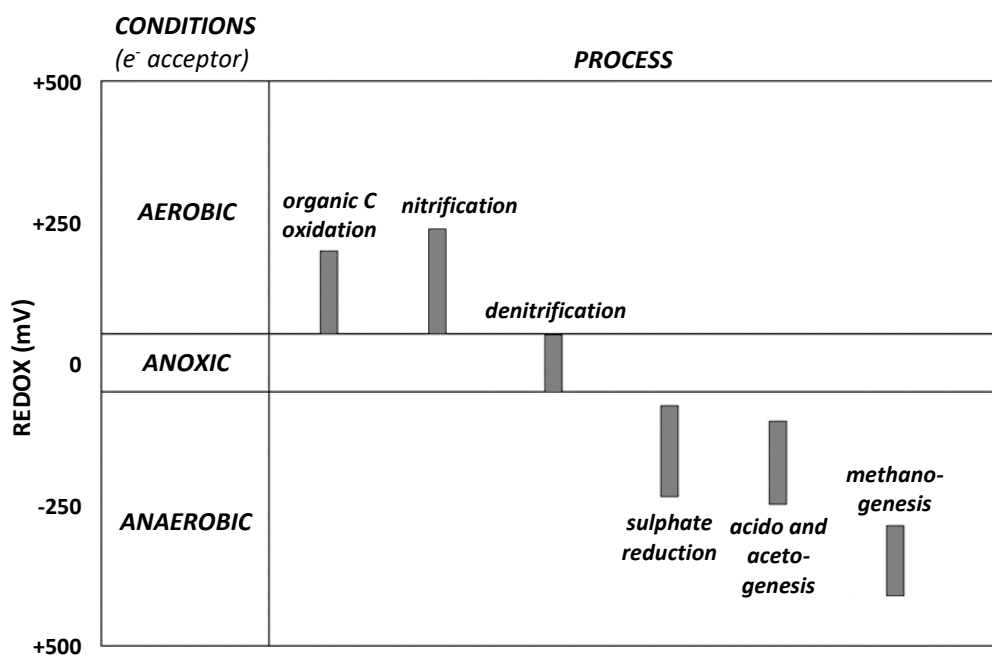


Figure 2.3 – Transformations taking place in biological treatment, as a function of electron acceptor and redox potential. Source: adapted from (VON SPERLING, 2007b).

Biological processes may be classified regarding the metabolic requirements of the microorganisms but also according to other aspects, as the type of biomass growth and hydraulic conditions in the reactor. All of those are presented in the following subsection.

### 2.2.2. Classification of Biological Processes

The main classification of biological processes is regarding the electron acceptor in the metabolic route of the microorganisms, as presented in section 2.2.1. As seen in Table 2.4, the processes may be aerobic, anoxic, anaerobic, facultative or a combination.

Table 2.4 – Classification of biological processes with respect to the electron acceptor used in the metabolism of the microorganisms. Source: adapted from (METCALF & EDDY, TCHOBANOGLOUS, *et al.*, 2003).

<i>Class</i>	<b>Description</b>
<i>Aerobic</i>	Biological processes that happen in the presence of oxygen.
<i>Anaerobic</i>	Biological processes that happen in the absence of oxygen.
<i>Anoxic</i>	Process in which the nitrogen contained in nitrate is biologically converted to nitrogen gas in the absence of oxygen.
<i>Facultative</i>	Biological processes in which microorganisms might act in the presence or absence of oxygen.
<i>Combined</i>	Combinations of aerobic, anoxic or anaerobic processes.

Following, Figure 2.4 illustrates the categorization of biological treatment processes regarding the type of biomass growth, i.e. in suspension (whether dispersed or flocculated), adhered to surfaces (biofilms), or a combination. The examples of processes listed within Figure 2.4 are given based on the type of biomass growth on which the treatment is based. Nevertheless, there may always be suspended growth in biofilm reactors and the other way around (BASSIN, DEZOTTI, 2008). The bulk of flocculated biomass is usually denoted as biological sludge, or simply sludge. Activated sludge is the designation of the most common configuration of suspended growth reactor, where the biomass is kept in suspension in an aeration basin followed by a secondary decanter that concentrates and recirculates part of the sludge to achieve the desired biomass concentration in the bioreactor.

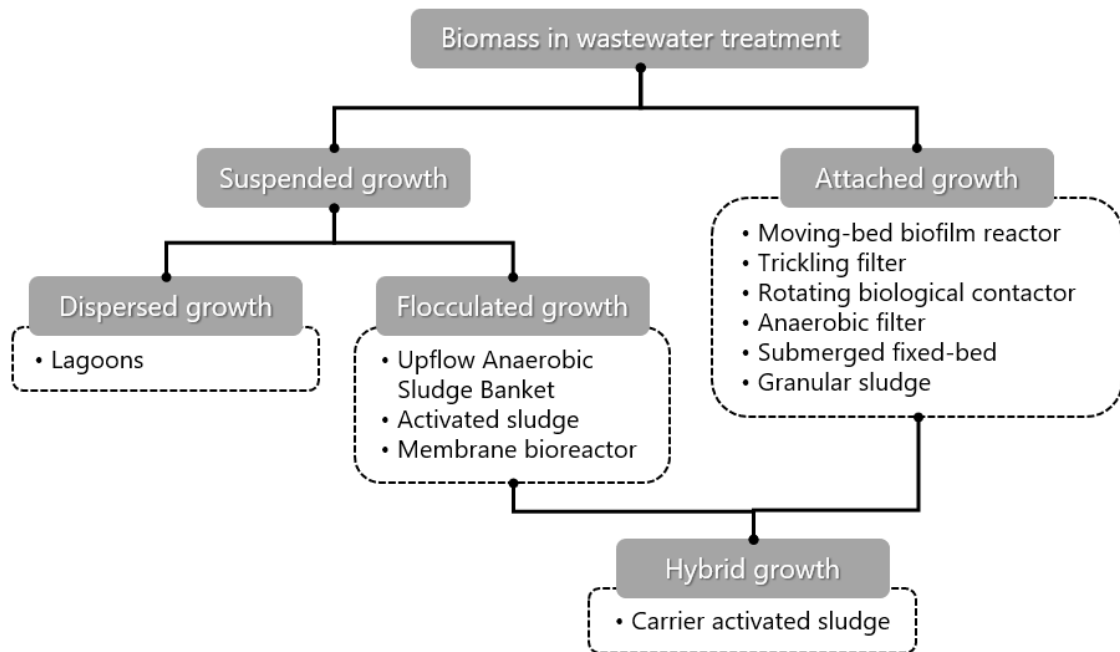


Figure 2.4 – Classification of secondary wastewater treatment processes with respect to the type of biomass growth and examples of technologies. Source: adapted from (MARA, HORAN, 2003).

Hydraulic conditions also serve as a categorization parameter for biological processes: intermittent (batch or semi-batch) or continuous flow; completely mixed or plug flow. This kind of classification is tightly related to the availability of substrates to the biomass in different times and positions in the reactor, therefore posing direct influence on the development of the microbial community and modelling of mass balances and reactions rates (VON SPERLING, 2007b).

Another way of classifying the secondary treatment processes is related to its function, that is, the removal of carbonaceous organic matter and/or nutrients, which is closely associated with the microbial groups that will be favored in the controlled reactional environment. This classification is detailed in Table 2.5 (METCALF & EDDY, TCHOBANOGLOUS, *et al.*, 2003).

Table 2.5 – Classification of biological processes in relation to their functionality.

Source: adapted from (METCALF & EDDY, TCHOBANOGLOUS, *et al.*, 2003).

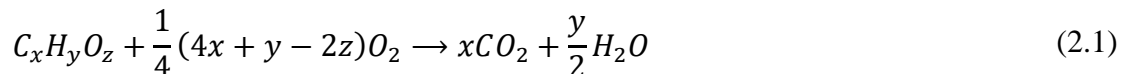
<i>Classification</i>	<i>Description</i>
<i>Carbonaceous BOD removal</i>	Biological conversion of organic matter to cell material and various gases and products.
<i>Nutrient removal</i>	Simultaneous removal of nitrogen and phosphorous.
<i>Nitrification</i>	Sequential conversion of ammonia to nitrite and then nitrate.
<i>Denitrification</i>	Reduction of nitrate/nitrite to dinitrogen and other gases.
<i>Phosphorous removal</i>	Removal of phosphorous by its accumulation in biomass and subsequent solids separation.
<i>Sludge stabilization (digestion)</i>	Aerobic or anaerobic stabilization of the organic matter in primary and secondary sludges.

Vast differences exist between the biological wastewater treatment processes based on each of the aforementioned categories. The distinctions may range from cost, operational, maintenance and performance attributes. Thus, the remaining topics from section 2.2 focus on briefly approaching fundamental points of bioreactors.

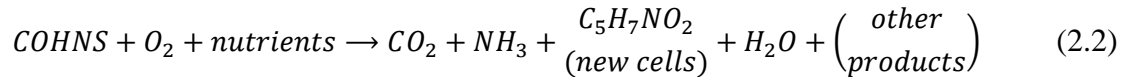
As the bench-scale experiments presented in this doctoral thesis focused on the aerobic removal of carbonaceous organic matter and nitrification, these are discussed in detail in the following sections (2.2.3 and 2.2.4).

### 2.2.3. Aerobic Biological Organic Matter Removal

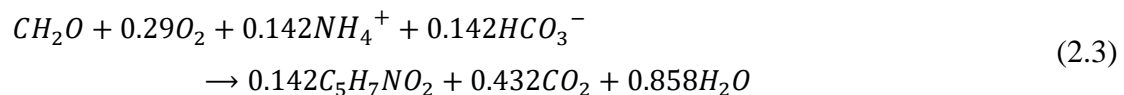
In the aerobic oxidation of organic matter, the biodegradable organic substances present in the wastewater serves as electron donor and carbon source, whereas oxygen is the electron acceptor. Chemo-organotrophic heterotrophic bacteria are responsible for the majority of the organic substrates metabolization, requiring sufficient contact time with the organic compounds, oxygen and nutrients (METCALF & EDDY, TCHOBANOGLOUS, *et al.*, 2014). Considering the complete metabolization of organic matter by aerobic microorganisms, a simplified global reaction can be expressed as Equation (2.1) (VON SPERLING, 2007b).



The given equation allows the calculation of the demand of oxygen for complete oxidation of a generic substrate. Nevertheless, it does not include the assimilation of carbon and nutrients for the production of new cells. A more general, yet unbalanced reaction, is given in Equation (2.2), where COHNS denotes non-specific organic matter as carbon source/electron donor (METCALF & EDDY, TCHOBANOGLOUS, *et al.*, 2014).

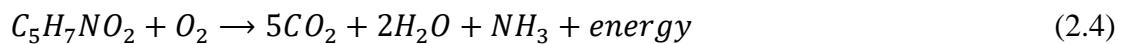


Balanced reactions will depend heavily on the composition of the carbon source, the nature of the nutrients sources and the chosen cell average formula. In the example above, phosphorous is not included in the cell composition, therefore a complete reaction could be written without a P source. Then, a stoichiometrically balanced equation for a certain substrate may be derived from the sum of specific half-reactions, considering the percentage of the substrate that is converted to energy ( $f_e$ ) and directed to cellular synthesis ( $f_s$ ). Various half-reactions and the full explanation of the calculation procedure are found throughout textbooks (GRADY, DAIGGER, *et al.*, 2011, HENZE, VAN LOOSDRECHT, *et al.*, 2008, METCALF & EDDY, TCHOBANOGLOUS, *et al.*, 2014, RITTMANN, MCCARTY, 2001, WIESMANN, CHOI, *et al.*, 2007). Equation (2.3) shows one example of a carbohydrates oxidation reaction with  $f_s$  equal to 0.71 mg of formed biomass COD per mg of carbohydrate COD oxidized, and ammoniacal nitrogen as N source (which most heterotrophic bacteria may use as sole N supply, preferable over other inorganic forms) (GRADY, DAIGGER, *et al.*, 2011, GRAY, 2004).



In this case, the fraction of the substrate conversion to biomass is equivalent to the cell yield. Typically for heterotrophic bacteria, the yield is around 0.7 mg COD biomass/mg COD removed, which may also be represented as mgVSS biomass/mg COD removed by multiplying by the adequate conversion according to the average cell formula (1.42 to 1.67 mg COD biomass/mg VSS biomass) (HENZE, VAN LOOSDRECHT, *et al.*, 2008).

Decaying cellular material resultant from cell death and lysis is also a common substrate for aerobic heterotrophic metabolism. This is known as endogenous respiration, as opposed to exogenous respiration, which uses external substrates coming in the wastewater. A simplified representation of the endogenous respiration is shown in Equation (2.4). Endogenous metabolism is a greater part of the overall metabolism at longer sludge ages and lower availabilities of external substrates (METCALF & EDDY, TCHOBANOGLOUS, *et al.*, 2014).



The pH span considered tolerable for the aerobic removal of organic matter is 6.0 to 9.0, but the best performance occurs nearer neutrality, between 6.5 and 8.5. Regarding dissolved oxygen, above 0.5 mg/L there is little influence on the biodegradation rate. Nevertheless, 2.0 mg/L is usual for aerobic reactors aiming at organic matter removal, as this concentration allows for maximum oxygen uptake for normal-sized biomass flocs. In terms of temperature, higher values up to 35-40°C increase the removal rate (GRAY, 2004, METCALF & EDDY, TCHOBANOGLOUS, *et al.*, 2014).

Sufficient concentration of nutrients (N and P) should also be guaranteed, particularly for industrial wastewater sources that lack it. When compared to other microbial groups, the aerobic heterotrophic bacteria have a higher resistance to toxicity (METCALF & EDDY, TCHOBANOGLOUS, *et al.*, 2014). However, various substances – as heavy metals; phenol, detergents, and other organics; high salt concentrations; high ammonia; etc. – may inhibit the activity of these microorganisms. Heterotrophic microorganisms are not affected by light, being able to grow whether in its presence or in the dark (GRAY, 2004).

#### **2.2.4. Biological Nitrogen Removal**

Despite this nutrient being mainly found as ammoniacal and organic nitrogen – soluble or particulate -, other forms of nitrogen are also observed in waste streams, as nitrite and nitrate. Mostly, the ammoniacal nitrogen is presented as ammonium when the pH is close to 7 and the temperature between 25 and 35°C. The percentage of free ammonia as a function of pH and temperature may be calculated, as described in appendix B, section B.6. Amongst other factors, the relevance of the ammoniacal nitrogen

distribution is due to the free ammonia volatility and its toxicity to fish and other aquatic organisms even at low concentrations.

Regarding nitrogen removal, there are physicochemical technologies options, however biological removal is usually more feasible and achieves better performances (AHN, 2006, ZHU, PENG, *et al.*, 2007). The biological nitrogen removal takes place in a controlled environment that favors natural steps of the biological nitrogen cycle, shown in summary in Figure 2.5.

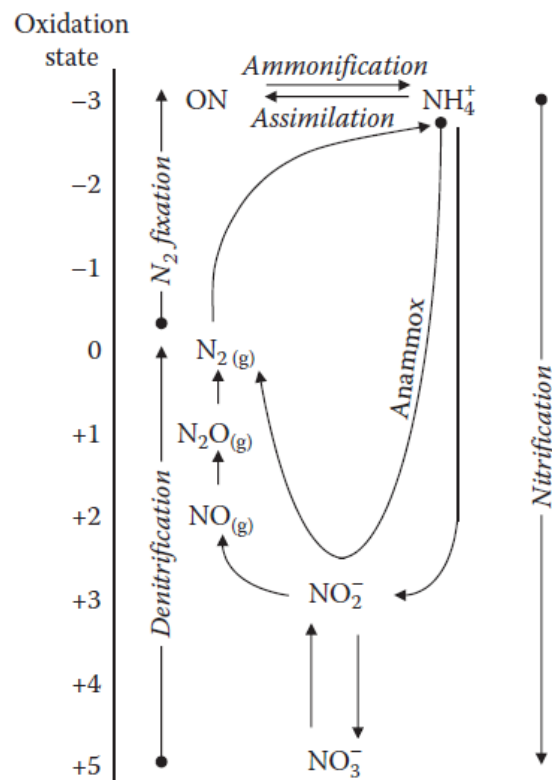
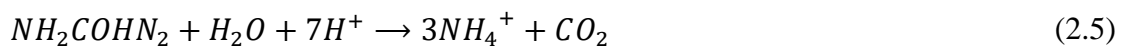


Figure 2.5 – Reactions within the biological nitrogen cycle. ON states for organic nitrogen. Source: (GRADY, DAIGGER, *et al.*, 2011).

Particulate organic nitrogen may be hydrolyzed to soluble organic nitrogen. Then, the latter goes through the transformation known as ammonification, being converted to ammoniacal nitrogen by heterotrophic bacteria. Equation (2.5) exemplifies this by the hydrolysis of urea.

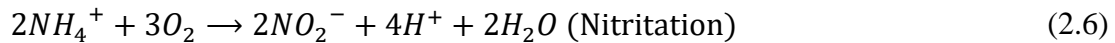


The most consolidated strategy for biological nitrogen removal includes the combination of nitrification and denitrification (SUN, NÀCHER, *et al.*, 2010). Nitrification is the limiting stage and also the most studied one (BASSIN, DEZOTTI, 2008).

Another relevant biological route for nitrogen removal is the anaerobic ammonium oxidation (anammox), which may result in more cost-effective nitrogen removal technologies (SUN, NÀCHER, *et al.*, 2010). As only nitrification was addressed during the experimental evaluations of this doctoral work, it is further explained below, whereas other processes from the nitrogen cycle may be better understood in the literature (BOTHE, FERGUSON, *et al.*, 2007).

#### 2.2.4.1. Nitrification

Nitrification is the energetically favorable biological stepwise conversion of ammoniacal nitrogen to nitrite and then to nitrate. Respectively, the steps are known as nitritation and nitrataion – both exergonic – and are shown simplified in Equations (2.6) and (2.7). The global reaction is represented in Equation (2.8), not considering the assimilation of nitrogen in cell material.



Based on Equation (2.8), complete nitrification requires 4.57 gO<sub>2</sub>/gNH<sub>4</sub><sup>+</sup>-N, where 3.43 gO<sub>2</sub>/gNH<sub>4</sub><sup>+</sup>-N is for oxidizing ammonium to nitrite and 1.14 gO<sub>2</sub>/gNO<sub>2</sub><sup>-</sup>-N is for oxidizing nitrite to nitrate. It is also possible to estimate the consumption of alkalinity by adding 2 mol of bicarbonate in Equation (2.8), resulting in equivalent 7.14 gCaCO<sub>3</sub>/gNH<sub>4</sub><sup>+</sup>-N. The alkalinity and oxygen are slightly lower when anabolism is considered, as will be seen ahead (METCALF & EDDY, TCHOBANOGLOUS, *et al.*, 2003).

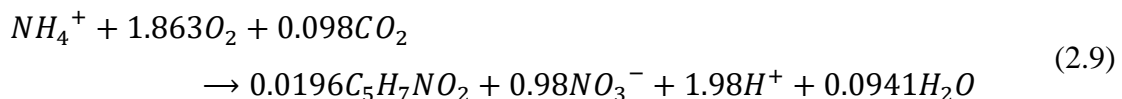
The reactions are promoted by aerobic chemo-lithoautotrophic - or simply autotrophic - bacteria, using inorganic compounds (ammonium and nitrite) as source of

energy; inorganic carbon source (CO<sub>2</sub>) for synthesizing cells; and oxygen as electron acceptor (GRAY, 2004).

Ammonia-oxidizing bacteria (AOB) is the group of bacteria responsible for the nitrification stage, it is constituted mainly by the *Nitrosomonas* genus, in addition to the genera *Nitrosococcus*, *Nitrosospira*, *Nitrosolobus*, *Nitrosovibrio*, etc. Nitrification also has an intermediary step where ammonia is transformed into hydroxylamine (NH<sub>2</sub>OH) that is then converted to nitrite (AHN, 2006, COLLIVER, STEPHENSON, 2000, METCALF & EDDY, TCHOBANOGLOUS, *et al.*, 2003).

Nitrification is performed by the group of bacteria known as nitrite-oxidizing bacteria (NOB), composed mainly of the genus *Nitrospira* and *Nitrobacter*, in addition to others such as *Nitrococcus*, *Nitrospina*, etc. (AHN, 2006, METCALF & EDDY, TCHOBANOGLOUS, *et al.*, 2014). Recently, it was found that members of the *Nitrospira* genus are capable of performing complete nitrification, the so-called comammox *Nitrospira* (DAIMS, LEBEDEVA, *et al.*, 2015).

Ammoniacal nitrogen and nitrite are used primarily in the catabolism of autotrophic nitrifying microorganisms as source of energy, being negligible the fraction of nitrogen assimilated as cellular material (anabolism), only around 1% of the ammonia converted (HENZE, VAN LOOSDRECHT, *et al.*, 2008). The balanced equations representing the nitrification while considering the anabolism depend on the percentage of nitrogen in the substrate that is converted to energy ( $f_e$ ) and the remainder that is directed to cellular synthesis ( $f_s$ ). Therefore, it is common to find distinct stoichiometry in different references. Some demonstrate how to get to the balanced equations (METCALF & EDDY, TCHOBANOGLOUS, *et al.*, 2003, RITTMANN, MCCARTY, 2001, WIESMANN, CHOI, *et al.*, 2007). One example is given in Equation (2.9), considering  $f_s = 0.05$  and the simplified cell composition  $C_5H_7NO_2$  (METCALF & EDDY, TCHOBANOGLOUS, *et al.*, 2003).



From Equation (2.9), it is implied that the autotrophic cell yield is 0.16 gVSS/gNH<sub>4</sub><sup>+</sup>-N. Most of it is related to the growth of AOB (0.14 gVSS/gNH<sub>4</sub><sup>+</sup>-N), and the remaining is due to NOB (0.02 gVSS/gNO<sub>2</sub><sup>-</sup>-N) (GRADY, DAIGGER, *et al.*, 2011). When compared to heterotrophic organisms, the yield values are considered low,

and so are the growth rates, so that nitrifiers are regarded as slow-growing microorganisms (WIESMANN, CHOI, *et al.*, 2007). The specific growth rate of AOB is higher than NOB, with this relation shifting at lower temperatures (GRADY, DAIGGER, *et al.*, 2011, MULDER, 2014). Furthermore, the consumed oxygen per mass unit of substrate oxidized is  $4.25 \text{ gO}_2/\text{gNH}_4^+\text{-N}$ , a bit inferior to the value previously shown without pondering nitrogen assimilation to cellular material. The alkalinity consumption in terms of calcium carbonate, calculated from Equation (2.9), is also lower, corresponding to  $7.07 \text{ gCaCO}_3/\text{gNH}_4^+\text{-N}$  (METCALF & EDDY, TCHOBANOGLOUS, *et al.*, 2003).

Given the slow growth and cell yield of nitrifiers, keeping sufficient sludge age and favorable conditions is critical to assure nitrification in the system. Some parameters especially important to track, that relate to the nitrifying performance, include the organic carbon to nitrogen ratio (C/N); alkalinity; temperature; and the presence of toxic or inhibiting compounds. As the cell yield is low, carbon dioxide present in the air suffices as carbon source. The carbon dioxide produced by heterotrophic microorganisms inhabiting the same environment may also serve as inorganic carbon source. Phosphorous is seldom the limiting nutrient in nitrification. Some micronutrients stimulate the spread of nitrifying bacteria in the following concentrations (in mg/L): Ca = 0.50; Cu = 0.01; Mg = 0.03; Mo = 0.001; Ni = 0.10; and Zn = 1.0 (METCALF & EDDY, TCHOBANOGLOUS, *et al.*, 2014).

Different authors agree that optimal nitrification takes place in the pH range from 7.0 to 8.5. Out of this span, the nitrifiers growth rate drops rapidly, with complete inhibition when pH is lower than 5. Many wastewaters have pH between 7 and 8, but the nitrification and the  $\text{CO}_2$  production by heterotrophic microorganisms make the pH in the bioreactor lower compared to the raw wastewater. Thus, unless the wastewater alkalinity is high enough, the pH in the reactor will most likely be below 8. The main concern is to keep the pH higher than 7 by, for instance, keeping the reactor's alkalinity above  $35 \text{ mgCaCO}_3/\text{L}$  (GRAY, 2004, VAN HAANDEL, VAN DER LUBBE, 2012). This may be done through addition of sodium bicarbonate, sodium hydroxide, magnesium hydroxide, calcium oxide, etc. (METCALF & EDDY, TCHOBANOGLOUS, *et al.*, 2003).

Dissolved oxygen content up to 3 or 4 mg/L contributes positively to the nitrification rate, being values above 2.0 mg/L highly recommended. Concentrations below 0.5 mg/L strongly inhibit the nitrification and may lead to partial nitrification,

resulting in high effluent nitrite concentration (GRAY, 2004, METCALF & EDDY, TCHOBANOGLOUS, *et al.*, 2003).

The optimum temperature for nitrification is between 30 to 35°C (GRAY, 2004, METCALF & EDDY, TCHOBANOGLOUS, *et al.*, 2003), but it may occur in lower temperatures. It is emphasized that high temperatures, above 45°C, disfavor the nitrification rate by lowering the microbial activity (MAYER, SMEETS, *et al.*, 2009, SHORE, M'COY, *et al.*, 2012).

Biodegradable organic matter may heavily and rapidly inhibit nitrification due to favoring the activity of heterotrophs. Their much faster growth rate makes them outcompete the nitrifiers for dissolved oxygen and nutrients. Thus, nitrification is associated with low organic loading conditions. Similarly, light can be a driving force for competition with photoautotrophs, resulting in a decrease in nitrification extent (GRAY, 2004).

### **2.2.5. Forms of Microbial Growth in Biological Treatment**

As shown before in Figure 2.4, most of the bioreactor technologies rely on the development of the microbial community whether in suspended agglomerates (flocs) or attached to support surfaces (biofilms). Suspended microbial agglomerates present density slightly higher than that of the water and are predominantly composed of bacteria surrounded by an organic matrix of EPS excreted by them, mostly proteins and polysaccharides. Besides functioning like a glue holding microorganisms and providing adhesion to surfaces, the EPS also confer mechanical protection to the microbes. Agglomeration facilitated by the EPS favors the increase of the floc to its full size (50 to 500  $\mu\text{m}$  on average, (VON SPERLING, 2007b)), contributing to sedimentation downstream of the bioreactor. Nevertheless, the microbial structure of the biomass may bring difficulties to the settling, for instance when there is a substantial presence of filamentous bacteria. Figure 2.6 depicts the structure of a microbial floc and its main components (BASSIN, DEZOTTI, 2008).

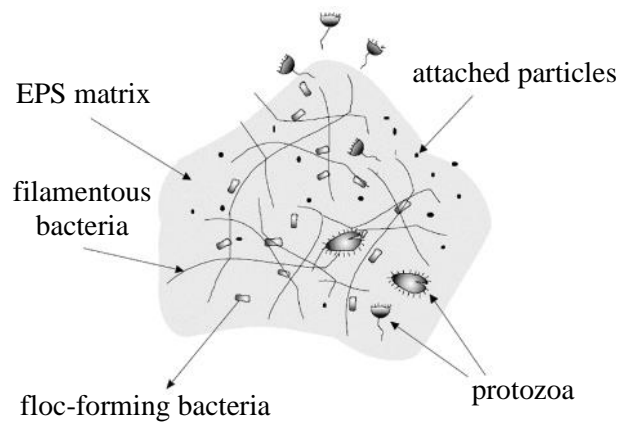


Figure 2.6 – Basic structure of a microbial floc. Source: adapted from (HORAN, 1990 apud VON SPERLING, 2007b).

The bulk of microbial flocs formed in the bioreactor - the sludge - has its characteristics given by the amount of filamentous microbes and by the average size of the flocs. When filaments are too scarce, the flocs have less structural resistance and are smaller, compromising the settleability of the sludge. On the other hand, excess of filaments may cause sludge bulking, leading to the formation of aggregates of flocs with the tendency to float instead of settling (BASSIN, DEZOTTI, 2008). Both scenarios regarding the presence of filaments are shown in Figure 2.7.

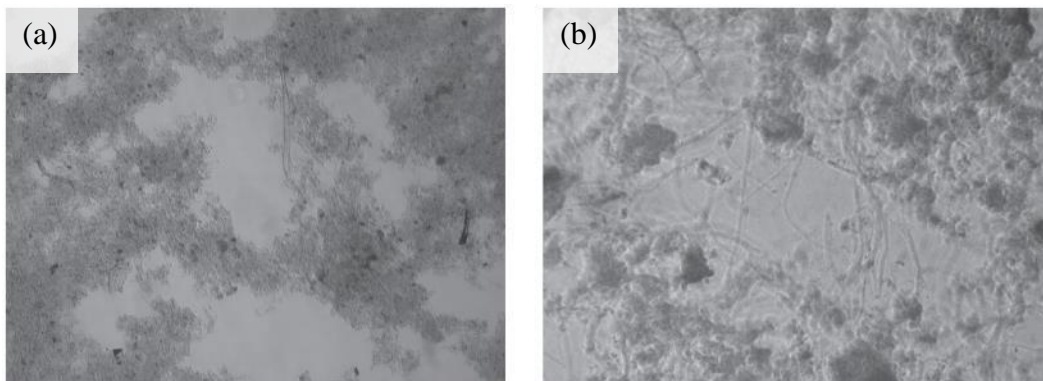


Figure 2.7 – Microbial flocs with scarcity (a) and abundance (b) of filaments. Source: (BASSIN, DEZOTTI, 2008).

Biofilms' formation mechanism starts with the adsorption of macromolecules onto the support surface, followed by the attachment of dispersed bacteria. Despite existing little evidence that EPS is responsible for the initial adhesion of microbes, once bacteria start colonizing the surface, they produce these exopolymers that serve as the

matrix for the biofilm growth. The stages of biofilm formation are displayed in Figure 2.8 (LEWANDOWSKI, BOLTZ, 2011).

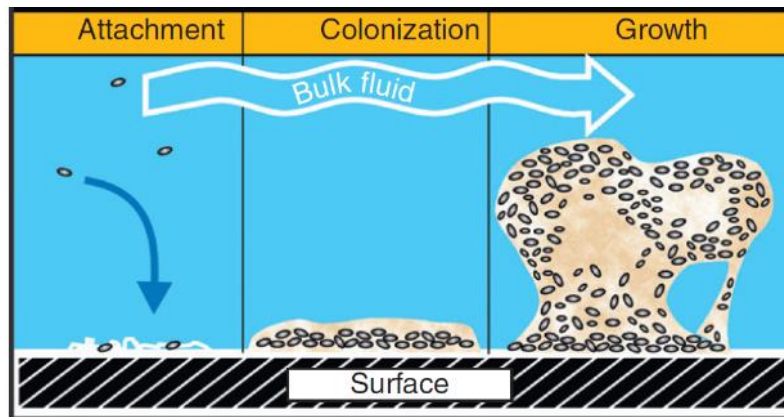


Figure 2.8 – Stages of biofilm formation. Source: (LEWANDOWSKI, BOLTZ, 2011).

When the EPS and microorganisms matrix is formed, it can propagate over the support surface and to the suspended phase via several mechanisms, as illustrated in Figure 2.9 (LEWANDOWSKI, BOLTZ, 2011).

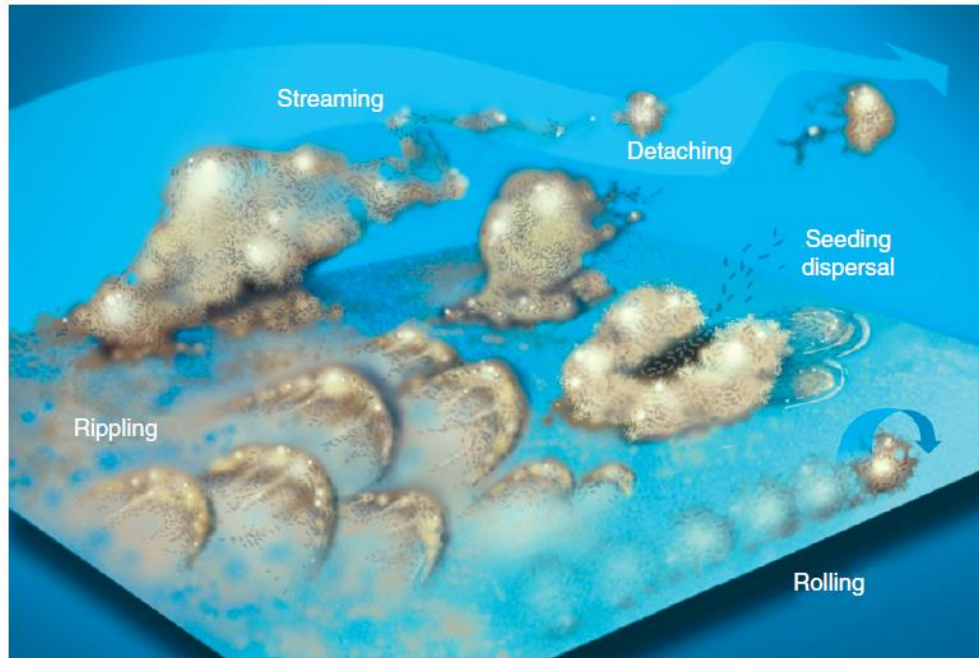


Figure 2.9 – Propagation of biofilm and its mechanisms. Source: (LEWANDOWSKI, BOLTZ, 2011).

Systems with attached biomass growth offer advantages in relation to suspended growth. As the biomass is immobilized inside the reactional volume, biofilms dissociate the sludge age (or sludge retention time, SRT) from the hydraulic retention time, making the performance of the system less dependent on sludge settleability. This dissociation allows SRT to be equivalent or higher than that of an activated sludge at lower HRTs, resulting in more compact bioreactors. Thus, the SRT is the main parameter differentiating the suspended and fixed growth (MARA, HORAN, 2003).

Also, by trapping the biomass in the reactor, the total biomass concentration inside biofilm processes may be comparable or higher than in activated sludge reactors with considerably lower volume (and, thus, HRT). Nevertheless, the effluent solids content is potentially lesser, as the biomass is retained inside the reactor and the possibly higher sludge age results in lower biomass yields (due to endogenous activity). Thereby, secondary solids separation units may be downsized or dismissed, also outcoming in smaller footprints (VAN HAANDEL, VAN DER LUBBE, 2012).

Additionally, the high SRT allows the development of slow-growing organisms that makes the treatment more efficient, as they may be able to oxidize otherwise persistent substances (ØDEGAARD, 2006). This specialization of the biomass, and the protection conferred by the biofilm, makes the immobilized biomass reactors more resistant to load, pH, flow rate, toxicity and temperature shocks than suspended growth bioreactors (VAN HAANDEL, VAN DER LUBBE, 2012).

The biomass specialization and biodiversity can be higher in biofilms not only because of the potential greater SRT, but because of the biofilm structure itself (MARA, HORAN, 2003, VON SPERLING, 2007b). Due to the diffusional control of the mass transfer of substances from the bulk into the biofilm, metabolic substrates and products (more on that in section 2.2.1, above) form concentration gradients providing various subsistence conditions in distinct depths of the biofilm. For instance, as the oxygen concentration decays while it diffuses deeper into the biofilm, the environment fades from aerobic to anoxic (if nitrate is present) and then anaerobic (METCALF & EDDY, TCHOBANOGLOUS, *et al.*, 2014). A typical representation of the biofilm structure and diffusion of substrates and products in and out of it is shown in Figure 2.10.

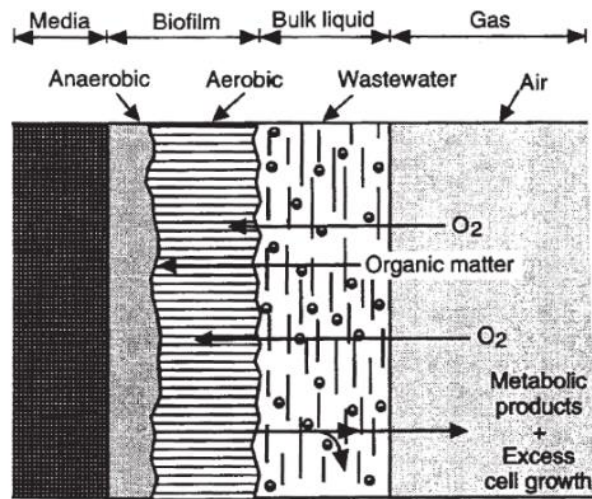


Figure 2.10 – Schematic view of biofilm structure and diffusion of substrates and products in and out of the microbial film. Source: (MARA, HORAN, 2003).

Depending on the hydraulic conditions, support type and substrates concentrations, the biofilm may be as thin as 100  $\mu\text{m}$  and as thick as 10 mm. This makes diffusion limitation a particularly important factor to be considered in attached biomass reactors. Also, the decreasing gradients of substrates through the biofilm depth makes the substrate utilization rate a function of the perpendicular distance to the support surface (MARA, HORAN, 2003, METCALF & EDDY, TCHOBANOGLOUS, *et al.*, 2014). This characteristic may lead to the existence of inactive layers, in relation to exogenous substrates, in the biofilm. The effect of the biofilm thickness on the substrates concentration gradient is portrayed in Figure 2.11. Something to notice is that diffusion may be a significant component of mass transfer towards the center of biomass flocs as well, with the formation of anoxic/anaerobic zones. However, to regular sized flocs (50 to 500  $\mu\text{m}$  (VON SPERLING, 2007b)) diffusion seldom represents a restrictive component to removal rates.

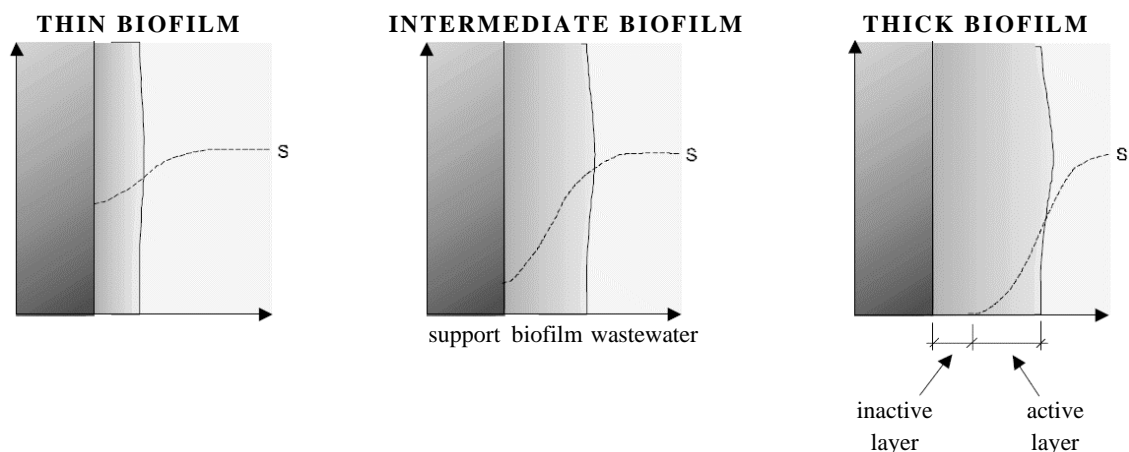


Figure 2.11 – Representation of the effect of the biofilm thickness on the substrate concentration ( $S$ ) gradient towards the support medium. Source: adapted from (VON SPERLING, 2007b).

### 2.2.6. Microorganisms and Ecology in Biological Wastewater Treatment

Unlike pure bacteria culture in labs, in natural environments and biological treatment systems the competition for survival between various species is intense. Both attached and suspended biomass systems have the microbial community dynamics dependent on the environmental and nutritional conditions of the matrix where the flocs or biofilm are found (BASSIN, DEZOTTI, 2008). Many microorganisms other than bacteria compose the microbiota. Generally, bacteria and protozoa are the main groups of microorganisms found in the biomass, whereas fungi and micrometazoa (micro-animals) may appear with less, yet considerable, significance (VON SPERLING, 2007b).

Two great groups may be addressed when classifying microorganisms present in aerobic reactors. The decomposers group comprises approximately 95% of the microbial community and contains mainly heterotrophic bacteria, fungi and osmotrophic<sup>2</sup> protozoa. They are responsible for metabolizing the substrates contained in the wastewater. The consumers group feed on bacteria and protozoa, posing great importance in keeping the

<sup>2</sup> The uptake of dissolved nutrients occurs by osmosis through the cell membrane.

ecological balance in the system. The microorganisms included in this group are phagotrophic<sup>3</sup> protozoa and micrometazoa (BASSIN, DEZOTTI, 2008).

Once an aerated activated sludge reactor is started, the natural development of the microbial community that composes the biomass is shown in Figure 2.12. It starts with the emergence of protozoa amoebae and bacteria. Initially, the food availability is high (high load), and after the bacterial population is well established, flagellated protozoa start taking amoebae's place. In a short span of time, bacteria diversity and abundance increase, then the organic load starts to fall. Free-swimming ciliates arise as they acquire food faster than amoebae and flagellates, making the number of ciliates increase proportionally to the rise in the number of bacteria. The mucoproteins and polysaccharides secreted by the free ciliates contribute to floc formation. After the flocs are stabilized, the organic matter further decreases and the oxygen raises, floc-predators ciliates emerge and predominate the protozoa group. As the sludge matures, micrometazoa and stalked ciliates begin to appear and multiply, feeding on the particulate material, including diverse bacteria and protozoa (BASSIN, DEZOTTI, 2008, VON SPERLING, 2007b).

---

<sup>3</sup> Nutrition by the engulfment of larger food particles by into the cell membrane.

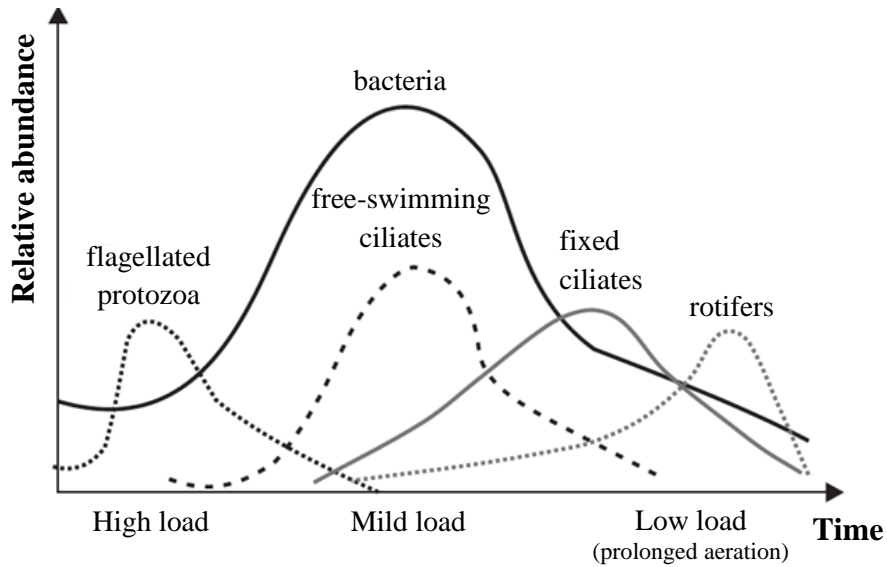


Figure 2.12 – Relative abundance over time of microbial groups in aerobic sewage treatment. Source: (BASSIN, DEZOTTI, 2008, CANLER, PERRET, *et al.*, 2011).

In a biofilm-based process, the succession of predominant groups of microorganisms over time is more likely to follow the behavior shown in Figure 2.13.

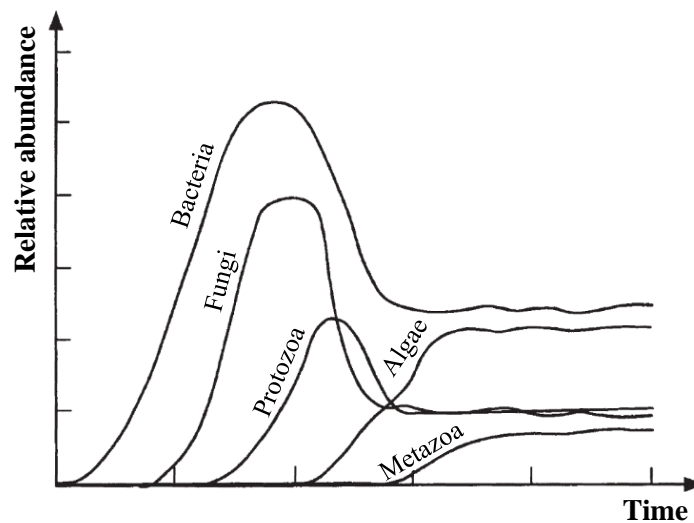


Figure 2.13 – Succession over time of relative abundance of microbial groups in a biofilm. Source: adapted from (IWAI & KITAO, 1994 apud MARA, HORAN, 2003).

Bacteria are prokaryotic and unicellular beings measuring around 1 to 2  $\mu\text{m}$ , with rapid movement and high capacity to adapt in diverse pH, temperature, salinity and pressure conditions. They take the major relevance in the degradation of organic matter and nutrients (MARA, HORAN, 2003, p. 57). Amidst other roles performed by bacteria,

they are responsible for the oxidation of carbonaceous organic matter; nitrification; floc formation, closely related to the settleability of the sludge and effluent clarification; and, in some cases, enhanced removal (accumulation) of phosphorous. Considering the metabolic characteristics, bacteria can be classified into groups related to their action in wastewater treatment systems, as seen before in Table 2.3. Some example genera are introduced in Table 2.6, along with their morphological growth type (BASSIN, DEZOTTI, 2008).

Table 2.6 – Example of bacterial genera found in biological reactors with respect to their metabolic function and their morphologic growth type. Source: adapted from (BENTO, HOFFMANN, 2007).

Class	- Carbon source - Energy source - Electron acceptor	Grow as	Genera examples
<i>Aerobic heterotrophic</i>	- Organic - Aerobic oxidation - Oxygen	Floc-forming, filamentous	- <i>Bacillus</i> - <i>Pseudomonas</i> - <i>Micrococcus</i> - <i>Alcaligenes</i> - <i>Flavobacterium</i> - <i>Zooglea ramigera</i>
<i>Fermentative</i>	- Organic - Fermentation - Organic carbon	Floc-forming	- <i>Aeromonas</i> - <i>Pasteurella</i> - <i>Alcaligenes</i>
<i>Denitrifiers (anoxic heterotrophic)</i>	- Organic - Reduction - Nitrate	Floc-forming, filamentous	- <i>Achromobacter</i> - <i>Alcaligenes</i> - <i>Arthrobacter</i> - <i>Bacillus</i> - <i>Flavobacterium</i> - <i>Pseudomonas</i> - <i>Moraxella</i>
<i>Nitrifiers</i>	- Inorganic - Ammonium aerobic oxidation - Oxygen	Aggregate (colonies)	- <i>Nitrosomonas</i> - <i>Nitrobacter</i>
<i>Phosphate accumulating organisms (PAO)</i>	- Organic - Poliphosphates and organic stored products - Oxygen or nitrate	Aggregate (colonies), filamentous	- <i>Acinetobacter</i> - <i>Pseudomonas</i> - <i>Moraxella</i>
<i>Sulfur oxidizers</i>	- Inorganic - Aerobic oxidation - Oxygen	Floc-forming, filamentous	- <i>Beggiatoa</i> - <i>Thiothrix</i> - <i>Thiobacillus</i>
<i>Sulphate reducers</i>	- Organic - Reduction - Sulphate	Floc-forming	- <i>Desulfovibrio</i> - <i>Desulfobacter</i>

In the microbial community, protozoa and micrometazoa - both composing the microfauna - are frequently found. High bacterial growth, oxygen and organic matter concentrations provide the ideal habitat for many protozoa species. Table 2.7 shows the

main classification of the groups of organisms commonly found in the microfauna in activated sludge systems.

Table 2.7 – Groups of organisms composing the microfauna in activated sludges systems. Source: adapted from (BASSIN, DEZOTTI, 2008).

Group	Classification	Description
<i>Ciliates</i> (protozoa)	Floc predators	<i>Possess dorsoventrally flattened cell and modified cilia grouped in the part that is in contact with the substrate. They are voracious bacteria predators.</i>
	Free swimming	<i>Possess cilia regularly distributed over the whole cell and swim freely between the flocs. They are carnivores and predators.</i>
	Fixed	<i>Fixed to the polymeric matrix with a peduncle. Some species form colonies. The cilia are located in the anterior region of the cell, next to the oral cavity.</i>
<i>Amoebae</i> (protozoa and others)	Testate	<i>Possess external shell made of proteins, silica, limestone, iron, amongst others.</i>
	Naked	<i>Soft body and undefined shape.</i>
<i>Flagellates</i> (protozoa and others)	Zooflagellates (protozoa)	<i>Non-pigmented flagellates presenting one or more flagella. Feed on solid matter or dissolved organic and inorganic substances.</i>
<i>Micrometazoa</i>	- Rotifers - Nematodes - Annelids - Tardigrades	<i>Pluricellular organisms from various phyla. Have low growth velocity and most are predators of bacteria and protozoa.</i>

Table 2.8 shows some of the most frequent genera observed in the microfauna of bioreactors.

Table 2.8 – Most frequent genera found in activated sludges for various organisms groups of the microfauna. Source: adapted from (BASSIN, DEZOTTI, 2008).

Phylum	Group	Common genera
Ciliophora	Free-swimming ciliates	<i>Paramecium, Colpidium, Litonotus, Trachelophyllum, Amphileptus, Chilodonella</i>
Ciliophora	Stalked ciliates	<i>Vorticella, Opercularia, Epistylis, Carchesium; and the suctoria Acineta, Podophrya</i>
Ciliophora	Free-swimming ciliates, floc predators	<i>Aspidisca, Euplotes, Stylonychia, Oxytricha</i>
Euglenozoa, Cercozoa, Heterokontophyta	Flagellates	<i>Bodo, Cercomonas, Monas, Oikomonas, Euglena, Peranema</i>
(various)	Amoebae	<i>Amoeba, Arcella, Actinophrys, Vahlkampfia, Astramoeba, Diffflugia, Cochliopodium</i>
Rotifera	Rotifers	<i>Philodina, Rotaria, Epiphanes</i>
Nematoda	Nematodes	<i>Rhabditis</i>
Annelida	Annelids	<i>Aeolosoma</i>

Eukaryotic microorganisms – such as fungi, protozoa and micrometazoa – have a relevant role in the organic matter oxidation and sludge floc formation, also contributing to the maintenance of a well-balanced bacterial community. The presence and distribution of the eukaryote community in a bioreactor give hints about the quality of the wastewater and the process performance, since these microorganisms may be sensitive to changes in the operating conditions. Some factors related to the presence of the eukaryotes are the efficiency of BOD and suspended solids removal; the sludge settleability; the aeration conditions; the presence of toxic compounds (heavy metals, ammonia, recalcitrant organics, etc.); the occurrence of organic overload; and the incidence of nitrification (BASSIN, DEZOTTI, 2008).

Identifying certain groups of microorganisms present in the biomass and their relative abundance may supply valuable indicators with regards to the effluent and treatment quality. Some possible correlations are listed in Table 2.9.

Table 2.9 – Treatment conditions related to the presence or predominance of certain groups of organisms in the biomass. Source: adapted from (BASSIN, DEZOTTI, 2008).

<i>Attribute of the microbial community</i>	<b>Expected characteristics</b>
<i>Predominance of flagellates and amoebae</i>	Start of operation or low sludge age.
<i>Predominance of flagellates</i>	Poor aeration and depuration, and organic overload.
<i>Predominance of pedunculated and free ciliates</i>	Good depuration.
<i>Presence of Arcella (rhizopod with shell)</i>	Good depuration.
<i>Presence of Aspidisca costata (free ciliate)</i>	Nitrification.
<i>Presence of Trachelophyllum (free ciliate)</i>	High sludge age.
<i>Presence of Vorticella microstoma (pedunculated ciliate) and low concentration of free ciliates</i>	Bad quality effluent.
<i>Predominance of Aeolosoma (annelids)</i>	Excess of dissolved oxygen.
<i>Predominance of filaments (bacteria or fungi)</i>	Sludge bulking.

Some relevant functions exercised by the protozoa in secondary wastewater treatment include: predation of bacteria, contribution for the effluent clarification; degradation of organic substances, reduction of effluent BOD; production of polysaccharides and mucoproteins that assist the floc or biofilm formation; interspecies interactions, helping to keep the ecological balance of the system; and reduction of the sludge production by the ingestion of flocculated bacteria.

In sludges from sewage treatment, the predominating micrometazoa are rotifers, being annelids, nematodes and tardigrades also found. Rotifers have a low growth rate and are more prone to appear in systems with high sludge age, as biofilm reactors. Among the functions performed by micro-animals in activated sludge processes, some are mentioned: assist to keep a healthy and active bacteria community through predation; act in the recirculation of minerals; consume free-living bacteria, reduce the effluent BOD and turbidity; and contribute to the ecological balance of the system. Nematodes may also assist in the creation of microchannels in the biomass agglomerates because of their bodies' shape and locomotion, improving the income of oxygen to the interior of the flocs. They feed on bacteria, protozoa, rotifers, tardigrades and other nematodes (BASSIN, DEZOTTI, 2008).

The balance between free-swimming ciliates, floc predator ciliates and rotifers expresses a good indicator of the system performance. Flagellates, amoebae, and free-swimming ciliates predominate at high food/microorganism ratios

(>0.2 gBOD/(gVSS·d)), generally associated with dissolved oxygen concentration below 0.5 mg/L in the aeration tank. For low food/microorganism ratios (<0.1 g BOD/(gVSS·d)), there is little presence of free ciliates, although with a high diversity of species. Finally, for medium food/microorganism ratios, it is expected high density of microorganisms (BASSIN, DEZOTTI, 2008).

Despite being rarely found in conventional treatment systems, fungi may also be part of the microbiota, particularly in favorable conditions: pH close to 5, high concentration of carbohydrates and nutrients deficiency. The most common species include *Geotrichum sp.*, *Cephalosporium sp.*, *Cladosporium sp.*, *Penicillium sp.* and *Fusarium sp* (BASSIN, DEZOTTI, 2008).

### **2.3. Moving Bed Biofilm Reactor (MBBR)**

The moving bed biofilm reactor is one kind of continuous flow, perfectly mixed, biological reactor with attached biomass growth. It was developed in Norway, between the late 1980s and the beginning of the 1990s, by professor Hallvard Ødegaard, from the Norwegian University of Science and Technology (NTNU). This technology gathers the features from the conventional activated sludge process with the ones of other biofilm processes, leaving apart the downsides (ØDEGAARD, 2006, ØDEGAARD, RUSTEN, *et al.*, 1994, VAN HAANDEL, VAN DER LUBBE, 2012).

In the MBBR, the biomass grows as biofilm attached to carriers that freely circulate within the reactional volume. Air, or oxygen, is injected at the base of the reactor assuring the movement of the carriers (thus improving mass transfer); supplying the oxygen necessary for the metabolism of microorganisms; and controlling the biofilm thickness by increasing turbulence. For anoxic or anaerobic MBBRs, agitation is kept by mechanical stirrers. Sieves are equipped at the reactor's outlet to maintain the biofilm supports inside the reactor. An illustration of the process is given in Figure 2.14.

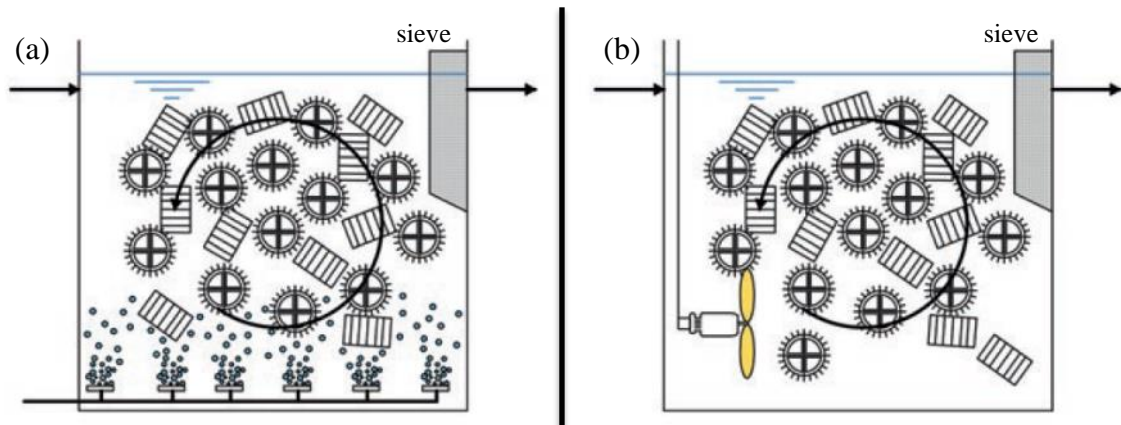


Figure 2.14 – Typical moving bed biofilm reactor setup, with the biofilm carriers kept in suspension whether by (a) aeration (aerobic MBBRs) or (b) mechanical stirring (anoxic or anaerobic MBBRs). Source: adapted from (BASSIN, DEZOTTI, 2018, RUSTEN, EIKEBROKK, *et al.*, 2006).

Initially, this kind of setup was commercialized by the company Kaldnes Miljøteknologi and, later, by AnoxKaldnes, nowadays a business unit from Veolia Water Technologies. The MBBR is a well-established technology, with more than 700 operating AnoxKaldnes™ MBBR units in the world, treating industrial or municipal wastewaters (ANOXKALDNES, 2014). Other MBBR suppliers complement the market dominated by AnoxKaldnes, such as Aqwise, Eimco, Brightwater, Siemens, Headworks and Degremont (VAN HAANDEL, VAN DER LUBBE, 2012).

The MBBR was developed and patented without biomass recirculation, differing from activated sludge systems. That said, it is important to differentiate it from its derivative system known as Integrated Fixed Film Activated Sludge (IFAS), which incorporates biomass recycle, being a hybrid reactor regarding biomass growth (VAN HAANDEL, VAN DER LUBBE, 2012).

Relatively short hydraulic residence time (15 to 90 minutes) is usually enough for carbonaceous organic matter removal, being the MBBR a compact system with high volumetric removal capacity. When substances with low biodegradability are present, it is desirable to apply longer retention times, favoring the assimilation of such compounds by the microbiota (REVILLA, GALÁN, *et al.*, 2016). It should be noticed that the HRT of MBBRs is conventionally the empty bed HRT, disregarding the volume occupied by the plastic body of the biofilm carriers. Despite the reduced HRTs, part of the particulate organic matter may get attached to the carriers and stay longer in the reactor, providing

enough time for hydrolysis and action of the microorganisms (VAN HAANDEL, VAN DER LUBBE, 2012). In fact, the extent of hydrolysis is smaller at elevated soluble biodegradable organic load, which is consequent of low HRTs and/or high soluble BOD, as seen in Figure 2.15 (ØDEGAARD, 2019).

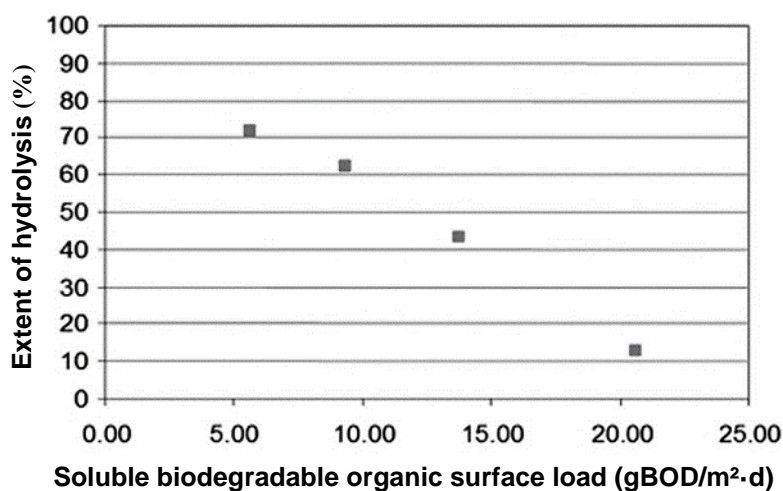


Figure 2.15 – Extent of hydrolysis of particulate organic COD to soluble COD as a function of the soluble biodegradable organic surface load. Source: adapted from (HELNESS AND SJØVOLD, 2001 apud ØDEGAARD, 2019).

Nitrification may be reached within the MBBR, being superior HRT possibly necessary for lowering an organic load that could disfavor the autotrophic nitrifying microorganisms in competition with the heterotrophs for oxygen and nutrients. Another way to achieve the desired nitrification extent is by positioning 2 or more MBBRs in series, as the first MBBR would deal with the high organic load and the second would offer a more favorable environment for the aerobic autotrophic nitrifiers.

Comparatively, the nitrification performance in one MBBR is higher than in a comparable activated sludge reactor. The same is not true for denitrification. One of the reasons is the fact that the nitrification in MBBRs is performed with DO between 3 to 7 mg/L, quite higher than in nitrification zones in activated sludge reactors. It makes the organic matter to be used for aerobic cell respiration instead of denitrification (that requires an anoxic environment), reducing the extent of the latter. As the oxygen level needs to be reduced, it is common that a deoxygenation system is installed before a denitrification MBBR (VAN HAANDEL, VAN DER LUBBE, 2012).

Eventually, systems with moving bed biofilm reactors are also demanded to remove phosphorous. However, plants equipped with MBBRs usually have the phosphorous removed by chemical precipitation/flocculation downstream of the MBBR and upstream the solids separation unit. For removing the phosphorous biologically, IFAS reactors can be used, where the suspended biomass plays a major role in this process (VAN HAANDEL, VAN DER LUBBE, 2012).

### **2.3.1. MBBR Features**

One of the principal advantages of the MBBR, differently from other biofilm reactors, is the utilization of the whole reactional volume for biomass growth, as in conventional activated sludge systems, meaning great volumetric capacity. It is also highlighted that the lack of sludge recycle, as other pure attached growth reactors, makes the effluent much lower in suspended solids concentration, downsizing the subsequent solids separation system when comparing the MBBR with the activated sludge reactor. The effluent solids come from biofilm sloughing or are already present in the influent wastewater. The advantages of the MBBR are overviewed in Table 2.10 (DEZOTTI, 2008, ØDEGAARD, 2006, VAN HAANDEL, VAN DER LUBBE, 2012). The reasoning supporting some of the stated features is found in section 2.2.5, as they are common benefits of biofilm systems against suspended growth ones.

Table 2.10 – MBBR overall features and benefits in comparison to activated sludge and other biofilm reactors.

<b>MBBR features</b>
<b>Overall features</b>
- Ease of operation and low need for maintenance.
- Liable to installation by small upgrades and adaptations of existing tanks or reactors.
- Applicable as an aerobic, anoxic, or anaerobic system.
- Various carrier models exist, offering unique features.
- Carriers filling ratio is easy to increase, allowing adaptation to load raises.
<b>Compared to other biofilm processes<sup>1</sup></b>
- Entire reactional volume used for biomass growth: high volumetric treatment capacity.
- Head loss much lower than in fixed bed biofilm reactors.
- Absence of issues with bed clogging in comparison with fixed bed processes.
<b>Compared to activated sludge reactors<sup>1</sup></b>
- SRT is not limited by HRT, possibly reaching higher sludge ages and specialization.
- Higher specialization confers greater resistance to load, pH, temperature, and toxic shocks.
- The specialized biomass has a better capacity to degrade otherwise recalcitrant compounds.
- Dampening of variations in nitrification performance, even at lower temperatures.
- Events of peak flow cannot washout the biomass.
- Concentration of biomass does not depend on the sludge settleability nor HRT.
- No need for sludge recycle, since the biomass grows in supports kept within the reactor.
- The suspended solids content is lower, downsizing the effluent solids separation unit.
- Much smaller footprint required than AS with similar capacity.
- The MBBR may be used when substantial organic load variations are expected, as the deeper zones of the biofilm may constitute a reservoir of biomass that may increase its contribution when the external zones are overloaded.

<sup>1</sup> Given similar capacities

As any other process configuration, the MBBR also present flaws. Some of its disadvantages and attention points are presented ahead (BASSIN, DEZOTTI, 2018, BASSIN, DEZOTTI, *et al.*, 2011, VAN HAANDEL, VAN DER LUBBE, 2012):

- Considerable acquisition cost of the carriers, that may surpass the economy provided by the smaller footprint compared to AS systems of same capacity.
- High energy consumption for adequate aeration.
- Incorrect design or operation of the MBBR may incur hydrodynamic problems, as the formation of stagnant regions near the sieves.

- Removing the carriers for reactor maintenance may be logistically tough.
- The supports may be subject to inorganic scaling (commonly calcium carbonate,  $\text{CaCO}_3$ ), reducing the available area for biomass formation and increasing the apparent density of the carriers, making it difficult to keep them in suspension. It is not advised to feed streams with calcium concentration over 200 mg/L.
- Foaming may trap carriers, mainly at the beginning of the reactor operation when carriers are empty, decreasing the treatment capacity.

The design of MBBRs depends majorly on the total area available for biofilm development, as this parameter defines the reactor capacity and, therefore, the surface organic load ( $\text{gCOD}/(\text{m}^2 \cdot \text{d})$ ) that may be applied (ØDEGAARD, 2019). Just like other biofilm-based processes, the diffusion of components into the biofilm is a quite relevant aspect. The effective biofilm thickness represents the deepness that the substrates can actually reach. Normally, the substrates cannot effectively diffuse deeper than 100  $\mu\text{m}$  towards the interior of the biofilm (RUSTEN, EIKEBROKK, *et al.*, 2006). Ideally, the biofilm should have a low thickness and be equally distributed through the protected surface of the carrier. In this sense, it is important to provide turbulence to the medium, which helps maintaining low biofilm thickness and improving the mass transfer from the bulk to the biofilm surface (VAN HAANDEL, VAN DER LUBBE, 2012). When compared to thin biofilms, thick ones geometrically reduce the contact area between the biofilm surface and the bulk, as illustrated in Figure 2.16 (WEF, 2010), potentially hindering the transfer of substrate and nutrients into the film. If the biofilm grows uncontrolled and eventually clogs the carrier, its surface exposed to the liquid may reduce significantly and diffusional problems are much more likely to affect the reactor performance, especially for carrier designs with a high height/diameter ratio.

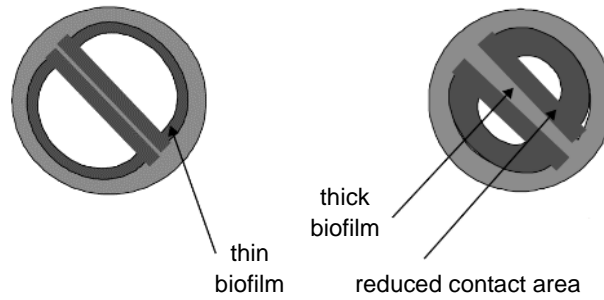


Figure 2.16 – Representation of the reduction of biofilm contact perimeter, therefore of the area, when the biofilm thickens. Source: adapted from (WEF, 2010).

The concentrations of substrates and oxygen are expected to gradually decrease across the biofilm thickness, given that the diffusional transport of solutes to the microorganisms may be slower than the degradation kinetics (XAVIER, PICIOREANU, *et al.*, 2003). Such gradients play a direct part in the distribution of biomass in the biofilm. The groups of microorganisms distribute spatially in function of the substrate and oxygen availability, as detailed before in section 2.2.5 (REVILLA, GALÁN, *et al.*, 2016).

It has been shown that the suspended biomass within the MBBR may have an important role in the treatment as well (LIMA, DEZOTTI, *et al.*, 2016). This contribution tends to be greater at higher HRTs (PICULELL, WELANDER, *et al.*, 2014). If the HRT of the MBBR is shorter than the critical SRT for free-growing microorganisms, the planktonic solids will come from the constant biofilm shearing and sloughing. Once these solids get to the bulk, regeneration and growth in suspension take place, contributing to the total activity in the reactor (MAŠIĆ, EBERL, 2014). As the suspended biomass is much less dependent on mass transfer by diffusion, it has more immediate access to substrates, especially if it detaches as smaller portions. Therefore, the activity of the suspended microbial community will be linked to the biofilm activity but will also be a function of the HRT and substrates concentration (PICULELL, 2016).

### 2.3.2. Biofilm Carriers

Regarding the carriers for biofilm growth - also known as supports, biomedia or media -, they should provide high protected surface area per unit for maximizing the reactor capacity, offering smaller footprints. Internal voids in the carriers represent the

actual surface where the biofilm grows, whilst the external surface is liable to constant collisions with other carriers, carrying a negligible amount of attached biomass.

Carriers with various sizes and shapes were historically developed for distinct applications. Some of the most popular models presented by AnoxKaldnes are detailed in Table 2.11, along with their main characteristics.

Table 2.11 – Several examples of commercial MBBR carriers from AnoxKaldnes and their main characteristics. Source: adapted from (BASSIN, DEZOTTI, 2018, MORGAN-SAGASTUME, 2018).

<i>Characteristics</i>	<i>Carrier Commercial Name</i>						
	<i>K1</i>	<i>K3</i>	<i>K5</i>	<i>Natrix C2</i>	<i>F3</i>	<i>Biofilm Chip M</i>	<i>Biofilm Chip P</i>
<i>Shape</i>							
<i>Protected area (m<sup>2</sup>/m<sup>3</sup>)</i>	500	500	800	220	200	1200	900
<i>Diameter (mm)</i>	9.1	25	25	36	46	48	45
<i>Height (mm)</i>	7.2	10	3.5	30	37	2.2	3.0
<i>Release (year)</i>	1989	2001	2010	2001	2007	2003	2005

A thorough description of AnoxKaldnes' carriers history is given elsewhere (MORGAN-SAGASTUME, 2018), including the most recent and innovative saddle-shaped Anox K™Z, created in 2014 and designed to auto control the biofilm thickness through the constant scraping resultant from the shocks between carriers. The biofilm thickness will be equal to the height of the grid over the surface of the carrier, that can be seen in Figure 2.17



Figure 2.17 – The Z carrier Z400, in reference to the 400 $\mu$ m height of the grid. Source: photo by Alan Werker (PICULELL, 2016).

Knowing that the water's density is approximately 1.0 g/cm<sup>3</sup> - or a little less when aerated -, the choice of a carrier's confection material with a density slightly lower than that of the water makes it easier to keep the carriers in suspension. This way, they will not have a great tendency neither to float nor settle. Usually, polyethylene or polypropylene are employed. These materials also deliver durability, an important attribute for the carriers to resist the constant collisions among them and the reactor's wall. The pioneer commercial carrier (K1) was made of high-density polyethylene (HDPE, 0.95  $\pm$  0.02 g/cm<sup>3</sup>), a material that is still regularly used in the production of more modern carrier designs.

The quantity of carriers inside the reactor is commonly specified by the carriers filling ratio, or filling degree. It is defined as the volume of the carriers dry bed - considering empty spaces - over the reactional volume. So, for a full-scale reactor with 3000 m<sup>3</sup>, the 50% filling ratio is given by a dry carriers bed of 1500 m<sup>3</sup>. Filling ratios up to 70% may be used in MBBRs, however values are usually lower than that for maintaining good hydrodynamics but enough for providing sufficient area for biofilm development (RUSTEN, EIKEBROKK, *et al.*, 2006). It might as well be convenient to work with lower filling degrees if increased pollutant loads are to be expected anywhere in the future, so that the reactor capacity may be expanded by the simple addition of more carriers. The maximum feasible filling ratio is usually within 55-65%, depending on the carrier shape (VAN HAANDEL, VAN DER LUBBE, 2012). The product of the filling ratio and the carrier's specific surface area indicates the effective specific surface area of the MBBR.

It should be pointed out that the plastic material may occupy a considerable fraction of the reactional volume. Carriers K1, K3 and K5 take around 11 to 14% of the reactional volume, whereas 23% is occupied by the BioChip M model, also from AnoxKaldnes (VAN HAANDEL, VAN DER LUBBE, 2012). This volume is conventionally not taken into consideration when calculating the HRT. Therefore, it shows how much the empty bed HRT (commonly used) is an overestimation of the actual value of the HRT.

As discussed before, in order to keep good mass transfer, the internal sections of the carriers should have enough space for the liquid to flow through it and for clogging prevention, which could substantially reduce mass transfer rates (VAN HAANDEL, VAN DER LUBBE, 2012). Figure 2.18 exhibits carrier media with clogged internal sections.



Figure 2.18 – Biofilm carriers (Kaldnes K1) with clogged voids due to poor mixing within the reactor. Source: lab-scale MBBR from pesticide research.

### 2.3.3. Aeration System

Usually, the aeration system is responsible for keeping the carriers in suspension with good hydrodynamics, for controlling the biofilm thickness, and for favoring mass transfer. Therefore, the aeration must be well distributed all over the base of the reactor by a robust aeration system. To guarantee adequate turbulence, medium-sized bubbles (4 mm holes) may be preferred over fine bubbles. Large bubbles, on the other hand, could hamper the transfer of oxygen to the liquid bulk due to decreased air-liquid contact area (BASSIN, DEZOTTI, 2018). In addition to the bubble size, the oxygen transfer efficiency from the bubbles to the liquid depends on the type of installed aeration system; the height of the liquid column; the shape of the biofilm carrier; the chosen biomedica filling ratio; and the temperature. Thus, the design of the aeration system should also consider the possibility of future increases of the carrier filling degree, consequent from raises in the

influent load to be treated. In an MBBR, medium-sized bubbles do not compromise the oxygen transfer to the liquid medium because adherence of the bubbles to carriers increase their residence time inside the reactor in comparison to activated sludge reactors. Furthermore, the shock of the bubbles with the carriers might break them into smaller bubbles, increasing the contact surface between gas and liquid phases (VAN HAANDEL, VAN DER LUBBE, 2012).

For carbonaceous organic matter removal, 2 mg/L is referred to as the minimum dissolved oxygen concentration in aerobic bioreactors (METCALF & EDDY, TCHOBANOGLOUS, *et al.*, 2014). Yet, due to diffusion limitations into the biofilm, required bulk DO concentrations may be higher. Keeping the DO at 2-3 mg/L in the MBBR, depending on the operational temperature, is usually sufficient for maintaining both microbial activity and a thin biofilm (BASSIN, DEZOTTI, 2018, RUSTEN, EIKEBROKK, *et al.*, 2006, VAN HAANDEL, VAN DER LUBBE, 2012).

Regarding nitrification, DO not rarely is the limiting substrate because of its concentration drop from the outer biofilm layer, containing heterotrophic microorganisms, to the inner portion where the autotrophic nitrifiers are located (HARREMOËS, 1982). This DO limitation to the nitrification rate is more pronounced at higher TAN concentrations, as Figure 2.19 illustrates. Consequently, a higher DO concentration is usually required, from 3 to 7 mg/L, depending on the temperature.

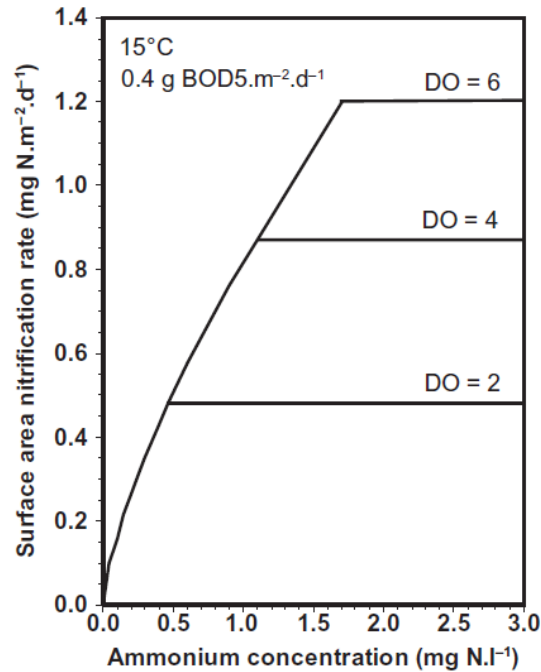


Figure 2.19 – Dependence of the nitrification rate with the ammonium concentration for some DO levels in an MBBR. Source: (RUSTEN, EIKEBROKK, *et al.*, 2006, RUSTEN, HEM, *et al.*, 1995, VAN HAANDEL, VAN DER LUBBE, 2012).

If the TAN concentration in the reactor is sufficiently above a critical minimum value, then the dissolved oxygen content starts limiting the nitrification rate. The higher the concentration of dissolved oxygen, the higher the nitrification rate will be. The relation between the nitrification rate and the dissolved oxygen content is approximately linear up to 10 mgO<sub>2</sub>/L (HEM, RUSTEN, *et al.*, 1994, VAN HAANDEL, VAN DER LUBBE, 2012).

#### 2.3.4. BAS Configuration

One typical plant configuration employing the MBBR is the so-called Biofilm-Activated Sludge, the BAS process from AnoxKaldnes. As suggested by the name, it consists of an MBBR as a pre-treatment step followed by a conventional activated sludge reactor, as depicted in Figure 2.20.

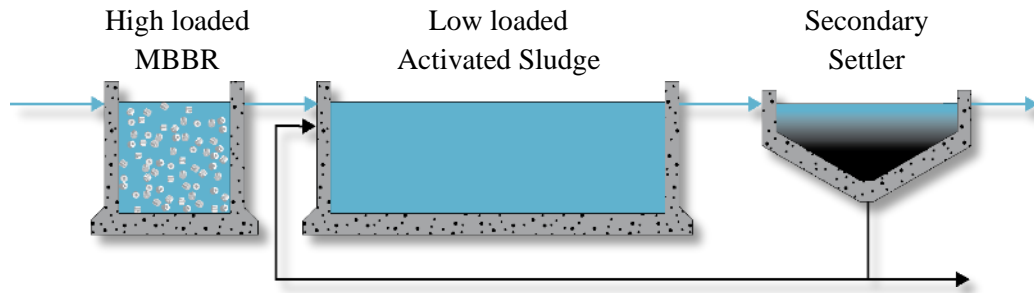


Figure 2.20 – Biofilm-Activated Sludge (BAS) configuration: a high loaded MBBR followed by a low loaded activated sludge reactor. Source: adapted from (VAN HAANDEL, VAN DER LUBBE, 2012).

Many times, this setup is resultant from the upgrade of an existing AS plant, cutting down the carriers acquisition cost when compared to the conversion to a full MBBR system. The MBBR step is designed to remove the readily available organic matter at a high rate, ending up as a very compact and high loaded bioreactor (VAN HAANDEL, VAN DER LUBBE, 2012). In a high-rate MBBR, the load should be not so high that the removal of the soluble and easily degradable COD would be constrained, but also high enough to minimize hydrolysis of incoming particulate organic matter, as seen previously in Figure 2.15 (ØDEGAARD, 2019).

Soluble COD removals ranging from 50 to 70% are usual in the MBBR, considerably reducing the organic load reaching the AS reactor (ANOXKALDNES, 2019, VAN HAANDEL, VAN DER LUBBE, 2012). This might be advantageous for protecting the more sensitive AS when the wastewater presents frequent oscillations in quality. Also, the lower load contributes to a higher sludge age in the AS, resulting in greater specialization of the biomass to remove the remaining slowly biodegradable COD. If nitrification is desired in the AS, it also is benefited by the load lowering (VAN HAANDEL, VAN DER LUBBE, 2012).

The fast-growing bacteria generated in the MBBR are not adapted to thrive in the environment of the downstream AS, low loaded with harder to degrade COD. Thus, those bacteria decay and have their decaying products consumed by the slow-growing bacteria. As a consequence of this predation relation, when compared to a similar low-loaded pure AS with similar capacity, in a BAS system a larger fraction of the microbial community of the AS will be comprised of slow-growing bacteria; the excess sludge production is 30 to 50% lower; problems with bulking sludge due to filamentous bacteria are minimized; and the demand for nutrient falls. The total HRT of a BAS system is only 30 to 50% than

that required for a similar COD removal by a pure AS system, while providing greater stability and resistance to disturbances (MALMQVIST, BERGGREN, *et al.*, 2004, VAN HAANDEL, VAN DER LUBBE, 2012).

One particular instance of the BAS process emerged in 2002, the nutrient-limited BAS (WELANDER, OLSSON, *et al.*, 2002). Once N or P availabilities are limited, the microbial community is stimulated to produce more EPS through the consumption of organic substrates, rather than new cells. Despite that the EPS-rich biomass is slimier (JENKINS, RICHARD, *et al.*, 2004), the easy biodegradation of the MBBR excess sludge in the AS lessens the sliminess and recycles nutrients into the process (SLADE, ELLIS, 2004). In comparison with the nutrients excess scenario, operating the BAS under limited nutrients availability further lowers the sludge production, improves its separability, and prevents excessive effluent N and P concentrations.

The BAS process has been broadly applied to wastewaters from the P&P industry (DALENTOFT, THULIN, 1997, MALMQVIST, WELANDER, *et al.*, 2007, REVILLA, GALÁN, *et al.*, 2018a, VILLAMAR, JARPA, *et al.*, 2009), but is also commercially offered by AnoxKaldnes for other sectors as municipalities, food, chemical, pharmaceuticals, and oil & gas (ANOXKALDNES, 2019).

#### **2.4. Brazilian Legislation on the Disposal of Industrial Wastewaters**

There exist many norms and laws that must be observed by industries and by public power to grant the right for disposal of industrial wastes in water bodies, and how industries should do it to diminish or extinguish their polluting potential. These regulations are a result of the development through time of policies on the environment and water resources. Systems composed of numerous organs, agencies, institutes, secretaries, counsels, committees, etc., are responsible for assuring the application of the policies. Summary of how the policies led to the creation of specific norms - in Brazil and the state of Rio de Janeiro - on the disposal of liquid industrial wastes in water bodies is given in Figure 2.21. The diagram is not extensive on systems that apply the policies, and neither on the organs that compose the systems. Instead, focus is given to those organs that provided resolutions applicable to the treatment and discharge of industrial wastewaters in water bodies, and the organs that concede the grants for disposal.

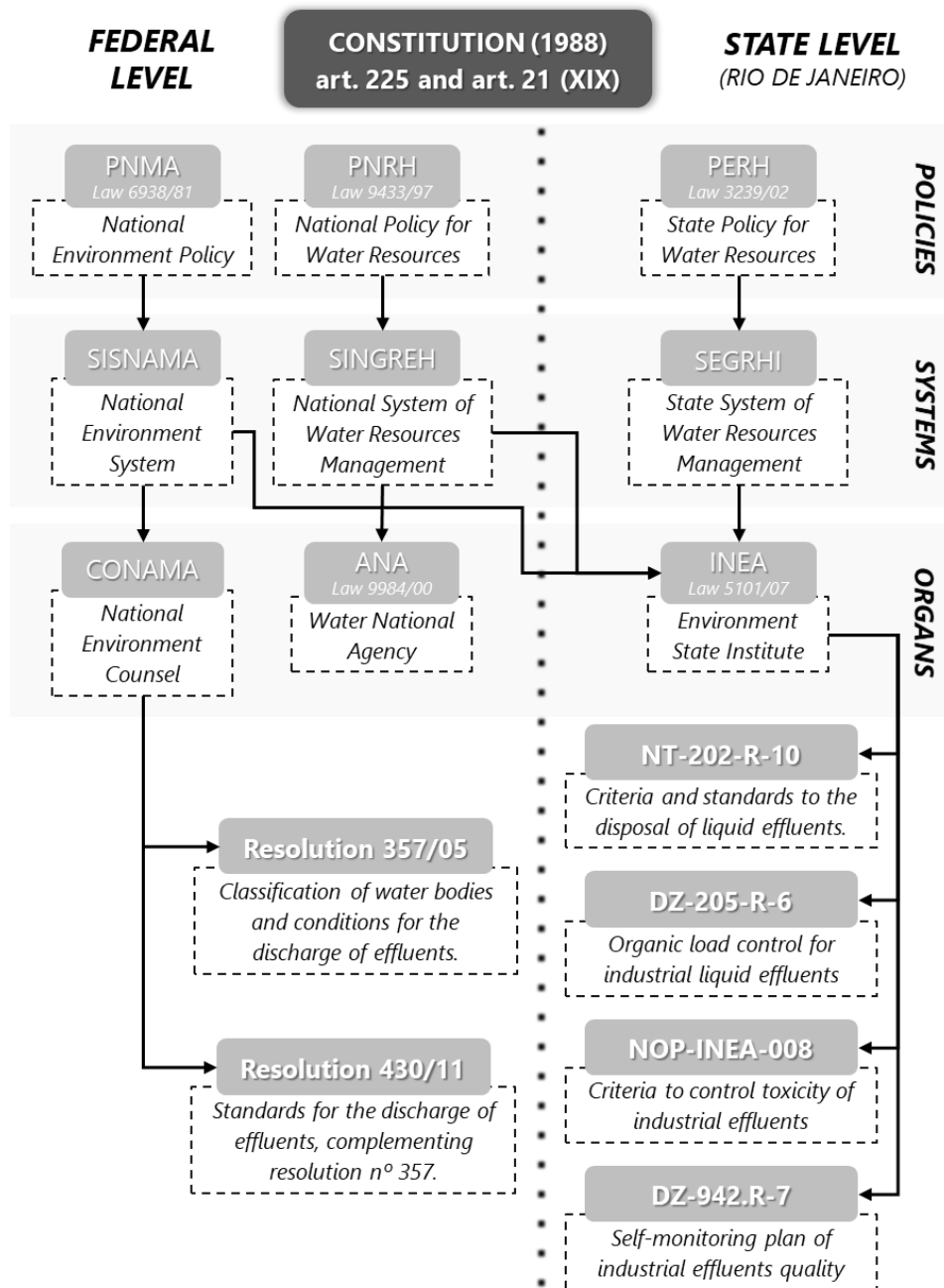


Figure 2.21 – Main Brazilian policies, associated systems and organs originating norms and usage grants related to the disposal of industrial wastewaters.

The description and practical implications of the federal resolutions and directives presented in Figure 2.21 are summarized below, focusing on those applicable to the treatment of the pesticide wastewater studied in part of this doctoral work.

- Resolution CONAMA n° 357/2005 – Disposes about the classification of water bodies and environmental directives for it. Also establishes conditions and standards for the discharge of wastewaters (CONAMA, 2005).

- Resolution CONAMA n° 430/2011 – Disposes about the conditions and standards for the discharge of wastewaters, complementing and altering Resolution CONAMA n° 357, from March 17, 2005 (CONAMA, 2011).

Within their texts, the resolutions classify water bodies to define specific directives for discharge in each class of water body. Some general conditions set by CONAMA for releasing wastewaters in water bodies include: pH between 5 and 9; total ammoniacal nitrogen concentration below 20.0 mgN/L; and limits for the toxic effects to the aquatic organisms present in the receiving body, with toxicity assessed for at least two trophic levels. The 3rd article of resolution 430/2011 grants autonomy to municipal or state environmental organs to establish other conditions and standards – or further restrict the existing ones –, considering the quality of the receiving body (CONAMA, 2011). That said, the state norms and directives shown in Figure 2.21 are described below.

- NT-202-R-10 – CRITERIA AND STANDARDS TO THE DISPOSAL OF WASTEWATERS; December 04, 1986 (revision). This technical norm applies to the direct or indirect discharge of wastewaters in inland or coastal, superficial, or subterranean water bodies in the state of Rio de Janeiro, via any discharge means, including public sewage systems. It states as standard for disposal, amongst other criteria, that the pH range must be between 5.0 and 9.0 and that the concentration of total ammoniacal nitrogen must be lower than 5.0 mg/L.
- DZ-205-R-6 – DIRECTIVE OF ORGANIC LOAD CONTROL FOR INDUSTRIAL WASTEWATERS; September 25, 2007 (revision). This directive covers industrial wastewaters as well as sanitary ones originated in industries when treated together with the industrial streams. Applied to this research with pesticide wastewater, the norm limits the effluent COD from chemical industries at 250 mg/L or 5.0 kg/d.
- NOP-INEA-008 – CRITERIA AND STANDARDS TO CONTROL ECOTOXICITY OF INDUSTRIAL WASTEWATERS; December 4, 2018. This technical norm defines the criteria over ecotoxicity of the industrial wastewater to be disposed of. It states that it is not allowed to discharge liquid industrial wastes in any water body when toxicity tests over 8 toxicity units. It also declares that after the second year of the norm publication, tests should result in less than 8 toxicity

units for organisms of, at least, two trophic levels; and starting at the fourth year after the norm publication, the reference value becomes 4, instead of 8.

- DZ-942.R-7 – DIRECTIVE OVER THE SELF CONTROL PROGRAMS OF WASTEWATERS; January 14, 1991. Defines which parameters should be monitored by the responsible for a polluting activity, and what frequency of monitoring should be respected for each parameter. Values thresholds are given by the other INEA or CONAMA's norms.
- NOI-INEA-14 – METHODOLOGY TO CALCULATE THE OPERATION QUALITY INDEX OF INDUSTRIAL WASTEWATER TREATMENT FACILITIES; May 6, 2015. Stablishes the methodology for calculating the quality index of operation of industrial wastewaters treatment facilities, aiming at periodical evaluation of treatment plants and contribution to quality improvements of receiving water bodies.

## **2.5. Pesticides: Industry, Wastewater, and its Treatment**

Chemical formulations denominated pesticides are designed to prevent or remedy the action of detrimental living organisms to agricultural crops by repelling, killing, or inhibiting the activity of such organisms. In Brazil, the federal law n° 7802/89, regulated by the federal decree n° 4074/02, defines pesticides as

products and agents of physical, chemical or biological processes meant to be used in the production, storage and processing sectors of agricultural products, pastures, protection of forests, whether native or planted, and other ecosystems and urban environments, hydric or industrial, with the objective to alter fauna or flora composition to protect them from the harmful action of living organisms considered noxious, as well as substances and products employed as defoliants, desiccants, stimulators and growth inhibitors (BRASIL, 1989, 2002, 2017).

Protection to agricultural cultivations is necessary for the productivity to follow the rise in food consumption occasioned by the demographic growth and change in eating habits (NATIONAL RESEARCH COUNCIL, 2000, OERKE, DEHNE, 2004). Besides

substantial losses in productivity, the action of plagues may deteriorate the final quality of agricultural goods, spoiling the financial performance of the activity (CERDA, AVELINO, *et al.*, 2017).

Naturally, the production loss extent depends on the type of cultivated product and climatic, ecological, and socioeconomic conditions. For instance, for barley crops the production loss potential is inferior to 50%, falling to an estimated 27% when practices for plague control are associated (OERKE, DEHNE, 2004). Pesticides constitute one major alternative for controlling plagues and boosting agricultural productivity. (TAKÁCS-GYÖRGY, TAKÁCS, 2011).

One of the ways of categorizing pesticides is according to the kind of plague it fights and the mechanism of action. Table 2.12 shows the main classes of pesticides. More specific classes can be found in the literature, including bactericide, avicides, algicides, amongst others (WANG, YUNG-TSE, *et al.*, 2004, WOOD, 2017, WORLD HEALTH ORGANIZATION, 2010).

Table 2.12 – Classification of pesticides according to the kind of plague and action.

Source: adapted from (SILVA, COSTA, 2012).

<i>Class</i>	<i>Action</i>
<i>Herbicide</i>	Products designed to eliminate or impede the growth of weed.
<i>Insecticide</i>	Chemicals or biological agents meant to eliminate insects.
<i>Fungicide</i>	Physical, chemical, or biological agents designed to fight fungi.
<i>Acaricide</i>	Chemicals intended to control or eradicate mites.
<i>Biological agents</i>	Organisms that act on the plague by parasitism or competition.
<i>Semiochemicals based pesticides</i>	Traps that emanate small doses of gases similar to natural pheromones capable of attracting and capturing insects.
<i>Household products</i>	Products destined to urban regions, mainly: domestic insecticides; molluscicides; rodenticides; and insect repellents.

The chemical nature of the active ingredients of pesticide products can also be utilized as categorization criteria. Five chemical groups include most of the existing pesticide compounds: halogenated organics; organophosphorus; organonitrogen; metallo-organic; and botanical and microbiological (WANG, YUNG-TSE, *et al.*, 2006). Further specification with regards to the chemical structure for each class of pesticide may be found elsewhere (WOOD, 2017, WORLD HEALTH ORGANIZATION, 2010).

There is also a guide presented by the World Health Organization (WHO) to categorize pesticides with respect to its danger to health. It is based on acute oral and dermal toxicity to rats, as measured by the median lethal dose (LD<sub>50</sub>) and indicated in Table 2.13 (WORLD HEALTH ORGANIZATION, 2010).

Table 2.13 – Pesticides classification with respect to the danger to health as defined by the WHO. Source: adapted from (WORLD HEALTH ORGANIZATION, 2010).

WHO Toxicological Classification	LD <sub>50</sub> in rats (mg/kg body mass)	
	Oral	Dermal
Ia Extremely hazardous	< 5	< 50
Ib Highly hazardous	5 to 50	50 to 200
II Moderately hazardous	50 to 2000	200 to 2000
III Slightly hazardous	> 2000	< 2000
U Unlikely to present acute hazard	> 5000	> 5000

Similarly, the ordinance n° 03 from the Brazilian National Secretary of Sanitary Surveillance (SNVS, Ministry of Health), dated from September 16, 1991, also presents criteria on median lethal dose on rats for classifying the toxicological risk of pesticides, differing liquid and solid formulations (Table 2.14). More specific criteria for each toxicological class are found in the ordinance original text (BRASIL, 1992).

Table 2.14 – Toxicological classification of pesticides according to the Brazilian ordinance n° 03 (SNVS, Ministry of Health). Source: (BRASIL, 1992).

(SNVS/MS) Toxicological Classification	LD <sub>50</sub> in rats (mg/kg body mass)			
	Solid Formulation		Liquid Formulation	
	Oral	Dermal	Oral	Dermal
I Extremely toxic	< 5	< 10	< 20	< 40
II Highly toxic	5 to 50	10 to 100	20 to 200	40 to 400
III Moderately toxic	50 to 500	100 to 1000	200 to 2000	400 to 4000
IV Little toxic	> 500	> 1000	> 2000	> 4000

Rigorous legislations are controlling the use of pesticides because of its danger to health and environment. Contamination of soil, and surface and underground waters

constitute some of the polluting capacity of those products. Another matter of intense debate is the consumption of food contaminated with pesticide compounds, with possible carcinogenic effects.

### **2.5.1. Pesticide Industry**

Manufacturing and formulating/packing are the main segments of the pesticide industry. The manufacture corresponds to the production of the active ingredients in technical grade purity, defined as technical products by Brazilian Federal Decree n° 4074/02. Industrial plants responsible for formulation perform the mixture of active ingredients with chemical additives and proceed with the conditioning and packing for the commercialization of pesticide products, referred to as formulated products by the mentioned decree (BRASIL, 2002, WANG, YUNG-TSE, *et al.*, 2004).

A series of steps is part of the manufacturing industries: chemical synthesis of active ingredients; separation; recuperation and purification; and product finishing. Many substitution reactions might be used for the synthesis stage, such as: chlorination; alkylation; and nitration. The separation steps are unit operations like filtration, decantation, extraction, and centrifugation. Recuperation and purification are employed altogether to recover solvents or reagents in excess, and typical processes are evaporation and distillation. At last, product finishing includes steps like drying, blending, pelletizing, packing and canning (WANG, YUNG-TSE, *et al.*, 2006).

Pesticide formulation industrial units blend the technical grade active ingredient with other substances that help to optimize a number of characteristics as storage, handling, application, effectiveness, or safety. The formulated product is then packed, being commercially presented in liquid form, or as solid grains or powder. The formulation can be done by the active ingredient manufacturer themselves or by selling the technical product to industries that will solely formulate the commercial pesticide. Operations related to formulation include dry mixing and grinding of solids, dissolving solids, and blending. Formulation of liquid products usually consists of batches in mixing-tanks equipped with mechanical stirrers and, possibly, cooling/heating systems (WANG, YUNG-TSE, *et al.*, 2006).

### 2.5.2. Pesticide Industries Wastewater

The wastewater used for this research was obtained from local pesticide formulation facilities, in Rio de Janeiro. So, detailing over pesticide wastewaters from manufacturing industries (i.e. that synthesizes the active ingredients) is not addressed in this work.

Pesticide formulation units have as major source of wastewater the washing and rinsing of lines and equipment between distinct batches for the formulation of different pesticide products. This periodic cleaning operation is needed to avoid cross-contamination. Sometimes the solvent used for the pesticide formulation is employed instead of water for the cleanup operation, then water is used for rinsing.

Other sources of liquid waste streams responsible for minor contributions comprise air pollution control devices (as water-scrubbing devices), drains from quality control labs, leakages/spillages/area runoff, external washing of equipment, washing of storage drums, etc. The amount of wastewater produced is usually not high, on average between 0.2 and 3.8 m<sup>3</sup>/d (WANG, YUNG-TSE, *et al.*, 2006).

The wastewater contains the active ingredients of the formulated product and other chemical additives diluted in water, and, potentially, other solvents utilized for washing. Some pollutant groups frequently found in pesticide waste streams include volatile aromatics, halomethanes, cyanides, haloethers, phenols, polynuclear aromatics, heavy metals, chlorinated ethanes and ethylenes, nitrosamines, phthalates, dichloropropane and dichloropropene, pesticides, and dienes. Additionally, conventional pollutants groups may be observed, such as ammoniacal nitrogen, biodegradable organic matter, suspended solids, chloride, etc. (WANG, YUNG-TSE, *et al.*, 2004).

Industrial pesticide wastewaters, generated by the manufacture of the active ingredients or formulation of the commercial products, have a high polluting impact due to usually having elevated toxicity, high concentration of organic matter with low biodegradability, and high pH. The presence of persistent and potentially carcinogenic pollutants makes this sort of waste particularly harmful to the environment and human health.

### 2.5.3. Treatment of Industrial Pesticide Wastewaters

Pesticide formulation plants have simpler operations for the management and treatment of wastewater than manufacture plants since the former produce much lower wastewater volume. Treatment or reuse should be the destination given to formulation plants residual streams. The same processes applied to treat waste streams from pesticide manufacturing industries may be used for pesticide formulation plants. It has been shown that the recycling of the treated water is possible if respected the quality required for each objective.

One of the most effective ways of dealing with waste streams is by diminishing and controlling their generation. Some techniques, as washing equipment with high-pressure sprays, can reduce the generated volume by more than 50%. Another applicable procedure is utilizing the residue from the previous cleanup to wash the system, or as makeup water, when the same pesticide contained in the residue is produced again. Beyond the reduction in the amount of wastewater, losses of active ingredients are also avoided (WANG, YUNG-TSE, *et al.*, 2006). A non-extensive list of processes, or categories of processes, that can be employed for pollution control of pesticide formulation plants is given in Table 2.15.

Table 2.15 – Main techniques applied in the management and treatment of wastewaters in pesticide manufacture and formulation industries. Source: adapted from (ATKINS, 1972, WANG, YUNG-TSE, *et al.*, 2006).

<i>Technique</i>	<i>Comment</i>
<i>Source Control</i>	Solutions that restrict the wastewater generation may be quite effective, downsizing the treatment operations.
<i>Steam or Vacuum Stripping</i>	Use of steam or vacuum to remove volatile organic compounds. May be effective in removing priority pollutant groups as volatile aromatics, halomethanes e chloroethanes. The condensate may return to the process.
<i>Activated Carbon Adsorption</i>	Adsorption onto granular or powdered activated carbon is a well-established process for pesticide removal. The saturated carbon is another residue to be managed.
<i>Resin Adsorption</i>	Adsorption onto synthetic polymeric resins has a similar principle than the activated carbon and is useful for removing and recovering specific compounds. Regeneration of resins is more viable than the activated carbon.
<i>Advanced Oxidation Processes (AOP)</i>	Many AOP can be applied with high efficiency to transform complex organic loads. Some plants use AOP to reduce the toxicity of the wastewater upstream of biological treatment. AOPs may be too expensive for high loaded streams.
<i>Hydrolysis (acid or alkaline)</i>	Acid or alkaline agents promote the hydrolysis of complex organics, leading to simpler substances. It may lessen toxicity yet generating undesired substances.
<i>Heavy Metals Precipitation</i>	Soluble metals may be precipitated and separated by operations such as coagulation/flocculation and filtration.
<i>Equalization</i>	Consists of a great capacity tank, stirred or aerated, that retains the wastewater for enough time for reducing variability in outlet flow and quality. Very adequate upstream sensitive processes, as biological ones.
<i>Neutralization</i>	pH adjusting for discharge or downstream processes, as bioreactors, adsorption on activated carbon or resins, or AOP.
<i>Biological Treatment</i>	Widely employed for the reduction of BOD, is usually the most feasible option. Pretreatment steps are common.
<i>Filtration</i>	May be used as pretreatment for removing suspended solids previous to adsorption on carbon or resin; or as tertiary treatment. Sand filter, micro and ultrafiltration are examples.

Biological processes are broadly used in the pesticide industries for reducing parameters as BOD and COD. The economic feasibility of bioreactors commonly stands out in comparison to other options. Nevertheless, pesticide wastewaters may contain toxic components that kill the microorganisms or inhibit their activity. Hence, pretreatment steps usually are placed before biological stages. Some factors affecting the biodegradability of pesticides are listed below (ATKINS, 1972, WANG, YUNG-TSE, *et al.*, 2006).

- Solubility and availability. Emulsified or chelated compounds are not readily available for metabolization by the microorganisms and are slowly degraded or inert to the treatment. DDT (dichlorodiphenyltrichloroethane) and its isomers, for instance, are highly insoluble in water.
- Molecular size. It may difficult the action of enzymes and reduce the degradation rate by the microorganisms.
- Molecular structure. Aliphatic organics, with linear or closed chain, are more biodegradable than aromatic substances. Hence, some pesticides, or even part of their molecules, cannot be easily degraded. Partial degradation may occur.
- Substitutions. Substitution elements usually make the chain more resistant to degradation, as in ethers and epoxides.
- Functional groups. Halogenic substitution in aromatic substances reduces biodegradability, with the number and place of the substituents playing a role in this. Substituents amine and hydroxyl normally improve biodegradability.

The removal mechanism may be a combination of metabolization by microorganisms, adsorption of pollutants on the sludge and volatilization to the air. In appropriate conditions, the biological treatment may remove priority, non-conventional and conventional (normally present in domestic sewage) pollutants (WANG, YUNG-TSE, *et al.*, 2006). A report from 1985 of the U.S. Environmental Protection Agency showed that, by the time, from 31 pesticide plants using biological treatment, 14 used aerated lagoons with retention time between 2 and 95 days, 13 had activated sludge reactors with HRT from 7.2 to 79 h, and 4 industries used trickling filter systems (USEPA, 1985 apud WANG, YUNG-TSE, *et al.*, 2006).

Studies with various standalone or combinations of physicochemical and biological processes, from the last 2 decades, are summarized in Table 2.16, where

performances and conditions of the treatment of pesticide wastewaters are provided. The fact that the majority of the studies are from the past 14 years indicates how the concern in achieving better treatment approaches to pesticide wastewaters increased concomitantly to the raising acknowledgement of pesticide substances as persistent organic pollutants, posing as micropollutants with various potential chronic toxic effects.

Table 2.16 – Literature review of researches assessing the treatment of pesticide wastewaters.

Ref. <sup>a</sup>	Waste type	Initial Concentration (mg/L)	Treatment	Results	Conditions
[1]	Synthetic	100 (1 of 3 pesticides)	(O <sub>3</sub> or O <sub>3</sub> /UV) + Batch AS	> 90%	<b>AOP:</b> 210 min <b>Batch AS:</b> up to 64 h HRT, 16 to 37°C
[2]	Synthetic	200 (DOC)	Photo-Fenton	15 to 50% DOC	pH 2.8   20 mg Fe <sup>2+</sup> /L   400 mg H <sub>2</sub> O <sub>2</sub> /L   sunlight
[3]	Synthetic	200 (pesticides)	Photo-Fenton + batch AS	100%	<b>Photo-Fenton:</b> 30°C, pH 2.8, 20 mg/L Fe <sup>2+</sup> , 100 mg H <sub>2</sub> O <sub>2</sub> /L, 2h <b>Batch AS:</b> 26.7°C, 5 h HRT
[4]	Synthetic	10 (malathion)	Nanofiltration Photo-Fenton	0.06 mg/L 0.08 mg/L	<b>Nanofiltration:</b> NF90   ΔP = 1120 kPa <b>Photo-Fenton:</b> pH 3   H <sub>2</sub> O <sub>2</sub> : Fe <sup>2+</sup> = 40:1   malation:H <sub>2</sub> O <sub>2</sub> = 1:100   135 min   UV-C (254 nm)
[5]	Synthetic	500 (TOC) 1000 (acetamiprid)	Integrated biofilter and electrolysis cell	85.4 % (TOC)	7 h HRT, 25°C, 20 mA/cm <sup>2</sup> current density
[6]	Synthetic	3 to 35 (Vydine)	Anaerobic-aerobic (fixed beds)	> 96 %	<b>Anaerobic:</b> 30°C, PET beads filling, 8 to 24 h HRT <b>Aerobic:</b> 22°C, PET beads filling, HRT = 2 times anaerobic reactor HRT
[7]	Synthetic	10 (mepiquat chloride)	TiO <sub>2</sub> /UV	0.54 mg/L	0.5 g/L TiO <sub>2</sub> P-25   180 min   pH 3   UV-A lamp
[8]	Real	10700 (COD) 3480 (TOC)	Aerobic batch	77.6 to 96.9 % (COD)	7 to 30 d HRT
[9]	Real	9650 (COD)	Anaerobic batch	87 to 91.5 %	15 to 30 d HRT, diluted raw pesticide wastewater (from ~250 to 9.65 g/L)
[10]	Real	3617 (COD)	Photo-Fenton + AS	99.2%	<b>Photo-Fenton:</b> pH 3   0.02 mmol Fe <sup>2+</sup> /L   45 min   0.4 mmol H <sub>2</sub> O <sub>2</sub> /L <b>AS:</b> 6h HRT   (industrial:sanitary) = (4:1)
[11]	Real	33700 (COD)	Fenton + MBBR	< 500 mg/L	<b>Fenton:</b> 97 mmol H <sub>2</sub> O <sub>2</sub> /L   40 mmol Fe <sup>2+</sup> /L   pH 3 (precipitation w/ Ca(OH) <sub>2</sub> until pH 7.5) <b>MBBR:</b> 3 kg COD/m <sup>3</sup> .d; HRT = 24h

Ref. <sup>a</sup>	Waste type	Initial Concentration (mg/L)	Treatment	Results	Conditions
[12]	Real	2500-5000 (COD)	Pressurized AS	85 to 92.5%	Aerobic, 0.1 to 0.4 MPa, 25°C, up to 10 h HRT
[13]	Real	200-500 (DOC)	Photo-Fenton + IBR	60 mg/L	<b>Photo-Fenton:</b> pH 2.8   20 mg Fe <sup>2+</sup> /L   sunlight <b>IBR:</b> two in series w/ recycle   20h HRT   carrier: Pall Ring   pH 7
[14]	Real	1662-1960 (COD) 513-696 (DOC)	IBR +: or UV or TiO <sub>2</sub> /UV or H <sub>2</sub> O <sub>2</sub> /UV or TiO <sub>2</sub> /H <sub>2</sub> O <sub>2</sub> /UV or Fenton or Photo-Fenton	- 41~56% DOC - 17% DOC - 23% DOC - 50% DOC - 50% DOC - 56% DOC - 56% DOC	<b>IBR:</b> pH 6.5-7.5   carrier: polypropylene <b>UV:</b> sunlight <b>TiO<sub>2</sub>:</b> 200 mg/L TiO <sub>2</sub> P-25 <b>H<sub>2</sub>O<sub>2</sub>:</b> 500 mg/L <b>Fenton:</b> pH 2.8   140 mg Fe <sup>2+</sup> /L   500 mg H <sub>2</sub> O <sub>2</sub> /L   475 min <b>Photo-Fenton:</b> pH 2.8   140 mg Fe <sup>2+</sup> /L   500 mg H <sub>2</sub> O <sub>2</sub> /L   120 min   sunlight
[15]	Real	3350 (COD) 2960 (TOC)	Photo-Fenton + SBR	- 99.3% COD - 99.4% TOC	<b>Photo-Fenton:</b> pH 3   (H <sub>2</sub> O <sub>2</sub> :Fe <sup>2+</sup> ) = (50:1)   (H <sub>2</sub> O <sub>2</sub> :COD) = (2:1)   UV-A   120 min <b>SBR:</b> DO > 3 mg/L   12 h HRT   (industrial:sanitary) = (3:1)
[16]	Real	0.1 (acetamiprid)	UV H <sub>2</sub> O <sub>2</sub> /UV Photo-Fenton PS/UV PS/Fe <sup>2+</sup> /UV	100% Removal: 90 min 45 min 20 min 30 min 30 min	<b>UV:</b> UV-C lamp (254 nm) <b>H<sub>2</sub>O<sub>2</sub>/UV:</b> 50 mg H <sub>2</sub> O <sub>2</sub> /L <b>Photo-Fenton:</b> 1 mg Fe <sup>2+</sup> /L   50 mg H <sub>2</sub> O <sub>2</sub> /L   UV-C lamp (254 nm) <b>PS/UV:</b> 100 mg PS/L <b>PS/Fe<sup>2+</sup>/UV:</b> 50 mg PS/L   1 mg Fe <sup>2+</sup> /L
[17]	Real	30100 (COD)	Coag/flocc + Fenton	91% COD	<b>Coagulation-flocculation:</b> polyferric chloride <b>Fenton:</b> H <sub>2</sub> O <sub>2</sub> stochoimetric
[18]	Real	183 (COD)	Fenton Photo-Fenton MWEUV/Fenton	- 48.7% COD - 64.0% COD - 77.9% COD	<b>Fenton:</b> pH = 5   0.6 mmol Fe <sup>2+</sup> /L   40 mmol H <sub>2</sub> O <sub>2</sub> /L   120 min <b>Photo-Fenton:</b> Same as Fenton + mercury-vapour lamp <b>MWEUV/Fenton:</b> pH = 5   0.8 mmol Fe <sup>2+</sup> /L   100 mmol H <sub>2</sub> O <sub>2</sub> /L   120 min   lamp w/ microwave generator

Ref. <sup>a</sup>	Waste type	Initial Concentration (mg/L)	Treatment	Results	Conditions
[19]	Real	3350 (COD) 2960 (TOC)	FeCAG/H <sub>2</sub> O <sub>2</sub> + SBR	- 99.6% COD - 99.6% TOC	<b>FeCAG/H<sub>2</sub>O<sub>2</sub></b> : 15 g FeCAG/L   300 mg H <sub>2</sub> O <sub>2</sub> /L   120 min <b>SBR</b> : DO > 3 mg/L   12 h HRT   pH = 7.0   (industrial:sanitary) = (3:1)
[20]	Real	357 (COD) 207 (DOC)	MBBR + MF + RO	Total: 99.2% COD (MBBR: 82 to 91% COD)	<b>MBBR</b> : Pre-denitrification layout; 0.72 kg COD/m <sup>3</sup>   12 + 24 h HRT; influent diluted with sewage and other chemical industries <b>MF</b> : 0.45 μm   2 bar <b>RO</b> : polyamide membrane   1.5, 2 e 2.5 MPa
[21]	Real	23390 (tCOD) 8160 (TOC)	EGSB + batch AS	59 to 62 % COD	<b>EGSB</b> : anaerobic at 35 or 55°C, 1 d HRT <b>Batch CSTR</b> : aerobic respirometry, 30°C, 24 h
[22]	Real	230 to 721 (COD)	MBBR + Physicochemical Post-treatment	64 to 89 % COD	<b>MBBR</b> : 6 h HRT, 26°C, wastewater mixed with 91.5% sewage and 4.7% landfill leachate

CSTR, completely stirred tank reactor; DOC, dissolved organic carbon; EGSB, expanded granular sludge bed; GAC, granular activated carbon; IBR, immobilized biomass reactor; MF, microfiltration; MWEUV, microwave electrodeless ultraviolet; SBR, sequencing batch reactor; RO, reverse osmosis; PS, persulfate; UV, ultraviolet.

<sup>a</sup> [1] (LAFI, AL-QODAH, 2006); [2] (ZAPATA, VELEGRAKI, et al., 2009); [3] (BALLESTEROS MARTÍN, SÁNCHEZ PÉREZ, et al., 2009); [4] (ZHANG, PAGILLA, 2010); [5] (LIU, ZHAO, et al., 2010); [6] (SHAWAQFEH, 2010); [7] (STAN, CRETESCU, et al., 2012); [8] (LIN, 1990a); [9] (LIN, 1990b); [10] (BADAWY, GAD-ALLAH, et al., 2006); [11] (CHEN, SUN, et al., 2007); [12] (JIN, PAN, et al., 2010); [13] (ZAPATA, OLLER, et al., 2010); [14] (MOREIRA, VILAR, et al., 2012); [15] (AFFAM, CHAUDHURI, et al., 2014); [16] (CARRA, SÁNCHEZ PÉREZ, et al., 2016); [17] (PLIEGO, ZAZO, et al., 2014); [18] (CHENG, LIN, et al., 2015); [19] (AFFAM, CHAUDHURI, et al., 2016); [20] (CAO, DEZOTTI, et al., 2016); [21] (GARCÍA-MANCHA, MONSALVO, et al., 2017); [22] (BACHMANN PINTO, MIGUEL DE SOUZA, et al., 2018).

Advanced oxidation processes, that might act with low selectivity and mineralize, or turn into less harmful subproducts, even the hardest-to-biodegrade substances, were thoroughly studied. They have been applied and investigated with different purposes: to mineralize already very low concentrations (down to ng/L) of specific substances, with a micropollutant point of view; to increase biodegradability upstream bioreactors, enhancing the secondary treatment performance; and to polish already biotreated effluents, acting as tertiary treatment. The same strategies are observed, but less frequently, with other physicochemical processes such as membrane separation or electrochemical technologies.

Biological configurations, alone or combined with physicochemical steps, were usually investigated for performance optimization over organic matter removal. In some cases, removal of particular pesticide substances was monitored in addition to general pollution parameters. Not rarely, dilution upstream the biological process with sanitary wastewater was used as a means to reduce the organic load, toxicity, and supply nutrients. Anaerobic, aerobic, and combined configurations were successfully investigated. The assessed types of bioreactors included: batch AS, AS, pressurized AS, sequencing batch reactor (SBR), expanded granular sludge bed (EGSB), immobilized biomass reactor (IBR), biofilter integrated with electrolysis cell, and the MBBR. From operational and performance points of view, the MBBR presents several advantages over other suspended or attached biomass processes, as seen in section 2.3.1.

Few were the applied studies of the MBBR as biological treatment for pesticide containing wastewaters (CAO, FONTOURA, *et al.*, 2016, CHEN, SUN, *et al.*, 2007). The most recent was performed during master studies conducted based on the preliminary results of this doctorate work. It combined the MBBR with a post-treatment train aiming industrial reuse (BACHMANN PINTO, MIGUEL DE SOUZA, *et al.*, 2018). Therefore, this study finds its niche in better studying the MBBR technology over a large number of operational conditions, expanding the knowledge base and application range of the MBBR for treating industrial pesticide wastewaters.

#### **2.5.4. Local Pesticide Formulation Industry**

According to information obtained with the pesticide formulation industry, the industrial raw (IR) wastewater has high COD, usually between 10000 and 16000 mg/L, being potentially even higher. The wastewater is generated with a flow rate of 7 m<sup>3</sup>/d and

its composition varies considerably, including fungicides, herbicides, pesticides, stabilizers, emulsifiers, thickeners, dyes, etc. Besides, there is seasonal variation of the produced pesticide products and, therefore, of the wastewater composition – as expected for the residuary stream of a pesticide formulation industry.

Pretreatment of the IR is performed with adsorption onto powdered activated carbon (PAC), aiming to reduce both COD and toxicity of the IR. The PAC adsorption is done to batches of 40 m<sup>3</sup> of liquid waste blended from diverse cleanup operations of the formulation plant. To this volume, 300 kg of PAC is added, corresponding to a PAC dosage of 7.5 g/L. The mixture is kept in agitation for at least 12 h at ambient temperature; then it is press filtered for retention of the suspended carbon. At the end of the process it is expected to reduce COD below 4000 mg/L (based on the INEA directive DZ-205.R-6 (INEA, 2007), and toxicity (ED<sub>50</sub>, median effective dose) above 25% v/v with *Vibrio fischeri*. Toxicity is only analyzed once the COD criterion is reached. In the case that the specifications are not met, the effluent is again processed with PAC.

Subsequently, the industrial pretreated (IPT) wastewater is mixed with the sanitary (S) sewage from the industrial site in an equalization tank. The latter has a nominal flow rate of around 168 m<sup>3</sup>/d and COD ranging from 100 to 150 mg/L, on average. From the nominal flow rates, it is known that the mixture proportion of IPT:S corresponds to 4:96 % v/v. Then, the mixture is fed to the activated sludge system with inlet COD ranging between 300 and 600 mg/L, and outlet COD ranging from 90 to 100 mg/L. In turn, the mean TAN concentration influent to the biological treatment is 13 mg/L, and lower than 5 mg/L in the treated wastewater. Typical characteristics of the different industrial streams are summarized in Table 2.17.

Table 2.17 – Nominal values for flow rate, COD and TAN concentrations for the different waste streams of the pesticide formulation industry.

<b>Stream</b>	<b>Total COD (mg/L)</b>	<b>TAN (mg/L)</b>	<b>Flow rate (m<sup>3</sup>/d)</b>
Industrial Raw (IR)	10000 to 16000	NA	7
Industrial Pretreated (IPT)	≤ 4000	NA	7
Sanitary (S)	100 to 150	NA	168
AS inlet	300 to 600	~ 13	175
AS outlet	90 to 100	< 5	175

NA, not available.

By the time of execution of the experimental activities of the pesticide research, the biotreated effluent was completely discharged into a local river. Therefore, the effluent conditions of the industrial treatment plant must meet the criteria established by applicable laws and norms, as overviewed above in section 2.4.. In the meantime, before its conclusion, this doctoral work branched into other research projects managed by colleagues assessing the feasibility of directing the MBBR effluent to the water treatment plant of the industry, that takes water from the same aforementioned river, instead of discharging the wastewater in the environment (BACHMANN PINTO, MIGUEL DE SOUZA, *et al.*, 2018, GAIOTO, 2019).

## 2.6. Pulp and Paper: Industry, Wastewater, and its Treatment

The sequential production of pulp and paper starts with the processing of raw cellulosic materials, from which a cellulosic/hemicellulosic fiber pulp is extracted and processed into paper products. The raw material is primarily classified as wood, nonwood (rice straw, wheat straw, sugarcane bagasse, cotton, etc.), or recycled fibers (wastepaper), which is increasingly becoming a major source for papermaking. Wood is the preferred raw material most of the time for their combined characteristics such as abundance, high cellulose content, high pulp yield, easiness of transporting and processing, etc. (EK, GELLERSTEDT, *et al.*, 2009, GOYAL, 2020b). A typical elemental composition of wood is given in Table 2.18.

Table 2.18 – Approximate elemental composition of wood materials. Source: adapted from (BAJPAI, 2018, GOYAL, 2020b).

Element	% of dry weight
Carbon	49.0 – 50.5
Hydrogen	5.8 – 6.1
Oxygen	43.5 – 44.5
Nitrogen	0.2 – 0.5
Sulphur	Max 0.05

Further classification of wood as soft or hard is usual. Softwood is acquired from evergreen coniferous trees as spruce, firs, hemlocks, pines and cedar. Deciduous trees like oaks, eucalyptus, maples and birches are the common source of hardwood (WANG, YUNG-TSE, *et al.*, 2006). Generic form of soft and hardwood trees appears ahead in Figure 2.22.

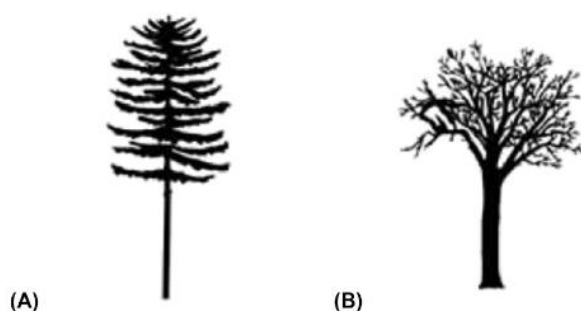


Figure 2.22 – Shape of a generic (a) softwood tree and a (b) hardwood tree. Source: (BAJPAI, 2018).

Considering classes of compounds, both hard and softwood are mainly constituted by cellulose, hemicelluloses (a class of compounds), lignin and wood extractives. In Table 2.19, the average percentages of dry weight for the main classes of substances may be observed (BAJPAI, 2018).

Table 2.19 – Typical composition of hard and softwood, based on North American species, by classes of compounds. Source: adapted from (BAJPAI, 2018).

Class	% of dry weight		Description
	Hardwood	Softwood	
<b>Cellulose</b>	40 - 50	45 – 50	White fibrous structure of wood
<b>Hemicelluloses</b>			White solid material filling out the fibers
<i>glucomannans</i>	2 - 5	20 – 25	
<i>xylans</i>	15 - 30	5 – 10	
<b>Lignin</b>	18 - 25	25 – 35	Adhesive polymer that holds the fibers
<b>Extractives</b>	1 - 5	3 – 8	Confer color, odor, and taste
<b>Ash</b>	0.4 – 0.8	0.2 – 0.5	Residue of complete combustion

Analyzing the descriptions given in Table 2.19, it is apparent that, in order to turn wood into fibrous paper products, pulp and paper industries desire to maximize the reclamation of cellulose - and hemicelluloses depending on the type of final product - while getting rid of lignin, extractives and ash. For so, these industries count on several processing strategies, addressed ahead.

### 2.6.1. Pulp and Paper Industry

P&P mills turn the raw material - mostly wood - into various types of paper products by the steps summarized in Figure 2.23. Each step comprises a series of operations and may differ from one industry to another. Pulp manufacture consists of mechanical and/or chemical breakdown of the wood chips to provide cellulose and hemicellulose fiber separation, while bleaching is the whitening of the pulp by means of chemical agents that attack residual lignin.

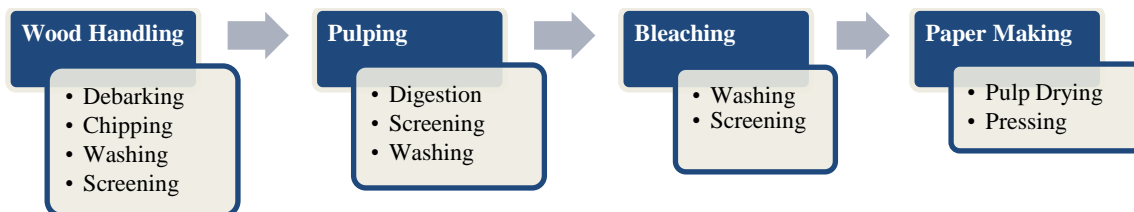


Figure 2.23 – Main processing steps employed by the pulp and paper making industries.

Wood handling is the first stage for pulp manufacturing, aiming at optimally preparing the raw wood for further processing. It usually begins at the forest by cutting trees into logs and debarking them, which could also sometimes be done in the industrial site. Those debarked logs are cut into chips about 20-30 mm long and screened for removing oversized pieces or fine particles. Washing might take place in between debarking and chipping and/or after screening, prior to the pulping stage (BAJPAI, 2018).

Once the chips are prepared, they are mechanically and/or chemically broken down to separate the cellulosic fibers used for paper making. Many pulping technologies have been developed through the history of pulp and paper industry, each presenting particular applicability according to factors such as raw material and desired final product. Some of the most applied pulping processes are summarized in Table 2.20.

Table 2.20 – Summary of the most commonly applied pulping processes. Source: adapted from (BAJPAI, 2018, WANG, YUNG-TSE, *et al.*, 2006).

Features	Pulping process				
	Mechanical	CTMP	NSSC	Kraft	Sulfite
<b>Mechanism</b>	Grinding stone, double disc refiners, steaming, followed by refining in TMP process	Chemical treatment using NaOH or NaHSO <sub>3</sub> + steaming followed by mechanical refining	Continuous digestion in Na <sub>2</sub> SO <sub>3</sub> + Na <sub>2</sub> CO <sub>3</sub> liquor using steam followed by mechanical refining	Cooking at 175 °C, 100-135 psi for 2-5 hours in NaOH, Na <sub>2</sub> S and Na <sub>2</sub> CO <sub>3</sub> ; efficient recovery of chemicals	Sulfonation at 125-175°C, 90-110 psi for 6-12 hours in (H <sub>2</sub> SO <sub>3</sub> + HSO <sub>3</sub> <sup>-</sup> ) with Ca <sup>2+</sup> , Na <sup>+</sup> , NH <sub>4</sub> <sup>+</sup> or Mg <sup>2+</sup>
<b>Raw Material</b>	Hardwood (poplar), softwood (balsam, fir, hemlock)	Hardwood and softwood	Hardwood (aspen, oak, alder, birch), softwood sawdust and chips	Any type of wood and nonwood	Any hardwood and non-resinous softwood
<b>Pulp charac.</b>	Low strength, soft pulp, low brightness	Moderate strength	Good stiffness and moldability	High strength brown pulp, difficult to bleach	Dull white-light brown pulp, easily bleached, lower strength than Kraft pulp
<b>Pulp yield</b>	92 – 96%	88 – 95%	70 – 80%	43 – 70%, depending on pulp finality	46 – 51%
<b>Paper products</b>	Newspaper, magazines, inexpensive writing papers, molded products	Newspaper, magazines, inexpensive writing papers, molded products	Corrugating medium	Bags, wrappings, white papers, cartons, corrugated board	Fine paper, sanitary tissue, wraps

TMP, thermomechanical pulp; CTMP, chemi-thermomechanical pulp; NSSC, neutral sulfite semi-chemical.

About 5 to 10% of the lignin content cannot be removed during the pulping process without significantly damaging the cellulosic content. This residual lignin imparts dark color to the pulp and needs sequential treatments with bleaching chemicals in order to produce white pulp (WANG, YUNG-TSE, *et al.*, 2006). Pulps are chemically bleached by one of two approaches where the chemicals attack the lignin, or specifically its chromophoric group. The former provides greater brightness whereas the latter has better pulp yield. Usually, a combination of chemical stages is employed for the bleaching process, with a wash of the pulp in between for removing the bleaching agent of the preceding step. A list of some of the most usual bleaching chemicals is given in Table 2.21, with a more extensive list found elsewhere (GOYAL, 2020a).

Table 2.21 – Description of some of the most common pulp bleaching stages. Source: adapted from (GOYAL, 2020a).

<i>Symbol</i>	<b>Stage description</b>
<i>A</i>	Acid wash - To remove metal elements from the pulp.
<i>C</i>	Chlorination - Elemental chlorine (Cl <sub>2</sub> ) is an effective de-lignifying agent. However, as it breaks lignin bonds, it adds chlorine atoms to the lignin degradation products, producing significant amounts of chlorinated organic material.
<i>D</i>	Chlorine dioxide - A highly selective chemical that can both de-lignify and brighten pulp. It oxidizes lignin but does not add chlorine atoms onto lignin fragments. However, small amounts of elemental chlorine and other chlorine compounds formed during the process react with degraded lignin to form chlorinated organics.
<i>CD</i>	Chlorine and chlorine dioxide are added together.
<i>E</i>	Alkaline extraction - Used to remove colored components from partially bleached pulps that have been rendered soluble in dilute warm alkali solution.
<i>H</i>	Sodium hypochlorite - An inexpensive de-lignifying agent formed by mixing elemental chlorine with alkali at the mill.
<i>N</i>	Nitrogen dioxide.
<i>O</i>	Oxygen - Oxygen removes lignin and modify other coloring components. The pulp reacts with oxygen in a pressurized vessel at high temperature and alkalinity.
<i>P</i>	Hydrogen peroxide - Often used at the end of a conventional bleaching sequence to prevent the pulp from losing brightness.
<i>W</i>	Wash - Pulp is washed at almost every stage to remove reactants of the preceding step.
<i>X</i>	Xylanase - Enzymatic pretreatment, in a TCF sequence, results in easier bleaching and delignification of the pulp, causing a bleach-boosting effect.
<i>Y</i>	Sodium hydrosulfite - Reductive bleaching. Good for recycled fibers.
<i>Z</i>	Ozone - An effective de-lignifying agent. It also brightens the pulp. Ozone attacks the cellulose fiber as well as the lignin.
<i>ZD</i>	Ozone and chlorine dioxide are added sequentially in the same stage.

TCF, total chlorine free.

Increased efficiency is usually achieved by using three to seven sequential stages, which decreases the total amount of chemicals needed as the complex structure of lignin interacts uniquely with each bleaching agent. Examples of conventional gaseous chlorine-based sequences are CEH, CEHD, CEHHD, CEHDED. However, there has been an increasing use over the last decades of bleaching sequences that reduce the production of chlorinated organics (AOX), substances associated with toxic effects in residual waters. More than 80% reduction of AOX emissions was attained since 1990 (ZODI, LOUVET,

*et al.*, 2011). Such sequences are whether elemental chlorine free (ECF), excluding the use of molecular chlorine; or even total chlorine free (TCF), excluding chlorine dioxide or any other chlorine-containing chemical. For ECF, a few common bleaching sequences are DED, (ZD)(EOP)DD, OD(EOP)D, whereas TCF sample trains are OAPP, OZEPY, OXZEPY, etc. (BAJPAI, 2018, GOYAL, 2020a). ECF bleaching dominates the market, while TCF production did not increase significantly since 1995. In North America, for instance, ECF responds for 96% of the bleached chemical pulp production (BAJPAI, 2018, CABRERA, 2017).

### **2.6.2. Pulp and Paper Industries Wastewater**

A number of factors influence the final quality of the wastewater from P&P industries. The most important ones are the type of raw material, the chosen pulping technology and bleaching sequence, and the amount of water used and wastewater recirculated in the process (POKHREL, VIRARAGHAVAN, 2004, VIRKUTYTE, 2017). For instance, nonwood raw materials generate wastewaters with a high amount of silica, and softwood presents greater polluting potential than hardwood. The pulping and bleaching stages generate the majority of the liquid wastes, with up to 85% originating in the bleaching stage (CABRERA, 2017, WANG, YUNG-TSE, *et al.*, 2006). Depending on the same factors as the quality of the wastewater, the volume discharged may vary from close to zero to 400 m<sup>3</sup> per ton of produced pulp (WANG, YUNG-TSE, *et al.*, 2006).

Overall, the liquid waste streams are primarily composed of degradation products of carbohydrates and lignin, and wood extractives, containing high COD, BOD, and concentration of AOX (in case of non-chlorine-free bleaching) (ZODI, LOUVET, *et al.*, 2011). High total suspended solids content is also common as a result of the wood preparation and pulp screening stages. Dark brown color of the residual water is attributed to lignin and its degradation products (WANG, YUNG-TSE, *et al.*, 2006). The BOD to COD ratio, often used to express the biodegradability of aqueous matrices, is usually within the range of 0.05 to 0.5, reflecting the great presence of recalcitrant compounds (ZODI, LOUVET, *et al.*, 2011). Even if the biodegradability is high enough to make the use of secondary treatment technologies feasible, limiting the concentrations of N and P is a concern point. These key nutrients needed for cell growth are usually deficient in wastewaters from the P&P industry, as could be expected by the average wood elemental

composition, previously shown in Table 2.18 (SLADE, ELLIS, 2004, WANG, YUNG-TSE, *et al.*, 2006).

The spent liquor from Kraft pulping is denominated black liquor, as 90-95% of the lignin solubilize to a mixture of lignin oligomers that imparts a dark brown color to the wastewater. Further cleavage of the oligomers results in phenylpropanoic acids, hydroxylated and/or methoxylated aromatic acids. The pulping process also results in dissolution of cellulose and hemicelluloses that are sensitive to alkali. Some inorganic constituents are found due to the chemical nature of the Kraft pulping, namely sodium hydroxide, sodium sulfate, sodium thiosulfate, sodium sulfide, sodium carbonate, and sodium chloride (WANG, YUNG-TSE, *et al.*, 2006). Nevertheless, this Kraft spent liquor goes through a recovery process that sequentially concentrates the black liquor by evaporation and burns the remaining organics, aiming for recovery of the inorganic chemicals through further steps (BAJPAI, 2018). Therefore, the condensate from the evaporator is the stream that actually follows to the treatment plant, containing toxicity, odor and 1000-34000 mg COD/L with a high contribution of methanol (60-90%) (WANG, YUNG-TSE, *et al.*, 2006, ZODI, LOUVET, *et al.*, 2011).

One of the major sources of color in the wastewater is the alkali extraction bleaching stages, due to ligninolytic substances (VIRKUTYTE, 2017). However, the characteristics of the bleaching effluent are highly dependent on the delignification degree of the unbleached pulp, the bleaching sequence, the type of raw material and the final desired brightness. Over 500 organic substances have been attributed to bleaching wastewaters, mostly derived from lignin, wood extractives and carbohydrates (CABRERA, 2017). Bleaching of kraft pulp may produce some pollutants that are among the hardest to remove from wastewater (ZODI, LOUVET, *et al.*, 2011)

A relevant control parameter that relates to the effluent COD is the kappa number, which quantifies the remaining lignin in the unbleached pulp by oxidative reactions. Higher lignin content is represented by a higher kappa number. If kappa number is low, then the amount of lignin to be removed by the bleaching sequence is smaller and so it is the use of bleaching chemicals, reducing the pollutant load. It should be noticed, however, that the kappa number is not supposed to decrease too much during the pulping process because it would negatively impact the pulp yield and physical properties (CABRERA, 2017).

### 2.6.3. Treatment of Industrial Pulp and Paper Wastewaters

Pollution prevention may take place by many actions that reduce the pollutant load from P&P industries. Best available technologies and practices, as follows in Table 2.22 for Kraft mills, are advisable in this sense. Overall, the measures include the process modifications aiming at cleaner operational practices and technologies (WANG, YUNG-TSE, *et al.*, 2006).

Table 2.22 – Main best available technologies guidelines, from the European Integrated Pollution and Prevention Control and the International Finance Corporation, for minimizing wastewater load in bleaching kraft pulp mills. Source: adapted from (CABRERA, 2017, WANG, YUNG-TSE, *et al.*, 2006).

<b>Best Available Technologies and Practices for P&amp;P Industry</b>
Dry debarking of wood.
Extended pulp delignification to a low kappa number.
Systems for collection and recycling of temporary and accidental discharges.
Closed screening stages.
Efficient washing of the pulp ahead of the bleaching.
Oxygen delignification ahead of the bleach plant.
ECF or TCF bleaching.
Improved process control of bleaching operations.
Removal of hexenuronic acids <sup>1</sup> by hydrolysis at the start of the bleach, for hardwood.
Partial closure of the bleach plant combined with increased evaporation.
Recycling of wastewater with or without simultaneous recovery of fibers.
Separation of contaminated and non-contaminated (clean) wastewaters.
Biological secondary wastewater treatment.

<sup>1</sup> Other color-giving substances, relevant in hardwood pulping and bleaching.

Other worth-mentioning cleaner technologies are organic solvent pulping, acid pulping, biopulping and biobleaching (enzyme-based), that are further addressed elsewhere (BAJPAI, 2018, WANG, YUNG-TSE, *et al.*, 2006).

Despite being able to reduce the potential of pollution, process modifications are not able to completely cease wastewater generation. Thus, end-of-pipe treatment technologies are necessary, from preliminary to tertiary solutions. Since the P&P wastewater quality and quantity may vary considerably from one pulp mill to another, it is important that the sector rely on varied technological options that may be applied in

diverse scenarios with few adaptations (WANG, YUNG-TSE, *et al.*, 2006). As for any industrial wastewater, there is a large number of alternatives for adequately treating the wastewater from P&P plants, dampening environmental impact and respecting regulations (KAMALI, ALAVI-BORAZJANI, *et al.*, 2019, ZODI, LOUVET, *et al.*, 2011).

Surveying the existing literature ends in a huge number of published studies assessing many different types of treatment for P&P waste streams. Over ninety references were gathered, starting in 1994, while searching the literature. One particular review article from 2016 provides an even more comprehensive list, with an overview of 206 investigations about the treatment of P&P wastewaters (ZODI, LOUVET, *et al.*, 2011). Figure 2.24 shows the percentage distribution of types of treatment employed in those 206 studies, amongst biological (B), chemical (C), mechanical (M), or combinations of those.

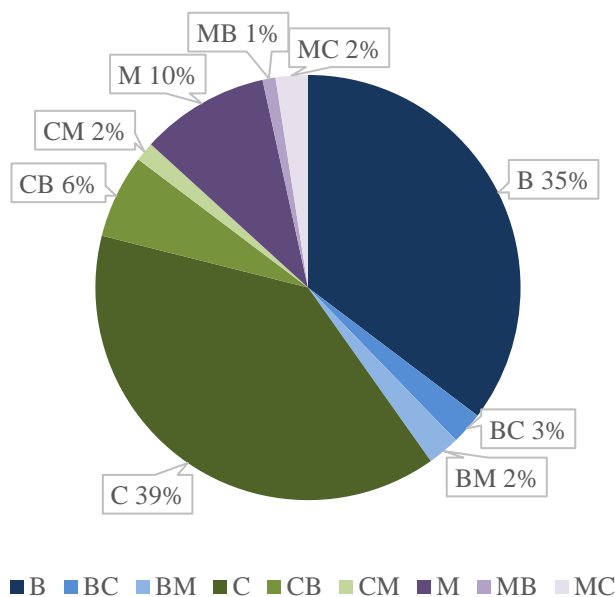


Figure 2.24 – Percentage distribution of 206 published studies, listed in a literature review (ZODI, LOUVET, *et al.*, 2011), by type of treatment investigated over P&P wastewaters: biological (B), chemical (C), mechanical (M), or a combination of those.

Investigations containing a biological stage, combined with other types of treatment or not, sums up to 47 % of the total, as seen in Figure 2.24. Secondary treatment is provided in existing industries by diverse aerobic and/or anaerobic biological technologies (WANG, YUNG-TSE, *et al.*, 2006). Acclimated microbial communities can

reduce BOD to levels below those that would be achievable with non-adapted biomass (ORDAZ-DÍAZ, ROJAS-CONTRERAS, *et al.*, 2014, ZODI, LOUVET, *et al.*, 2011). The scarcity of nutrients (N and P) for microbial growth in the P&P wastewater, mentioned in section 2.6.2, is often overcome with the supplement of external nutrients sources. One drawback when dosing nutrients is the need for continuous monitoring of the biotreated stream to avoid excessive N and P effluent concentrations, that could be harmful to receiving water bodies. The addition of nutrients is done upstream of the bioreactor in soluble forms. However, alternative approaches have been investigated, as adding solid N and P salts with low solubility, or incorporating bacteria capable of fixing atmospheric nitrogen to the process (WANG, YUNG-TSE, *et al.*, 2006).

From the data summarized in Figure 2.24, numerous were the investigated biological treatment technologies, including: activated sludge, aeration ponds, upflow anaerobic sludge blanket (UASB), constructed wetland, upflow anaerobic filter, various mono or mixed cultures of specific bacteria strains, various specific yeast strains (mono or mixed culture), tertiary algal treatment, anaerobic and aerobic trickling filters, anaerobic granular activated carbon biofilm reactor, anaerobic bioelectrochemical, SBR, anaerobic/aerobic membrane bioreactor (MBR), etc. Particularly, the Biofilm-Activated Sludge configuration has been effectively applied (DALENTOFT, THULIN, 1997), with multiple reports of pilot and full-scale plants (MALMQVIST, WELANDER, *et al.*, 2007, VILLAMAR, JARPA, *et al.*, 2009), and over 90 operating plants around the world (REVILLA, GALÁN, *et al.*, 2018b).

Summarized operational conditions of the MBBR stage of various studies with the BAS process treating P&P industrial wastewater are listed in Table 2.23. Some research has also been conducted on computational modelling, simulation and optimization of the BAS configuration (REVILLA, GALÁN, *et al.*, 2016, 2018b, REVILLA, VIGURI, *et al.*, 2014)

Table 2.23 – Summary of the MBBR stage operational characteristics of studies evaluating the BAS process over the treatment of P&P wastewater.

Ref. <sup>a</sup>	HRT (h)	$f$ (%)	$a$ (m <sup>2</sup> /m <sup>3</sup> )	$(f \cdot a)$ (m <sup>2</sup> /m <sup>3</sup> )	VLR (kg/(m <sup>3</sup> ·d))	SLR (g/(m <sup>2</sup> ·d))	P/COD (%)	N/COD (%)
[1]	5-24	30	NA	NA	4.5-9.0	NA	NA	NA
[2]	NA	10	900	90	NA	NA	0.2-0.3	1.1-2.1
[3]	5-45	30	340	102	2-6	20-59	NA	NA
[4]	3-38	16.3	850	139	0.2-7.5	1.4-54	0.3-1	1-5
[5]	3.3	10	900	90	5.7-13	63-144	dosed	dosed
[6]	12-24	50	NA	NA	0.8-1.6	NA	0.41	2.1
[7]	3-48	16.3	850	139	0.20-7.67	1.4-55	0.12-0.74	0.4-3.7
[8]	4-85	21-43	305	65-132	0.24-2.65	3.72-20.1	>0.32	0.35-1.8
[9]	3-7	30-50	220-300	66-150	8.7-30.8	58-467	limit.	limit.
[10]	8.6	33	220	73	19.4	266	0.17	0.77
[11]	12-15	20	300	60	10-30	167-500	limit.	limit.
[12]	2.4-3	50	300	150	13.4-16.7	89-111	0.06-0.15	0.9-1.5
[13]	13-22	58	350	203	2.5-3.5	12-17	0.52	2.2
[14]	NA	50-67	333	167-223	15-25	67-150	excess	excess
[15]	0.6-25	47-70	350	175-235	17-55	72-314	excess	excess
[16]	4.9	15	800	120	9-16	77-133	0.08-0.62	0.4-2.6
	1.6-4.9	45	800	360	11-48	31-133		

$f$ , carrier filling ratio;  $a$ , carrier specific surface area;  $(f \cdot a)$ , reactor effective specific surface area; VLR, volumetric loading rate; SLR, surface loading rate; NA, not available.

<sup>a</sup> [1] (BRINK, SHERIDAN, *et al.*, 2018); [2] (REVILLA, GALÁN, *et al.*, 2018a); [3] (BRINK, SHERIDAN, *et al.*, 2017); [4] (BAEZA, JARPA, *et al.*, 2016); [5] (OLIVEIRA, 2014); [6] (REZENDE, MOUNTEER, *et al.*, 2012); [7] (JARPA, POZO, *et al.*, 2012); [8] (VILLAMAR, JARPA, *et al.*, 2009); [9] (MALMQVIST, WELANDER, *et al.*, 2007); [10] (RANKIN, AERT, *et al.*, 2007); [11] (MALMQVIST, BERGGREN, *et al.*, 2004); [12] (WELANDER, OLSSON, *et al.*, 2002); [13] (JAHREN, RINTALA, *et al.*, 2002); [14] (DALENTOFT, THULIN, 1997); [15] (RUSTEN, MATTSSON, *et al.*, 1994); [16] This study.

Examination of Table 2.23 shows that reactors with low to medium effective specific surface area ( $f \cdot a$ ) were studied. They employed whether low filling degrees with great carrier specific surface, or high filling degrees with lower carrier specific surface. Regarding the carrier filling ratio, it has been shown that it is a major effect influencing the microbial community in biofilms and is, as well, linked to the performance of organic matter and nitrogen removal (CALDERÓN, MARTÍN-PASCUAL, *et al.*, 2012).

Publications listed in Table 2.23 lack discussion with regards to the distribution and role of the suspended and attached biomass fractions. It is known that the planktonic biomass might have a significant part in the MBBR performance, and that the HRT is directly linked to the extent of that part (LIMA, DEZOTTI, *et al.*, 2016, PICULELL, WELANDER, *et al.*, 2014). For a similar capacity, a smaller reactor with high effective specific surface area would rely more on the biofilm, while a larger one with lower effective specific surface area would take more advantage of the activity of the planktonic biomass. As in the BAS system consumption of the suspended biomass exiting the biofilm stage is an important component in the AS step, more challenging may be the design of the MBBR. Finally, studies in Table 2.23 do not discuss in depth how the nutrients availability affects performance, neither the solids leaving the MBBR, nor the efficiency of nutrients utilization for organic matter removal, essential knowledge for minimizing consumption and discharge of N and P.

#### **2.6.4. Södra Cell Värö Pulp and Paper Industry**

The experimental lab-scale work developed during the study with P&P wastewater was conducted with real residuary water from the pulp producing Cell Värö mill, from the Swedish company Södra. Softwood - pine or spruce trees - is the main raw material used by the industry for manufacturing up to 700,000 t/yr of paper and textile pulp by means of the Kraft process (SÖDRA, 2020). The Kraft pulp is then bleached by ECF bleaching sequence, which was not specified by the industry. Then, the wastewater comprises the bleach and debarking waste streams, leachate from the waste pile, and filtrate from the final pulp screening.

A full-scale nutrient-limited BAS system is in operation treating the industrial wastewater since July 2002 (MALMQVIST, BERGGREN, *et al.*, 2004), with the MBBR stage currently designed to abate 30 to 50% of the soluble COD. Previous published study performed at the same industrial site informed that the treatment plant consists of cooling towers followed by dosing of nutrients, pH adjustment with NaOH, and the BAS. The industry informed that the BAS is composed of a 4000 m<sup>3</sup> MBBR followed by a 20000 m<sup>3</sup> activated sludge, with design and current nominal flows of 34000-37000 and 18000 m<sup>3</sup>/d, respectively. Consequently, the correlated design and nominal HRTs are 2.6-2.8 h and 5.3 h. It should be noticed that, when the BAS was implemented, the bleaching

technology was TCF, which certainly makes the wastewater distinct from the one produced nowadays (MALMQVIST, WELANDER, *et al.*, 2007).

When started, the MBBR stage was first filled with 20% of the Natrix™ O (300 m<sup>2</sup>/m<sup>3</sup>) carrier. In 2004, due to increased load, additional Natrix™ M2 (220 m<sup>2</sup>/m<sup>3</sup>) were added, raising the carrier filling ratio up to 50% (MALMQVIST, WELANDER, *et al.*, 2007). Currently, the Natrix carriers were switched by the more modern Anox K™Chip P carriers (BioChip P, 900 m<sup>2</sup>/m<sup>3</sup>), which are carriers specially designed for optimal organics removal from P&P industrial wastewater (MORGAN-SAGASTUME, 2018). As told by Södra, the current carrier filling ratio is 19%, for an MBBR effective specific surface area of 171 m<sup>2</sup>/m<sup>3</sup>. For comparison, only 14% fill of BioChip P would provide as much total area as the previous fill with Natrix carriers.

In terms of performance, in the past, the BAS was reported to remove 60 to 75% of the total incoming COD, with 30-40% abated in the biofilm step. Sludge production was quite low, with solids yield averaging 0.07 kg TSS/kg COD removed. Finally, effluent N and P were 7-8 mg/L and 0.6-0.7 mg/L, respectively, with unknown supplementation dose in the inlet stream (MALMQVIST, WELANDER, *et al.*, 2007).

## 3. METHODS AND EXPERIMENTAL SETUPS

This section describes the materials and methods applied throughout the studies with the pesticide formulation and the P&P wastewaters, including the receipt of the industrial wastewaters, the operation of the bench-scale reactors and associated procedures, description of the operational phases, batch assays, and others. The operational strategies employed for each independent study are summarized in Figure 3.1.

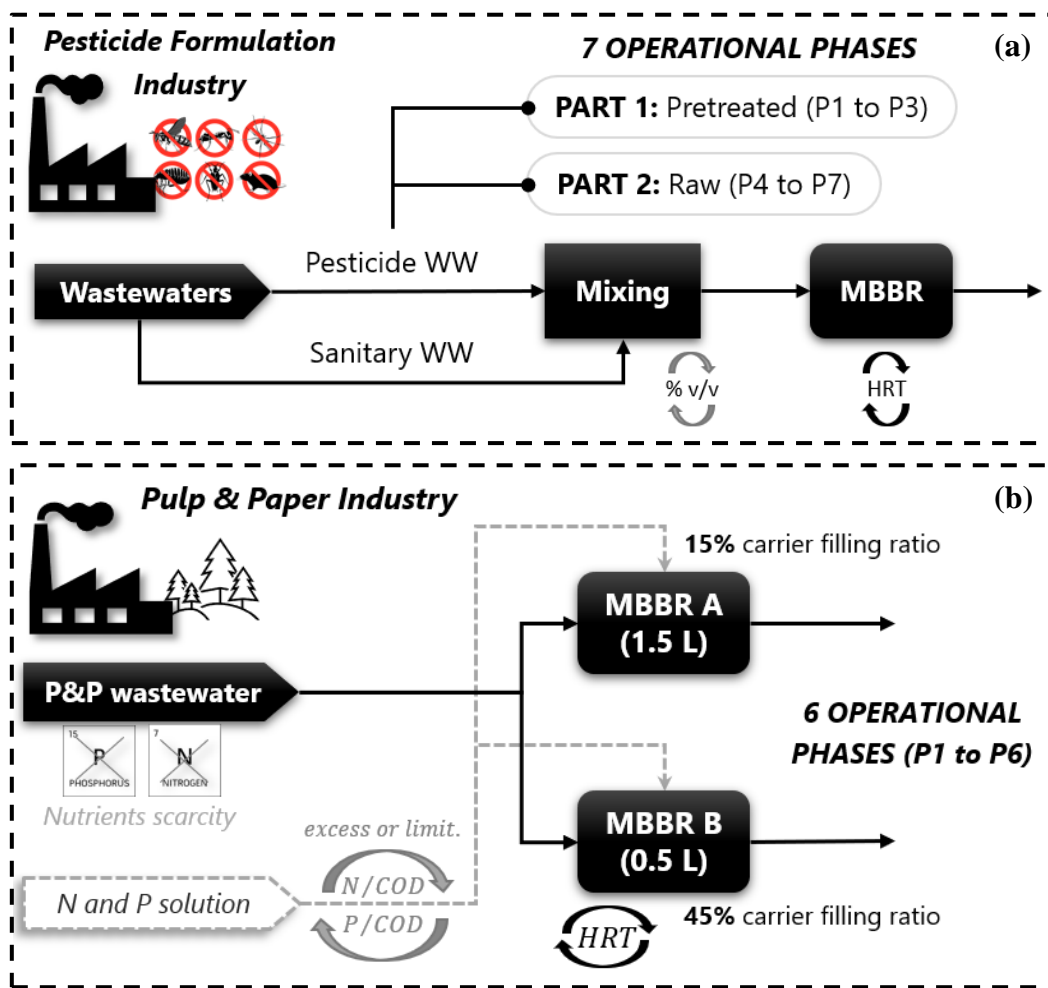


Figure 3.1 – Operational strategy summary of the pesticide (a) and P&P (b) researches.

Analytical methods and calculation procedures are considered background knowledge that may spoil the natural reading flow. This is true particularly for readers already familiar with the usual measurement techniques for the monitored parameters and

calculations of the derived ones. Hence, analytical methods are described in Appendix A and calculation procedures in Appendix B.

### 3.1. Pesticide Wastewater Research

#### 3.1.1. Receipt and Storage of Wastewaters

The industrial wastewater was provided by a local pesticide formulation industry, described in section 2.5.4. Altogether, 3 qualities of wastewaters were part of the study: the industrial raw; the industrial pretreated with adsorption on PAC (section 2.5.4); and the sanitary from the industrial site. They were better described in section 2.5.4, above. As a reference for the understanding of this work and for simplifying the notation utilized, acronyms for the waste streams collected at the industrial facility are defined in Table 3.1.

Table 3.1 – Definition of the acronyms used for the identification of each waste stream and differentiation from one collected lot to another.

<b>Wastewater</b>	<b>Acronym</b>	<b>Lots distinction</b>
Industrial Raw	IR	-
Industrial Pretreated	IPT	IPT0, IPT1, IPT2
Sanitary	S	S1, S2, ... , S20

The mixture of the IPT (or IR) with S will be simply referred to as feed or upstream/inlet/influent stream to the MBBR. As for the exiting flow of the MBBR, it will be called the downstream/effluent/outlet stream.

The first and only collection of IR took place on May 25, 2016. Nine containers of IR were received, of which three had a volume of 20 L and six had 5 L, as seen in Figure 3.2. The containers were stored in a refrigerator in the temperature range from 4 to 6°C. As the nine containers represented three distinct lots, two were taken and blended, resulting in 20 L of IR that were pretreated in the lab (section 3.1.2, below). The other 70 L were stored for later direct utilization in the continuous operation of the MBBR.



Figure 3.2 – Industrial raw pesticide wastewater containers received on May 25, 2016.

Unlike the samples of IR, delivered in great quantity at once, the receipt of IPT and S wastewaters occurred multiple times in 10 or 20 L containers, limited to the available space in the refrigerator (4 to 6°C), where the samples were stored to minimize biodegradation prior to their use in the experiments.

Figure 3.3 contains the timeline and received volumes of each lot of S and IPT. The first lot of IPT (IPT0) corresponds to the treatment of the received IR in the lab with adsorption on powdered activated carbon.



Figure 3.3 – Timeline of the receipt of IPT and S lots, with received volume in parentheses and respective day of MBBR operation timeline next to the vertical dashed line. Day 0 is highlighted in black text balloon.

Table 3.2 and Table 3.3 list the characteristics of each lot of pesticide (IPT and IR) and sanitary wastewaters, respectively.

Table 3.2 – Characteristics of each IPT lot and the IR lot in terms of physicochemical parameters (average values are shown).

Lot	tCOD (mg/L)	sCOD (mg/L)	DOC (mg/L)	TN (mg/L)	TAN (mg/L)
<b>IPT (mean)</b>	6100	6000	1613.8	226.3	42
IPT 0	6000 <sup>a</sup>	6000	1264	346.5	82
IPT 1	9700 <sup>a</sup>	9400	2891	294.0	28.2
IPT 2	2600	2600	686.5	38.3	17.1
<b>IR</b>	16900	12300	NA	NA	150

NA, not available.

<sup>a</sup> Diluted COD down to 3500 mg/L, as described in section 3.1.2.

Table 3.3 – Characteristics of each S lot and the related average of physicochemical parameters.

Lot <sup>a</sup>	N <sup>b</sup>	tCOD (mg/L)	sCOD (mg/L)	TAN (mg/L)
S1	4	76	NA	NA
S2	6	173.2	48.6	71.5
S3	9	441.7	27	60.4
S4	6	108	13.6	25.4
S5	2	0	0	3.4
S6	4	471.5	81.3	37.7
S7	5	258.5	73.9	30.1
S8	6	313	134.4	56.0
S9	9	173.2	67	34.6
S10	2	203	159.5	28.9
S11	5	204.7	146.4	28.5
S12	4	215.7	139.1	29.0
S20	18	321.3	174.7	55.9
Average	-	227.7	88.8	38.4

NA: Not Available.

<sup>a</sup> Lots that were not used (13, 14, 15 and 19) or used during the non-monitored period (16, 17, 18) are not included.

<sup>b</sup> Number of monitored days during which the reactor was fed with the corresponding lot.

### 3.1.2. Pretreatment with Powdered Activated Carbon (PAC) Adsorption

The first lot of industrial pretreated wastewater (IPT0) was produced in the lab by treating the IR with reproduction of the PAC adsorption as performed at the industrial site. As stated in section 2.5.4, the real scale PAC adsorption uses a dosage of 7.5 g PAC/L and 12 h contact time at room temperature. If necessary, the adsorption is repeated until COD below 4000 mg/L and toxicity (ED<sub>50</sub>) above 25% v/v with *Vibrio fischeri* (based on the INEA directive DZ-205.R-6 (INEA, 2007)) are obtained.

In the lab, 20 L of IR were treated at room temperature, around 22°C. For this purpose, 12 L buckets were used with a mechanical stirrer (Fisatom 711S, up to 2000 rpm) providing the needed agitation, as seen in Figure 3.4.



Figure 3.4 – Lab-scale system for reproducing the real scale adsorption onto powdered activated carbon.

Due to the 12 L capacity of the experimental setup, the IR was processed in two consecutive batches containing 10 L. The 7.5 g PAC/L dosage was initially respected, and the contact time was 18 h. After the consecutive batch adsorptions, the final content of both were mixed and homogenized to compensate eventual differences between the consecutive batches. The whole content was, then, filtered through a glass fiber filter ( $< 2 \mu\text{m}$  pore size) for PAC exclusion and COD was quantified to decide on the necessity, or not, for more adsorption batches (in case of  $\text{COD} > 4000 \text{ mg/L}$ ). At the end, four PAC adsorption steps were run, as listed in Table 3.4.

When proceeding with more batch adsorptions, the total volume was always divided by two, but adjustments were done to the PAC dosage and the contact time, aiming to reach more rapidly the desired COD. A simple estimation was used to adjust the PAC dosage based on the remaining COD to be removed and the ratio between the previous dosage and COD removal.

Table 3.4 – COD results and treatment conditions for each batch adsorption on PAC.

Stage	Batch	Treated volume (L)	Final volume (L)	Initial sCOD (mg/L)	Final sCOD (mg/L)	PAC dosage (g/L)	Contact time (h)
PAC 1	1	20.5	19	24000	19000	7.5	18
	2					7.5	18
PAC 2	1	19	17	19000	17800	6	18
	2					7.5	22
PAC 3	1	17	15.5	17800	13000	7.5	22
	2					20	22
PAC 4	1	15.5	12	13000	6000	30	22
	2					50	22

Even after the four PAC adsorption stages - with increasing PAC dosage -, the sCOD was still above the criterion of 4000 mg/L. Decision was made to stop the adsorption treatment and, instead, to dilute the final effluent to reach a COD of 3500 mg/L. This was advantageous for saving resources and time; and for increasing the produced IPT volume. Also, the focus of the study was the MBBR, and not the PAC adsorption.

The proportion IPT:water was calculated for final COD of 3500 mg/L, resulting in 55:45 ratio. A COD of 3500 mg/L was chosen instead of 4000 mg/L because the latter is a threshold condition, rarely observed in practice. After dilution, a sample was sent for microtoxicity analysis with *Vibrio fischeri* within the pesticide formulation industrial site. The result of ED<sub>50</sub> (t = 15 min) was 34.84 % v/v, being adequate to the toxicity criterion (> 25% v/v). Therefore, both COD and toxicity were within the criteria after PAC adsorption and dilution.

### 3.1.3. MBBR System Setup

For studying the efficiency of the moving bed biofilm reactor on the removal of organic matter and ammoniacal nitrogen from pesticide formulation plant wastewater, the experimental setup drawn in Figure 3.5 was used.

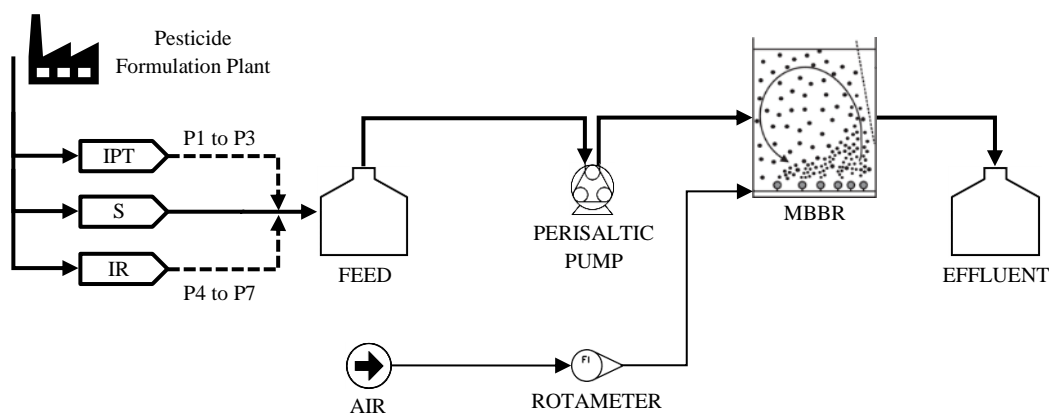


Figure 3.5 –Experimental setup schematic diagram. P1 to P7 denote the operational phases 1 to 7, described in section 3.1.5.

The bench-scale MBBR was set using a cylindrical glass reactor with 300 mL working volume and 5.5 cm internal diameter. For working with around 50% filling degree (as defined in section 2.3.2), the reactor was filled with 149 K1 carriers. This carrier is made of HDPE and, as detailed in Table 2.11, it has 500 m<sup>2</sup>/m<sup>3</sup> protected specific surface area, 9.1 mm diameter, and 7.2 mm height.

Throughout the research, the MBBR feed was stored in 10 to 20 L containers and under refrigeration (4 to 6°C) for preventing early biodegradation. The content of the feed container was replaced once a week, on average.

During the first three phases, the feed was produced by mixing the IPT with S, and, eventually, with water. The latter was for diluting the COD of the IPT down to 3500 mg/L (see section 3.1.2), whenever an IPT lot with COD over that was received. Once diluted, the IPT was blended with S, with the proportion of each (on a volume basis) defined by the corresponding phase, to produce the desired amount of feed. Measurement of the involved volumes was conducted in graduated cylinders or containers.

Mixing and aeration were provided by compressed air bubbled through the base of the reactor. The air was initially supplied by a porous stone with the flow regulated by a rotameter. Subsequently, to improve the turbulence, the air was injected through a silicon hose with a 3 mm internal diameter, fed by a compressor Jeneca AP2000, with flow rate of around 1.6 L/min.

Flexible silicone hoses were connected to a peristaltic pump (Watson Marlow 323S), that transferred the feed from the refrigerator to the reactor. A picture of the

operating system is shown in Figure 3.6. During the entire operation, the reactor was kept under room temperature, controlled between 21 to 25°C by air conditioning.



Figure 3.6 – The operating lab-scale MBBR system.

#### 3.1.4. MBBR Startup and Inoculum

During the startup, the reactor was inoculated for the development of the biofilm in the carriers. The inoculum consisted of around 20 mL of concentrated activated sludge and 12 carriers colonized with biofilm replacing 12 empty carriers. Both the activated sludge and the carriers were taken from operating bench-scale reactors in the lab fed with synthetic wastewater simulating domestic sewage. The MBBR in operation during the startup may be seen in Figure 3.7



Figure 3.7 – MBBR in operation during the startup phase.

While the real wastewater was not available, the MBBR was fed for approximately 5 months with synthetic wastewater composed of 0.29 g glucose/L, 0.35 gNaHCO<sub>3</sub>/L, 0.105 gNH<sub>4</sub>Cl/L, 0.01 gMgSO<sub>4</sub>/L, 0.0281 gK<sub>2</sub>HPO<sub>4</sub>/L, 0.0219 gKH<sub>2</sub>PO<sub>4</sub>/L, and 0.5 mL of trace metal solution/L. The latter is described elsewhere (VISHNIAC, SANTER, 1957). The theoretical COD was around 310 mg/L (calculated as shown in section B.4, and in accordance to the nominal range informed by the industry, section 2.5.4), which may be considered 100% biodegradable for glucose as carbonaceous substrate. As the corresponding TAN and P concentrations were 27 and 10 mg/L, respectively, the COD:N:P ratio was 100:9:3, more than enough to ensure adequate growth conditions to the bacterial community (as explained in section 2.2.1).

### **3.1.5. MBBR Operational Phases**

For assessing the MBBR performance, the operational phases described in Table 3.5 were executed, each one complementing different information regarding the robustness of the process and its response to the variations in the influent concentration and composition. In phase 4, the reactor started to be fed with the industrial raw wastewater (instead of the pretreated one) mixed with the sanitary wastewater. The time gaps observed between phases 3 and 4, and 5 and 6, correspond to periods with minimal monitoring of the reactor, not representative of any of the phases. This was due to issues unrelated to this doctoral work.

Table 3.5 – MBBR operational phases and their characteristics throughout the pesticide wastewater study.

Phase →	P1	P2	P3	P4	P5 <sup>a</sup>	P6 <sup>a</sup>	P7 <sup>a</sup>	
<sup>b,c</sup> HRT (h)	3.3	3.3	6.6	6.7	6.1	6.6	6.7	
<sup>b</sup> VLR (kgCOD/(m <sup>3</sup> ·d))	2.9	6.2	1.7	1.6	1.4	1.8	2.5	
<sup>b</sup> SLR (gCOD/(m <sup>2</sup> ·d))	11.4	24.5	6.7	6.1	5.2	7.1	9.7	
% v/v	Sanitary	96	92	92	98	98	97	96
	Industrial (quality)	4 (IPT)	8 (IPT)	8 (IPT)	2 (IR)	2 (IR)	3 (IR)	4 (IR)
<sup>b</sup> pH	In	8.0	8.3	7.6	6.9	7.9	8.2	7.7
	Out	7.4	8.2	7.3	6.0	8.5	7.9	7.1
Duration (d)	Start	0	88	155	390	418	653	704
	End	87	154	234	417	458	703	742

<sup>a</sup> pH adjustment was conducted.

<sup>b</sup> Average values for the entire experimental phase.

<sup>c</sup> Small deviations from the nominal values of HRT (namely 3 and 6 h) are due to practical limitations in the system operation. HRT was controlled by changing the rotation of the peristaltic pump, which corresponded to 1.67 and 0.83 mL/min for the HRT of 3 and 6 h, respectively.

During phase 1, the operational conditions of the moving bed biofilm reactor were similar to those of the industrial treatment plant in terms of the influent composition. The following variables were addressed in the 3 initial phases: two distinct hydraulic retention times (3 and 6 h); various qualities of the industrial wastewater; and two proportions of the pretreated industrial pesticide wastewater within the mixture with sanitary wastewater.

Then, phases 4 to 7 were intended to investigate the response of the system when subjected to non-pretreated pesticide wastewater. For this purpose, HRT was maintained invariant at 6 h and the effect of gradual increases in the proportion of IR to S on the system performance was evaluated.

### 3.1.6. MBBR Monitored Parameters

Assessment of the MBBR performance for treating the pesticide wastewater depends on the choice of monitored parameters and the frequency of measurement. The main indicators monitored were: chemical oxygen demand (tCOD, pCOD and sCOD);

DOC; TN; TAN; pH; and suspended solids (TSS, VSS and FSS). An extensive list and approximate analysis frequencies are detailed in Table 3.6.

Table 3.6 – Monitored parameters and their approximate analysis frequencies.

Frequency →	2-3 times per week	1 time per week	2-3 times per phase	1 time per phase
Parameters	<ul style="list-style-type: none"> <li>• COD</li> <li>• TAN</li> <li>• TN<sup>a</sup></li> <li>• DOC<sup>a</sup></li> <li>• pH</li> <li>• Temperature</li> </ul>	<ul style="list-style-type: none"> <li>• Turbidity</li> <li>• TSS, VSS</li> </ul>	<ul style="list-style-type: none"> <li>• Nitrite</li> <li>• Nitrate</li> <li>• DO</li> </ul>	<ul style="list-style-type: none"> <li>• TAS, VAS</li> <li>• Microscopy<sup>b</sup></li> <li>• FISH<sup>b</sup></li> <li>• N<sub>2</sub>O gas<sup>c</sup></li> </ul>

FISH, fluorescence *in situ* hybridization; TAS, total attached solids; VAS, volatile attached solids.

<sup>a</sup> Only until phase 3 (included).

<sup>b</sup> Except phase 1.

<sup>c</sup> Phases 4 and 5, only.

### 3.1.7. Biofilm Batch Trials for Nitrification and Organic Matter Removal

Batch trials were performed by operating the MBBR in batch mode during a certain span of time after draining its content and filling it with fresh feed. Samples were taken in various predetermined instants and immediately filtered through cellulose nitrate membranes - with nominal 0.45 µm pore size - to interrupt microbial activity on the substrates. sCOD and TAN analysis were done to construct concentrations versus time curves and determine maximum removal rates, as detailed in section B.11. Table 3.7 summarizes the conditions under which the tests were conducted. Temperature was maintained similar to that of reactor continuous operation so that the maximum removal rates derived from the batch trials could be compared to the apparent removal rates.

Table 3.7 – Experimental conditions during the batch trials.

<b>Condition</b>	<b>Description</b>
Wastewater composition	Same as the end of each phase of continuous operation
Total duration	5 h (P1) or 7 h (P2 to P7)
Wastewater volume	0.25 L (P1 to P3) or 0.3 L (P4 to P7)
Sampling instants (min)	15, 30, 45, 60, 90, 120, 150, 180, 240, 300, 360, 420
Attached solids analysis	6 carriers taken at end of the trials
Temperature	Same as continuous operation ( $21 \pm 1^\circ\text{C}$ )
Aeration	Same as continuous operation

At the end of each trial, 6 carriers were taken for analyzing attached solids with the procedure explained in section A.10. Hence, it was possible to calculate the maximum specific removal rate of TAN and COD, according to the calculation procedure explained in section B.11.

## **3.2. Pulp and Paper Wastewater Research**

### **3.2.1. Receipt and Storage of Wastewater**

The industrial pulp and paper wastewater was provided by a local Swedish industry (Södra Cell Värö, described in section 2.6.4) in periodical collections of about 1 m<sup>3</sup>. Every wastewater sampling was done at the entrance of the industrial BAS treatment facility, designed to abate 30 to 50% of the sCOD. To assure consistency, each batch was sequentially numbered and used, not being mixed with the remainders of previous lots. A Wedholms Milk Cooling Tank DF 183AD, with 1.25 m<sup>3</sup> capacity, was used to store and refrigerate the wastewater (at  $6.2 \pm 2.4^\circ\text{C}$ ) to minimize biodegradation upstream the reactional systems.

The raw material used by the industry is mainly softwood (pine or spruce trees) for paper and textile pulp production by means of the Kraft process, followed by ECF bleaching with chlorine dioxide. Data regarding the individual characterization of each wastewater lot collected at the industrial site, along with the period that each lot was fed to the reactors, are shown in Table 3.8. Lots 5 and 6, in particular, had lower COD as a result of dilution of the wastewater in the industry.

Table 3.8 - Average characteristics of the different wastewater lots, at the time of collection at the industry. “Start” and “End” refers to the operational timescale of the MBBRs.

Lot	tCOD (mg/L)	sCOD (mg/L)	TAN (mg/L)	PO <sub>4</sub> <sup>3-</sup> -P (mg/L)	TSS (mg/L)	VSS/TSS (%)	pH	Start (d)	End (d)
L1	3000	2900	0.0	1.7	82	66	6.8	0	57
L2	3000	2900	0.0	1.1	16	92	7.6	58	116
L3	3700	3600	0.0	1.4	30	87	7.2	117	168
L4	3050	3000	0.0	0.9	22	90	7.2	169	215
L5	2400	2350	0.0	5.6	18	89	7.0	216	248
L6	2100	2000	0.0	1.2	18	80	7.4	249	302
L7	3300	3250	0.0	1.6	31	90	7.4	303	337
<b>Average</b>	2935	2860	0.0	1.6	29	86	7.3	-	-

As seen in Table 3.8, ammoniacal nitrogen was always absent in all wastewater lots and the P/COD was only around 0.06%, with exception of lot 5, for which it amounted to 0.23%. Suspended solids content was always quite low and pH was adequate for biological treatment. Nitrate and nitrite were absent or negligible (<0.1 mg/L) whenever tested.

### 3.2.2. MBBRs Experimental Setup

Glass cylinders were utilized for setting up two bench-scale MBBRs, designated as A and B, with respective working volumes of 0.52 and 1.58 L. Both reactors were filled with 77 pieces of AnoxK<sup>TM</sup>5 carriers (protected specific surface area of 800 m<sup>2</sup>/m<sup>3</sup> and 25 x 3.5 mm (diameter x height)) (BASSIN, DEZOTTI, 2018), providing carrier filling ratios of 45 and 15%, respectively. Thus, reactor A had an effective specific surface area of 360 m<sup>2</sup>/m<sup>3</sup>, while for reactor B it was 120 m<sup>2</sup>/m<sup>3</sup>. The reactors had glass jackets for the circulation of heating water that maintained the reactional temperature at 35.0 ± 0.3°C during their entire operation. Peristaltic pumps were employed to continuously feed reactors A and B from a common source of wastewater, whilst an overflow pipe kept the volume constant, as depicted in Figure 3.8. During the first 5 days of operation, both reactors were inoculated twice with 60 mL of activated sludge that had been recently collected at the industry and kept refrigerated (4°C) until use.

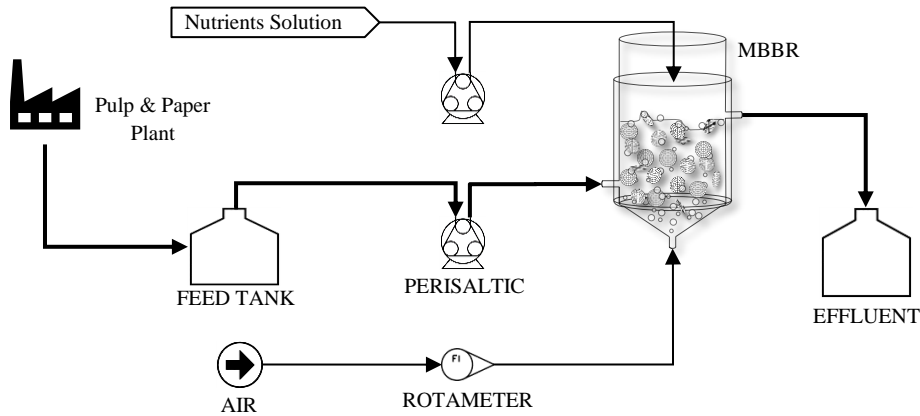


Figure 3.8 - Experimental setup schematic diagram (identical for both MBBRs, out of scale).

A picture of the operating bioreactors is shown in Figure 3.9, where the reactors A and B are highlighted.

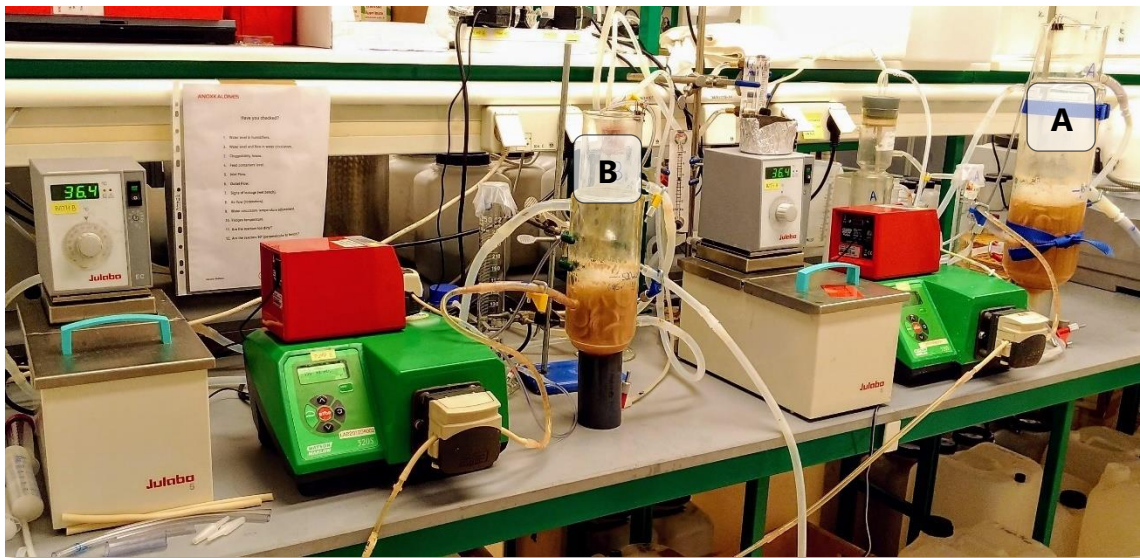


Figure 3.9 – The lab-scale MBBR system experimental set-up, with reactors A and B highlighted.

The bottom part of the reactors was conical with connection for compressed air injection as medium-sized bubbles, providing mixing and dissolved oxygen for the microorganisms. Mean DO concentrations within reactors A and B for the entire study were  $3.7 \pm 0.7$  mg/L and  $3.6 \pm 0.7$  mg/L, respectively. The pH, not controlled, averaged  $8.3 \pm 0.1$  and  $8.2 \pm 0.2$  for reactors A and B, respectively. Sampling of treated effluent

for periodical analysis was made using a syringe and silicone hose from atop the reactors, thrice or twice a week.

### 3.2.3. Operational Phases

The performance of the MBBRs was assessed during 6 operational phases under a variety of conditions, including the variation of nutrients availability, for both reactors, and HRT, for reactor B, as disposed in Table 3.9. Also shown in Table 3.9 are the average soluble volumetric loading rate (sVLR) and soluble surface loading rate (sSLR), that were dependent on the organic matter content of the wastewater lots. The duration of each phase and the number of monitored dates,  $n$ , are also listed in Table 3.9. Please note that  $n$  is not exactly reflected in the graphs and averages presented in the results section, as outliers and non-representative spans of time (due to identified experimental issues) have been excluded. The non-uniformity in phases duration, particularly for phases 4 to 6, was a consequence of specific practical and personal time issues.

Table 3.9 – P&P research operational phases and its characteristics, duration, and number  $n$  of analysis dates.

Phase →		P1	P2	P3	P4	P5	P6
HRT (h)	A	4.9	4.9	4.9	4.9	4.9	4.9
	B	1.6	1.6	1.6	3.2	4.9	4.9
	(A/B)	3.07	3.05	3.07	1.53	0.99	0.98
sVLR (kg/(m <sup>3</sup> ·d))	A	14	16	10	9	11	15
	B	43	48	32	13.8	11	15
sSLR (g/(m <sup>2</sup> ·d))	A	116	133	88	77	95	125
	B	121	133	89	39	31	41
Nutrients		Excess	P limit	N limit	N limit	N limit	Excess
P/COD <sub>in</sub> (%)		0.56	0.08	0.44	0.62	0.39	0.55
N/COD <sub>in</sub> (%)		2.6	1.3	0.7	0.7	0.4	2.5
Start-End (d)		6-90	91-222	223-265	266-286	287-325	326-337
$n$		29	43	16	7	12	4

Concentrated nutrients solutions - prepared with tap water, reagent grade dihydrogen potassium phosphate (KH<sub>2</sub>PO<sub>4</sub>) and ammonium chloride (NH<sub>4</sub>Cl) - were supplied by peristaltic pumps at a flow rate that provided the intended nitrogen and

phosphorous availability for each experimental phase. For excess of nutrients, N/COD and P/COD ratios in the feed were primarily planned for nominal values of 2.5% and 0.5%, respectively. These are common reference values to ensure a sufficient amount of nutrients for cell growth in biological processes, considering a wastewater biodegradability level of 50% (WEF, 2010). When P was restrained, the nominal ratio of P/COD was set to approximately 0.1%, alike the nominal value used in the full-scale industrial treatment plant. For N limitation, its proportion to COD was set empirically to allow a theoretical sCOD removal between 30 and 50% in both reactors, based on the N utilization per unit of COD removed from the previous phase. Once set, it was kept constant within 0.4-0.7% N/COD and as similar as possible for both reactors.

The nutrients solutions concentrations were chosen to provide low flow rates and dilution factors to the wastewater streams, less than 0.8% for most phases. Exceptions were phases 4 to 6 for reactor B, during which the dilution factor reached a maximum of 2.2%.

### 3.2.4. Monitored Parameters

The MBBR performance when treating the P&P wastewater was evaluated by monitoring a number of parameters in the influent and effluent streams, and within the reactor. Table 3.10 lists all the monitored parameters with their respective approximate frequencies of analysis.

Table 3.10 – Monitored parameters and their approximate analysis frequencies.

Frequency (→)	2-3 times per week	2-3 times per phase	1 time per phase
Parameters	<ul style="list-style-type: none"> <li>• COD</li> <li>• TSS, VSS</li> <li>• TAN</li> <li>• TN</li> <li>• Phosphate</li> <li>• pH</li> <li>• Temperature</li> <li>• DO</li> </ul>	<ul style="list-style-type: none"> <li>• Nitrate</li> <li>• Nitrite</li> <li>• Stereomicroscopy (carriers)</li> </ul>	<ul style="list-style-type: none"> <li>• TAS, VAS</li> <li>• Microscopy (suspended and attached biomass)</li> <li>• DNA sequencing</li> </ul>

### 3.2.5. Kincannon-Stover Kinetic Model

Continuous operation data of reactor B was fitted to the Kincannon-Stover kinetic model for obtaining the maximum substrate utilization rate and the biodegradability of the wastewater. This model has been primarily developed for describing the substrate removal in rotating biological contactors under steady-state conditions based on total biofilm surface area (KINCANNON, STOVER, 1982 apud HOSSEINY, BORGHEI, 2002). As the suspended solids might not be negligible in concentration and activity inside the MBBR (LIMA, DEZOTTI, *et al.*, 2016, PICULELL, WELANDER, *et al.*, 2014), the model has been successfully adapted to be used in relation to the total reactor volume instead of area (HOSSEINY, BORGHEI, 2002). The kinetic model can be seen in combination with the substrate steady-state mass balance in Equation (3.1).

$$\begin{aligned}
 r &= \frac{(C_i - C_e)}{HRT} \text{ (STEADY - STATE MASS BALANCE)} \\
 r &= \frac{U_{max} \left( \frac{C_i}{HRT} \right)}{K_B + \frac{C_i}{HRT}} \text{ (KINETIC MODEL)} \\
 \frac{(C_i - C_e)}{HRT} &= \frac{U_{max} \left( \frac{C_i}{HRT} \right)}{K_B + \frac{C_i}{HRT}} \tag{3.1}
 \end{aligned}$$

Where  $r$  is the volumetric rate of substrate removal;  $HRT$  is the hydraulic retention time;  $C_i$  is the influent substrate concentration;  $C_e$  is the effluent substrate concentration;  $K_B$  is the saturation constant; and  $U_{max}$  is the maximum substrate removal rate. Linearization of the model results in Equation (3.2).

$$\frac{HRT}{(C_i - C_e)} = \frac{K_B}{U_{max}} \left( \frac{HRT}{C_i} \right) + \frac{1}{U_{max}} \tag{3.2}$$

Basically, if plotting  $1/VRR$  (the inverse of the volumetric removal rate, VRR) against  $1/VLR$  (the inverse of the volumetric loading rate) results in good linear regression, then the  $K_B$  and  $U_{max}$  parameters can be calculated with the slope and interception of the obtained line. This plot was possible for reactor B since it was operated at three distinct HRT, generating sufficiently scattered VLR and VRR data.

Only data from lot 6, over the course of phases 3, 4 and 5, was used for the linear regression, after outliers removal by Cook's Distance analysis (section B.12), as those phases had similar N restriction.

Additionally, it can be demonstrated that the biodegradable fraction of the wastewater feeding an MBBR that fits to the Kincannon-Stover model is estimated by the ratio  $U_{max}/K_B$ , Equation (3.3), by assuming that maximum possible removal is attained in the limit when HRT tends to infinity (BRINK, SHERIDAN, *et al.*, 2017).

$$\lim_{HRT \rightarrow \infty} \left( \frac{C_i - C_e}{C_i} \right) = \frac{U_{max}}{K_B} \quad (3.3)$$

### 3.2.6. Batch Trials with Biomass Fractions for COD Removal

To examine individual maximum organic matter oxidation rate, batch trials were performed with both attached and suspended biomass fractions. A batch activity test was also performed with BioChip P carriers sampled at the full-scale BAS system installed at the P&P industry, at the end of operational phase 2.

For the attached biomass fraction batch trials, a known number of carriers was taken from the reactor, gently rinsed with tap water for removing suspended flocs adhered to the carriers and placed back in a clean closed reactor. It was filled with excess nutrients and a measured volume of fresh P&P wastewater previously subjected to filtration in a glass fiber filter (< 2  $\mu\text{m}$  pore size), to avoid interference from suspended solids eventually present in the feed. As for the suspended fraction batch assay, concentrated sludge from each MBBR was mixed with fresh filtered raw P&P wastewater, in a fixed proportion of 1 part of concentrated sludge to 4 parts of wastewater. The concentrated sludge was obtained by allowing the effluent that had recently been collected from the reactors to settle for 40 min, and then removing most of the supernatant.

The reactional medium, containing whether attached or suspended biomass, was kept at about the same temperature and DO as in continuous MBBRs operation. Samples of 6 mL were taken every 20 minutes for an assay duration of 4 - 7 hours, and then analyzed for tCOD and sCOD. For the batch assays conducted with the biofilm in phase 5, the duration was extended for more than one day until the COD stabilized, so that comparison of the final and initial COD content could indicate how much of the organic matter was biodegradable by the established microbial community.

Whilst substrates and oxygen are in excess, the removal rate equals the maximum removal rate and remains constant (HENZE, VAN LOOSDRECHT, *et al.*, 2008). When plotting concentrations against time, the slope of linear regression of initial data represents the maximum volumetric organic matter removal rate, as detailed in section B.11. For calculating the maximum surface and specific removal rates, corrections regarding the sampled volume were done for every data point. For calculating the specific maximum substrate removal rate from the suspended biomass batch trials, the pCOD at the start of the trial was defined as the content of suspended solids throughout the assay. Whenever necessary, the theoretical value of 1.42 g pCOD/g VSS was used to convert pCOD to VSS (HENZE, VAN LOOSDRECHT, *et al.*, 2008).

For a fair comparison between apparent and maximum removal rates, the former were calculated with average data from continuous reactors operation with the same wastewater lot and phase of the respective batch trial. All removal rates are expressed in terms of sCOD.

When comparing maximum removal rates and apparent ones for phases with nutrient limitation, it should be considered that the batch trials were not executed with such constraints. However, as the data from batch trials fitted properly a zero-order reaction model, the activity is independent of the concentration of substrates. Therefore, the maximum activity should be the same for a given microbial community whether exposed to excess or limitation of nutrients.

## 4. PESTICIDE RESEARCH: RESULTS AND DISCUSSION

This chapter presents and discusses the results obtained throughout the MBBR operation with the pesticide formulation wastewater. Naturally, for being a project that assessed the technical viability of substituting the secondary treatment existing in the treatment plant at an industrial site, details about the operation of the industrial treatment plant are frequently regarded (section 2.5.4).

### 4.1. MBBR General Aspects

Over the course of the MBBR operation, several events had the potential to alter the tendency and interpretation of the results. Overall, the events included: changes in sanitary wastewater lot; changes in industrial pesticide wastewater lot; and operational phase shifts. The timeline of the MBBR operation with the events that may influence the observed MBBR results is given in Figure 4.1. In graphs presented in the upcoming subsections of this chapter, labels are used to identify phase transitions and pesticide wastewater lot changes, assisting the interpretation of the results.

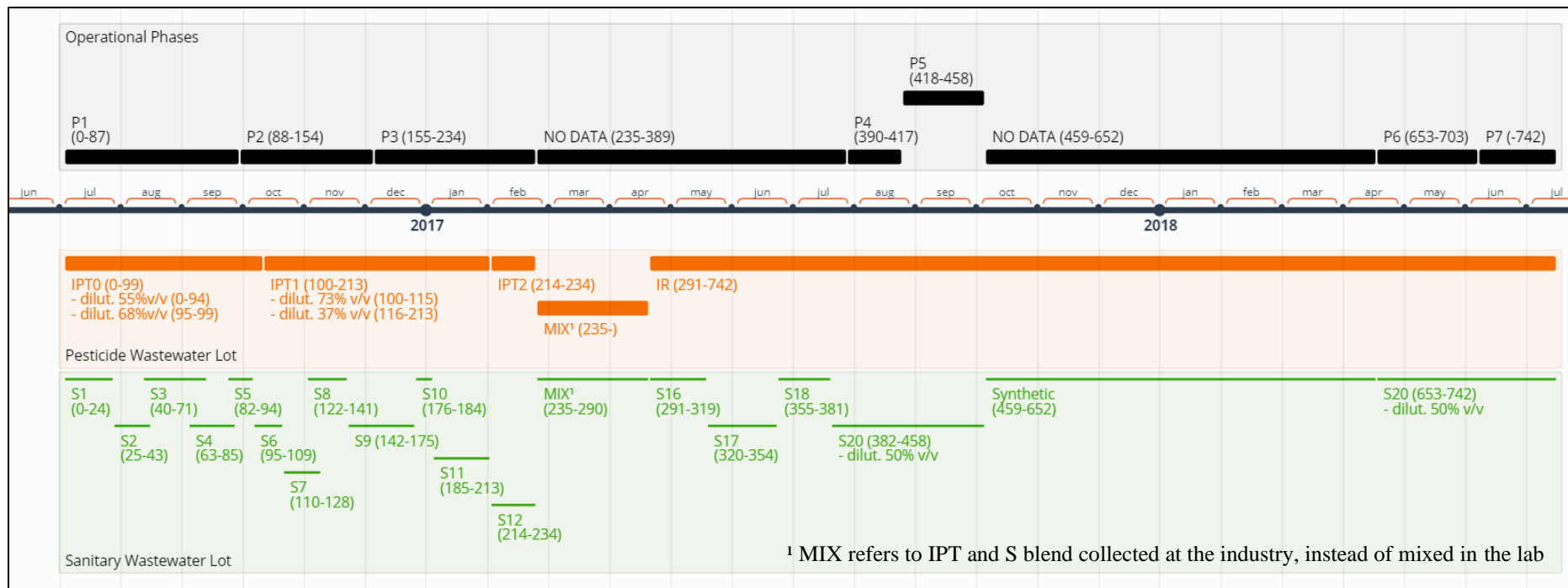


Figure 4.1 – Timeline of MBBR operation, with time range (in days) for each operational phase and wastewater lots given in parentheses as (start-end). Dilution of pesticide or sanitary wastewater with water is also specified, as percentage of IPT or S, whenever applicable. “NO DATA” correspond to periods with minimal monitoring, as explained in section 3.1.5.

The average values for the main monitored parameters, upstream and downstream the MBBR, are given in Table 4.1, for each operational phase.

Table 4.1 – Summary of MBBR average inlet and outlet monitored parameters in each operational phase.

Phase	tCOD (mg/L)			sCOD (mg/L)			TAN (mg/L)			TSS (mg/L)		VSS/TSS (%)		Turbidity (NTU)	
	in	out	%	in	out	%	in	out	%	in	out	in	out	in	out
<b>P1</b>	458	58	84	160	34	80	60	28.8	57	373	84	72	86	8.9	1.6
<b>P2</b>	838	207	74	458	122	74	39	26.1	36	291	100	67	93	27.8	13.0
<b>P3</b>	467	133	71	281	103	63	27	1.3	95	164	48	63	56	22.1	8.8
<b>P4</b>	442	160	64	309	136	55	30	14.8	50	82	49	72	71	57.0	19.1
<b>P5</b>	348	123	65	266	118	58	28	2.7	90	101	53	60	40	43.9	7.7
<b>P6</b>	530	223	55	388	148	66	31	7.2	77	49	39	38	59	28.2	18.1
<b>P7</b>	687	283	58	524	176	66	37	11.7	69	41	58	40	59	48.1	33.5

When assessing Table 4.1 with respect to influent tCOD and TAN, it can be seen that the reactor robustness has been tested throughout the operation, since the influent conditions surpass the average inlet characteristics of the industrial treatment plant (described in section 2.5.4, Table 2.17). For some dates, the inlet tCOD exceeded more than two times the nominal maximum (600 mg/L), whereas the average influent TAN was always more than two times the nominal average entering the industrial activated sludge plant (13 mg/L).

It is understood that the excess in comparison to the nominal operation of the industrial treatment facility is due to the sampling location for this research project. While the nominal values informed by the industry refer to concentrations past the equalization tank, the samples delivered to the laboratory were taken upstream of the equalization tank. As the tank is aerated at ambient temperature and has a long residence time (around 10 days), biodegradation most likely occurs prior to the treatment plant.

#### 4.1.1. Visual Observations

Before the results obtained are presented and discussed specifically, some relevant visual inferences may be done when looking naked eye to the MBBR and its effluent. The reactor, for instance, had intense scum formation (Figure 4.2) while the IPT had inadequate dilution (days 100 to 115, Figure 4.1), in phase 2, due to wrongly measured

IPT COD. During this span of time, the industrial portion of the organic load was twice the planned for phase 2.



Figure 4.2 – MBBR system showing scum formation during the inadequate IPT dilution (days 100 to 115, Figure 4.1).

The visual inspection of the inlet and outlet streams help evidencing the improvement of the aspect provided by the MBBR treatment. This is translated in reduced effluent parameters as COD, turbidity and suspended solids concentration, as seen in Table 4.1 and will be further addressed ahead. Examples of the appearance before and after the bioreactor are shown in Figure 4.3 for some dates. The least limpid appearance is for the date 27/10/16 (day 115), comprehended in the inadequate IPT dilution period.

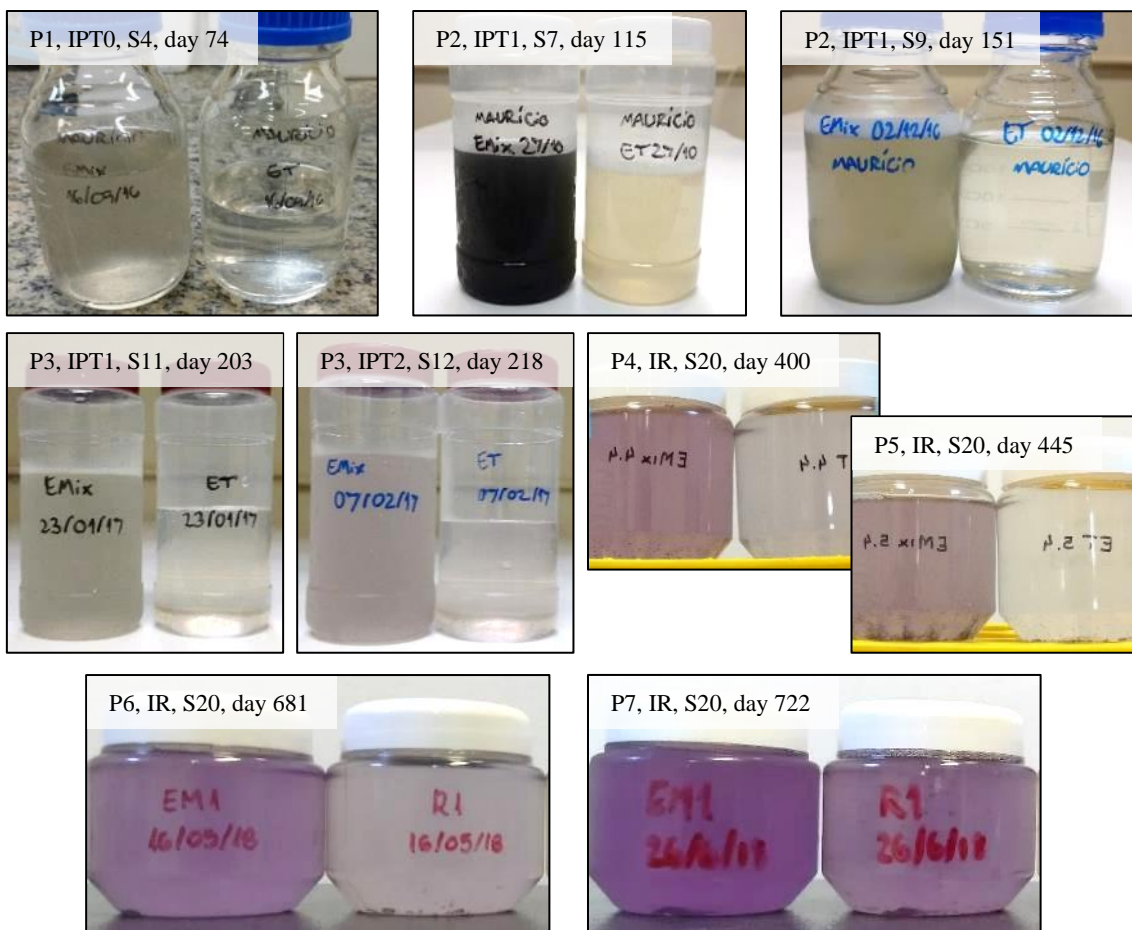


Figure 4.3 – Appearance of inlet (left) and outlet (right) streams of the MBBR. Phase, pesticide wastewater lot, sanitary wastewater lot, and day of operation are given in the upper left corner of each image.

Overall, observation of the carriers showed a uniform biofilm with normal thickness and density, with no apparent excessive sliminess. Starting at phase 4, the biofilm accumulated some purple color, which was the color of the IR wastewater. Example pictures of biofilm carrier taken via stereomicroscopy (section A.16) is shown in Figure 4.4.



Figure 4.4 – Stereomicroscopy micrographs of the biofilm carriers in phase 7.

### 4.1.2. pH

Effluent pH is one of the parameters specified by legislation, in the technical norm INEA NT-202.R-10, for the disposal of liquid effluents (INEA, 1986), as presented in section 2.4. The graph in Figure 4.5 evidences that for every phase the effluent pH is within the upper and lower limits established by the norm, 9.0 and 5.0, respectively.

As introduced in section 2.2.4.1, the optimal pH for nitrification lies between 7 and 8.5, even though it is possible with lower removal rates for lower pH values. Hence, in phases 1, 2 and 3, the average outlet pH was not a hindrance to the occurrence of nitrification and no adjustment to alkalinity was needed. Nevertheless, for some dates during phases 1 and 3, the pH was between 6 and 7.

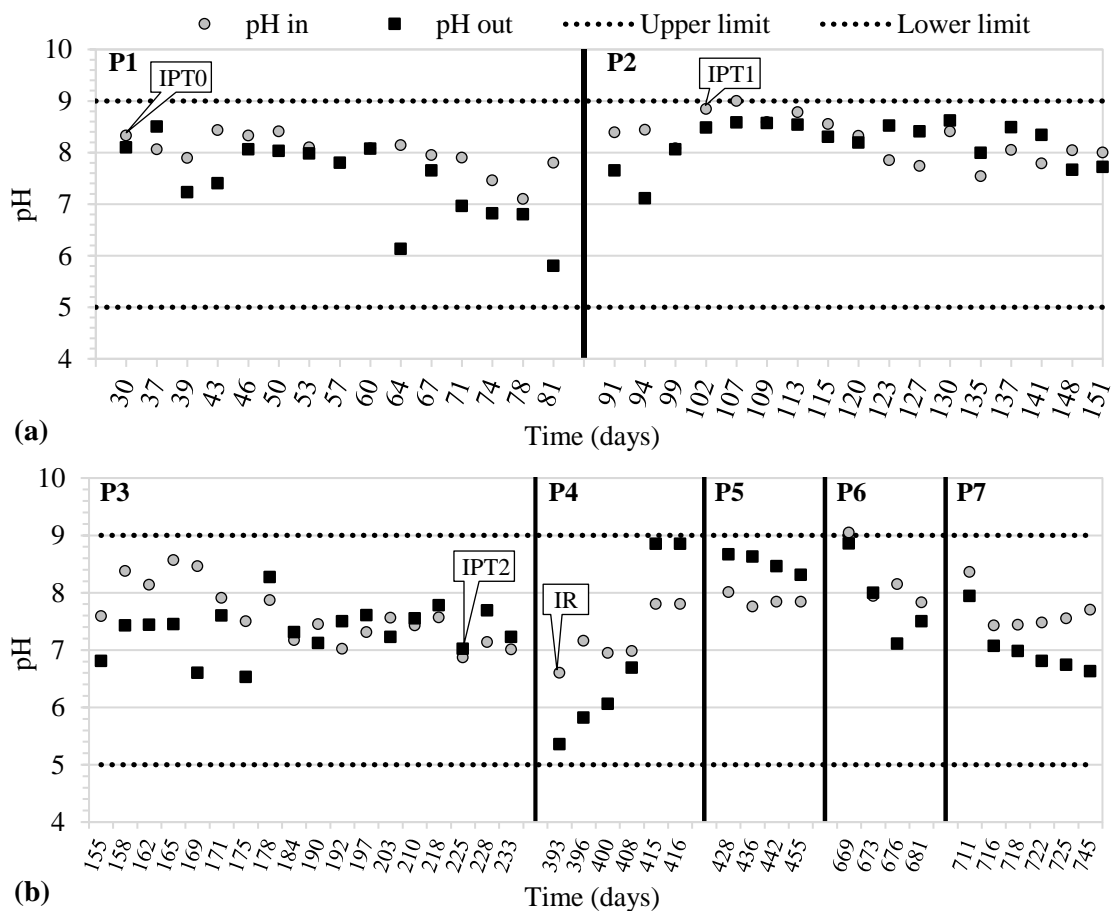


Figure 4.5 – MBBR inlet and outlet pH during phases 1 and 2 (a) and phases 3 to 7 (b). Text balloons identify changes in pesticide wastewater lot. Upper and lower discharge limits are given by dotted horizontal lines. Time, x-axis, is out of scale.

## 4.2. Organic Matter Removal

Time series of the inlet and outlet total COD – and the respective percentage removal - throughout all phases is given in Figure 4.6. Columns are divided into sCOD and pCOD fractions. Even if the INEA directive states limit in terms of total COD, it is relevant to evaluate the soluble and particulate fractions in order to understand what kinds of phenomena may be inducing the tCOD variance. For instance, excessive biofilm detachment or resuspension of decanted solids would bring up the pCOD, whilst the soluble portion would remain stable. In the graphs, text balloons indicate the change of the industrial wastewater lot used to prepare the reactor feed. Transitions from one phase to the following are depicted as black vertical lines and identified with P1, P2, P3, P4, P5, P6 and P7. Average tCOD values and their standard deviations for each phase were provided above, in Table 4.1.

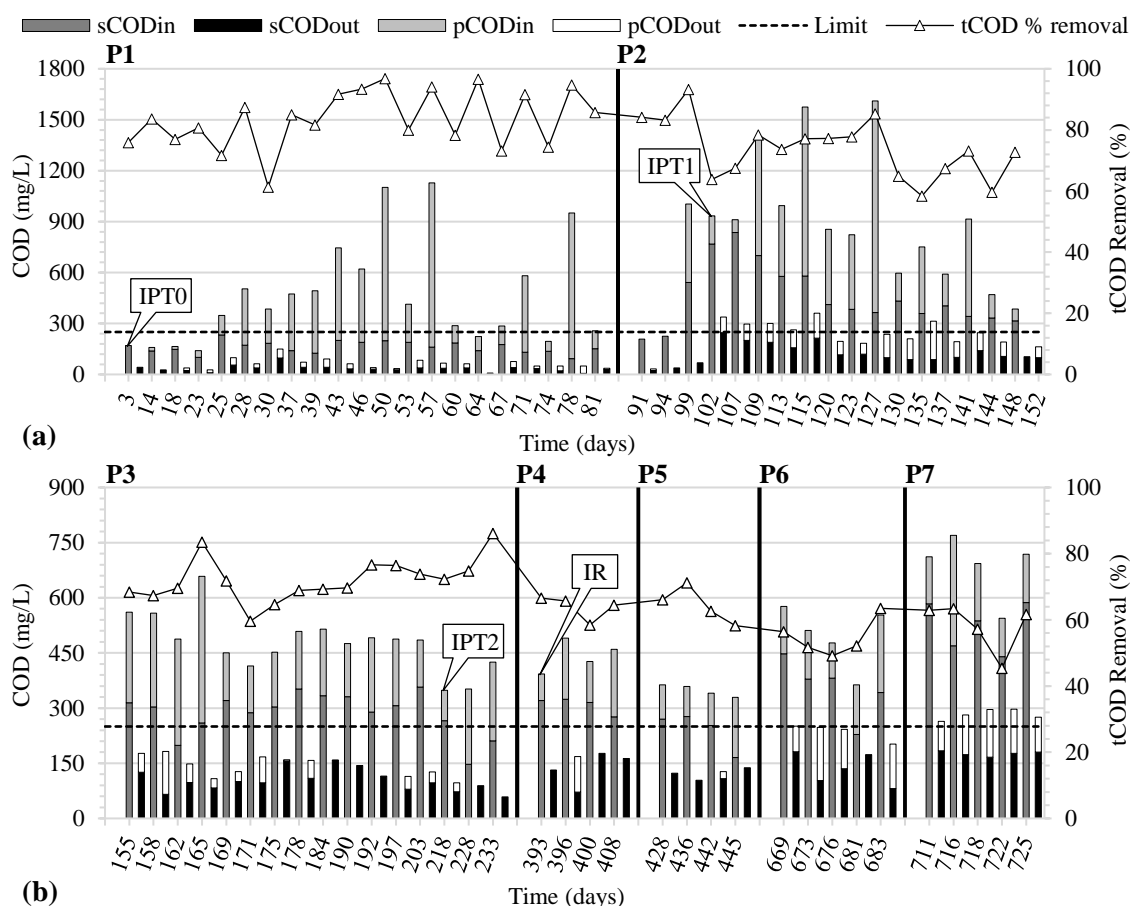


Figure 4.6 – MBBR inlet and outlet COD and removal percentage during phases 1 and 2 (a) and phases 3 to 7 (b). Text balloons identify changes in pesticide wastewater lot. The discharge limit is given by the dotted horizontal line. Time, x-axis, is out of scale.

Throughout phase 1, the total COD average removal was 83.5%, with mean effluent tCOD of 58 mg/L, presenting great variation, though always below the discharge limit of 250 mg/L imposed by local regulation (INEA, 2007). Meanwhile, the mean outlet sCOD was 34 mg/L. Nevertheless, assessment of sCOD is more realistic since, at real scale, any variations in outlet pCOD could probably be managed by a solid-liquid separation unit, usually the secondary clarifier. As the purpose of the lab-scale experiment was just the evaluation of the role of the bioreactor in the overall treatment, such a device was not installed in the bench setup. It should also be considered that the influent pCOD proceeded almost in its totality from the sanitary wastewater, usually of easy biodegradability.

At the beginning of phase 2, after doubling the proportion of the pretreated industrial wastewater (IPT) from 4% to 8% (v/v), the reactor performance remained quite stable, although for this period the COD of the sanitary wastewater was particularly low.

Along the change of the lot of IPT (IPT 0 to IPT 1) there was a period that the dilution described in section 3.1.3 was inadequate, particularly from days 100 to 115, raising considerably the inlet sCOD. Therefore, during this span of time, the average outlet sCOD increased significantly from 43 mg/L (IPT 0, phase 2) to 201 mg/L (IPT 1, days 100 to 115). In terms of total COD, the legal limit was exceeded within this period due to the particulate fraction. After correcting the dilution, the average outlet sCOD remained 106 mg/L to the end of phase 2 (days 120 to 152), while tCOD was below the 250 mg/L legal threshold. The exception was the day 135, at which abnormally high pCOD is observed – as seen in Figure 4.6 – likely due to accidental manual agitation of the MBBR content during the sampling process, resuspending solids decanted in the corner bottom of the reactor.

As phase 3 started, the HRT was adjusted from 3 to 6 h. Nevertheless, the outlet sCOD with IPT 1 did not change (110 mg/L, days 155 to 203), suggesting that the remaining COD was not biodegraded by the existing microbial community for that HRT/contact time with the waste stream. This means that the HRT of 3 h was enough to achieve maximum organic matter removal for that wastewater quality, as is confirmed by comparing the maximum and apparent removal rates (section 4.4). Theoretically, there may be a critical HRT that would lead to a wastewater-biomass contact time high enough for the growth and thrive of more specialized microorganisms that could further degrade the industrial compounds. In this scenario, the easily biodegradable matter could be degraded mainly by the suspended biomass and free-living bacteria, that are present in higher quantity for superior HRT, if the organic load suffices (PICULELL, WELANDER, *et al.*, 2014).

Finally, the average effluent sCOD when changing industrial wastewater lot to IPT 2 was lower, close to 74 mg/L (days 218 to 233), until the end of phase 3. These observations about the remaining sCOD show how the simple seasonal variation of the industrial wastewater can significantly change the performance of the reactor due to the existence of different fractions of persistent organic matter.

Starting in phase 4, the industrial lot was changed to raw pesticide wastewater (IR) which was fed to the reactor at growing proportions from 2 to 4% v/v. In Figure 4.7, it can be observed that the average outlet sCOD increases somewhat linearly for growing fractions of influent sCOD coming from the IR. This points out to a crescent amount of persistent sCOD in the reactor effluent concurrent to the raise in IR proportion, even if

the reactor was operating only at low to moderate organic loading rates (i.e., 5 to 15 gCOD/(m<sup>2</sup>·d)) (VAN HAANDEL, VAN DER LUBBE, 2012).

When relating the average sCOD removal with the incoming IR sCOD portion (Figure 4.7), both expressed in concentration units (mg/L), a linear tendency shows that 0.65 mg/L of sCOD is depleted for each unit increment of influent IR sCOD to the MBBR. In other words, 65% of the industrial COD is degradable by the MBBR, and removals higher than that are only possible since the IR is mixed with S, that is, most likely, more biodegradable. One should notice that these inferences from the series presented in Figure 4.7 are only possible because the sanitary part of the feed remained sufficiently stable, so that changes in sCOD removal and outlet sCOD can be attributed solely to increments in IR content.

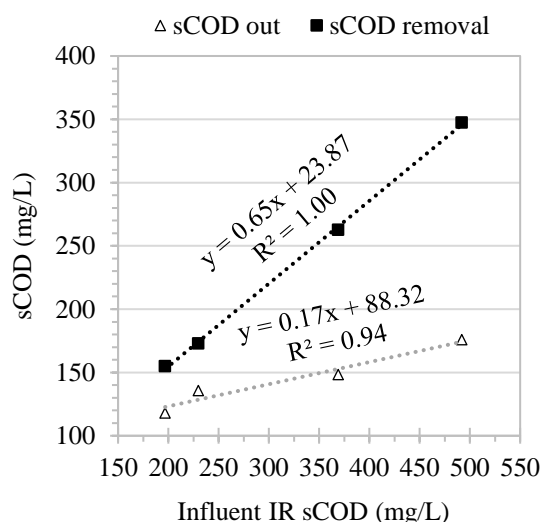


Figure 4.7 – Mean value of outlet sCOD and removal of sCOD in relation to influent IR sCOD (phases 4 to 7).

In phases 6 and 7, the sCOD of the sanitary wastewater was particularly low due to its degradation during storage, responding for only 8% and 4%, respectively, of the sCOD fed to the MBBR. Consequently, it was expected that the reactor performance was governed by the IR biodegradability level. Indeed, the inferred 65% sCOD degradability of the IR is very close to the average sCOD percentage removal for phases 6 and 7 (Table 4.1), both 66%. Therefore, the reactor was working at its full potential for that biomass-wastewater contact time and biofilm maturity. The latter might be a crucial factor for determining the biodegradability of certain wastewater as the biomass might continuously specialize in biofilms for long times, especially for heavily polluted industrial waste

streams. Under full-scale (industrial) scenario and long operation times, it may be possible that once recalcitrant compounds could be made susceptible to biodegradation by immobilized biomass harbored in the plastic media.

Phases 2 and 3 have shown that the IPT proportion can be pushed up from 4% to 8% v/v while still respecting the norm discharge threshold of COD of 250 mg/L, considering efficient solids removal. Still, environmental responsibility needs to be taken into consideration as higher proportions of industrial wastewater will mean greater fractions of non-biodegradable pesticide compounds reaching water bodies. The same can be said for when changing feed to raw pesticide wastewater mixture but still getting effluent within the COD limit, as seen for the effluent sCOD from phases 4 to 7. It should be highlighted that pesticide substances may be harmful even in very low concentrations, standing as micropollutants, and their further removal by means of tertiary treatment options should be strongly considered (LUO, GUO, *et al.*, 2014).

Dissolved organic carbon analysis were performed only during the initial 3 phases of the MBBR operation. Therefore, the discussion of organic matter removal performance is completely done in terms of COD. However, it is valuable to register the obtained average ratios sCOD/DOC, as listed in Table 4.2. Soluble COD is used instead of the tCOD to eliminate the influence of the great variation of pCOD in the feed, thanks to the sanitary portion.

Table 4.2 – MBBR influent and effluent sCOD/DOC ratio for operational phases 1 to 3.

Phase	Inlet sCOD/DOC	Outlet sCOD/DOC
P1	3.8 ± 0.9	4 ± 2.1
P2	3.1 ± 0.4	3.3 ± 2.6
P3	3.4 ± 0.4	2.9 ± 1.2
Mean	3.4 ± 0.7	3.4 ± 2

Quite variable with the nature of the wastewater is the COD/TOC ratio. The higher the value, the greater might be the amount of inorganic compounds liable to oxidation, in the COD analysis, that is present in the sample. Domestic sewage presents COD/TOC ratio close to 2.3, while industrial wastewaters may have values higher than 20 (DEZOTTI, 2008). As seen in Table 4.2, the values are closer to what is expected for wastewaters of sanitary nature, which is in accordance with the fact that the feed mixture was 92-96% v/v sewage for the assessed phases.

### 4.3. Nitrogen Removal

As may be seen in section 3.1.1, there was almost always considerable TAN content in the feed of the MBBR. The mechanisms of nitrogen removal and nitrification performance were monitored during the operation and the results are presented and discussed below.

#### 4.3.1. Removal Mechanism and Nitrogen Species Distribution

In the feed, nitrogen was present majorly as ammoniacal nitrogen, on average  $96\pm 4\%$ , whilst nitrate and nitrite were practically absent whenever analyzed. The industrial wastewater may constitute a relevant source of organic nitrogen, however, its dilution with the sanitary sewage diminishes the importance of TN coming from the industrial portion. Also accounting that the TN was not monitored after phase 3 (due to technical issues) and that there were relevant inconsistencies related to the TN results, then the nitrogen removal will be quantitatively described in terms of total ammoniacal nitrogen. Finally, it is possible that an important part of the organic nitrogen in the IR is not liable to ammonification, passing inert through the reactional volume.

In the MBBR effluent, nitrite was present in concentrations lower than 1 mgN/L most of the time, whereas nitrate was measured in levels that indicate TAN removal by nitrification, regardless of quantification issues that made it difficult to state accurate values. The approximate distribution of the inorganic nitrogen species in the MBBR is shown in Figure 4.8. Nitrate responded on average for 92% of the sum of oxidized nitrogen forms (i.e., nitrate and nitrite). It is qualitatively safe to assume that the main mechanism of ammonia removal was nitrification. The presence and relative abundances of AOB and NOB (section 4.3.3) reinforces this statement.

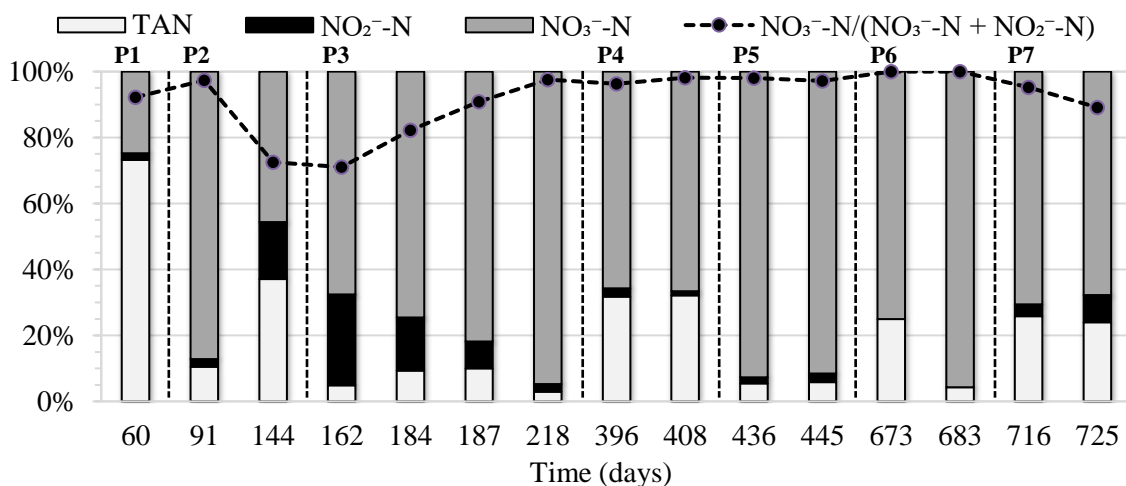


Figure 4.8 – Relative distribution of inorganic nitrogen species in the MBBR effluent for various operating days. Vertical dashed lines depict phases transitions. Time is out of scale

Nitrogen species distribution in the liquid phase was assessed as described in section B.5. Some of the quantitative issues observed with the nitrogen species distribution include: i) negative organic nitrogen when subtracting the sum of inorganic species from TN; ii) outlet TN much higher or lower than the incoming TN, which could only be justified for small or medium differences; iii) generated nitrate and nitrite substantially greater than the removed TAN, which is even more inconsistent when not ignoring that some nitrogen is anabolized. Therefore, it was decided to only discuss the species distribution qualitatively.

Considering 12.4% of the biomass as nitrogen, assuming that the incoming suspended solids were completely degraded in the MBBR, and that the outlet volatile suspended solids are the produced biomass, then assimilation of nitrogen by anabolism was calculated (as explained in section B.7). It corresponded on average to 12% of the removed TAN, for phases 5, 6 and 7, where the assumptions could be taken more safely as inlet suspended solids were much lower.

Free ammonia concentration in the liquid phase was estimated based on the ammonia/ammonium equilibrium (METCALF & EDDY, TCHOBANOGLOUS, *et al.*, 2003) and it represented less than 4% of TAN most of the time for the prevailing operational temperature and pH, as calculated by Equation (B.7), section B.6. Thus, even if the medium chemical composition, ionic strength and the airflow could shift the

equilibrium towards free ammonia, it is plausible that ammonia volatilization had little significance in TAN removal.

Under certain conditions, intermediate steps of the nitrification process may lead to N<sub>2</sub>O production. It may be stripped off by the air stream going through the reactor; or even oxidized by heterotrophic denitrifying bacteria present in deeper zones of the biofilm, where oxygen availability is rather low (BOTHE, FERGUSON, *et al.*, 2007). Despite being of little relevance quantitatively for the overall nitrogen balance, nitrous oxide is a potent greenhouse gas, 300 times stronger than carbon dioxide. So, even low amounts emitted are important to account for (KAMPSCHREUR, TEMMINK, *et al.*, 2009). Therefore, by the end of phases 4 and 5, the off-gas was sampled and analyzed for N<sub>2</sub>O content, resulting in, respectively, 423 ppb and 180 ppb emitted, that is, discounting the N<sub>2</sub>O content in the atmospheric air.

#### **4.3.2. Nitrification Performance**

The time series of inlet and outlet TAN concentration for all experimental phases, accompanied by their respective percentage removal, are presented in Figure 4.9. Black vertical lines depict the transitions from one phase to the following and are identified as P1, P2, P3, P4, P5, P6 and P7. The change of the industrial wastewater lot used to prepare the reactor's feed is indicated in text balloons. Table 4.1 shows the averages of the data presented in the graphs.

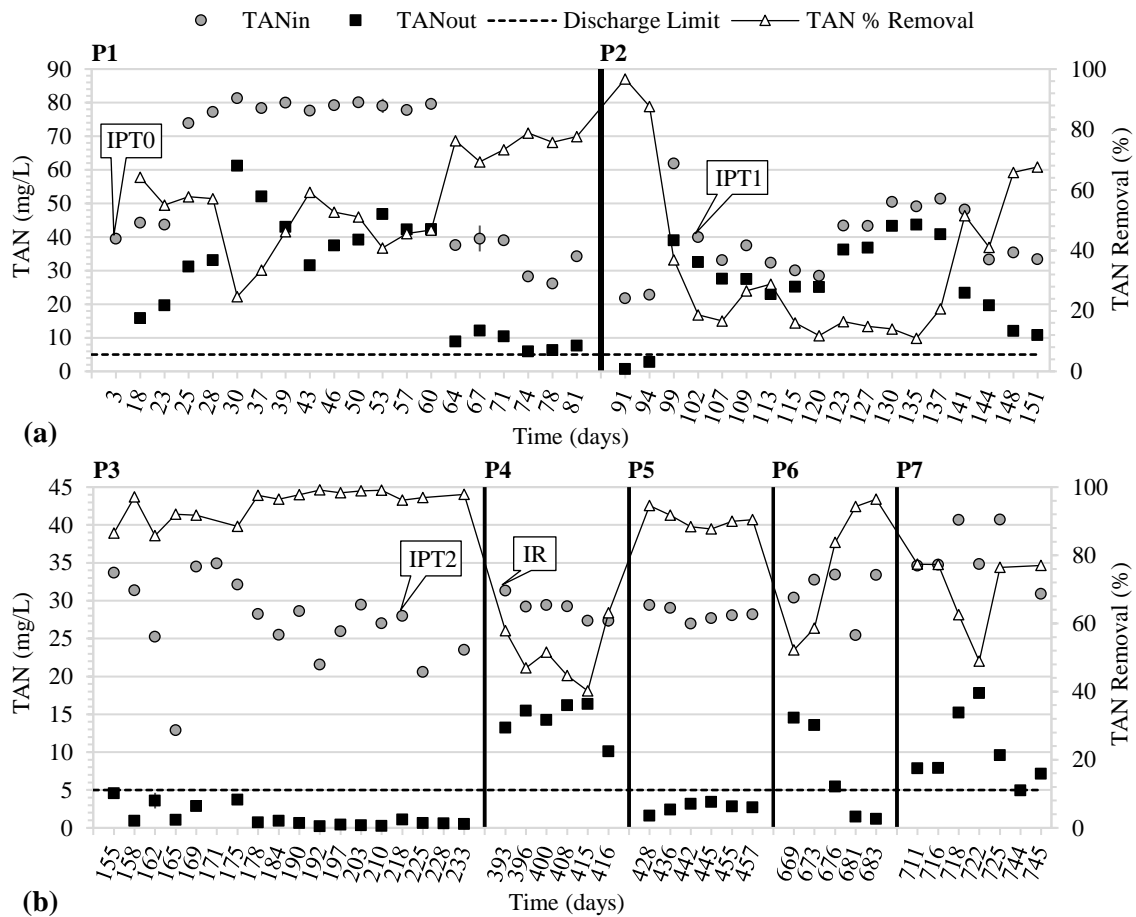


Figure 4.9 – MBBR inlet and outlet TAN concentrations and removal percentage during phases 1 and 2 (a) and phases 3 to 7 (b). Text balloons identify changes in pesticide wastewater lot. Time, x- axis, is out of scale.

The time period from days 25 to 60, within phase 1, is highlighted with an average inlet TAN of approximately 80 mg/L. During that time span, the effluent was never below 30 mg/L on TAN, considerably above the maximum of 5 mg/L demanded by the local technical norm INEA NT-202.R-10 (INEA, 1986). Nevertheless, this feeding condition is unlikely to happen on real scale, where the typical TAN concentration is 13 mg/L (section 2.5.4). Right after the shift of the S lot responsible for the high TAN content, immediate raise in TAN removal efficiency was noticed.

Although the HRT increase was not relevant for the COD removal, the same cannot be said about the TAN removal, that rose concurrently to the HRT raise in phase 3, as can be seen in Figure 4.9 (b).

During phases 1 and 2, the effluent TAN was most of the time higher than the regional discharge limit of 5 mgN/L (INEA, 1986). TAN removal varied substantially but had low averages of 57% and 36% in phases 1 and 2, respectively. It was particularly low

when the sCOD was higher, from days 99 to 137, averaging only 19%. It was in this time span that the expressive raise of the organic load fed to the MBBR, consequent to the beginning of phase 2 and the incorrect dilution of IPT1 (days 100-115, Figure 4.1). The reason for the low TAN removal is possibly related to the competition of nitrifiers with heterotrophic organisms in the biofilm for oxygen, nutrients and space due to high availability of organic matter and faster growth of heterotrophic microorganisms compared to autotrophic nitrifiers. There can also be some inhibition caused by substances present in the industrial wastewater IPT1. Inhibition by ammonia may be discarded because a similar TAN concentration – around 40 mg/L – was registered between days 64 and 81 with good associated TAN removal. Doubling the HRT in phase 3 attenuated these factors and TAN removal reached almost completion, 95% on average, with mean effluent TAN of 1.4 mg/L. Changing the IPT1 for IPT2 during phase 3 had no impact on nitrification performance.

The feed TAN concentration was almost always 2 or more times the nominal value informed by the industry (13 mg/L, section 2.5.4). The reason for such difference is, probably, because in the industrial treatment plant there is an aerated equalization tank with HRT in the order of 10 days. That is a long residence time and, with aeration and environment temperature above 20°C, there is probable biodegradation of pollutants in the aeration tank itself. Equalization was not necessary or replicated in the lab-scale system. All along phases 4 to 7, the average inlet TAN concentration of 32 mg/L is representative regardless of the proportion of raw industrial wastewater in the influent, as the TAN was coming mainly from the sewage portion and it was stable through the period.

Once the feed started being prepared with the IR, the average inlet pH significantly decreased to 6.9 when compared to the average 7.9 for phases 1 to 3. As a consequence, the pH in the reactor went down to a mean value of 6.0 in phase 4. This is far from the optimal range of 7 to 8.5 for nitrification (VAN HAANDEL, VAN DER LUBBE, 2012) and could explain the limited TAN removal over the course of phase 4, with an average 14.8 mg/L outlet TAN. Hence, phase 5 presented the same approximate 2% proportion of industrial raw wastewater but with adjustment of alkalinity by the addition of sodium bicarbonate in the proportion to guarantee the equivalent of 7.14 g CaCO<sub>3</sub>/g removed TAN (VAN HAANDEL, VAN DER LUBBE, 2012). The raise in nitrification performance reflects the importance of that adjustment, as for phase 5 the mean removal

was 91% compared to 50% in phase 4. The average effluent TAN was 2.7 mg/L, always below the discharge limit.

As the IR proportion was increased from 2 to 3% v/v in phase 6, the TAN removal immediately dropped to 52%. However, it was consistently recovered through the days reaching an average of 95% in the last two operational days of phase 6, with 1.3 mg/L of effluent TAN. Increasing the non-pretreated industrial load in phase 7 had again a negative impact on nitrification, as the average removal went down to 69% and the effluent TAN concentration increased up to 11.7 mg/L, not showing early signs of recovery. Because the only changed parameter from phase 5 to 7 is the IR proportion, possibly it led some substances to inhibitory concentrations. This may be better evaluated by assessing the relative abundance of AOB and NOB over the course of the study.

#### 4.3.3. Assessment of Nitrifying Community (AOB and NOB) by FISH

Samples of biofilm taken from the reactor at the end of phases 2 to 7 were fixed for subsequent fluorescence in situ hybridization (FISH), as detailed in section A.17. Relative abundance percentages of AOB and NOB in relation to the total bacterial population were obtained. The average results are graphically summarized in Figure 4.10. Examples of images taken are shown in Figure A.3, section A.17.

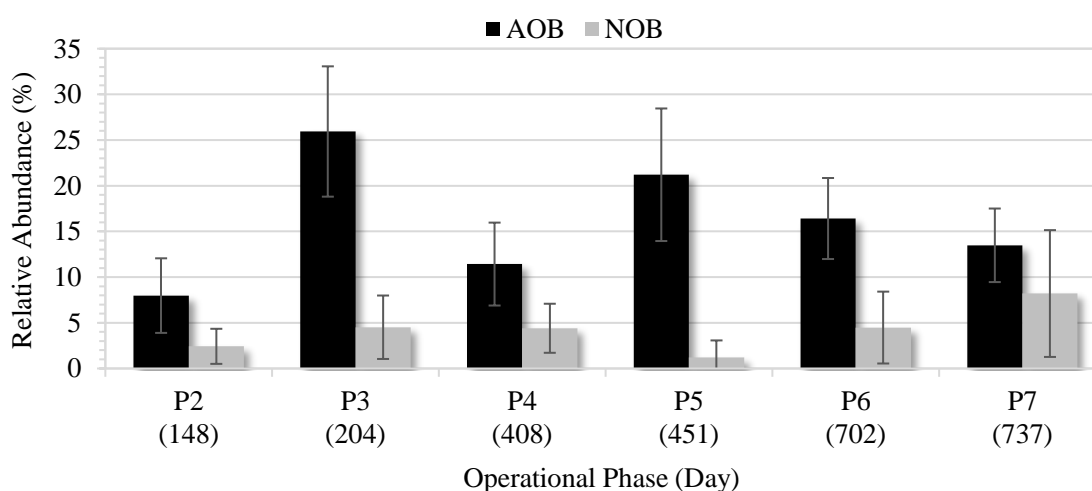


Figure 4.10 – Relative abundance of AOB and NOB in relation to the total bacterial community at the end of phases 2 to 7, as determined by FISH analysis.

In all operational phases, AOB and NOB were detected with a greater abundance of the former in relation to the latter, by a factor of 2.6 to 18 times. As discussed in section 2.2.4.1, NOB are slower-growing organisms in comparison to AOB, especially at higher temperatures, besides having much lower cell yield (GRADY, DAIGGER, *et al.*, 2011, MULDER, 2014). Therefore, it is plausible that AOB were always more abundant than NOB. Also, it helps clarifying the fact that no statistically significant difference is observed for NOB abundance from phase to phase.

By comparing phase 2 with phase 3, AOB relative abundance increased from around 8% to 26%. This result is consistent with the previously discussed results that showed the enhance of nitrification performance concurrently to the HRT raise. Nevertheless, when moving to phase 4, the AOB community diminished significantly to 11.4%. Two distinct effects are likely responsible for that: (i) the change to the raw industrial wastewater - whose components could exert some inhibitory effect on ammonium oxidizers -, (ii) and the insufficient alkalinity. This last effect (ii) is reinforced with the transition to phase 5, as the proportion of AOB increased to 21.2% when alkalinity in the feed started to be adjusted. Then, the abundance of AOB decreased stepwise to 16.4 and 13.5% in phases 6 and 7, respectively. Since for phases 5 to 7 the only change was the proportion of IR, with constant incoming TAN concentration, the possibility of inhibitory effect over AOB is supported. The comparisons made in this paragraph are supported by ANOVA statistics with 95% confidence, and 90% when comparing phases 5 and 7.

Meanwhile, despite the lack of statistical significance of the difference in the relative abundance of NOB from phases 5 to 7, it seems clear that the inhibitory effect on AOB was not observed on NOB. If some remarkable inhibition affected the NOB population, nitrite accumulation could be an outcome, but it was not observed during the reactor operation (Figure 4.8). A study with 100 substances of industrial relevance revealed that the AOB are more prone to inhibition by organics than NOB (GRADY, DAIGGER, *et al.*, 2011, HOCKENBURY, GRADY, 1977).

It is remarkable that even in the presence of a complex industrial matrix, the nitrifiers always represented more than 10% of the microbial community. It is true, however, that organic load did not pose as an impediment for most of the MBBR operation, as it was, most of the time, low to moderate (5 to 10 g/(m<sup>2</sup>·d)) (VAN HAANDEL, VAN DER LUBBE, 2012)), or even low (< 5 g/(m<sup>2</sup>·d)), if considering the limited biodegradability.

The maximum nitrifying activity obtained in the batch trials, presented below, may give support to the statements made regarding the inhibitory effect on AOB resulting from the increment of IR concentration.

#### **4.4. Biofilm Batch Trials**

The curves of sCOD concentration over time for the batch trials performed at the end of each operational phase are contained in Figure 4.11, as well as the TAN concentration curves. Data points that were used for linear regression and calculation of the maximum removal rates have red outlines. Batch trials were performed under pseudo-stationary conditions at the end of each operational phase, as specified in section 3.1.7.

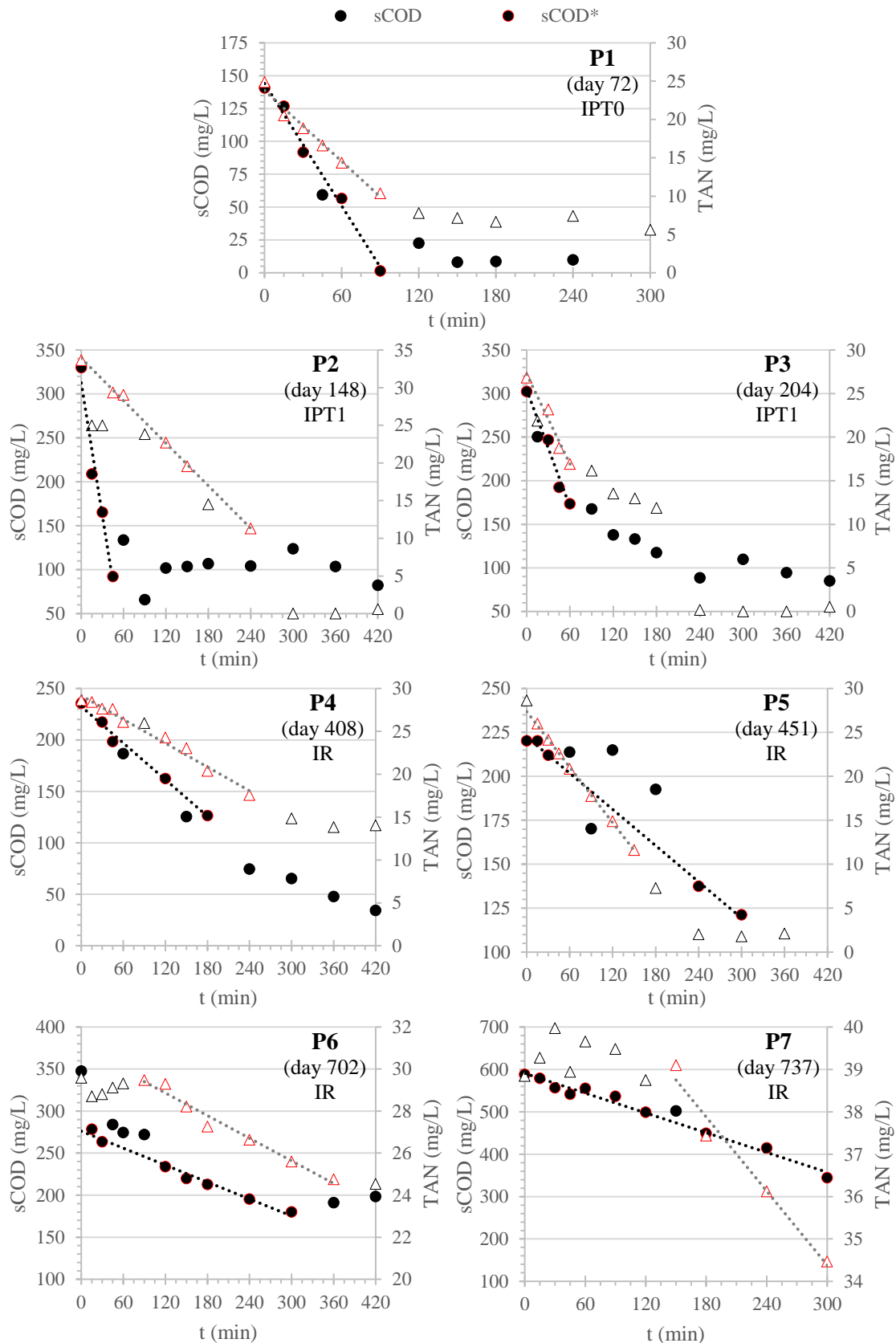


Figure 4.11 - sCOD (black circles) and TAN (white triangles) over time for batch trials, from phases 1 to 7 (P1 to P7). The data points with red outline were used to calculate the maximum removal rates.

For phases 1, 2, 3 and 6, the maximum sCOD removal seemed to be attained within the duration of the batch trial, reaching somewhat stable final sCOD that were comparable with average effluent sCOD from continuous operation at the end of each respective phase. Despite not reaching a final stable level of sCOD, the removal during batch trial for phase 5 was also close the continuous operation removal. For phase 1, when the industrial load was lower, the maximum removal was achieved between 1 and 1.5 h duration; on phase 2, it took between 45 min to 2 h; on phase 3, between 3 and 4 h; and on phase 6, somewhere between 4 and 5 h is needed to get to sCOD final level. As in the 4 phases the time required for maximum removal was below the continuous operation HRT, it is expected that raises in HRT would not extend the removal of organic matter.

Final sCOD values were around 10 mg/L in the batch trial of phase 1, and close to 100 mg/L for batch trials of phase 2 and 3. The vast difference demonstrates the increase of the non-biodegradable organic matter fraction comparing the IPT1 lot (collected in the industrial site) to the IPT0 lot (produced in the lab). If the recalcitrant fraction was of equal magnitude, then 20 mg/L sCOD would be expected after maximum removal in batch trials of phases 2 and 3. It helps to show how seasonal variations of the pesticides formulation may significantly change the non-biodegradable fraction.

In the first 5 batch trials, maximum TAN removal was obtained within the test duration, reaching a considerably stable level. In phase 1, it took between 1.5 to 2 h to achieve final TAN concentration; in phase 2, necessary time was between 4 and 5 h; from 3 to 4 h in phase 3; from 4 to 5 h in phase 4; and from 3 to 4 h in phase 5. As in phases 1, 3, 4 and 5 the required time to get to the minimum TAN content was lower than the HRT, it may be inferred that increases in HRT would not provide wider TAN removal. However, for phase 2 time for maximum nitrification was higher than the HRT. Therefore, it was expected that bringing up the HRT, when switching to phase 3, would improve the nitrification efficiency, which was confirmed as discussed in section 4.3.2.

Final concentrations reached in the trials for phases 1, 3, 4 and 5 are compatible with the effluent TAN quantified for dates next to realization of the batch trials. With regards to phase 2, the TAN concentration at 3 h of the batch removal curve - that was the HRT for that phase - is consistent with the outlet TAN registered for the last dates of phase 2.

The linear regressions done for the red-outlined data points of each dataset confirm the zero-order kinetics regarding the removal of sCOD and TAN, with correlation

( $R^2$ ) over 0.95 in all cases. Table 4.3 presents the calculated maximum specific removal rates, as detailed in section B.11, and the biofilm quantifications that followed the batch trials at the end of each operational phase. The TAS was expressed in  $\text{g/m}^2$  but also in  $\text{g/L}$  for better comparison with the TSS results. For each phase, Table 4.3 also shows the average apparent specific removal rate (section B.11) from operational days during which the reactor feed had the same composition as that used for each respective batch trial. The restraint to those days allowed a more accurate comparison with the maximum specific removal rates results. Total suspended solids concentrations from those dates were also used for calculating the fraction of suspended solids within the total (suspended and attached) biomass ( $f_{SS/TS}$ ).

Table 4.3 - Biofilm quantification, fraction of suspended solids in the MBBR ( $f_{SS/TS}$ ), apparent specific removal rates and maximum specific removal rates for each phase.

Phase	TAS (g/L)	TAS (g/m <sup>2</sup> )	$\frac{\text{VAS}}{\text{TAS}}$ (%)	TSS <sup>a</sup> (mg/L)	$f_{SS/TS}$ <sup>b</sup>	Specific Removal Rate			
						(mg sCOD/gVS.h)		(mg TAN/gVS.h)	
						Max <sup>c</sup>	App. <sup>d</sup>	Max <sup>c</sup>	App. <sup>d</sup>
P1	4.5	17.8	85	50	1.1%	20.3	8.9	2.2	1.9
P2	1.4	5.6	96	80	5.3%	188.3	46.4	3.7	4.1
P3	2.3	9.2	86	54	2.3%	61.9 12.6	16.3	4.9	2.0
P4	2.6	9.9	96	49	1.9%	17.0	10.5	1.5	0.9
P5	4.3	16.3	77	53	1.2%	8.0	6.1	2.1	1.3
P6	6.9	27.1	88	39	0.6%	10.1	5.6	0.6	0.7
P7	5.3	20.8	89	58	1.1%	38.1	10.9	1.5	1.0

<sup>a</sup> Average for the days with the same feed as that used for the respective batch trial.

<sup>b</sup> Calculated by the ratio of TSS to the sum of TAS and TSS.

<sup>c</sup> VS equals VAS, as in the batch trials only attached solids were present (section 3.1.7).

<sup>d</sup> VS equals VAS plus VSS, as this rate is related to continuous operation (presence of both biomass fractions).

The volatile attached solids concentration falls in between, or above, the typical range of a conventional activated sludge system, 1.5 to 5.0 g VSS/L (VON SPERLING, 2007c), offering equal or higher capacity in much lower volume with higher sludge age due to solids immobilization in the plastic media. Also, the TAS values are compatible with the typical range reported for MBBRs, i.e., 2 – 8 g/L (VAN HAANDEL, VAN DER LUBBE, 2012).

On the other hand, the suspended solids in the reactor accounted, on average, for only 1.9% of the total biomass, with a maximum of 5.3% in phase 3. These results are similar to those found in other studies where MBBR systems were used as biological treatment stage for industrial wastewater (BACHMANN PINTO, MIGUEL DE SOUZA, *et al.*, 2018, BASSIN, RACHID, *et al.*, 2017, CAO, FONTOURA, *et al.*, 2016). The low contribution of the suspended sludge to the total solids in the reactor implies that the apparent specific removal rate is mainly attributed to the attached solids activity. Therefore, the comparison between the apparent specific removal rate and the maximum specific removal rate is fair. It should be noticed that this does not mean that the suspended biomass had a low specific removal rate. In fact, it could be even higher than the biofilm specific removal rate because the planktonic solids are not exposed to oxygen and substrates diffusion limitations.

Neither the change from IPT to IR, from phase 3 to 4, nor the increase in the IR proportion from phases 4 to 7, showed to cause biofilm detachment, as the  $f_{SS/TS}$  remained low and quite stable. Thus, it is possible to infer that the reduction in nitrification performance was not due to biofilm loss, but likely attributed to some industrial wastewater components, which were present in higher concentrations when the proportion of either IPT or IR was increased. In fact, VAS reached levels much higher than in phase 3, where the best performance in nitrification was achieved, reaffirming that reductions in nitrification performance were not due to biofilm losses.

When assessing the amount of volatile attached solids within the total attached solids, it is noticeable that, except for phase 5, it was characteristic of sludges with a low accumulation of inorganic material, exhibiting VAS/TAS ratio within 85% to 90% (VAN HAANDEL, VAN DER LUBBE, 2012). This does not mean that the influent stream is free or low in inorganic solids but implies that this particulate inert material was not accumulating in the biofilm. Such observation is relevant as it shows the biofilm does not tend to lose its capacity of metabolizing pollutants due to inert material accumulation.

Regarding the sCOD, for all experimental phases, the maximum specific removal rate exceeded 1.8 to 12.5 times the rate observed during normal operational conditions. This is expected as the reactor is designed to provide nitrification, requiring higher HRT and resulting in lower organic loading rates than if only COD abatement was desired. The HRT is, thus, designed to guarantee the ammoniacal nitrogen removal, significantly overcoming the needed contact time for biodegradable organic matter metabolism.

In the batch trial of phase 3, two consecutive linear trends were observed, allowing two different sCOD maximum removal rates to be calculated, as seen in Figure 4.11. This is probably due to the depletion of the most easily biodegradable substrate fraction at the beginning of the batch test, leading to a shift in the removal rate to a lower value as the experiment progressed. However, it is unclear why the same trend was not observed for other batch trials.

Maximum TAN specific removal rates were much closer to the apparent ones than what is observed for the COD removal rates, with a maximum difference of 2.2 times in phase 3. It makes sense that the highest ratio between the maximum and apparent rates was found in those particular experimental conditions, as it had the greatest nitrifying performance, as displayed in Table 4.1 and Figure 4.9b. In the other phases, the apparent rate was nearer to the maximum removal rate, meaning that the reactor was operating closer to the edge of its nitrification capacity.

It is important to consider that, during the batch trials, the biofilm was exposed to higher industrial load in comparison to regular operation. Therefore, substances that can possibly inhibit the metabolism of some microorganisms were present in greater concentrations. In fact, when observing Figure 4.11, it is seen that the batch assays carried out in phases 6 and 7 had delayed start of TAN removal and reached final concentrations (24.5 and 34.5 mg/L) much higher than the effluent averages during continuous operation for such phases (7.2 and 11.7 mg/L). Supposition is made that the nitrification began only after the heterotrophic community depleted some inhibiting compounds to lower concentrations.

Both sCOD and TAN maximum removal rates were lower for batch trials performed with IR (P4 to P7) than those obtained with IPT (P1 to P3). This suggests that the pretreatment of the pesticide wastewater, and the consequent decrease of the industrial organic load, is indeed beneficial for the biological activity in pesticide-containing wastewater scenario. Nevertheless, the absence of pretreatment did not lead to substantial changes in the biofilm quality in terms of eukaryotic community, as seen in section 4.6, further below.

The information about the maximum removal rates is useful to design the reactor HRT, so it is high enough to allow complete nitrification extent. Ideally, the real apparent rate is lower than the maximum, since the operation may be subject to events that will need nitrification to be pushed further or will reduce the nitrification rate of the nitrifying community. Such events may include variations of temperature, pH, dissolved oxygen,

carbonaceous or nitrogenated loads, etc. Although, an excessively higher real apparent rate indicates underutilization of the system capacity.

#### 4.5. Suspended Solids Assessment

In Figure 4.12, the trends in influent and effluent total (volatile and fixed) solids may be evaluated for each operational phase. The percentage of TSS removal and the ratio VSS/TSS in the outgoing stream of the MBBR are also shown. Summary of average influent and effluent TSS and VSS/TSS for each operational phase is given in Table 4.1.

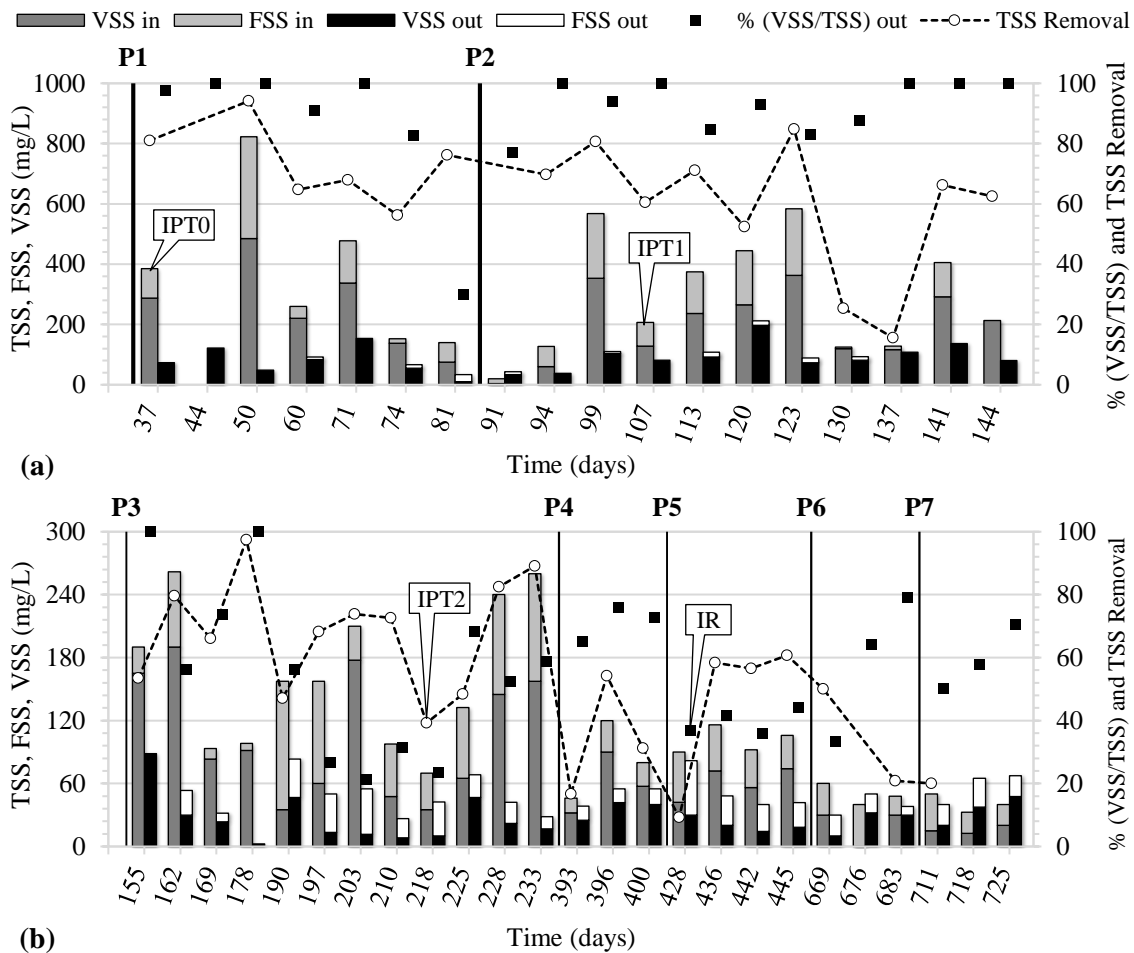


Figure 4.12 – MBBR influent and effluent suspended solids distribution during (a) phases 1 to 3 and (b) phases 4 to 7. Sum of VSS and FSS corresponds to TSS. Text balloons identify changes of pesticide wastewater lot. Time, x-axis, is out of scale.

As previously evidenced by the pCOD series (Figure 4.6), the high variability in influent total suspended solids in the feed, mainly during phases 1 and 2, reinforce the assumption that the solids were accumulating in the feed container due to the lack of agitation and constant changes of sanitary wastewater lot. Starting at phase 4, lower and more stable inlet TSS concentrations were due to constant utilization of the same sanitary wastewater lot (S20), which was low in solids. Regarding the effluent TSS concentration, rare events may have caused higher values. These events may be a consequence of organic shock loads, or sampling mistakes that could, for instance, resuspend biomass settled in the bottom corners of the reactor or cause detachment of biofilm.

The highest inlet solids concentrations were observed in phases 1 and 2, on average 373 and 291 mg/L, respectively. In those cases, when effluent TSS concentration is analyzed with respect to the incoming solids, it is seen that the microbial consortium was able to hydrolyze most of the particulate matter so that a low effluent TSS was noticed, averaging 84 (phase 1) and 100 mg/L (phase 2). If the COD is assessed for these phases (Figure 4.6 (a), days 120 to 148), it is seen that the outlet sCOD was mostly not varying with inlet pCOD fluctuations, indicating that the solids that entered the system were not only converted to soluble forms but also degraded. The HRT has an essential role in this, since the particles need to have enough contact time in the reactor for them to be converted into soluble matter and then metabolized.

From phase 3 onwards, effluent TSS never surpassed 90 mg/L, and the average was only between 39 and 58 mg/L. As a reference, the mean TSS content was 68 mg/L during the whole operation, whilst pure MBBR systems treating municipal sewage tend to have effluent TSS in the range 150 to 250 mg/L (VAN HAANDEL, VAN DER LUBBE, 2012). Thus, the MBBR was capable of resisting and dealing well with the oscillating incoming solids load, always producing an effluent with quite low suspended solids content.

One important parameter presented in Figure 4.12 is the percentage of volatile suspended solids, in relation to the total suspended solids. This ratio helps in understanding the nature of the solids leaving the MBBR. Volatile solids are generally associated with organic matter, whether as biomass or organic solids that went inert through the retention time in the reactor. On the other hand, the fixed suspended solids indicate an inorganic fraction, mostly inert to the action of the microorganisms.

In the feed there was a great variation of the VSS/TSS ratio, with values as low as 20% and as high as 100%, averaging around 70%. Despite this instability, it is clear that

a substantial part of the incoming solids is organic, most likely liable to biodegradation, as the solids came majorly from the sanitary wastewater. Usually, when the influent volatile fraction was low, so it was the concentration of total suspended solids. The great variation of the VSS/TSS ratio is certainly related to the constant changes in S lot, as those presented great inconstancy – even to the naked eye – regarding the particulate matter, both in quality and in quantity.

During the entire study, the average VSS proportion in relation to the incoming and effluent total suspended solids corresponded to 62% and 70%, respectively. As the fixed solids fraction remained high in the MBBR effluent, it suggests that the inorganic portion of the solids, incapable of producing EPS, was not attaching to the biofilm but staying in the suspended phase. In fact, the biofilm persisted with a great percentage ratio of VAS/TAS, as seen in section 4.4.

The lowest proportions of outgoing VSS were registered during phase 3 (average 56%), when the bioreactor was well adapted to the operational conditions. In that case, there is less biomass detachment and, then, reduction of the effluent TSS concentration, that gets richer in fixed solids remainders from the feed. Moreover, the greater HRT compared to the previous phases favors the biodegradation of both the incoming VSS and the sloughed off biofilm. So, the higher HRT justifies the lower VSS/TSS in phase 3. It is highlighted that the higher HRT could lead to superior TSS content if the load was higher, which would favor the activity of planktonic solids.

Even though the TSS leaving the reactor was low, even for the most severe operational conditions, it is advisable that the MBBR installation by the industry is followed by solids separation stage, such as a secondary settler. This is because the industrial operation is carried for longer times and more extraordinary events that involve biofilm excess detachment may happen. Therefore, a step for solids retention is essential in order to prevent the disposal of excessive TSS and pCOD in the receiving water body.

#### **4.6. Biofilm Microscopy**

At the end of each phase, except phase 1, microscopy was used to observe the microfauna established in the biofilm and the qualitative abundances of some groups of microorganisms. Micrographs of the end of each phase are contained in Figure 4.13, with indications of the identified organisms. The selected pairs of micrographs, for each

experimental phase, can be considered as good representatives of the overall observed biofilm quality.

By the end of each phase, protozoa and micrometazoa were spotted in considerable quantities through microscopical observations (Figure 4.13). The images attest to good stratification of the microfauna, with observations of nematodes, rotifers, fixed and free-swimming ciliates, and amoebae. The slow-growing organisms are characteristic of mature, low-loaded, biofilms (Figure 2.13)

Abundance of rotifers was noticed, which relates to high sludge age and low load. This kind of microorganism is common in biofilm reactors. Rotifers, as well as nematodes and ciliates, are bacteria predators, contributing to the clarification of the wastewater, as confirmed by previously presented results for pCOD, TSS and turbidity.

Even at the highest industrial wastewater concentration, in phase 7, rotifers and ciliates were still present. As the eukaryotic community is susceptible to toxic effects, the relative steadiness of the microfauna indicates stable and tolerable toxicity of the wastewater (PAPADIMITRIOU, PALASKA, *et al.*, 2007). This might suggest that higher trophic levels found in receiving water bodies might be unaffected as well by the persistent substances. This is important and is a requirement of the local environmental legislation (NOP-INEA-008, see section 2.4).

Eventual observations of the suspended sludge revealed similar characteristics to the biofilm and a low amount of free-living bacteria, which is consistent with the high presence of micro-animals and protozoa, and overall low turbidity of the MBBR effluent. Additionally, there was no relevant filamentous bacteria development, which, along the good biomass density and size, is an indication of good sludge settleability (BASSIN, DEZOTTI, 2008, MARA, HORAN, 2003). As the reactor was exposed to the raw pesticide-producing industry wastewater, the biofilm accumulated the purple color characteristic of the IR lot.

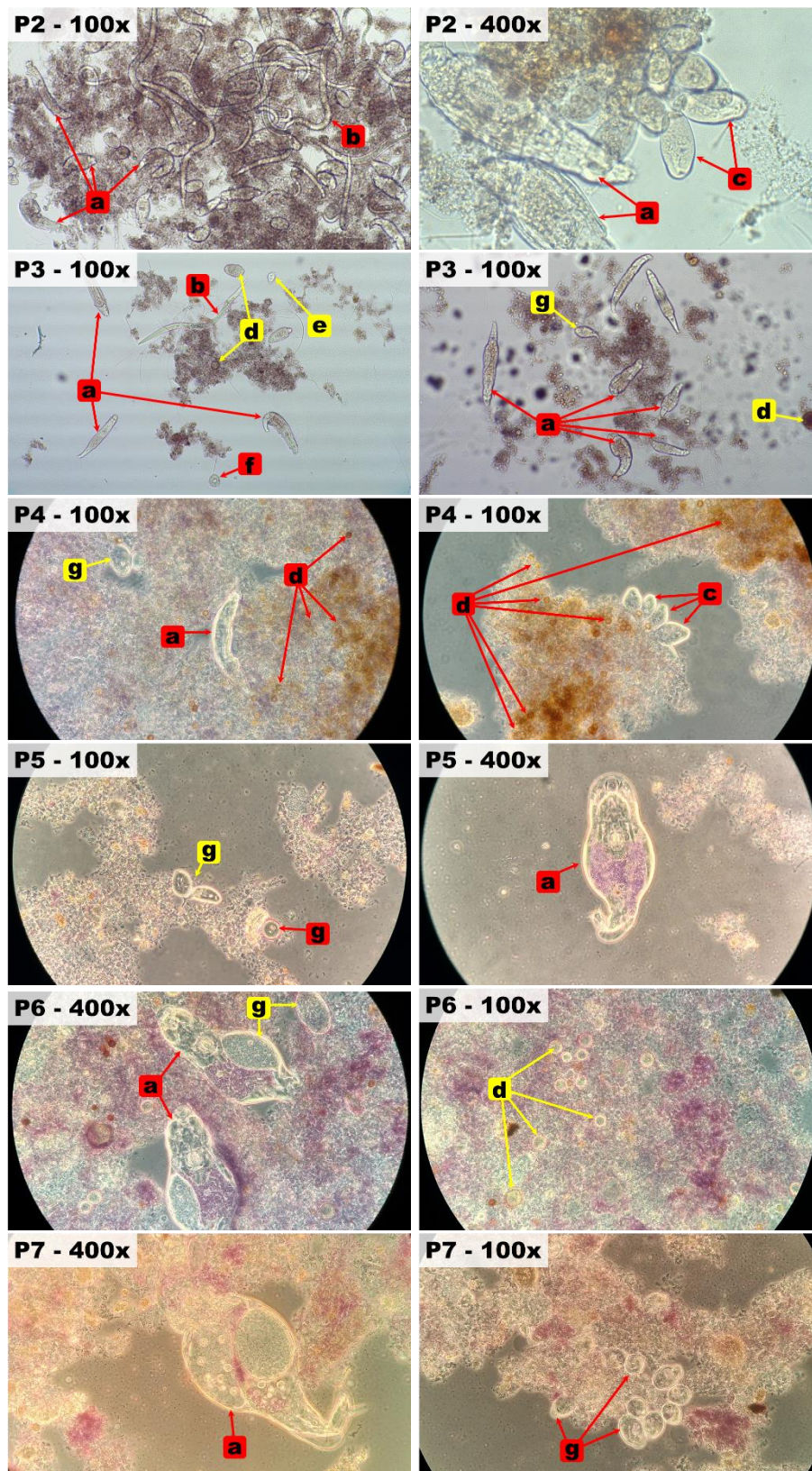


Figure 4.13 – Micrographs taken at the end of phases 2 to 7, with magnifications of 100 or 400x. Letters indicate identified organisms: (a) Rotifera; (b) Nematoda; (c) Ciliophora (*Epistylis* sp.); (d) shelled amoebae; (e) flagellate; (f) Ciliophora (*Vorticella* sp.); (g) Ciliophora. Yellow color refers to uncertain identifications.

## 5. P&P RESEARCH: RESULTS AND DISCUSSION

The content of this chapter is dedicated to present and discuss the results from the operation of the parallel MBBRs employed to evaluate the treatment of P&P wastewater. Considering that real wastewater was fed to the systems, information regarding its characteristics and the industrial treatment process currently employed at the P&P industry were firstly presented in sections 3.2.1 and 2.6.4, respectively.

### 5.1. General Aspects

The timeline of the MBBRs operation can be seen in Figure 5.1, where the time span of each operational phase and the utilization of each wastewater lot is given. Remarkable periods of time with potential effect on the results are also shown, being described in Table 5.1.

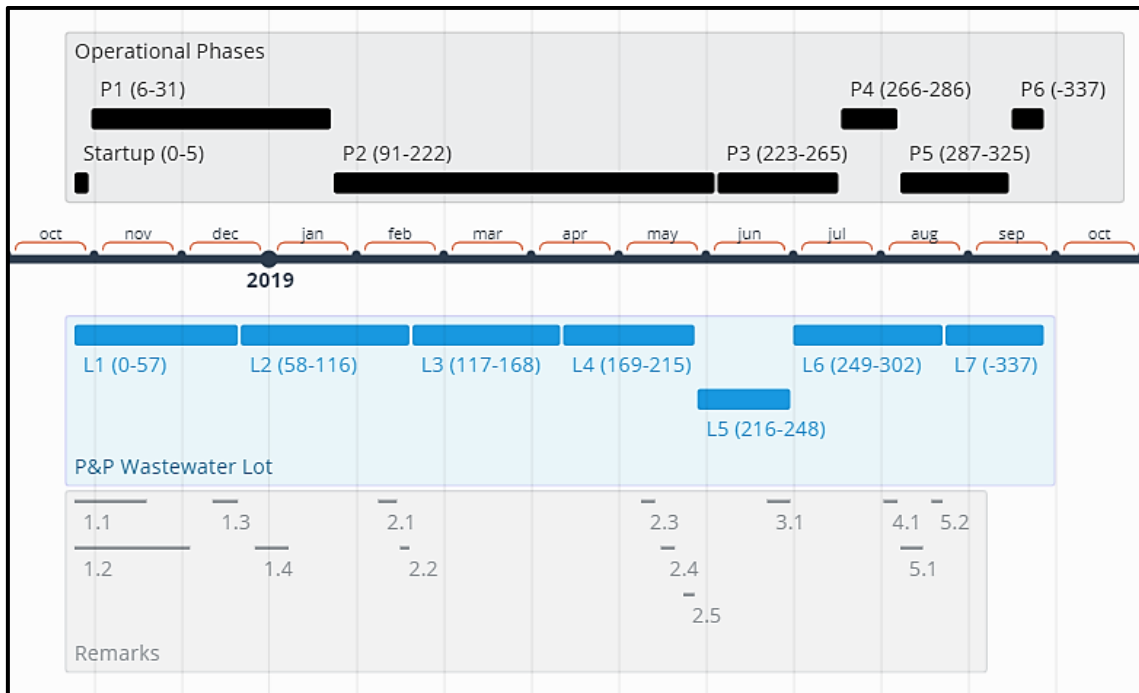


Figure 5.1 – Timeline of the MBBRs operation, with duration the of each phase and wastewater lot specified, in days, as (start-end). Remarks are described in Table 5.1.

Table 5.1 – Remarkable time spans throughout MBBRs operation with potential impact on results interpretation.

Label <sup>a</sup>	Lot	(Start-End) Description
1.1	L1	(0 – 25) Before dosing nutrients directly to the reactors (dosage was done to feed containers kept inside fridges).
1.2	L1	(0 – 40) Before the feed was transferred to a 1 m <sup>3</sup> cooled tank, instead of being kept in individual low capacity containers. Reactors were fed directly from the tank using peristaltic pumps.
1.3	L1	(48 – 57) Feed tank content showed signs of degradation.
1.4	L2	(63 – 75) Mechanical mixing of the feed tank was kept on as a strategy to obtain homogenous temperature and prevent degradation.
2.1	L2	(106 – 112) Intermediary tank was placed between the feed tank and reactors, with overflow back to the feed tank. Feed showed signs of degradation.
2.2	L2	(113 – 116) Flow reduction (and nutrients) by half to make remaining L2 last until L3 was available. Feed has further degraded.
2.3	L4	(196 – 201) Nutrients solution was mismade.
2.4	L4	(203 – 208) Feed tank content froze, concentrating COD.
2.5	L4	(211 – 215) Altered wastewater after thawing (much lower COD).
3.1	L5	(240 – 248) Feed tank content froze, concentrating COD.
4.1	L6	(281 – 286) Feed tank content showed signs of degradation.
5.1	L6	(287 – 295) Feed tank content showed signs of degradation.
5.2	L6	(298 – 302) Feed tank content showed further signs of degradation.

<sup>a</sup> phase.remarknumber

Overall, the biofilm developed on the carriers surface had seemingly adequate thickness, as may be seen in selected micrographs taken under the stereomicroscope, shown in Figure 5.2.

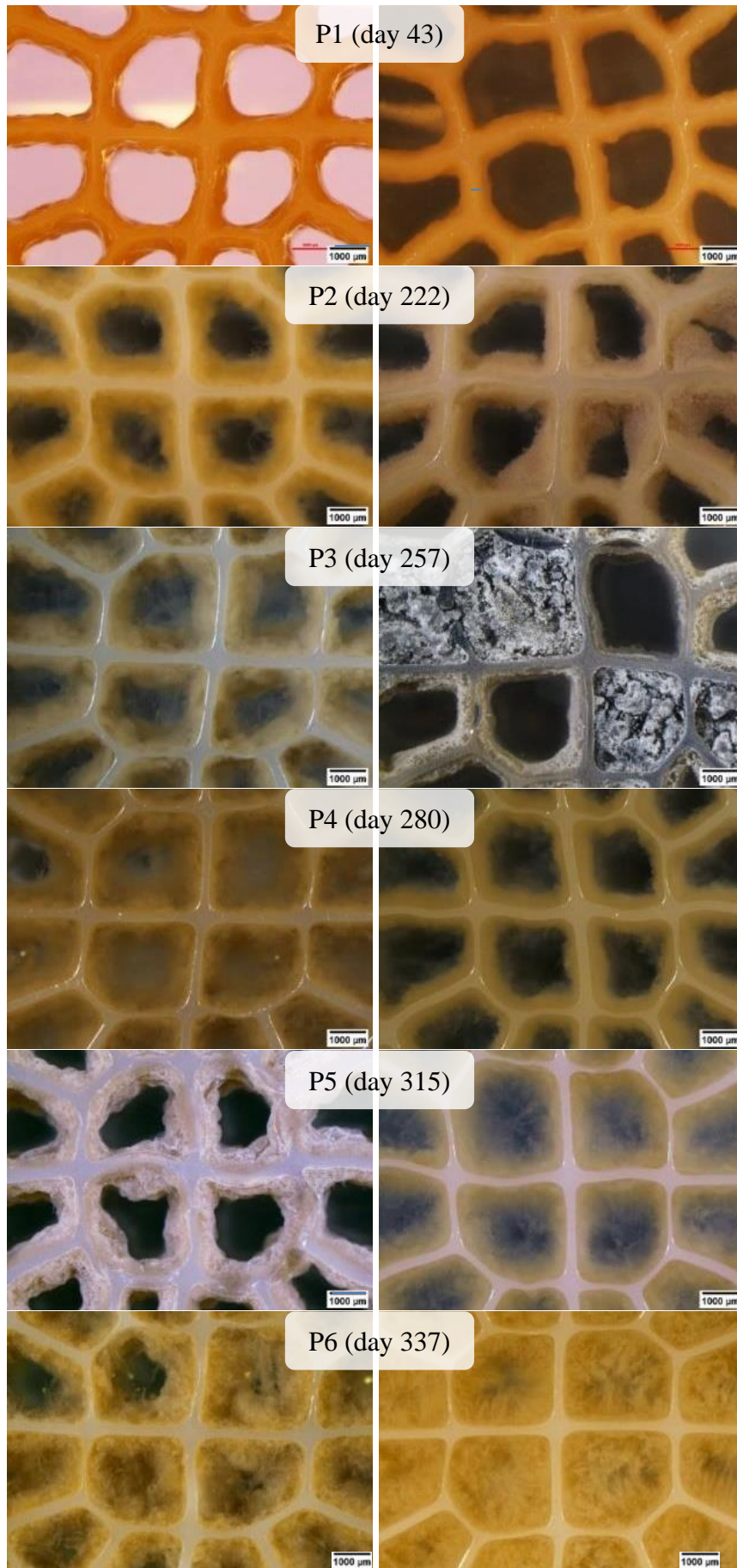


Figure 5.2 – Stereomicroscopy of the carriers from reactors A (left) and B (right).

The thickness of the biofilm was overall lower than 800  $\mu\text{m}$ , without clogging issues, except for phase 6. As may be observed in Figure 5.2, some of the voids in the carriers from reactors A and B seem completely occupied by the biofilm. The same micrographs taken with maximum backlight intensity, Figure 5.3, show that there is a dense biofilm almost blocking some of the carrier sections. In addition to the fact that there is no complete blockage of the carriers, the low height of the K5 carrier model helps reducing the extent of diffusional problems.

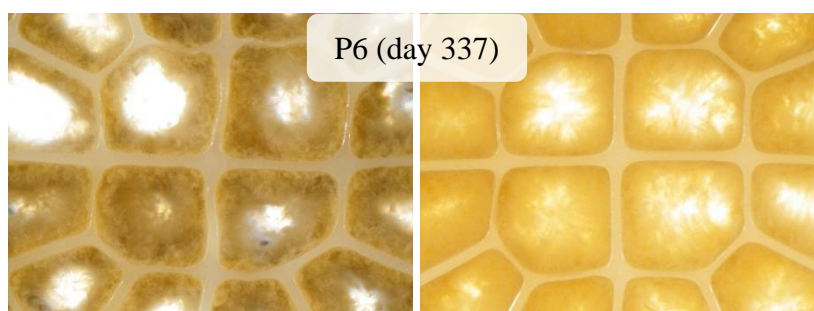


Figure 5.3 – Stereomicroscopy of carriers from reactor A (left) and B (right) with maximum backlight intensity.

The photo of the carrier of reactor B in phase 3 was taken less than 2 weeks after a major operational event: the freezing of the feed storage tank that resulted in concentrated COD entering the reactors (event 3.1, Table 5.1). Since reactor B had threefold higher VLR in this phase, the peak organic load provoked by the event resulted in biofilm darkening and great detachment, and foaming, as shown in Figure 5.4. The event was followed by rapid biofilm detachment and regeneration. Some clogged ash-like voids persisted longer in the carriers before detachment (Figure 5.2), while the normal-looking voids are from after the biofilm loss.

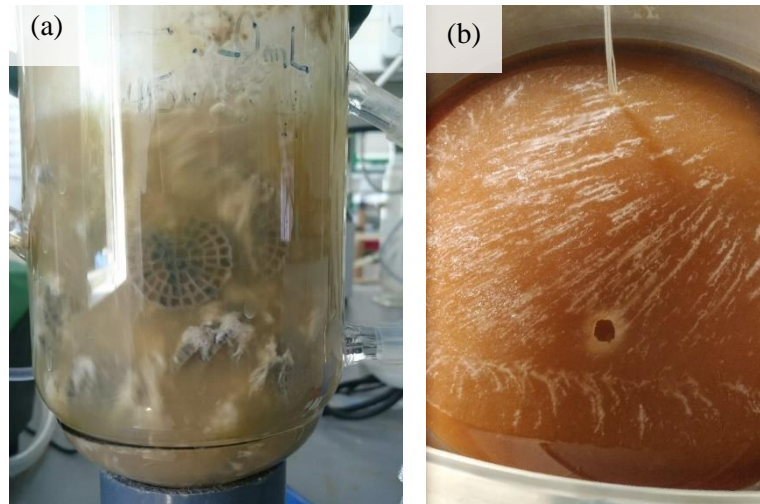


Figure 5.4 – (a) Darkening and loss of reactor B's biofilm on day 241, (b) during the freezing event in the feed tank.

The performance of reactor B was rapidly recovered after that and other disturbing events. For both reactors A and B, the influent and effluent average characteristics for a variety of parameters at each operating phase, along with their removal percentages (when applicable), are summarized in Table 5.2. As mentioned in section 3.2.2, the pH in reactors A and B was on average  $8.3 \pm 0.1$  and  $8.2 \pm 0.2$ , respectively, for the whole operation.

Table 5.2 – Summary of MBBR influent and effluent monitored parameters on each operational phase.

Parameter	Operational phase						
	P1	P2	P3	P4	P5	P6	
tCOD	in	2948	3203	2130	1891	2325	3046
	A out	2130	2572	1610	1409	1734	2197
	A -%	27.8	19.5	25.4	23.2	24.6	27.9
	B out	2462	2855	1712	1483	1559	2051
	B -%	17.1	11.8	20.3	21.7	32.1	32.7
sCOD	in	2870	3189	2099	1854	2297	2982
	A out	1492	2183	1253	1133	1434	1557
	A -%	48.0	32.0	40.2	38.8	37.5	47.8
	B out	1946	2551	1422	1117	1293	1467
	B -%	32.3	19.7	32.5	39.7	44.2	50.8
sSRR	A	56.4	41.6	35.3	29.7	35.8	59.6
	B	39.3	25.7	28.7	15.3	13.6	20.8
sVRR	A	6.7	4.9	4.2	3.5	4.2	7.0
	B	14.1	9.2	10.3	5.5	4.9	7.4
TSS	in	41.1	30.6	20.8	8.5	14.6	41.9
	A out	533.7	372.1	346.6	239.0	238.6	566.6
	B out	394.8	191.3	228.6	335.8	252.6	492.8
VSS/TSS	in	85.7	86.6	79.6	90.0	89.2	80.9
	A out	88.7	93.8	90.2	85.7	94.3	88.1
	B out	82.1	92.6	92.5	88.8	90.5	88.6
PO <sub>4</sub> <sup>3-</sup> -P	A in	17.1	2.5	8.1	12.2	12.5	17.0
	B in	17.4	2.6	8.2	11.9	12.6	16.7
	A out	8.7	0.0	4.5	9.5	9.3	8.2
	B out	6.9	0.1	5.0	9.2	9.5	9.4
TAN	A in	82.2	41.5	15.9	14.3	14.5	77.7
	B in	80.0	42.3	15.9	14.0	14.6	76.3
	A out	17.5	7.3	0.0	0.0	0.0	17.2
	B out	22.3	14.7	0.0	0.0	0.0	18.8

Detailed results and discussion with regards to COD removal, solids production, nutrients utilization and batch activity tests are detailed in subsequent sections.

## 5.2. COD Removal

Knowing that the reactors' feed is very low in solids (55±48 mg pCOD/L) and that the exiting solids from the MBBR would be consumed in an AS step of a BAS system, the discussion about organic matter removal will be focused solely on the sCOD

fraction. For both reactors, the inlet and outlet sCOD levels over the course of the six operational phases are shown in Figure 5.5, which also displays the sCOD removal percentages.

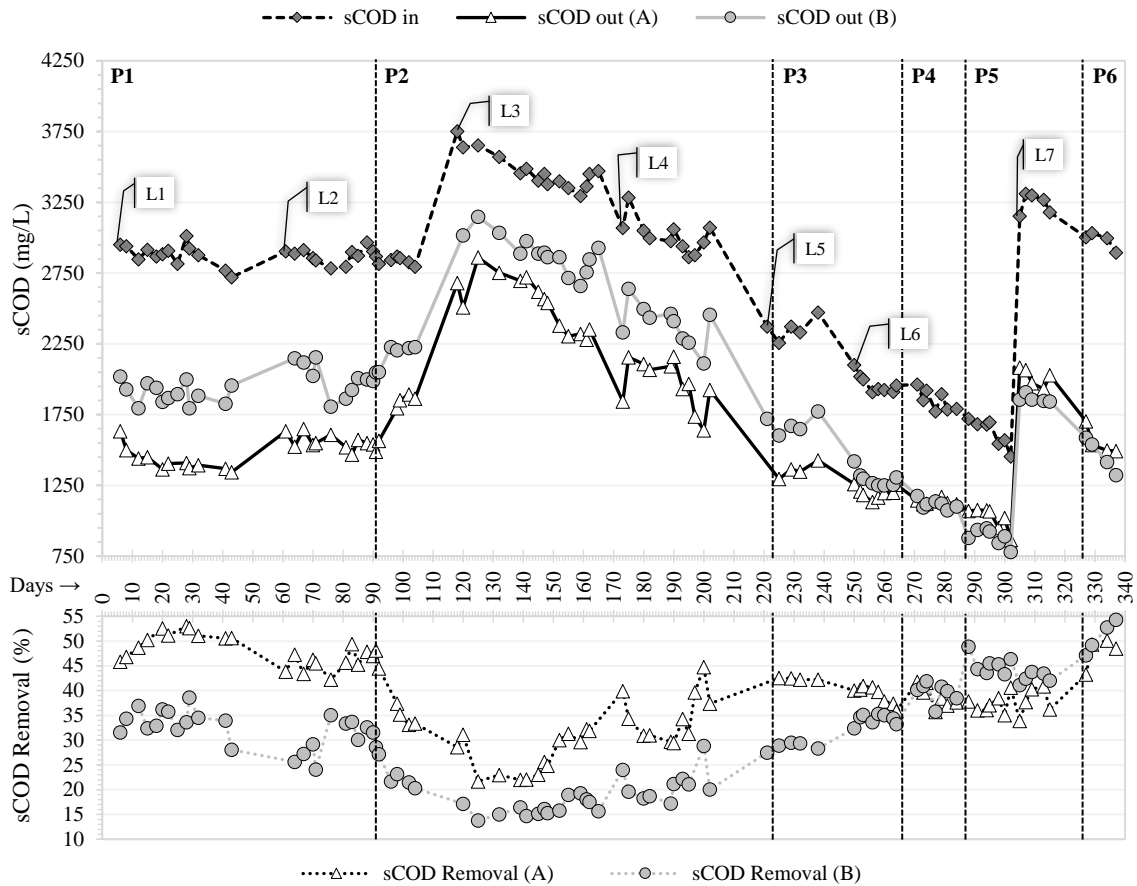


Figure 5.5 – Inlet and outlet sCOD for both reactors and their respective sCOD removal percentages during the whole operation. Changes of pulp & paper wastewater lot and transition between operating phases are identified by text balloons and vertical dashed lines, respectively.

Average sCOD removal during phases 1 to 6 for reactor A were  $48 \pm 3$ ,  $32 \pm 7$ ,  $40 \pm 2$ ,  $39 \pm 2$ ,  $38 \pm 2$  and  $48 \pm 3$  %; while for reactor B they corresponded to  $32 \pm 4$ ,  $19 \pm 4$ ,  $32 \pm 3$ ,  $40 \pm 2$ ,  $44 \pm 2$ , and  $51 \pm 3$  %. It can be seen that up to phase 3, while reactor A had 3 times higher HRT than reactor B (and 1/3 VLR), the sCOD removal of reactor A was on average 1.5 times higher, regardless of the excess or limitation of nutrients. As in this period the reactors had the same total area for biofilm growth and corresponding SLR, the difference in sCOD removal is attributed to the distinct HRT (and so the VLR) and, most likely, the role of the suspended biomass (as will be further discussed).

Looking at phases 5 and 6 - when the VLR is the same for both reactors and SLR is 3 times lower in reactor B - it seems that, at 4.9 h HRT, there is no proportional advantage in having a 3 times higher filling degree (and reactor specific surface area). While N was limited (phase 5), sCOD abatement in reactor B is just slightly better than in reactor A ( $1.18 \pm 0.07$  times) ( $F = 57$ ,  $p < 0.001$ ). With nutrients in excess (phase 6), no statistically significant difference ( $F = 1.81$ ,  $p = 0.22$ ) was found when comparing sCOD reduction from reactors A and B, although the number of data points was low, potentially hindering the statistics. This lack of difference was due to both reactors reaching maximal removal of the biodegradable sCOD, as will be confirmed ahead

For restricted nutrients availability, there should exist an intermediary HRT for reactor B (lower than that of reactor A) where the performances of the two MBBRs match. That was indeed observed during phase 4, when the outlet concentrations were very alike ( $1133 \pm 19$  and  $1117 \pm 33$  mg/L for reactors A and B, respectively), showing no statistically relevant difference in sCOD removal percentage ( $F = 0.55$ ,  $p = 0.47$ ). This condition shows that, when in limitation of nitrogen, a threefold higher filling degree could permit a 33% lower reactional volume without compromising the removal of sCOD, resulting in a more compact MBBR or BAS solution.

During phase 6, the nutrients were again dosed in excess to assess how biofilm maturity may affect the performance of the reactors, assuming all other conditions are identical (inlet COD was quite similar in phase 1 and 6, and there were no changes in the raw material and pulping and bleaching processes at the industry between the two phases). By assessing the data of phases 1 and 6 for reactor A, there was no statistically significant difference regarding organic matter removal ( $F = 0.016$ ,  $p = 0.90$ ). Hence, shifts in biofilm community over time (as discussed in section 5.6) did not result in observable capacity change to assimilate otherwise recalcitrant COD fractions. As the seed for the bioreactors was taken at the long-term operating industrial BAS, it is possible that biofilm maturation in the lab-scale MBBRs had minor weight.

The data of reactor B – while fed with lot 6, from phases 3 to 5 - was fitted to the Kincannon-Stover kinetic model (section 3.2.5). Below, Figure 5.6 displays the resulting plot and linear regression, from which maximum substrate removal rate and biodegradability could be defined.

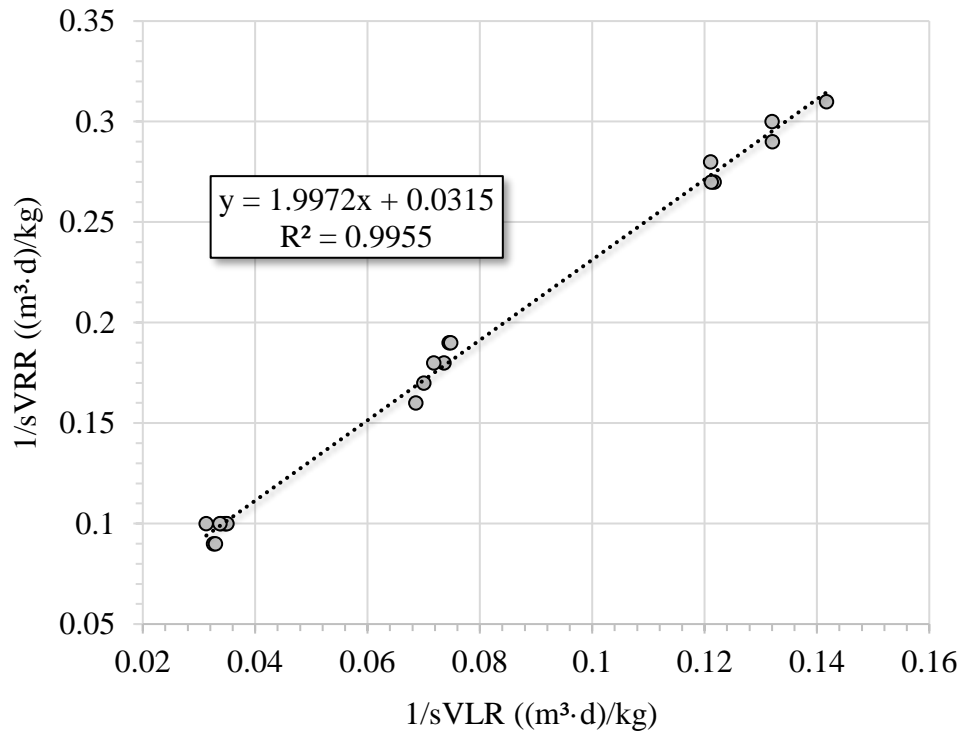


Figure 5.6 - Plot of data from reactor B according to the linearized Kincannon-Stover model ( $n = 20$ ) (see section 3.2.5).

The constant upstream sCOD deterioration of the untreated lot 6 (that may be seen in Figure 5.5,  $sCOD_{in}$ ) could result in poor adequation to the Kincannon-Stover model due to continuous change of the maximum substrate consumption rate. Nevertheless, the correlation coefficient ( $R^2$ ) was higher than 0.99, showing excellent fit to the model. The maximum substrate removal rate ( $U_{max}$ ) and the saturation constant ( $K_B$ ) were, respectively, 30.6 and 60.8  $kg/(m^3 \cdot d)$ . It means that the estimated biodegradability ( $U_{max}/K_B$ ) was 50.3%, which is coherent to what was obtained for lots 7 and 1 during batch trials (46%, see section 5.5, ahead), and also to what have been reported for P&P wastewaters in some previous studies (40-74% (BAEZA, JARPA, *et al.*, 2016, BRINK, SHERIDAN, *et al.*, 2018, OLIVEIRA, 2014)). Assuming that the biodegradability did not change significantly throughout the study – given the constancy of raw material and industrial process –, it is seen that reactor A, in phases 1 and 6, and reactor B, in phase 6, have achieved maximum removal of sCOD (48-51%). As commented in section 3.2.1, the lower initial COD of lot 6 was a result of dilution, which does not affect its biodegradability ratio.

Finally, comparison of the average sVRR of reactor B during phases 3, 4 and 5 (10.3, 5.5 and 4.9 kg/(m<sup>3</sup>·d), respectively, Table S1) with  $U_{max}$  (30.6 kg/(m<sup>3</sup>·d)) shows that reactor B was not overloaded, because it was working with apparent removal rates far below its maximum capacity. In practice, this means that reactor B would not lose performance for higher pollutant concentrations, disregarding the possibility that certain compounds could reach inhibitory levels, such as previously observed for phenol (BRINK, SHERIDAN, *et al.*, 2017). Consequently, in the studied scenarios, the HRT role is relevant as it directly affects the wastewater-biosolids contact time and the suspended mass concentration and activity but is not associated with overload at lower values of this parameter.

The results demonstrate how important it is to weigh volumetric and surface properties of an MBBR, rather than simply projecting its performance based on biofilm activity. Certainly, aspects related to the operation of the AS stage in the BAS configuration need to be taken into consideration, such as the MBBR effluent solids concentration and biomass quality.

### 5.3. Solids Production

Overall, the average solids yield per phase for both MBBRs ranged from 0.25 to 0.47 g TSS/g sCOD removed, as seen in Table 5.3. Reduced solids yield is one of the main features of the nutrient-limited BAS configuration, as reassured when assessing previously reported values, spanning from 0.07 to 0.20 g TSS/g sCOD removed (MALMQVIST, WELANDER, *et al.*, 2007, REVILLA, GALÁN, *et al.*, 2018a, WELANDER, OLSSON, *et al.*, 2002). Pure AS system of a full-scale plant had a reduction from 0.28 to 0.15 g TSS/g sCOD removed past the implementation of the MBBR pretreatment (SOINTIO, RANKIN, *et al.*, 2006). Yet, another study presented the average yield of pure full-scale MBBR system compared to BAS full-scale applications, with a substantial difference from 0.75 to 0.16-0.20 g TSS/g sCOD removed, respectively (REVILLA, GALÁN, *et al.*, 2018a).

When comparing the solids yield between both reactors, no statistically relevant disparity is observed for any phase ( $F < 2$ ,  $p > 0.05$ ), as evidenced by the statistics of one-way ANOVA, given in Table 5.3. It means that, quantitatively, there is no difference in the solids production between two given MBBRs that are designed for the same performance but favoring either planktonic (reactor A) or attached biomass activity

(reactor B) – as long as both are fed with the same P&P wastewater and identical nutrients availability.

Therefore, it is expected that whenever reactor A presents higher sCOD removal, it will also present greater suspended solids concentration (phases 1 to 3) in the same proportion; and TSS values will be alike once sCOD removals are equivalent (phase 4 to 6). Confirmation of such trend is seen in Table 5.3, where p-value for TSS data is above 0.05 for when both reactors had comparable COD removal (phases 4 and 6; phase 5 not suitable to ANOVA), and below 0.05 for when reactor A had superior COD removal, which was indeed in similar proportion than that observed for TSS concentration (phases 1 to 3). The percentage of volatile solids exiting the reactors (VSS/TSS) is, most of the time, greater than 85%, which is characteristic for sludges with a low accumulation of inorganic material (VAN HAANDEL, VAN DER LUBBE, 2012).

Table 5.3 – Average suspended solids concentration, percentage of volatile suspended solids relative to total suspended solids, and sludge yield at each operational phase, for both reactors. Standard deviation within brackets and one-way ANOVA statistics (F and p values), comparing reactors A and B, are also listed.

Parameter		P1	P2	P3	P4	P5	P6
TSS (mg/L)	In	41 (38)	31 (23)	21 (12)	8.5 (3)	15 (6)	42 (20)
	A	534 (159)	372 (136)	347 (108)	239 (87)	239 (99)	567 (91)
	B	395 (107)	191 (85)	264 (167)	336 (200)	267 (131)	493 (146)
	F/p <sup>a</sup>	10.3/0.003	>12/<0.003 <sup>b</sup>	8.5/0.011 <sup>b</sup>	0.61/0.46	NA <sup>c</sup>	0.73/0.42
VSS/TSS (%)	A	89 (10)	94 (10)	90 (13)	86 (14)	94 (8)	89 (10)
	B	82 (9)	93 (8)	93 (3)	89 (14)	91 (7)	90 (5)
Yield ( $\frac{g\ TSS}{g\ sCOD}$ )	A	0.38 (0.10)	0.35 (0.09)	0.39 (0.08)	0.37 (0.15)	0.29 (0.09)	0.40 (0.05)
	B	0.41 (0.11)	0.30 (0.10)	0.35 (0.17)	0.47 (0.29)	0.25 (0.08)	0.32 (0.09)
	F/p <sup>a</sup>	1.29/0.26	NA <sup>c</sup>	0.71/0.41	0.30/0.60	1.05/0.32	1.91/0.21

<sup>a</sup> One-way ANOVA statistic comparing the mean values for reactors A and B in each phase.

<sup>b</sup> Calculated by lot, instead of by phase, so the data fitted normal-like distribution.

<sup>c</sup> Data did not attend to normality condition required for the ANOVA test.

Another factor that was evaluated regarding the impact on the sludge yield is the nutrients availability. For so, ANOVA was performed for reactor A yield from phase 1 to 6, and the same was done for reactor B yield for phases 1 to 3 (no HRT variation). No statistically relevant difference is seen for reactor A ( $F = 1.92$ ,  $p = 0.10$ ), neither for

reactor B ( $F = 1.79$ ,  $p = 0.19$ ), despite that the ANOVA for reactor B was made without phase 2 data, as it did not fit to normal-like distribution. Hence, there seems to be sufficient evidence that the solids yield was not impacted dramatically by restraining the nutrient availability. Although care should be taken for this conclusion (as the statistical analysis may be negatively impacted by high standard deviation and small size of dataset), it is supported by a former study that only observed the influence of nutrients limitation on the biosolids yield of the total BAS and not on the biofilm stage. The BAS had the yield decreased from 0.2 to 0.05-0.10 g TSS/g sCOD removed when moving from excess to restriction of nutrients, respectively, whereas the biofilm stage remained at 0.30 g TSS/g sCOD removed regardless of the nutrients availability (WELANDER, OLSSON, *et al.*, 2002).

#### **5.4. Efficiency of Nutrients Utilization for COD Removal**

The average ratios of sCOD removed over consumed P and N are shown, respectively, in Figure 5.7a and Figure 5.7b, for every operational phase and both MBBRs. Higher ratios mean more sCOD removed per unit of consumed N or P, therefore greater efficiency of nutrients usage for organic matter removal. The average influent nutrient dosages, N/sCOD and P/sCOD, ratios are given in Table 3.9. Effluent concentrations of the restrained nutrients were always negligible during each respective limitation. Nitrite and nitrate were always absent in the reactors, discarding the occurrence of nitrification, which would really be unlikely to take place under the applied high organic loads.

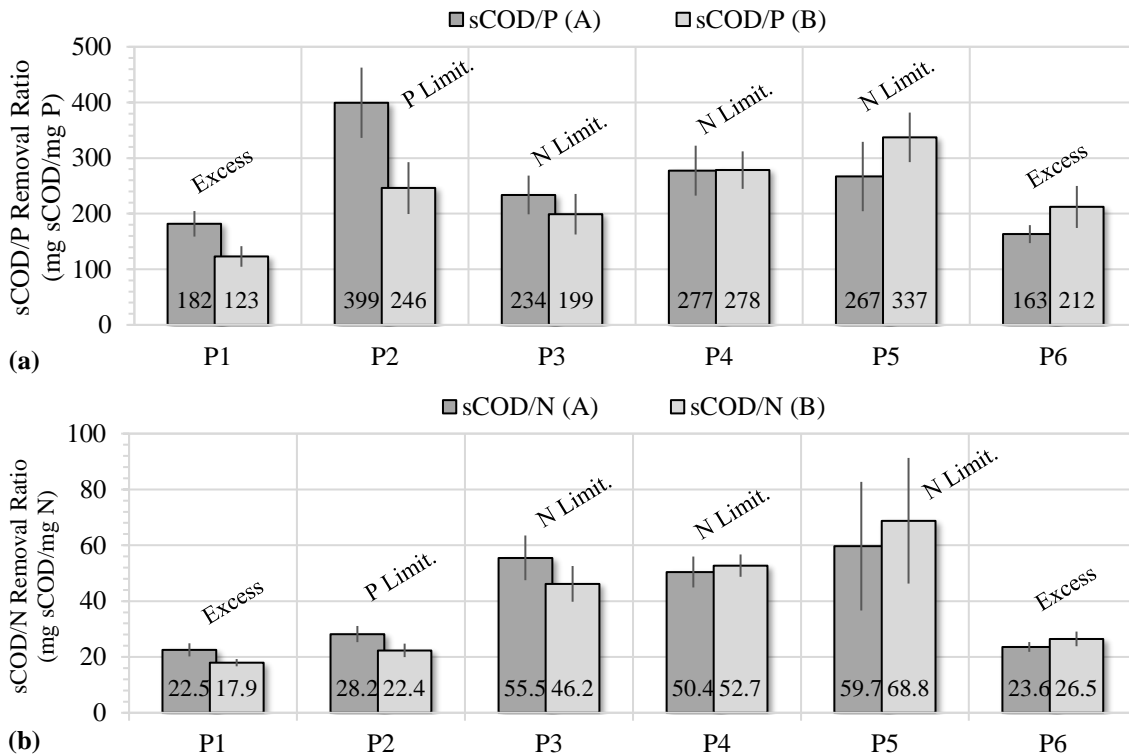


Figure 5.7 - Average ratio of sCOD removed over consumed P (a) or N (b) for both reactors and each operational phase. Error bars show standard deviation. Text labels above columns refer to nutrients availability condition.

It is known that EPS quality and yield, which potentially impact the proportion of organic matter to nutrients consumption, are directly related to the species of microbes present and the type of available substrate (NOUHA, KUMAR, *et al.*, 2018, STOUTHAMER, 1992). Time of operation may drive to changes in bacterial profile. Therefore, the efficacy in utilization of N and P in relation to biofilm maturity in reactor A was assessed by looking at phases 1 and 6. No statistically relevant disparities were observed neither for N ( $F = 0.68$ ,  $p = 0.42$ ) nor P ( $F = 2.2$ ,  $p = 0.16$ ). Seemingly, no major changes in EPS production that could alter the sCOD/nutrients consumption ratio resulted from biofilm maturation. Consequently, for reactor A, every comparison valid with phase 1 could also be done with phase 6. It is remarkable that despite the low number of data points in phase 6, the same levels of nutrient utilization efficiency of phase 1 were rapidly reached without need for adaptation of the microbial community. In fact, for both bioreactors, no need for long adaptation time was observed for any phase transition, even with sharp shifts in nutrients availability.

The effect caused by the limitation of each nutrient in its utilization efficiency may be assessed by comparing phases 1 and 6 (excess) with the respective nutrient-

limited phases. In this sense, phase 4 onwards are not analyzed for reactor B, as there were parallel changes in the HRT. Both reactors were more efficient in P usage when P was limited (phase 2,  $F > 46$ ,  $p < 0.001$ ). Indeed, under these conditions, it was observed that the sCOD/P removal ratio was 2.2 and 2.5 times higher than the averages from phases 1 and 6 for reactor A, and 2.0 times the mean of phase 1 for reactor B. In terms of N use, reactor A reduced 2.1 to 2.7 times more sCOD per unit of consumed N in phases 3 to 5 than in phases 1 or 6 ( $F > 85$ ,  $p < 0.001$ ). In turn, reactor B was 2.6 times more efficient in N utilization in phase 3 than in phase 1 ( $F > 30$ ,  $p < 0.001$ ).

The results show that the abundant nutrient is also used more efficiently while the other is restrained. At phase 2 (P limitation), removal of sCOD per unit of consumed N was 1.25 and 1.20 times greater than at phases 1 and 6, for reactor A ( $F = 20$ ,  $p < 0.001$ ); and 1.25 times the average from phase 1, for reactor B ( $F = 21.5$ ,  $p < 0.001$ ). Likewise, comparing the P utilization efficiency in reactor A at phases 3 to 5 (N limitation), it was 1.29 to 1.70 times higher than that observed in phases 1 and 6 ( $F > 18$ ,  $p < 0.001$ ). Efficacy of P usage was also higher at phase 3 (N limitation) for reactor B than in phase 1 by a factor of 1.62 ( $F = 25.4$ ,  $p < 0.001$ ). Hence, the efficiency in using both N and P for sCOD removal increases independently of which nutrient is limited. Even though, this trend is much more evident for the limiting nutrient (2.00 to 2.65 times) than for the plentiful one (1.20 to 1.70 times). Further investigation is necessary for explaining this outcome.

Nutrient (or other substrates) limitation is known to give an ecological advantage to EPS-producing bacterial strains (JAYATHILAKE, JANA, *et al.*, 2017, XAVIER, FOSTER, 2007), besides influencing the quality and boosting the amount of EPS produced (HOA, NAIR, *et al.*, 2004). EPS production may be more than 2 times more intensive in energy utilization than cell growth, demanding greater substrate oxidation for ATP production (STOUTHAMER, 1992). This partially explains the greater carbonaceous substrate removal per unit of consumed P and N.

Another factor to be taken into consideration is the EPS composition, which has major contributions from carbohydrates and proteins (NOUHA, KUMAR, *et al.*, 2018). Since carbohydrates are free of N and P, their synthesis contributes for greater COD consumption per unit of N and P utilized (i.e., higher COD/N and COD/P ratios). Proteins, on the other hand, have close to 17% w/w of N and no P in their composition (VENTURA, 2006), hence contributing to higher COD/P consumption ratios only. Previous study has shown that cuts in availability of both N and P boost the carbohydrates content (with the

effect of P being more pronounced), while protein content is increased just by N limitation, with no observed effect from P availability (HOA, NAIR, *et al.*, 2004).

For assessing how the HRT impacts the efficiency of nutrients use, data from reactor B may be assessed within phases 3 to 5 (increasing HRT and constant N limitation) and phase 1 against phase 6 (different HRT and nutrients excess). Phosphorous is more efficiently used with increasing HRTs ( $P5/P3 = 1.69$ ,  $P6/P1 = 1.72$ ) for the proposed comparisons ( $F > 28$ ,  $p < 0.001$ ), whereas statistically relevant difference for nitrogen usage efficiency was observed during nutrients abundance ( $P6/P1 = 1.47$ ,  $F = 54$ ,  $p < 0.001$ ) but not during N restriction (phases 3 to 5,  $F = 2.7$ ,  $p = 0.09$ , considering only lot 6 for meeting normality criteria).

Despite the duality of results for nitrogen in reactor B, the discussion about the HRT effect is supported by comparing reactors A and B to each other while reactor A had a higher HRT (phases 1 to 3). Reactor A was always more efficient than B in N (1.26, 1.26 and 1.20 times, phases 1 to 3) and P (1.48, 1.62 and 1.17 times, phases 1 to 3) utilization ( $F > 5$ ,  $p < 0.05$ ). Therefore, there is sufficient evidence that the HRT positively affects the sCOD/nutrients consumption ratio for both excess or limitation of N or P. It can be hypothesized that nutrients are more efficiently used by the planktonic biomass, as raises in HRT favors the suspended solids concentration and activity (as can be seen in section 5.5, ahead). Actually, the divergence between the reactors disappears at phase 4 ( $F < 0.78$ ,  $p > 0.39$ ), when the HRT still differs but the suspended solids concentration is comparable (Table 5.3), reinforcing the hypothesis.

Effect of carrier filling degree and effective specific surface area of the reactors was addressed by comparing reactor A with reactor B at phases 5 and 6, as they have 120 and 360  $m^2/m^3$  but same HRT and nutrients availability. With excess N and P (phase 6), reactor B seemed to have greater sCOD/P and sCOD/N consumption ratio than reactor A (1.30 and 1.12 times, respectively), but no statistically significant contrast was confirmed ( $F < 6$ ,  $p > 0.05$ ). During nitrogen limitation (phase 5), the average B/A ratios of P and N utilization were 1.26 and 1.15, respectively, but the statistics were inconclusive. Thus, it is uncertain if - at the same HRT - the greater filling degree impacts positively the consumption efficacy of N and P.

If considering the highest achieved average ratios of sCOD to nutrient consumption, it may be estimated what would be the minimum nutrients dosage for achieving maximum sCOD removal. Using 48% as biodegradability ratio (see section 5.2), individual minimum dosages would be 20 mgN/L (reactor B, phase 5) and 3.5

mgP/L (reactor A, phase 2). Reactor B, during phase 5, also achieved the best average combined minimum dosage, with the aforementioned dose of N and 4.1 mgP/L. This would represent an approximate sCOD:N:P dosage proportion of 100:0.70:0.14, taking into account the non-biodegradable sCOD portion as well. Assessing reactor A only, the minimal overall nutrients proportion was also observed in phase 5, with sCOD:N:P at 100:0.80:0.18. Thus, considering the operating of phase 5, combining greater HRT and N limitation is the optimal way to minimize supplementation of N and P simultaneously.

One computational study performing simulations for two full-BAS scenarios - differing in total HRT - treating P&P wastewater found minimal sCOD:N:P ratio to be 100:0.74:0.105 for the lower HRT scenario (with 76% sCOD removal), and 100:0.44:0.08 for the higher HRT case (with 85% sCOD removal) (REVILLA, GALÁN, *et al.*, 2018a). Quantitatively, it may not be precise to compare the mentioned computational results with this study, particularly considering that here the full BAS is not contemplated and that the referenced research only provided relative inputs of the scenarios, not absolute values. Nevertheless, there is an agreement that greater HRT allows savings in nutrients dosing. It should be noted that such minimal dosages are on a threshold, meaning that fluctuations in incoming sCOD would possibly cause incomplete removal of the biodegradable portion. In the context of the BAS, however, small oscillations in the MBBR effluent conditions should be dampened by the AS step.

### **5.5. Activity Batch Trials with Attached and Suspended Biomass**

Data obtained from biofilm quantification and batch trials performed at the end of each phase was used to calculate the maximum volumetric, surface and specific sCOD removal rates for attached and planktonic biomass fractions, which were compared to apparent removal rates from continuous operation, as explained in section 3.2.6. The sCOD depletion curves over time for each reactor during the biofilm and planktonic biomass batch assays are displayed in Figure 5.8.

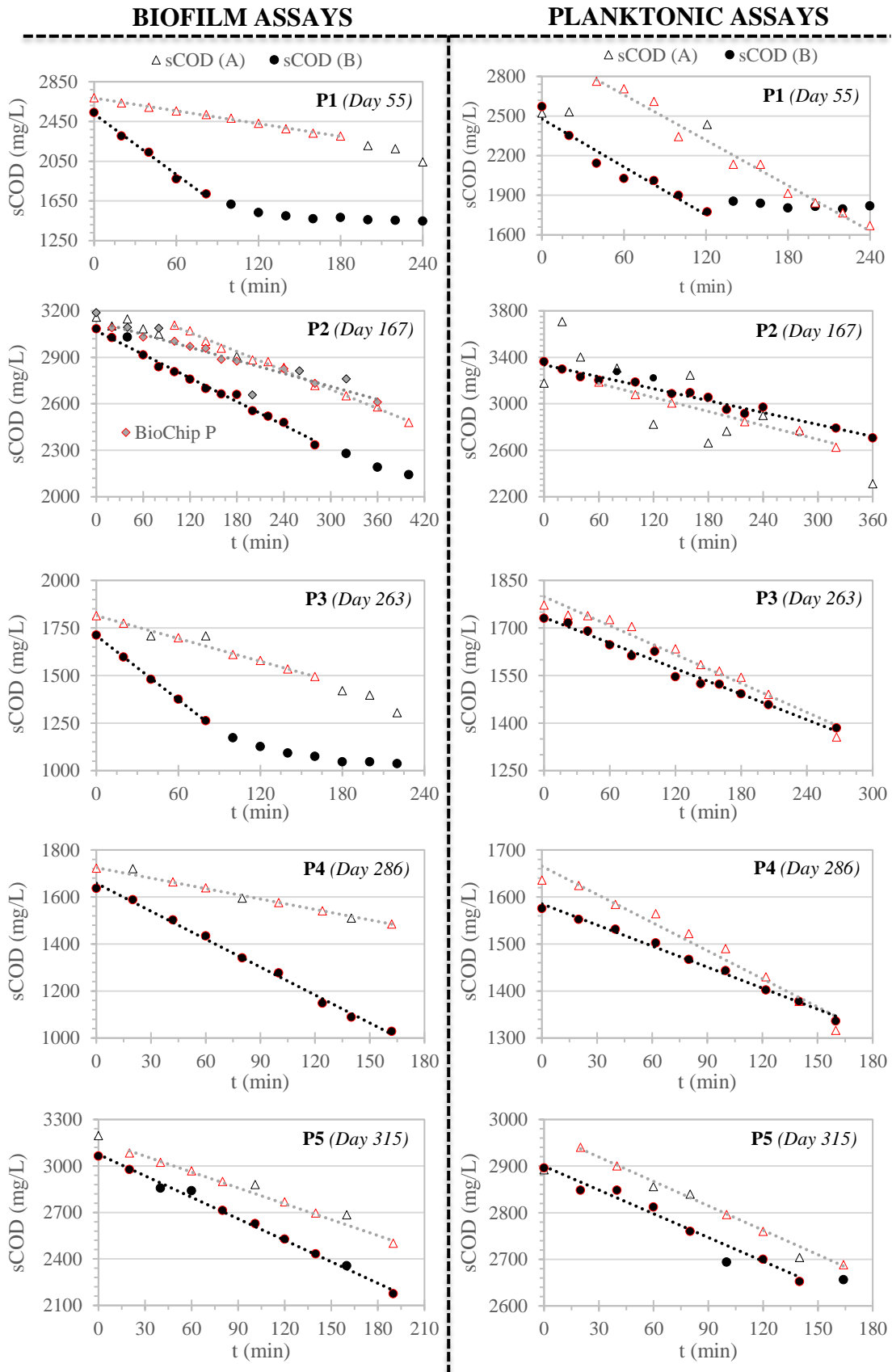


Figure 5.8 – sCOD over time for biofilm and planktonic batch trials for reactors A and B, from phases 1 to 5. Red outlined data points were used for linear regressions.

Biodegradability determination through extended batch assays during phase 5 was performed, as explained in section 3.2.6. Despite not shown in the phase 5 biofilm graph in Figure 5.8, somewhat stable final sCOD of  $1714 \pm 18$  and  $1664 \pm 4$  mg/L (6 measurements from 0.74 to 1.19 d duration) were attained for reactors A and B, respectively. Then, a comparison was done with the respective initial sCOD levels of 3232 and 3064 mg/L, seen in Figure 5.8, resulting in estimated biodegradability levels of 46.3% and 45.7%, averaging 46.0%. Regardless of not being operated for particularly long duration, the biofilm batch assay of reactor B of phase 1 also reached a constant final level of 1455 mg sCOD/L (Figure 5.8). Contrasted to the initial sCOD (2688 mg/L, Figure 5.8), that represents a 45.9% biodegradability. It should be highlighted that the batch trial with suspended solids cannot be analyzed in this sense because the fresh wastewater is mixed with a concentrated sludge solution that has different biodegradable fraction.

Batch assays of phase 1 and 5 were run with lots 1 and 7 of the P&P wastewater, respectively. The obtained 46% biodegradability is comparable to that of lot 6 (50.3%), determined via data fitting to Kincannon-Stover model (section 5.2, above), which is congruent with the consistency of the P&P wastewater quality over time.

For analyzing the biofilm activity, it should be considered that substrates are not uniformly available along the depth of biofilm, due to the diffusional nature of mass transfer throughout it. The thicker and denser the biofilm, the more diffusion problems intensify, resulting in varying specific removal rates across the biofilm and less active inner layers of biomass (VON SPERLING, 2007b). Density and thickness of the biofilm are hard to control from one phase to another, being subject to fluctuations of many operational parameters. That is why, when assessing the biofilm activity alone, surface removal rates – instead of specific removal rates - better show trends and responses to variations in the process, as the total area is not bound to any condition.

Figure 5.9a displays, for reactors A and B: i) their apparent surface removal rates, as calculated from continuous operation, ii) the biofilm maximum surface removal rates, and iii) the surface concentrations ( $\text{g/m}^2$ ) of VAS at the end of each phase. Since the reactors apparent surface removal rates assign the whole activity in the reactors solely to the total area (i.e., to the biofilm), they were presented just to verify if it is clearly wrong to neglect the conversions taking place in the suspended phase by comparison with the maximum surface removal rates (therefore weighting relatively the roles of attached and suspended fractions).

In Figure 5.9b, planktonic specific removal rates, as calculated from continuous operation (apparent) and batch trials (maximum), are shown together with the ratio of total suspended solids to total solids (i.e. suspended plus attached) in the reactors ( $f_{SS/TS}$ ). In this case, the apparent specific removal rates were calculated considering only the suspended solids concentration, ignoring attached solids. Such an approach was for discussion purposes only as, naturally, both fractions were simultaneously active in continuous operation.

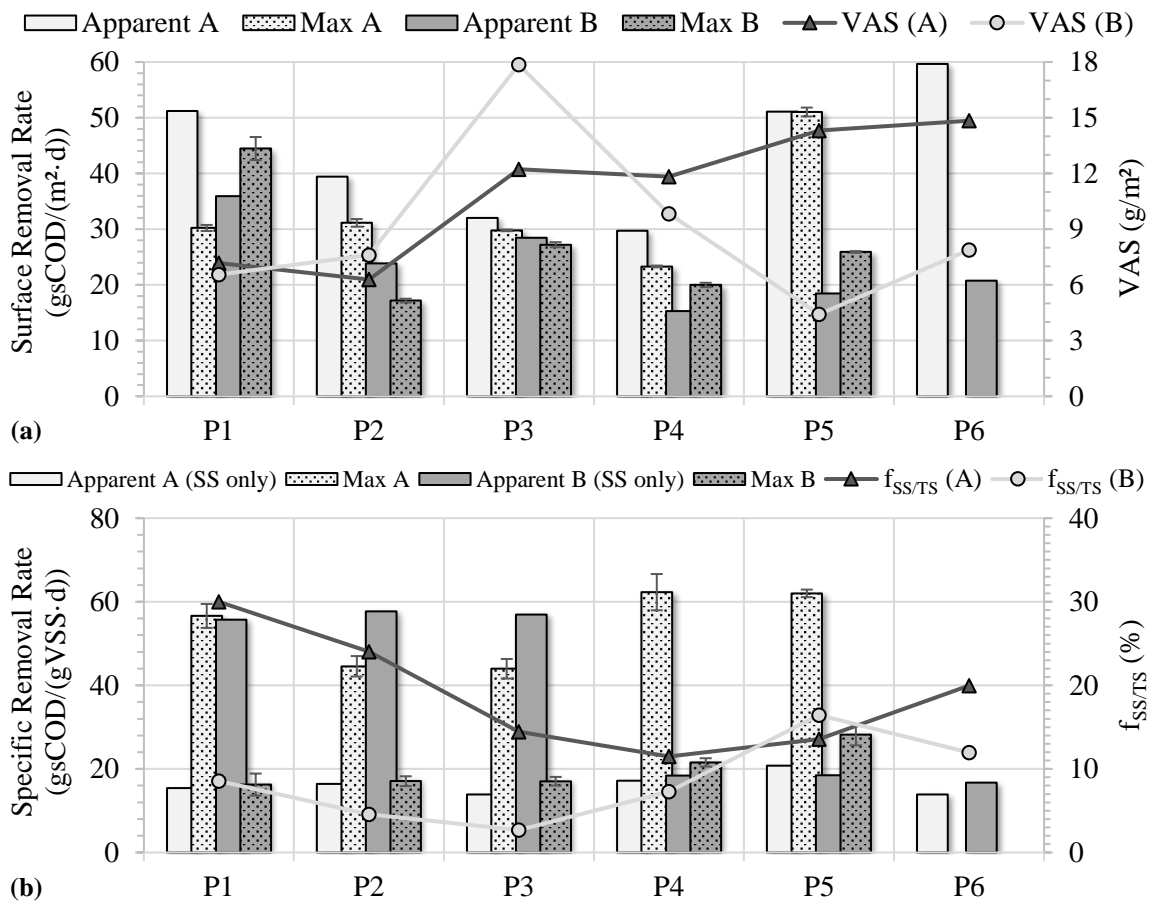


Figure 5.9 – (a) Biofilm maximum and apparent sCOD surface removal rates, and surface concentration of VAS; and (b) planktonic maximum and apparent (suspended solids only) specific removal rates, and percentage of suspended solids over total biosolids ( $f_{SS/TS}$ ), in phases 1 to 6, for reactors A and B. Maximum rates are not available for phase 6.

Greater HRT values promote superior suspended solids content with higher overall activity if the organic load suffices (PICULELL, WELANDER, *et al.*, 2014). Indeed, while reactor A has higher HRT than reactor B (phases 1 to 4), the former has

substantially higher maximum planktonic specific removal rate and  $f_{SS/TS}$  (Figure 5.9b) than the latter - 2.5, 4.8 and 5.4 times in phases 1, 2 and 3, respectively. Reactor B, in phases 3 to 5, had sequential increases in its planktonic maximum specific removal rate and  $f_{SS/TS}$  alongside the HRT. In spite of both reactors having 4.9 h HRT and similar  $f_{SS/TS}$  (around 15%) in phase 5, reactor A planktonic maximum specific removal rate is still 2.20 times higher than that of reactor B. It is supposed that, for having a threefold higher surface loading rate (Table 3.9), reactor A was more dependent on the activity of the suspended biomass fraction than reactor B. However, further investigation is necessary to justify why the biofilm maximum surface removal rate in reactor A at phase 5 stood out from the values determined from phases 1 to 4 (51.0 against average 28.6 g/(m<sup>2</sup>·d)).

When observing reactor A during all phases (4.9 h HRT, Figure 5.9a), the apparent surface removal rate was higher than (or equivalent to) the maximum biofilm surface removal rate, suggesting that the activity of the suspended biomass plays a relevant role in the COD metabolization (otherwise apparent activity could not be superior to the maximum activity). The opposite was noticed for reactor B through phases 1 to 3 (HRT of 1.6 h): its apparent (SS only) specific removal rate was much higher than the maximum planktonic specific removal rate (Figure 5.9b). This indicates that a significant part of the biological activity is happening in the biofilm. It should be reminded that the apparent surface removal rate and the apparent planktonic (SS only) removal rate were presented only to stress the relevance of the opposing respective biomass fraction in the overall activity.

Another sign of the role of different biomass fractions is the initial effect caused by the transition from nutrients excess (phase 1) to P limitation (phase 2). For reactor A, the maximum planktonic removal rate decreased by a 0.79 factor (Figure 5.9b) and the biofilm maximum surface removal rate was unaffected (Figure 5.9a). For reactor B, the opposite was noticed, with a 0.38-fold reduction in biofilm maximum removal rate and unchanged planktonic maximum specific removal rate. Supposedly, the magnitude of this effect was much higher for the biofilm maximum surface removal rate in reactor B (0.38 factor), than that for the reactor A maximum planktonic specific removal rate (0.79 factor), because the biofilm is more subjected to mass transfer limitations that intensify at lower nutrients concentration.

Finally, the activity trials conducted for the BioChip P carriers from the full-scale BAS plant, using wastewater lot 3, resulted in a biofilm maximum surface removal rate of 23.9 g/(m<sup>2</sup>·d). The determined values for reactors A and B during phase 2, when P was

restricted (like the industrial BAS) were 31.1 and 17.2 g/(m<sup>2</sup>·d), respectively. Since the HRT of the full-scale MBBR is within the 2.6-5.3 h range (considering the design and nominal flow rates), the results might be considered compatible, even if that reactor has been in operation for much longer, which could result in substantial differences in the microbial community when compared to much less mature biofilms with distinct biofilm history. Such microbiome distinctions may be evaluated by DNA screening from biofilm samples, as seen below in section 5.6.

### **5.6. Assessment of Biofilm Bacterial Profile**

As described in section A.18, biofilm samples from the end of each operational phase were submitted to DNA screening based on V1-V3 region of 16S rRNA, enabling the investigation of the attached microbiome. The results were related to the operational conditions shifts promoted over phases and to differences between reactors. In addition, DNA screening was also performed for the biofilm from carriers (BioChip P) taken at the full-scale BAS system at the industrial site that sourced the P&P wastewater.

It should be highlighted that the samples were only from biofilm extraction and, therefore, they do not necessarily describe the whole microbiome in the reactor. Certainly, shearing and detachment mechanisms do bring similarities to the suspended and attached microbial profiles, but depending on the HRT, there may be substantial divergences between the biomass fractions.

The 13 biofilm samples yielded 155 to 769 ng/μL of extracted DNA and a total of 369,120 sequences registered after quality control and bioinformatics processing. The sequence reads per sample ranged from 24,743 to 32,187. From all the reads, 799 distinct operational taxonomic units (OTUs) were found, with each sample within the span of 128 to 351 OTUs. Around 79% of the total OTUs could be assigned at the genus taxonomic level, comprising 253 unique, previously cultured, genera, as seen in Table 5.4 in which upper taxa data is also shown.

Table 5.4 – Number of OTUs assigned at various taxonomical levels and amount of corresponding unique taxa.

<b>Taxon</b>	<b>OTUs</b>	<b>Unique taxa</b>
Kingdom	799 (100%)	1
Phylum	736 (92.1%)	25
Class	721 (90.2%)	47
Order	713 (89.2%)	79
Family	683 (85.5%)	145
Genus	630 (78.9%)	253

Table 5.5 lists the number of sequence reads and their associated identified OTUs for each biofilm sample, as well as the day of sampling in the operational timescale of the lab-scale MBBRs. Richness indexes (i.e., measures of the number of microbes species found) in the form of observed OTUs and Chao1 indexes are also presented in Table 5.5. The latter accounts for rare OTUs to estimate not observed ones (CHAO, 1984, GOTELLI, CHAO, 2013). Hence, the greater the difference between Chao1 and OTUs, the more undetected rare OTUs. At last, Table 5.5 contains Shannon entropy and Gini-Simpson diversity indices of each sample (alpha diversity). These parameters weigh together the richness and evenness (i.e., measure of how evenly abundant the OTUs in the environment are) of the microbial community. Shannon and Gini-Simpson indices quantify, respectively, the uncertainty of predicting the OTU of a randomly taken sequence from one sample, and the probability of getting distinct OTUs from two consecutive random sequences. Therefore, both metrics are proportional to diversity, as they are higher in a richer and more even pool of reads (GOTELLI, CHAO, 2013).

Table 5.5 - Richness and alpha diversity indices for the 13 biofilm samples. Linear color scale goes from white to grey with increasing values for every index.

Phase	Day	DNA		Richness indexes				Alpha diversity indexes			
		Sequence Reads·10 <sup>-3</sup>		Observed OTUs		Chao1		Shannon		Gini-Simpson	
		A	B	A	B	A	B	A	B	A	B
P1	55	27.7	24.7	237	238	269	266	3.87	4.06	0.960	0.969
P2	167	30.3	30.8	223	163	274	187	3.14	2.76	0.913	0.875
P3	263	25.8	25.6	342	248	380	327	3.95	3.37	0.950	0.913
P4	286	25.8	29.9	399	341	447	387	4.29	3.68	0.963	0.917
P5	315	32.2	31.1	337	366	402	435	2.72	3.44	0.728	0.892
P6	337	29.3	26.8	426	324	479	360	4.18	4.16	0.947	0.970
Chip	169	29.2		337		368		4.09		0.967	

Accounting together all phases, the Venn diagram displayed in Figure 5.10 shows how many of the overall 799 OTUs were detected exclusively in one of the reactors, shared by each pair of them, or shared by all biofilm sources. Relative abundance represented by those groups of OTUs in each phase is also indicated, in *italic*, as a percentage of the amount of sequences read in that phase.

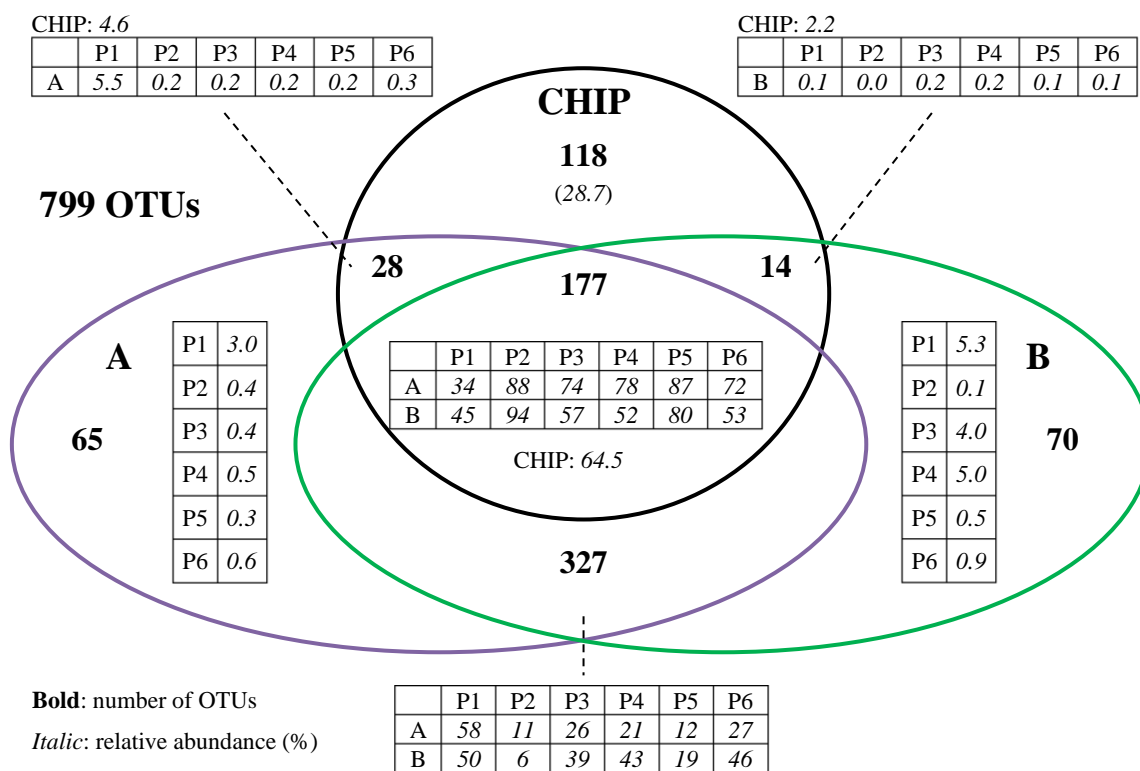


Figure 5.10 – Distribution of unique and shared OTUs (accounting all phases) amongst reactors A and B and the BioChip P, and the relative abundance of each group of OTUs in each operational phase (P1 to P6), expressed as a percentage of the total reads.

Accounting for all phases, Figure 5.10 shows that only 177 OTUs were identified in reactors A, B and in the BioChip P, which is only 22% of the 799 unique OTUs. Nonetheless, those sum up 68.3% of all the sequence reads in the 13 samples. The 327 OTUs that are shared only by reactors A and B correspond to 29% of sequences read over the two reactors and all phases. On the other hand, OTUs that appear exclusively in the biofilms of reactors A or B – shared or not with the BioChip P - give little contribution to their individual bacterial profile, representing no more than 5.5% relative abundance (reactor A and CHIP, phase 1, Figure 5.10). Thus, the bulk of the microbial community in reactors A and B (average 97.8%) are present in both of them, whether also in the BioChip P or not. That indicates that OTUs unique to reactor A or B, that could be due to HRT and filling ratio differences, play a minor role in the overall microbial composition.

In contrast, the 118 OTUs observed exclusively in the BioChip P showed a relative abundance of 28.7% within the bacterial community in its biofilm. Hence, the majority of the OTUs observed in the BioChip P were whether unique or also seen in

reactors A and B (64.5%, Figure 5.10). It suggests that the biofilm microbiomes in reactors A and B are overall more similar to each other than to the BioChip P biofilm. However, when looking specifically at phase 2, when reactors A and B were constrained in phosphorous, alike the BioChip P, 88% and 94% of their microbial communities are composed by OTUs that were found in all three biofilms. Therefore, the existing disparity between the biofilms from lab-scale and the full-scale seems to be mostly related to the difference in nutrients availability at phases 1 and 3 to 6. Distinct biofilm history, maturity and environment of the BioChip P may also differ its microbiome.

The visualization of unique OTUs does not account for differences in the evenness of the microbial communities. Therefore, further comparison of the similarity or disparity between the microbial communities of each sample (beta diversity) made use of non-metric multidimensional scaling (NMDS) analysis based on the Bray-Curtis distance between each sample, as explained in section B.12. Figure 5.11 displays the two-dimensional ordination plot from the NMDS analysis (stress = 0.142), where each point reflects the microbiome composition of each sample. Thus, when comparing two samples, the farther the points are from each other, the greater is the disparity between the bacterial profiles. The contrary is true, the closer the points, the more similar the microbiomes.

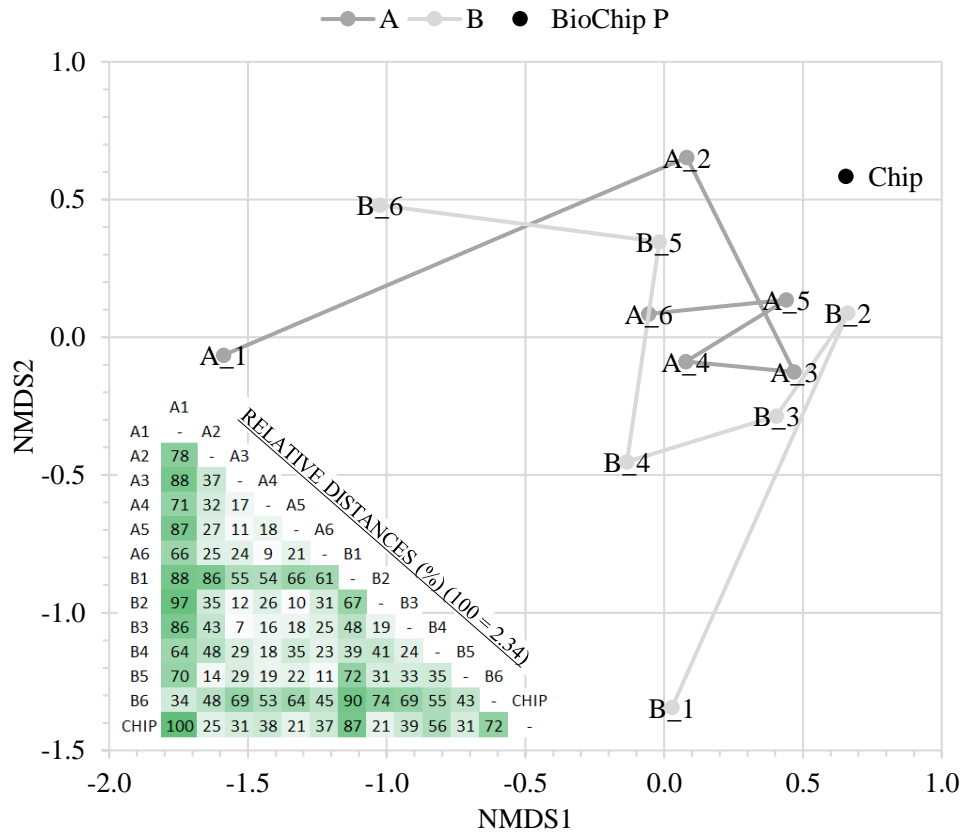


Figure 5.11 – Non-metric multidimensional scaling (NMDS) analysis based on the Bray-Curtis distance (BRAY, CURTIS, 1957) of 13 samples and 374 OTUs. Prior to the analysis, OTUs with no more than 0.1% relative abundance in any sample have been removed. The label at each point identifies the biofilm source (A, B, or Chip from the full-scale) in each phase (1 to 6). Heatmap in the lower-left corner show the relative Euclidean distances between each pair of samples within the NMDS plot.

In phase 1, when reactors A and B had a threefold difference in HRT and nutrients were abundant, the greatest disparity between the microbiomes of the two reactors, in the same phase, was noticed (points A\_1 and B\_1). Once phosphorous was restricted in phase 2, the microbial communities of reactors A and B became more similar between them and were amongst the most alike to the BioChip P biofilm. This result is in accordance with the relative abundances of OTUs observed in all biofilms in this experimental condition (Figure 5.10). Hence, it was clear that within short-term operation under similar operating conditions the lab-scale reactors could develop biofilms comparable to that of the BioChip P, which has been operating with P scarcity for some years. Nonetheless, the difference in maturity resulted in a richer but less diverse biofilm in the BioChip P than in reactors A and B (in phase 2), as indicated by

higher richness and alpha diversity indices (Table 5.5).

When the biofilms were analyzed at the end of phase 3 (limited N, threefold HRT difference), the highest similarity between the bacterial profile of reactors A and B was reached (Figure 5.11, A\_3 and B\_3). The biofilms of reactors A and B remained similar to each other, with slowly increasing disparity, up to phase 5. Once nutrients were made abundant again in phase 6, both biofilms became closer to that of reactor A in phase 1, period when the same HRT and nutrients availability conditions were applied.

When observing the heatmap of relative distances in Figure 5.11, it is evident that the points A\_1, B\_1 and B\_6 - all correspondent to excess of nutrients - are the farthest away from the rest of the samples. As the microbiomes became much more similar during phases 2 to 5 - when P or N were restrained - it is possible that the nutrients limitation is a major factor controlling the microbial community composition, disregarding HRT and filling ratio distinctions. Once nutrients were in excess, the HRT difference presented considerable effect on the disparity of the biofilms in reactors A and B, since B\_1 (1.6 h HRT) is one of the farther points from A\_1 (4.9 h HRT) but B\_6 (4.9 h HRT) is the closest point to A\_1. The fact that the A\_6 point did not become as close to A\_1 could be potentially associated with the low duration of phase 6 (12 days).

The filling ratio, apparently, also led to shifts in microbial community composition, as observed from the results of phase 6, when the filling fraction was the only distinction between the operating conditions of the reactors. However, the Euclidean distance from point A\_6 to B\_6 was only about half of the maximum distance observed in phase 1 (Figure 5.11), when the HRT and filling fraction were different between the two reactors. Nutrients restriction seemed to limit considerably the effect of different filling ratios, because in phase 5 the distance from A\_5 to B\_5 was close to half that noticed in phase 6. Consideration should be made to the fact that the biofilms in the parallel reactors naturally build different histories, and this could also be partly responsible for the observed distinctions.

The multivariate statistical analysis via NMDS is based on the relative abundance of the OTUs in each sample. However, various OTUs may be assigned to a given genus or upper taxonomic levels (family, order, class or phylum). The higher the taxonomic level, the more distinct OTUs are gathered into a single group, making it possible to assess the similarity of microbiomes by a substantially lower number of relative abundances.

Therefore, the microbial community was evaluated at different taxonomic levels,

starting with phylum (Figure 5.12). The results revealed that the dominant 10 phyla accumulated more than 98% of the reads in the 13 samples.

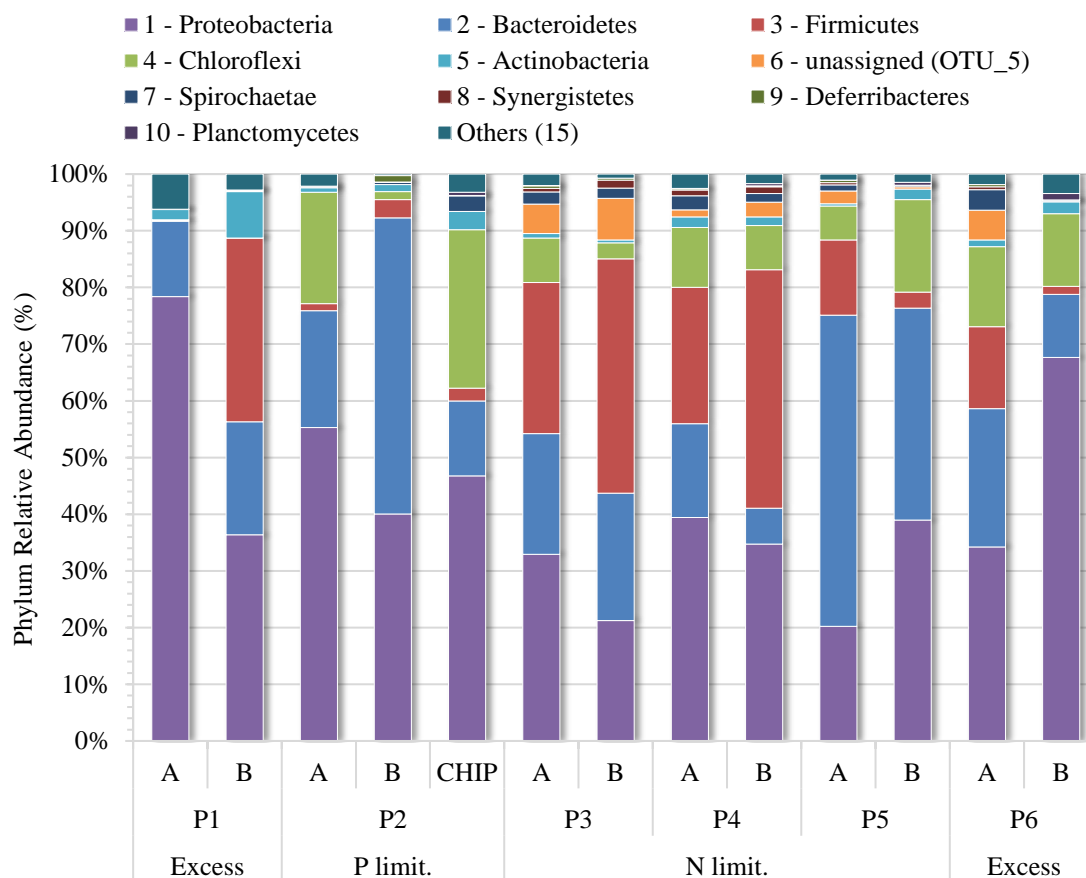


Figure 5.12 – Relative abundance of the 10 most common phyla amongst the 13 samples, for each operational phase and each reactor. Nutrients (N or P), whether in excess or limited, are indicated below each phase.

By analyzing Figure 5.12, it is clear that four phyla – Proteobacteria, Bacteroidetes, Firmicutes and Chloroflexi - dominated the microbial community in whichever condition, with no other phylum ever representing more than 10% relative abundance in any sample. Out of the 25 identified phyla, those represented 92% of all reads. Nevertheless, the distribution of dominance among them shifted from one reactor to another and between distinct operational conditions.

One of the remarkable shifts is regarding the presence of Firmicutes in relation to phosphorous availability. While for every phase with P excess (other than phase 2) it responded for more than 13% in at least one reactor, during phase 2 (and in the BioChip P) it was no higher than 3.2%. The hypothesis that the Firmicutes community was

disfavored during phosphorous restriction is reinforced by the fact that in phase 1 Firmicutes was practically absent in reactor A and highly abundant in reactor B (32%), but in phase 2 it was scarce in both reactors. However, once excess phosphorus conditions were reestablished in phase 3, this phylum became considerably abundant in the two reactors (27% and 41% in A and B, respectively). The little presence of Firmicutes in other scenarios (reactor A phase 1, and reactor B phases 5 and 6) could have resulted from another factors.

The frequency of Chloroflexi phylum correlated positively to the increasing HRT in reactor B under N limitation (i.e., phases 3 to 5). Its relative abundance was, respectively, 2.9, 7.8 and 16.3% at HRT of 1.6, 3.2 and 4.9 h. The same is true for Proteobacteria, whose abundance raised stepwise from 21.2 to 34.7 then 39.0%. Another concordant observation is that reactor A had more Chloroflexi and Proteobacteria than reactor B as long as the former had higher HRT, up to phase 4. In the two remaining phases (5 and 6), when the HRT was the same, reactor B had a higher carrier filling degree and superior relative abundance of the Proteobacteria phylum. These remarks related to higher HRT or filling degree are, in deeper analysis, associated with the organic load: when SLR was the same, the reactor with lower VLR (A, higher HRT) had more Proteobacteria and Chloroflexi; when VLR was the same, the reactor with lower SLR (B, higher filling degree) had more of the mentioned phyla.

The unassigned phylum OTU\_5 was absent during phases 1 and 2, and in the BioChip P. It became the 8<sup>th</sup> most relevant phylum starting at phase 3, when N was made scarce, with a relative abundance ranging from 0.4 to 7.4%. Presumably, this OTU better thrives in N-deprived conditions, despite representing 5.2% of the bacterial profile in reactor A at the end of phase 6. Nevertheless, the short duration of phase 6 (12 days) could pose as a reason for the microbial community not to be completely readapted to excess of N and P. Another hypothesis is derived from the fact that OTU\_5 was completely absent (0 reads) before phase 3: the detection of that OTU in the samples was simply a matter of contamination from an unknown source in the lab where the experiments were run, or from the periodic change of wastewater lot. Either way, it has shown capacity to be selected in an environment low in nitrogen.

At more specific taxonomical levels, the 10 most abundant taxa correspond to a lower percentage of the total reads. Hence, at class level, Figure 5.13 displays the 15 (instead of 10) most abundant ones, grouping 96.1% of the sequence reads.

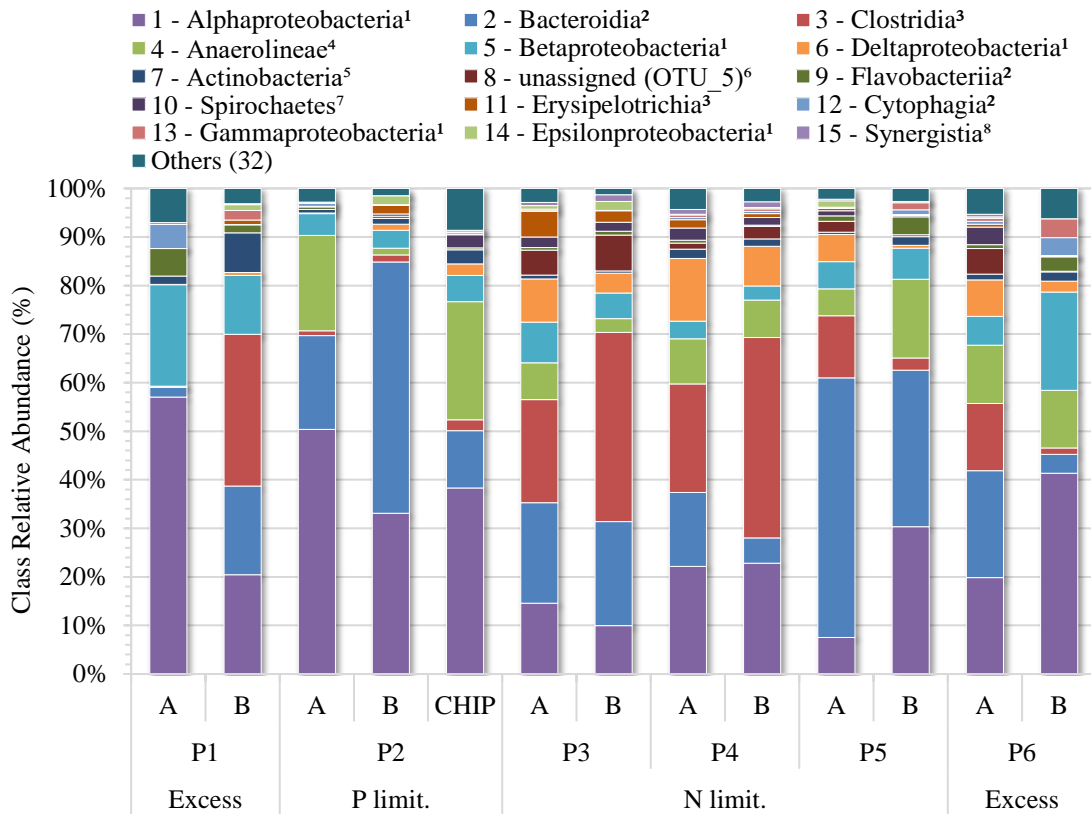


Figure 5.13 – Relative abundance of the 15 most common classes amongst the 13 samples, for each operational phase and each reactor. Nutrients (N or P), whether in excess or limited, are indicated below each phase. Superscript number refers to the phylum that each class belongs to, according to the rank in Figure 5.12.

The previously commented dominance of four phyla is made clearer when assessing the relative abundance distribution at class level, because 11 of the 15 most abundant classes belong to Proteobacteria, Bacteroidetes, Firmicutes or Chloroflexi phyla. Overall, the observation made at phylum level seemed to confirm, with few exceptions, at class evaluation, as is the case of the organic load remark about Proteobacteria and Chloroflexi. The same thing is true to classes Clostridia and Erysipelotrichia, members of the Firmicutes phylum, that were practically absent during P limitation. To obtain further insights about the functional role of microbes or relations to operational conditions, it is necessary to look at abundance distribution at more specific taxa.

The 40 most abundant genera amongst all the 13 biofilm samples from the two reactors and operating phases are listed in Table 5.6. It includes uncultured genera and unassigned OTU, justifying the unmatched number of unique genera shown above in Table 5.4. The most abundant genera in the samples of reactor A and the BioChip were

*Mangroviflexus* and *Rhizobium*. In reactor B, the most abundant microorganisms were from genera *Mangroviflexus*, the chemoautotroph *Acetobacterium* and the aerobic heterotroph *Proteiniphilum*.

Table 5.6 - Relative abundance of the 40 most abundant genera amongst all the 13 biofilm samples from each reactor (A or B) and phase (1 to 6). Square root color scale goes from white to red with raising abundance. Superscript number refers to the phylum that each genus belongs to, according to the rank in Figure 5.12.

i	Genus	Relative Abundance (%)												Chip	Global
		A						B							
		P1	P2	P3	P4	P5	P6	P1	P2	P3	P4	P5	P6		
1	<i>Mangroviflexus</i> <sup>2</sup>	0.3	18	19	14	52	20	0.3	28	19	3.3	30	3.2	11	17
2	<i>Rhizobium</i> <sup>1</sup>	21	19	1.4	4.3	0.5	2.0	7.6	1.8	0.1	2.8	4.4	4.7	6.7	5.8
3	<i>Acetobacterium</i> <sup>3</sup>	0.0	0.0	0.4	0.5	0.0	0.1	0.0	0.0	23	30	0.2	0.1	0.0	4.1
4	<i>Thioclava</i> <sup>1</sup>	0.0	3.8	0.6	1.2	1.2	0.7	5.7	4.7	5.3	4.4	5.1	0.4	5.8	3.0
5	<i>Proteiniphilum</i> <sup>2</sup>	1.3	0.2	0.7	1.0	0.9	2.0	2.7	23	1.6	1.8	0.5	0.4	0.7	3.0
6	<i>Caenispirillum</i> <sup>1</sup>	0.0	13	1.3	0.3	0.8	0.5	1.3	9.7	0.3	0.3	2.8	0.4	0.0	2.5
7	<i>Desulfofustis</i> <sup>1</sup>	0.0	0.0	3.8	7.5	4.6	6.2	0.0	0.0	2.5	6.6	0.2	0.1	0.0	2.4
8	uncultured (OTU_2) <sup>4</sup>	0.0	0.0	0.0	0.6	0.8	4.0	0.0	0.8	2.4	6.5	8.8	5.4	0.6	2.4
9	<i>Christensenellaceae R-7</i> <sup>3</sup>	0.0	0.0	3.8	6.5	3.6	5.0	0.4	0.7	5.5	4.2	0.4	0.2	0.8	2.4
10	uncultured (OTU_12) <sup>4</sup>	0.0	15	3.5	2.3	1.6	1.1	0.0	0.3	0.1	0.6	2.9	1.1	0.4	2.3
11	<i>Pleomorphomonas</i> <sup>1</sup>	0.0	0.3	4.6	3.7	1.5	1.1	2.5	7.1	3.2	1.1	0.1	0.0	1.3	2.0
12	unassigned OTU (OTU_5) <sup>6</sup>	0.0	0.0	5.2	1.2	2.3	5.2	0.0	0.0	7.4	2.6	0.4	0.1	0.0	1.8
13	<i>Dehalobacter</i> <sup>3</sup>	0.0	0.0	5.7	5.1	1.7	1.6	4.2	0.0	3.5	1.8	0.3	0.2	0.6	1.8
14	<i>Devosia</i> <sup>1</sup>	16	0.7	0.1	0.1	0.0	3.2	0.0	0.0	0.0	0.1	0.2	2.5	0.0	1.7
15	<i>Desulfovibrio</i> <sup>1</sup>	0.0	0.0	4.8	5.2	0.9	1.0	0.5	1.1	1.5	1.4	0.2	0.2	1.0	1.3
16	uncultured (OTU_13) <sup>1</sup>	0.0	0.1	2.1	1.6	0.8	2.3	0.4	2.4	0.1	1.0	0.4	0.2	4.1	1.2
17	<i>Propionivibrio</i> <sup>1</sup>	0.1	0.0	4.0	0.6	2.4	0.6	0.9	1.8	3.0	0.4	0.3	0.1	1.0	1.2
18	<i>Erysipelothrix</i> <sup>3</sup>	0.0	0.0	5.4	1.7	0.5	0.6	0.9	1.8	2.4	0.8	0.2	0.1	0.0	1.0
19	<i>Rhodobacter</i> <sup>1</sup>	0.1	0.1	0.2	2.0	0.2	0.8	0.0	0.0	0.0	6.0	3.2	0.4	0.1	1.0
20	<i>Hyphomicrobium</i> <sup>1</sup>	1.3	1.5	0.5	1.0	0.2	0.7	0.0	0.0	0.0	0.3	1.6	4.4	2.1	1.0
21	<i>Anaerolinea</i> <sup>4</sup>	0.0	0.1	1.1	2.7	1.7	4.0	0.0	0.0	0.0	0.0	0.0	0.1	3.0	1.0
22	<i>Azoarcus</i> <sup>1</sup>	1.1	0.4	1.3	0.3	2.0	0.6	0.0	0.2	0.2	0.2	4.3	0.3	1.2	1.0
23	uncultured (OTU_26) <sup>1</sup>	3.1	0.0	0.0	0.1	0.0	0.0	0.0	0.0	0.0	0.0	0.0	9.3	0.0	0.9
24	<i>Flavobacterium</i> <sup>2</sup>	0.8	0.5	0.5	0.3	1.1	0.7	0.7	0.4	0.8	0.3	3.3	1.2	0.2	0.8
25	<i>Xenophilus</i> <sup>1</sup>	7.3	0.0	0.0	0.0	0.0	1.0	0.0	0.0	0.1	0.4	0.0	1.2	0.0	0.8
26	<i>Starkeya</i> <sup>1</sup>	1.7	0.2	0.1	1.5	0.0	1.0	0.0	0.0	0.0	0.2	0.9	4.3	0.2	0.7
27	<i>Noviherbaspirillum</i> <sup>1</sup>	0.0	0.0	1.5	1.4	0.6	1.3	0.1	0.0	1.1	1.1	0.1	0.0	2.1	0.7
28	uncultured (OTU_730) <sup>1</sup>	0.0	0.0	0.3	1.5	0.8	1.5	0.6	0.0	0.2	1.2	0.2	0.0	2.4	0.7
29	<i>Dysgonomonas</i> <sup>2</sup>	0.0	0.1	0.0	0.0	0.0	0.0	9.4	0.3	0.0	0.0	0.0	0.0	0.0	0.7
30	<i>Treponema</i> <sup>7</sup>	0.0	0.1	1.4	1.4	0.7	1.5	0.0	0.3	1.3	0.7	0.2	0.2	0.9	0.7
31	<i>Candidatus Riegeria</i> <sup>1</sup>	0.0	1.8	0.9	0.2	0.3	0.3	0.1	2.7	0.2	0.1	0.1	0.0	1.3	0.6
32	<i>Methylobacillus</i> <sup>1</sup>	0.4	1.0	0.0	0.0	0.0	0.2	1.5	0.0	0.0	0.2	0.3	4.2	0.0	0.6
33	<i>Fastidiosipila</i> <sup>3</sup>	0.0	0.0	1.0	1.5	0.3	1.1	0.8	0.1	1.0	1.4	0.1	0.3	0.0	0.6
34	<i>Stappia</i> <sup>1</sup>	1.0	3.4	0.3	0.5	0.2	0.8	0.2	0.1	0.0	0.1	0.1	0.0	0.3	0.6
35	<i>Wolinella</i> <sup>1</sup>	0.0	0.1	0.7	0.1	1.3	0.3	1.2	1.8	0.9	0.2	0.0	0.0	0.4	0.5
36	<i>Ruminiclostridium</i> <sup>3</sup>	0.0	0.0	1.5	1.3	0.3	0.6	2.4	0.0	0.7	0.6	0.0	0.0	0.0	0.5
37	uncultured (OTU_30) <sup>4</sup>	0.0	0.0	0.0	0.0	0.0	0.0	0.0	0.0	0.0	0.0	0.0	0.0	6.7	0.5
38	<i>Ruminococcaceae UCG-004</i> <sup>3</sup>	0.0	0.0	0.5	0.3	3.4	0.9	0.0	0.0	0.8	0.1	0.2	0.0	0.0	0.5
39	<i>Xanthobacter</i> <sup>1</sup>	0.2	0.0	0.0	0.2	0.0	0.0	0.0	0.0	0.0	0.0	0.1	1.2	4.9	0.5
40	<i>Shinella</i> <sup>1</sup>	1.6	0.7	0.3	0.5	0.2	0.4	0.8	0.8	0.0	0.3	0.1	0.5	0.4	0.5
-	Others (504)	43	21	22	26	11	25	55	10	12	17	28	53	40	27
	Phase	P1	P2	P3	P4	P5	P6	P1	P2	P3	P4	P5	P6	-	-

As may be seen in Table 5.6, it is hard to explain most of the microbial abundance in each reactor at genus level, even looking at the globally most abundant 40 genera. Other genera responded from 10 to 55% in every sample.

At the end of phase 5, the genus *Mangroviflexus* alone was responsible for 52% of the bacterial community in reactor A, and 30% in reactor B. These numbers are quite high for a single genus in such a complex matrix and environment, and it is reflected by the steep drop in the alpha diversity indices shown in Table 5.5. Organisms belonging to this genus were first found in naturally occurring anaerobic cellulose-degrading microbial consortium from mangrove soil (GAO, XU, *et al.*, 2014). These strict anaerobic fermentative heterotrophic bacteria are able to degrade mono and disaccharides resultant from the breakdown of cellulose (DING, STEWART, *et al.*, 2016), with growth conditions at 22-39°C and pH 5.0-8.5. For having light yellow color and dominance in the majority of the samples, *Mangroviflexus* may have contributed to the color of the biofilm (that can be observed in Figure 5.2) (ZHAO, GAO, *et al.*, 2012).

*Mangroviflexus* was also reported in some biological treatment systems: in the anaerobic granular sludge of a UASB reactor treating textile wastewater (ZENG, HAO, *et al.*, 2017); in an aerobic granular SBR treating a mixture of 30% municipal and 70% industrial (printing, dyeing, chemical, textile and beverage) wastewaters (LIU, LI, *et al.*, 2017); and in the sludge of a pit latrine (CHANGARA, SANYIKA, *et al.*, 2019).

As anaerobic microorganisms, *Mangroviflexus*-related bacteria were likely located in deeper (oxygen-deprived) zones of the MBBRs biofilm and expectedly had little abundance in the suspended phase. Since the inoculum of the MBBRs was suspended sludge from the full-scale plant and anaerobic organisms are slow-growing, it is reasonable that phase 1 was the one with the lowest presence of *Mangroviflexus*.

Another bacterial genus that could be related to the inoculum source is the aerobic heterotrophic *Rhizobium*. Both reactors A and B had the greatest abundance of this genus in phase 1, 21 and 7.6%, respectively. The first phase tends to reflect the most of the microbial profile of the activated sludge inoculum from the full-scale plant. *Rhizobium* is well-known for its capability of nitrogen-fixing through endosymbiotic relations with leguminous plants (BITTON, 2011). Recently, this mutualism was extended to microalgae species occurring in wastewater treatment, as *Chlorella vulgaris*, with potential benefits of this association for the treatment of synthetic wastewater (FERRO, COLOMBO, *et al.*, 2019, KIM, RAMANAN, *et al.*, 2014). Then, it may be supposed that it could thrive in the activated sludge, where there is dependence on the recycle of

nitrogen assimilated in the MBBR, which could be not readily available at any given moment or position in the aeration basin.

Also capable of fixing atmospheric nitrogen are the anaerobic organisms of the genus *Desulfovibrio* (BITTON, 2011), as well as members of the Desulfobulbaceae family (genus *Desulfofustis*, in Table 5.6) (DEKAS, CHADWICK, *et al.*, 2014). *Desulfovibrio* and *Desulfofustis* genera had peak abundances in nitrogen-restricted phases (3 to 5), while small contributions were observed in nitrogen-rich phases (1 and 6), with exception of reactor A in phase 1. However, it is unsure if these microorganisms could benefit from nitrogen-fixing metabolism due to the low solubility of N<sub>2</sub> in water and the diffusional barrier in the biofilm. On the other hand, while the competition for other nitrogen sources would be intense, dinitrogen would face low competition for its utilization.

Actually, the change in nitrogen availability in phase 3, seemed to imply a major shift in the microbial communities, as many genera that were absent (or practically absent) in phases 1 and 2 became relevant in phase 3. In both reactors, the following genera had relevant raises in abundance in phase 3, in comparison to the previous phases: *Desulfofustis*<sup>1</sup>, *Christensenellaceae R-7*<sup>3</sup>, unassigned OTU\_5 (as discussed at phylum taxon, Figure 5.12), *Dehalobacter*<sup>3</sup>, *Noviherbaspirillum*<sup>1</sup>, *Treponema*<sup>7</sup>, *Fastidiosipila*<sup>3</sup>. Some other genera had the same behavior but only in reactor A (*Pleomorphomonas*<sup>1</sup>, uncultured OTU\_13<sup>1</sup>, *Propionivibrio*<sup>1</sup>, *Erysipelothrix*<sup>3</sup>, *Anaerolinea*<sup>4</sup>, *Ruminiclostridium*<sup>3</sup>) or in reactor B (*Acetobacterium*<sup>3</sup>, uncultured OTU\_2<sup>4</sup>). One should notice that 5 of the just-mentioned genera belong to Firmicutes phylum, in accordance with the discussion made above. In contrast, *Caenispirillum*<sup>1</sup>, for instance, was abundant in reactors A (13%) and B (9.7%) only in phase 2, probably selected by the P restriction. The same was noticed for the genus *Proteiniphilum*<sup>2</sup> in reactor B (23%), and the uncultured (OTU\_12) in reactor A (15%). Therefore, it is clear that not only nutrient limitation is a major factor controlling the biofilm biodiversity – as discussed from the NMDS analysis (Figure 5.11) – but also which is the restrained nutrient.

The aerobic heterotrophic organisms of the genus *Devosia* seemed to be favored in excess availability of nutrients and higher HRT, as the most representative abundances were noticed during phase 1 in reactor A, and phase 6 in reactors A and B. During the

nutrient-limited phases, these organisms did not thrive, with relative abundances averaging 0.13% in both MBBRs, from phase 2 to 5, and in the BioChip P.

The 4<sup>th</sup> most abundant genus, *Thioclava*, had no great peak abundances like *Mangroviflexus* or *Acetobacterium*. Instead, it was consistently present with an abundance lower than 6%, particularly in reactor B and in the BioChip P. Most of the facultative sulfur-oxidizing *Thioclava* species are yellow coloured, compatible with the yellowish appearance of the biofilm (Figure 5.2) (CHANG, BIRD, *et al.*, 2018). They grow as short rod-shaped bacteria, however, some may also grow as filaments with swollen ends (CHANG, BIRD, *et al.*, 2018, SOROKIN, TOUROVA, *et al.*, 2005). Other genera to which well-known filamentous bacteria belong that were found in the samples are, in order of overall abundance: *Anaerolinea*, *Flavobacterium*, *Trichococcus*, *Acinetobacter*, *Candidatus Alysiosphaera*, *Mycobacterium*, *Streptococcus*, members of the Bacteroidetes class (unassigned OTU\_205), and members of the Saprospiraceae family (*Lewinella*, *Phaeodactylibacter*, CYCU-0281, and uncultured OTUs 542 and 982) (NIELSEN, KRAGELUND, *et al.*, 2009). While *Thioclava* responded for 3.0% of the overall abundance, the other 13 OTU summed up for only 0.7%. Indeed, while the limited nutrients could favor filamentous bacteria, the predominant cause of filamentous growth is low food-to-microorganism ratio, not attended in the high loaded MBBRs (BITTON, 2011). Despite less than 4% seems low abundance, the microscopic observation of the biomass (section 5.7) may better tell about the importance of the presence of filaments.

It is worth mentioning that none of the nitrifying genera (presented in section 2.2.4.1), AOB or NOB, were ever detected, taking into account all the sequence reads in all the 13 samples. This fact reassures that nitrification was not taking place in the reactors and that the removal of TAN was exclusively attributed to bacterial assimilation.

Based on the Venn diagram in Figure 5.10, it was observed that the unique OTUs in the BioChip P responded for a great part of the total sequence reads of that sample (28.7%). Looking at those OTUs, it is also possible to observe which (if any) exclusive taxa were present only in the BioChip P and their relative abundance. In terms of phyla, Dictyoglomi, Omnitrophica and TM6 were present only in the biofilm of the BioChip P. However, they answered for only 0.05% of the bacterial microbiome. The first phylum is represented by the genus *Dictyoglomus*, whereas the other two exclusive phyla are from OTUs not assigned at genus level. Other genera observed uniquely in the BioChip P sample were *Ancalomicrobium*, *Aquicella*, *Candidatus Alysiosphaera*, *Candidatus Chloroploca*, *Candidatus Promineofilum*, *Candidatus Sarcinathrix*, *Chloronema*,

*Chryseobacterium*, *Dokdonella*, *Dolo\_07*, *Ignavibacterium*, *mle1-48*, *Mycobacterium*, *Nordella*, *Oxobacter*, *Patulibacter*, *Pelolinea*, *Phaeodactylibacter*, *Prosthecomicrobium*, *RB349*, *Skermanella*, *Sporobacter* and other 28 uncultured genera. They sum up to 19.7% of the total sequences of the BioChip P biofilm, including the 5<sup>th</sup> (*RB349*), 2<sup>nd</sup>, 12<sup>th</sup>, and 19<sup>th</sup> (three uncultured genera from Anaerolineaceae family) most abundant genera.

Reactor A was the only with the presence of the Chrysiogenetes and Gemmatimonadetes phyla, which accounted for only 0.005% of the microbiome, considering the 6 phases. They were represented by the genera *Desulfurispirillum* and *Gemmatimonas*. Other genera exclusively observed in reactor A were the *Alkaliflexus*, *Bacillus*, *Chelatococcus*, *CYCU-0281*, *Emticicia*, *Intestinibacter*, *Leptolinea*, *Ornatilinea*, *Parapedobacter*, *Rhizomicrobium*, *Silanimonas*, *T78*, *Thermoanaerobaculum*, and other 5 uncultured genera (from families Anaerolineaceae, Christensenellaceae and Porphyromonadaceae). All the genera unique to reactor A did not amount more than 0.17% of the overall sequences over all phases.

No phylum was present solely in reactor B. Nevertheless, the genera that appeared only in this system along the phases were *Ferrovibrio*, *Jonesia*, *Methylophaga*, *Novispirillum*, *Ottowia*, *Pseudorhodobacter*, *Pseudoxanthobacter*, *Ruminococcaceae UCG-014*, *Schumannella*, *Stella*, *Streptococcus*, *Syntrophobotulus*, and other 6 uncultured genera (from families Anaerolineaceae, Chitinophagaceae, Lachnospiraceae, Peptococcaceae and Rhodospirillaceae). These genera, accounted together in all phases, represented 0.33% of the microbial composition in reactor B.

In addition to the bacterial profile, the biomass may also be investigated for the presence and quality of the microfauna community and microbial agglomerates. This is addressed in the next section.

### **5.7. Microscopy of Suspended and Attached Biomass**

Once per phase, micrographs of the suspended and attached biomass were taken for investigation of the quality and diversity of the microfauna, as well as sludge characteristics. Figure 5.14 and Figure 5.15 display, respectively, pictures taken with 100x or 200x magnification under optical microscope (section A.15). Microorganisms that could be identified are pointed out.

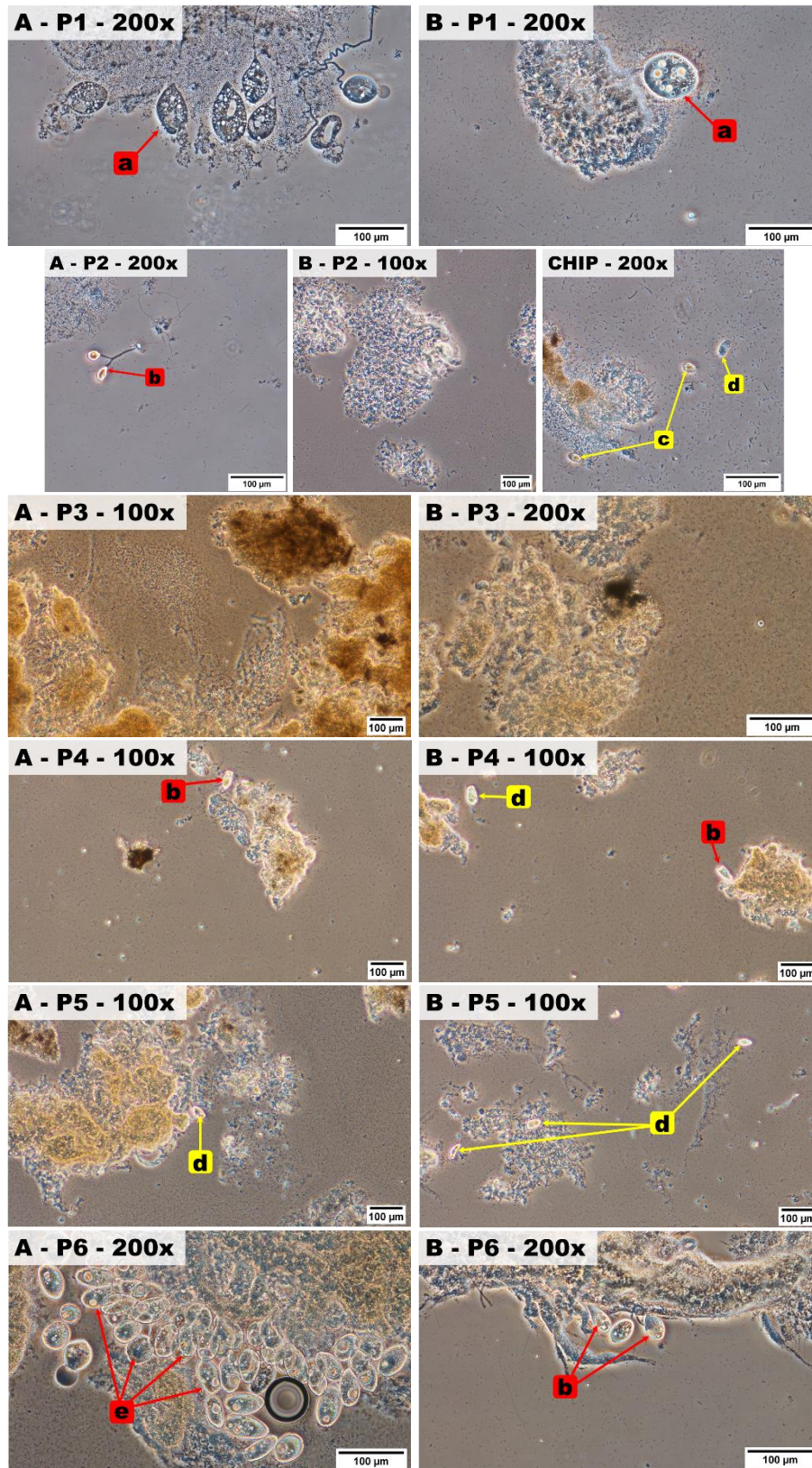


Figure 5.14 – Biofilm micrographs taken at the end of each phase and reactor (magnifications of 100 or 200x). Identified organisms are indicated: (a) Ciliophora (*Vorticella* sp.); (b) Ciliophora (Peritrichia); (c) flagellate; (d) Ciliophora; (e) Ciliophora (*Epistylis* sp.). Yellow color refers to uncertain identifications.

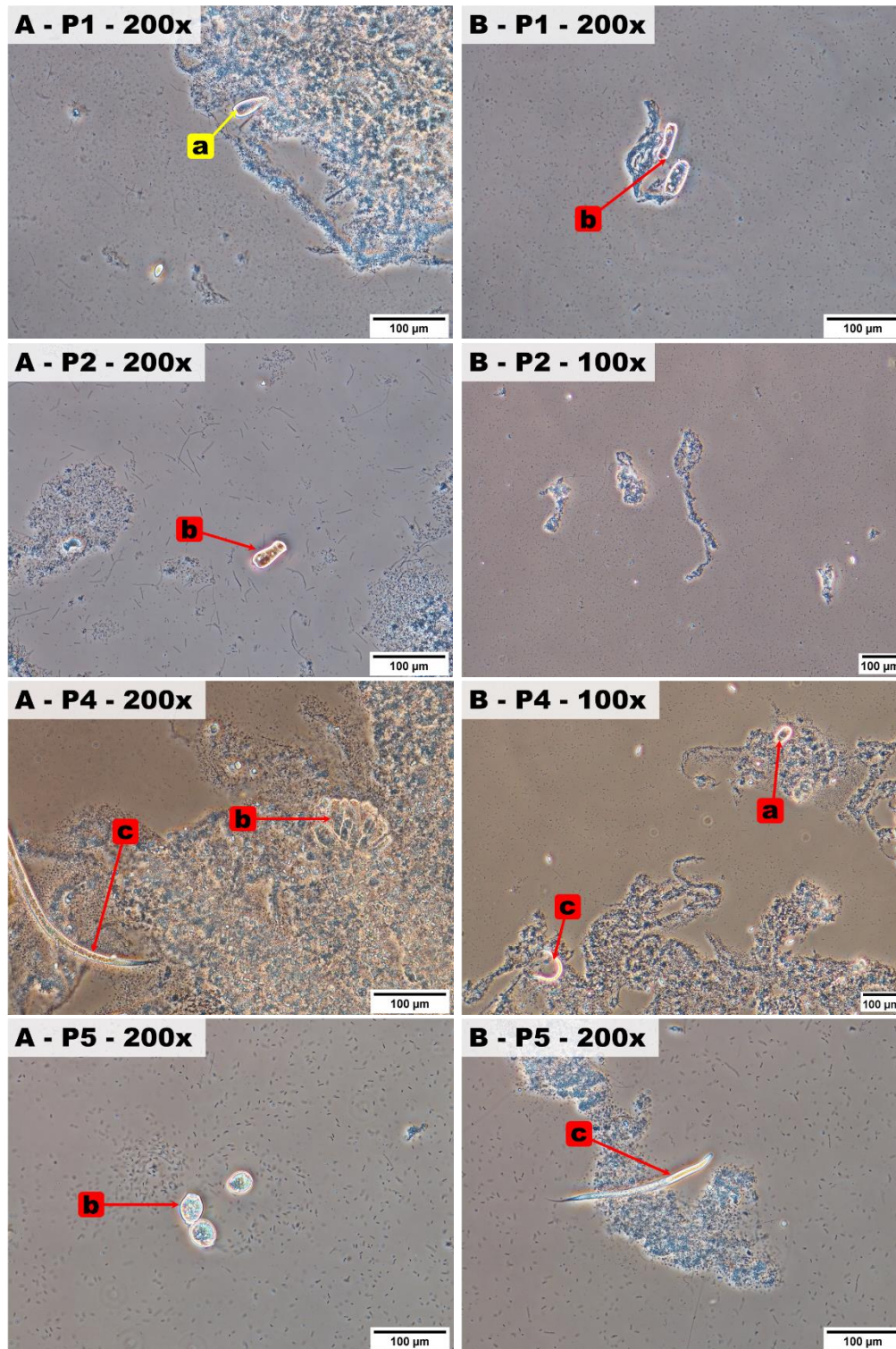


Figure 5.15 –Micrographs of suspended biomass of each reactor at the end of each phase (except phases 3 and 6) (magnifications of 100 or 200x). Identified organisms are indicated: (a) Ciliophora; (b) Ciliophora (Peritrichia); (c) Nematoda. Yellow color refers to uncertain identifications.

Overall, the biofilm presented constant presence of protozoa as small free-swimming flagellates and ciliates, as well as stalked ciliates, which were predominant. In turn, metazoans were mostly absent, with no rotifers and rare nematodes registered. However, in the suspended fraction of the biomass, the nematodes that are seen in phase 4 (Figure 5.15) are most likely originated in the biofilm, as these slow-growing organisms would not be able to multiply before being washed, due to the low suspended biomass retention time.

In one previous work with P&P wastewater from ECF bleached Kraft pulp from Canadian industry, the microfauna inside lab-scale aerobic SBRs was quantified at 35 and 45°C (MORGAN-SAGASTUME, ALLEN, 2003). The authors found that at 35°C a diverse and active microfauna community was established with stalked ciliates, small free-swimming ciliates, flagellates, rotifers, rotifer cysts, and nematodes. However, the shift to 45°C caused mostly small free-swimming flagellates and ciliates to persist, as a probable consequence of deflocculation (JENKINS, RICHARD, *et al.*, 2004).

An activated sludge reactor aerated with pure oxygen had the microfauna systematically investigated while treating wastewater from P&P mills at 35 to 40°C, and SRT of 3.7 days (BERNAT, KULIKOWSKA, *et al.*, 2017). No micrometazoa were observed and only 5 protozoa taxa were identified in 24 samples over 5 months, including small flagellates, crawling ciliates (*Chilodonella uncinata*), free-swimming ciliates (*Sathrophilus muscorum*), and attached ciliates (*Vorticella infusionum*, *Vorticella octava*). The latter was the most abundant group while the temperature remained between 34 to 36°C.

In phase 6, the biofilms had a burst of the protozoa population, consequently also raising their relative abundance in the suspended phase (photos not available). Most of the protozoa in the biofilm were colony-forming stalked ciliates, while free-living protozoa were in a similar proportion compared to previous phases. These characteristics suggest a biofilm providing good depuration and clarification of the wastewater (as seen in section 2.2.6) (BASSIN, DEZOTTI, 2008).

No phase nor reactor had filamentous microorganisms observed whether in the suspended or attached phase. This is in accordance with the scarcity of filamentous bacteria in the biofilm, as stated in the previous section, but also demonstrating that no filamentous fungi were present as well and that the suspended phase also did not provide conditions for the development of filamentous bacteria. Regarding *Thioclava* filamentous morphology shown and described in the literature, it was not recognized in the pictures

(SOROKIN, TOUROVA, *et al.*, 2005), so that supposedly only small rod-shaped *Thioclava* spp. were present.

## 6. CONCLUSIONS

Ahead, conclusions are taken individually for each of the two research projects conducted along the course of this work. Nevertheless, some common conclusions might be pointed out:

- The moving bed biofilm reactor (MBBR) has, indeed, shown the capability to handle upstream oscillations of the wastewaters robustly, showing reasonable to none effects on the health of the treatment. Even when more sharply affected by events, such effects had an acute nature, with fast recovery of steadiness.
- Despite the MBBR being a biofilm technology, dissociating the biofilm concentration and age of the hydraulic retention time (HRT), this parameter was capable of heavily influencing the performance of the treatment system and the biomass dynamics inside the reactor. Its association with the incoming load and the pollutant/biosolids contact-time is the reason for it.
- A greater participation of the suspended biomass in the MBBR requires a combination of sufficiently high organic load and HRT. For the low loaded reactor treating wastewater from pesticide industry, at 6 h HRT, the proportion of suspended solids to the total biosolids in the reactor never exceeded 2.3%. In turn, at a lower HRT (4.9 h), the high loaded MBBR treating pulp and paper (P&P) wastewater achieved up to 30% suspended solids in the total biomass within the reactor. Finally, high organic load in a short 1.6 h HRT resulted in a maximum of 8.5% of planktonic solids.
- Sourcing nutrients both by directly dosing chemicals or blending the industrial wastewater with sanitary sewage are successful approaches. Although the latter also reduces load and reduces toxicity, it might not be feasible for industries producing high effluent flow rates, as is the case for many P&P industries.

### 6.1. Conclusions of the Pesticide Research

Over the long-term operation of the MBBR fed with the mixture of pesticide formulation (whether pretreated, IPT, or raw, IR) wastewater with sanitary sewage, it was

possible to evaluate which conditions allow the application of this technology for the secondary treatment in the industrial site. Seven operational phases were completed, with variations of the HRT (3 or 6 h), IPT quality and proportion (4 or 8% v/v), substitution of the IPT by IR, and proportion of the IR (2 to 4% v/v).

Throughout 742 days, the pesticide-containing wastewater was efficiently treated in an MBBR operated at HRT of 6 h, even for stressed conditions. Removal reached up to 84% COD and 95% TAN when the IPT was used in the feed, and up to 66% COD and 91% TAN with IR. However, differences in pesticide wastewater proportion and quality impacted outlet COD and TAN levels, revealing the presence of persistent compounds and their adverse effects on nitrification, even under mild organic loading rates.

Since the apparent COD removal rates were always substantially lower than the maximum rates, it was shown that even at 3 h, or when fed with the IR wastewater, the reactor was abating COD below its full capacity. Then, the main reason affecting the effluent COD was the presence of persistent, non-biodegradable, compounds sourced from the pesticide waste stream. That was demonstrated by the raises in effluent COD when shifting between distinct IPT lots or when increasing proportion of the IR. Indeed, a maximum biodegradability of 65% was found for the IR, in the mixture with sanitary sewage. Furthermore, the MBBR was capable of hydrolyzing and degrading incoming particulate COD. Therefore, the effluent suspended solids and turbidity were low, with mean proportion of suspended biomass to total biomass within the reactor of only 1.9%.

Nitrification took place in the MBBR as the main mechanism of nitrogen conversion. This was confirmed through direct analysis of nitrogen compounds, obtainment of TAN maximum removal rates using batch assays, and assessment of the nitrifying community by FISH. During the experiments, the extent of nitrification was negatively affected by the lower HRT/higher organic load in the initial phases, which favored heterotrophs in the competition with the nitrifiers. In addition, the IR wastewater constrained nitrification, mainly by inhibition of AOB, that were the dominant nitrifiers in relative abundance but less resistant to inhibiting chemicals. Despite that the replication of the pre-treatment with PAC adsorption in the lab attested how the process is laborious and expensive, it has an important role in preserving the nitrification performance in the secondary treatment. Nevertheless, microscopy observations suggested tolerable and steady toxicity to the overall microbiota, as evidenced by the stable presence of micrometazoa and protozoa.

In general, the reactor was tested in diverse and extraordinary feeding conditions, in terms of wastewater composition, COD, TAN and TSS. It is possible to conclude that under the nominal conditions of the industrial treatment plant, an HRT of 3 h could suffice for adequate treatment. However, instabilities in the feed could easily cause the biological system to produce an effluent that may not meet the discharge criteria. Hence, MBBR operation at 50% filling degree (at 250 m<sup>2</sup>/m<sup>3</sup>) and 6 h HRT seems to be a safe alternative for the treatment of the pesticide formulation wastewater, with robustness to resist shocks while guarantying nitrification and organic matter removal.

Beyond the robustness, the MBBR substituting the existing activated sludge plant means savings in space, given the compactness of the reactor; easiness of operation and maintenance; needlessness of sludge recycle lines; and minimization of the sizing of the secondary solids separation unit. Therefore, the MBBR enables the reduction of the operational complexity of the secondary treatment of the pesticide formulation wastewater.

## **6.2. Conclusions of the P&P Research**

Over the course of 337 days, the parallel operation of two MBBRs differing on the reactor's specific surface area has shown that the balance between volumetric and surface properties may lead to optimal reactor design that prioritizes either greater volume/HRT/nutrient dosing efficiency or carrier filling degree/compactness. A threefold higher carrier filling ratio would allow a 33% smaller MBBR without compromising the performance of organic matter removal. Higher HRT (factor of 3) was associated with a greater concentration of suspended solids (by 1.4 to 2.1 times) that had a higher maximum specific sCOD removal rate, by up to 2.5 times, and represented as much as 30% of the total biomass in the reactor. Batch assays confirmed that higher HRT/lower filling degree provided greater activity in the suspended biomass fraction, whereas lower HRT/higher filling degree had the activity concentrated in the attached biomass fraction. At each reactor, shifting from excess to limitation of nutrients availability seemed to reduce the maximum sCOD utilization rate from the most active biomass fraction while the less active fraction remained unchanged regarding this rate. This effect was more substantial in the reactor designed to favor biofilm activity.

The ratio of sCOD removed by N or P consumed increased at 3 times higher HRT, as much as 1.7 times for P and 1.5 times for N, suggesting that the planktonic solids utilize

nutrients more efficiently for COD removal than the attached biomass. Restricting one nutrient availability (N or P) was another factor that improved simultaneously the efficacy of N and P utilization for sCOD removal, by up to 2.7 times for the restricted nutrient and 1.7 to the abundant one. The best observed scenario for savings in nutrients supplementation involved the highest HRT (4.9 h) during N limitation. For such case, the minimal sCOD:N:P proportion of 100:0.70:0.14 would grant depletion of the biodegradable sCOD. As the P/COD ratio originally present in the wastewater was eventually greater than 0.14% and N was consistently absent, limiting N availability is even more suitable. The effect of the carrier filling ratio on the efficiency of N and P utilization for sCOD removal seemed to be positive but was statistically inconclusive.

Excellent fit of data from continuous reactor operation to the Kincannon-Stover kinetic model was made possible by the HRT variation, which revealed maximum volumetric removal rate of 30.6 kg/(m<sup>3</sup>·d) and 50.3% biodegradability of the wastewater. It was consistent with the biodegradability obtained via extended biofilm batch trials (46%). Maximum biodegradable sCOD removal was reached at excess of nutrients, 4.9 h HRT and 15 or 45% carrier filling ratio, while only 32% of the sCOD was removed at 1.6 h and 45% filling ratio.

DNA sequencing of biofilm samples revealed that the two reactors shared many microorganisms at differing abundances, with little quantitative importance of those found solely in one of the reactors. Nutrients limitation was a primary factor shaping the biofilm microbiome, in spite of other operational differences. Nevertheless, once N and P were in excess, the HRT had a substantial influence on the microbial community composition, whereas the filling ratio played a minor role. While P was limited, the microbial profile of the reactors had the highest similarity to that of the BioChip P, from the full-scale MBBR at the industry, also restricted in phosphorous. Even though, there was a high number of OTUs detected uniquely in the BioChip P, whose relative abundance was 29%. Long-term maturity, distinct biofilm history and environment are possible reasons for the remarkable differences.

This study further assessed the effect of important factors relevant to the design and operation of MBBR reactors for P&P wastewater treatment, as in the nutrient-limited BAS configuration, such as HRT and volumetric load, carrier filling degree and specific surface area, and nutrients dosing. All of those factors have shown to have relevant effects on the reactors COD removal performance and the associated consumption of nutrients,

the distribution and activity of attached and suspended biomass fractions, and the composition of biofilm microbial community.

## 7. SUGGESTIONS AND ADVICES FOR FUTURE WORKS

Due to the peculiarities of each kind of wastewater and operational aspects of each study, individual suggestions are presented in the following subsections. However, a common suggestion would be to monitor key chemical substances of industrial interest in addition to general pollution parameters. That could bring specific substance-related perceptions about the performance of the reactors and the biosolids and microbial community dynamics.

### 7.1. Suggestions Arising from the Pesticide Research

Since the nitrification efficiency is relevant due to the TAN level of the sanitary wastewater, and that the initial phases demonstrated that the 3 h HRT is insufficient because of the organic load, another MBBR configuration could be tested, as reactors in series, aiming to grant efficient TAN removal even at lower HRTs.

Possibly, it would be valuable to substitute the real sanitary wastewater for a synthetic solution simulating it. As the variability of the quality of the sewage produced in the industrial site was considerably high, it implied too many oscillations in the feed quality. Disregarded the fact that the oscillation was a good thing to reaffirm the robustness of the MBBR, it also inferred in a lot of noise in the data, disturbing interpretations of some aspects.

Operating a parallel MBBR fed only with the sanitary portion of the wastewater could help dealing with such noise. Additionally, it could reveal the biodegradability of each pesticide lot and clarify some of the effects of the industrial pesticide wastewater fraction on the performance of the reactor and the microbial community. Regarding the latter, biomolecular techniques that could describe the bacterial profile would potentially give insights about the key bacterial strains in the biofilm and how its bacterial community changed after alterations of the wastewater lot and when shifting from pretreated to raw pesticide wastewater.

Performing toxicity assays in the MBBR exiting stream would clarify if the increasing persistent COD, consequent to the raises in the proportion of the pesticide wastewater in the feed, is impactful beyond the effect of organic load reaching water

bodies. Despite toxicity evaluations were planned, practical issues prevented them from being executed.

After the last operational phase, it would be interesting to raise the HRT of the MBBR and see if a greater wastewater/biomass contact time and lower load would provide greater removal of the remaining COD and recovery of nitrifying capacity. Extending the last phase for some weeks would be interesting too, as nitrifiers have been reported to have slow acclimation to some inhibiting conditions (GRAY, 2004).

## **7.2. Suggestions Arising from the P&P Research**

As presented in section 5.6, limiting N or P produce different effects in the biofilm microbiome. Therefore, strategies of lowering both N and P – simultaneously or stepwise - could also be investigated. Would the bacterial strains be selected in the same manner, resulting in similar final bacterial profiles?

Performing DNA analysis in suspended solids as well would provide further understanding of the peculiar roles played by the attached and suspended biomass, as different abundances could be expected in the established planktonic community. In the same context, assessing the bacterial profile of the inoculum that seeded the lab reactors could clarify which bacterial strains were selected during the bench-scale reactors operation.

Changing the source of wastewater to another P&P industrial site employing different raw material and pulping and bleaching technologies could elucidate to which extent the conclusions of the research apply to generic P&P wastewaters.

Submitting the wastewater of the MBBRs to a lab-scale activated sludge system and performing the same evaluations on the second step of a full BAS has the potential to derive even more practical insights about the operation of this system for the treatment of P&P wastewaters.

## 8. REFERENCES

AFFAM, A. C., CHAUDHURI, M., KUTTY, S. R. M., *et al.* "Combination of FeGAC/H<sub>2</sub>O<sub>2</sub> advanced oxidation process and sequencing batch reactor for treatment pesticide wastewater", **Environmental Earth Sciences**, v. 75, n. 4, p. 349, 16 fev. 2016. DOI: 10.1007/s12665-015-4988-0. .

AFFAM, A. C., CHAUDHURI, M., KUTTY, S. R. M., *et al.* "UV Fenton and sequencing batch reactor treatment of chlorpyrifos, cypermethrin and chlorothalonil pesticide wastewater", **International Biodeterioration & Biodegradation**, v. 93, p. 195–201, set. 2014. DOI: 10.1016/j.ibiod.2014.06.002. .

AHN, Y.-H. "Sustainable nitrogen elimination biotechnologies: A review", **Process Biochemistry**, v. 41, n. 8, p. 1709–1721, ago. 2006. DOI: 10.1016/j.procbio.2006.03.033. .

ALBERTSEN, M., KARST, S. M., ZIEGLER, A. S., *et al.* "Back to Basics – The Influence of DNA Extraction and Primer Choice on Phylogenetic Analysis of Activated Sludge Communities", **PLOS ONE**, v. 10, n. 7, p. e0132783, 16 jul. 2015. DOI: 10.1371/journal.pone.0132783. .

AMANN, R. I., BINDER, B. J., OLSON, R. J., *et al.* "Combination of 16S rRNA-targeted oligonucleotide probes with flow cytometry for analyzing mixed microbial populations.", **Applied and Environmental Microbiology**, v. 56, n. 6, p. 1919–1925, 1990. DOI: 10.1128/AEM.56.6.1919-1925.1990. .

ANOXKALDNES. **AnoxKaldnes™ MBBR & BAS technology**. . [S.l.: s.n.]. , 2019

ANOXKALDNES. **AnoxKaldnes™ MBBR**. . Canada, [s.n.]. , 2014

APHA, AWWA, WEF. **Standard Methods for the Examination of Water and Wastewater (23rd edition)**. 23rd. ed. USA, American Public Health Association; American Water Works Association; Water Environment Federation, 2017.

ATKINS, P. R. **The pesticide manufacturing industry: current waste treatment and disposal practices**. 1st. ed. USA, EPA, 1972.

BACHMANN PINTO, H., MIGUEL DE SOUZA, B., DEZOTTI, M. "Treatment of a pesticide industry wastewater mixture in a moving bed biofilm reactor followed by conventional and membrane processes for water reuse", **Journal of Cleaner Production**, v. 201, p. 1061–1070, nov. 2018. DOI: 10.1016/j.jclepro.2018.08.113. .

BADAWY, M. I., GAD-ALLAH, T. A., GHALY, M. Y., *et al.* "Combination of photocatalytic and biological processes as an integrated system for treatment and recovery of industrial wastewater containing pesticides", **Afinidad**, v. 63, n. 526, p. 478–487, 2006. .

BAEZA, R., JARPA, M., VIDAL, G. "Polyhydroxyalkanoate Biosynthesis from Paper Mill Wastewater Treated by a Moving Bed Biofilm Reactor", **Water, Air, & Soil Pollution**, v. 227, n. 9, p. 299, 4 set. 2016. DOI: 10.1007/s11270-016-2969-x. .

BAJPAI, P. **Biermann's Handbook of Pulp and Paper**. 3rd. ed. India, Elsevier, 2018.

BALLESTEROS MARTÍN, M. M., SÁNCHEZ PÉREZ, J. A., CASAS LÓPEZ, J. L., *et al.* "Degradation of a four-pesticide mixture by combined photo-Fenton and biological oxidation", **Water Research**, v. 43, n. 3, p. 653–660, fev. 2009. DOI: 10.1016/j.watres.2008.11.020. .

BASSIN, J. P., DEZOTTI, M., "Moving Bed Biofilm Reactor (MBBR)". **Advanced Biological Processes for Wastewater Treatment - Emerging, Consolidated Technologies and Introduction to Molecular Techniques**, 1st. ed. Brazil, Springer, 2018. p. 37–74.

BASSIN, J. P., DEZOTTI, M., "Tratamento primário, secundário e terciário de efluentes". **Processos e Técnicas para o Controle Ambiental de Efluentes Líquidos**, 1st. ed. Rio de Janeiro, Brazil, E-papers, 2008. p. 53–226.

BASSIN, J. P., DEZOTTI, M., ROSADO, A., "Molecular Biology Techniques Applied to the Study of Microbial Diversity of Wastewater Treatment Systems". **Advanced Biological Processes for Wastewater Treatment - Emerging, Consolidated Technologies and Introduction to Molecular Techniques**, 1st. ed. Brazil, Springer, 2018. p. 205–294.

BASSIN, J. P., DEZOTTI, M., SANT'ANNA, G. L. "Nitrification of industrial and domestic saline wastewaters in moving bed biofilm reactor and sequencing batch reactor",

**Journal of Hazardous Materials**, v. 185, n. 1, p. 242–248, jan. 2011. DOI: 10.1016/j.jhazmat.2010.09.024. .

BASSIN, J. P., RACHID, C. T. C. C., VILELA, C., *et al.* "Revealing the bacterial profile of an anoxic-aerobic moving-bed biofilm reactor system treating a chemical industry wastewater", **International Biodeterioration & Biodegradation**, v. 120, p. 152–160, maio 2017. DOI: 10.1016/j.ibiod.2017.01.036. .

BENTO, A. P., HOFFMANN, H., "Microbiologia e Ecologia de Sistemas Aeróbios de Tratamento de Esgotos". In: SCHIMIDELL, W., SOARES, H. M., ETCHEBEHERE, C., *et al.* (Org.), **Tratamento Biológico de Águas Residuárias**, Florianópolis, [s.n.], 2007. .

BERNAT, K., KULIKOWSKA, D., DRZEWICKI, A. "Microfauna community during pulp and paper wastewater treatment in a UNOX system", **European Journal of Protistology**, v. 58, p. 143–151, abr. 2017. DOI: 10.1016/j.ejop.2017.02.004. .

BITTON, G. **Wastewater Microbiology**. 4th. ed. Hoboken, US, Willey-Blackwell, 2011.

BOLGER, A. M., LOHSE, M., USADEL, B. "Trimmomatic: a flexible trimmer for Illumina sequence data", **Bioinformatics**, v. 30, n. 15, p. 2114–2120, 1 ago. 2014. DOI: 10.1093/bioinformatics/btu170. .

BOTHE, H., FERGUSON, S. J., NEWTON, W. E. **Biology of the Nitrogen Cycle**. 1st. ed. Netherlands, Elsevier, 2007.

BRASIL. **Decreto nº 4.074, de 4 de janeiro de 2002**. 2002. Disponível em: [http://www.planalto.gov.br/ccivil\\_03/decreto/2002/d4074.htm](http://www.planalto.gov.br/ccivil_03/decreto/2002/d4074.htm). Acesso em: 27 abr. 2020.

BRASIL. **Lei nº 7.802, de 11 de julho de 1989**. 1989. Disponível em: [https://www.planalto.gov.br/ccivil\\_03/leis/17802.htm](https://www.planalto.gov.br/ccivil_03/leis/17802.htm). Acesso em: 27 abr. 2020.

BRASIL. **Ministério do Meio Ambiente - Agrotóxicos**. 2017. Disponível em: <http://www.mma.gov.br/seguranca-quimica/agrotoxicos>. Acesso em: 7 set. 2017.

BRASIL. **Portaria nº 03/92 (SNVS/MS)**. . Brasília, Brasil, [s.n.], 1992

BRAY, J. R., CURTIS, J. T. "An Ordination of the Upland Forest Communities of Southern Wisconsin", **Ecological Monographs**, v. 27, n. 4, p. 325–349, fev. 1957. DOI:

10.2307/1942268. .

BRINK, A., SHERIDAN, C., HARDING, K. "Combined biological and advance oxidation processes for paper and pulp effluent treatment", **South African Journal of Chemical Engineering**, v. 25, n. 2018, p. 116–122, jun. 2018. DOI: 10.1016/j.sajce.2018.04.002. .

BRINK, A., SHERIDAN, C. M., HARDING, K. G. "A kinetic study of a mesophilic aerobic moving bed biofilm reactor (MBBR) treating paper and pulp mill effluents: The impact of phenols on biodegradation rates", **Journal of Water Process Engineering**, v. 19, n. August 2016, p. 35–41, out. 2017. DOI: 10.1016/j.jwpe.2017.07.003. .

CABRERA, M. N., "Pulp Mill Wastewater: Characteristics and Treatment". **Biological Wastewater Treatment and Resource Recovery**, 1st. ed. [S.l.], InTech, 2017. . DOI: 10.5772/67537.

CALDERÓN, K., MARTÍN-PASCUAL, J., POYATOS, J. M., *et al.* "Comparative analysis of the bacterial diversity in a lab-scale moving bed biofilm reactor (MBBR) applied to treat urban wastewater under different operational conditions", **Bioresource Technology**, v. 121, p. 119–126, out. 2012. DOI: 10.1016/j.biortech.2012.06.078. .

CANLER, J.-P., PERRET, J.-M., DUCHÈNE, P., *et al.* **Aide au diagnostic des stations d'épuration par l'observation microscopique des boues activées**. France, Editions Quae, 2011.

CAO, S. M. S., DEZOTTI, M., BASSIN, J. P. "MBBR followed by microfiltration and reverse osmosis as a compact alternative for advanced treatment of a pesticide-producing industry wastewater towards reuse", **The Canadian Journal of Chemical Engineering**, v. 94, n. 9, p. 1657–1667, set. 2016. DOI: 10.1002/cjce.22542. .

CAO, S. M. S., FONTOURA, G. A. T., DEZOTTI, M., *et al.* "Combined organic matter and nitrogen removal from a chemical industry wastewater in a two-stage MBBR system", **Environmental Technology**, v. 37, n. 1, p. 96–107, 2 jan. 2016. DOI: 10.1080/09593330.2015.1063708. .

CAPORASO, J. G., KUCZYNSKI, J., STOMBAUGH, J., *et al.* "QIIME allows analysis of high-throughput community sequencing data", **Nature Methods**, v. 7, n. 5, p. 335–336, 11 maio 2010. DOI: 10.1038/nmeth.f.303. .

CAPORASO, J. G., LAUBER, C. L., WALTERS, W. A., *et al.* "Ultra-high-throughput microbial community analysis on the Illumina HiSeq and MiSeq platforms", **The ISME Journal**, v. 6, n. 8, p. 1621–1624, 8 ago. 2012. DOI: 10.1038/ismej.2012.8. .

CARRA, I., SÁNCHEZ PÉREZ, J. A., MALATO, S., *et al.* "Performance of different advanced oxidation processes for tertiary wastewater treatment to remove the pesticide acetamiprid", **Journal of Chemical Technology & Biotechnology**, v. 91, n. 1, p. 72–81, jan. 2016. DOI: 10.1002/jctb.4577. .

CERDA, R., AVELINO, J., GARY, C., *et al.* "Primary and Secondary Yield Losses Caused by Pests and Diseases: Assessment and Modeling in Coffee", **PLOS ONE**, v. 12, n. 1, p. e0169133, 3 jan. 2017. DOI: 10.1371/journal.pone.0169133. .

CHANG, R., BIRD, L., BARR, C., *et al.* "Thioclava electrotropha sp. nov., a versatile electrode and sulfur-oxidizing bacterium from marine sediments", **International Journal of Systematic and Evolutionary Microbiology**, v. 68, n. 5, p. 1652–1658, 1 maio 2018. DOI: 10.1099/ijsem.0.002723. .

CHANGARA, M., SANYIKA, W., BANGIRA, C., *et al.* "Physico-chemical properties and bacterial community structure dynamics during the mesophilic anaerobic digestion of pit latrine faecal sludge", **Water SA**, v. 45, n. 3 July, p. 338–348, 31 jul. 2019. DOI: 10.17159/wsa/2019.v45.i3.6730. .

CHAO, A. "Nonparametric Estimation of the Number of Classes in a Population", **Scandinavian Journal of Statistics**, v. 11, p. 265–270, 1984. .

CHEN, S., SUN, D., CHUNG, J.-S. "Treatment of pesticide wastewater by moving-bed biofilm reactor combined with Fenton-coagulation pretreatment", **Journal of Hazardous Materials**, v. 144, n. 1–2, p. 577–584, jun. 2007. DOI: 10.1016/j.jhazmat.2006.10.075. .

CHENG, G., LIN, J., LU, J., *et al.* "Advanced Treatment of Pesticide-Containing Wastewater Using Fenton Reagent Enhanced by Microwave Electrodeless Ultraviolet", **BioMed Research International**, v. 2015, p. 1–8, 2015. DOI: 10.1155/2015/205903. .

COLLIVER, B. B., STEPHENSON, T. "Production of nitrogen oxide and dinitrogen oxide by autotrophic nitrifiers", **Biotechnology Advances**, v. 18, n. 3, p. 219–232, maio 2000. DOI: 10.1016/S0734-9750(00)00035-5. .

CONAMA. "Resolução n 357, 18 de março de 2005", **Diário Oficial**, n. 053, p. 58–63, 2005. DOI: nº 053, de 18/03/2005. .

CONAMA. **Resolução n 430, 16 de maio de 2011**. . [S.l: s.n.], , 2011

DAIMS, H., BRÜHL, A., AMANN, R., *et al.* "The Domain-specific Probe EUB338 is Insufficient for the Detection of all Bacteria: Development and Evaluation of a more Comprehensive Probe Set", **Systematic and Applied Microbiology**, v. 22, n. 3, p. 434–444, set. 1999. DOI: 10.1016/S0723-2020(99)80053-8. .

DAIMS, H., LEBEDEVA, E. V., PJEVAC, P., *et al.* "Complete nitrification by *Nitrospira* bacteria", **Nature**, v. 528, n. 7583, p. 504–509, 24 dez. 2015. DOI: 10.1038/nature16461. .

DAIMS, H., NIELSEN, J. L., NIELSEN, P. H., *et al.* "In Situ Characterization of *Nitrospira*-Like Nitrite-Oxidizing Bacteria Active in Wastewater Treatment Plants", **Applied and Environmental Microbiology**, v. 67, n. 11, p. 5273–5284, 1 nov. 2001. DOI: 10.1128/AEM.67.11.5273-5284.2001. .

DALENTOFT, E., THULIN, P. "The use of the kaldnes suspended carrier process in treatment of wastewaters from the forest industry", **Water Science and Technology**, v. 35, n. 2–3, p. 123–130, 1997. DOI: 10.1016/S0273-1223(96)00923-7. .

DEKAS, A. E., CHADWICK, G. L., BOWLES, M. W., *et al.* "Spatial distribution of nitrogen fixation in methane seep sediment and the role of the ANME archaea", **Environmental Microbiology**, v. 16, n. 10, p. 3012–3029, out. 2014. DOI: 10.1111/1462-2920.12247. .

DEZOTTI, M. **Processos e Técnicas para o Controle Ambiental de Efluentes Líquidos**. 1st. ed. Rio de Janeiro, Brazil, E-papers, 2008.

DING, W., STEWART, D. I., HUMPHREYS, P. N., *et al.* "Role of an organic carbon-rich soil and Fe(III) reduction in reducing the toxicity and environmental mobility of chromium(VI) at a COPR disposal site", **Science of The Total Environment**, v. 541, p. 1191–1199, jan. 2016. DOI: 10.1016/j.scitotenv.2015.09.150. .

DOBLE, M., KUMAR, A. **Biotreatment of Industrial Effluents**. 1st. ed. UK, Elsevier, 2005.

DODGE, Y. **The Concise Encyclopedia of Statistics**. 1st. ed. Germany, Springer, 2008.

EDGAR, R. C. "UPARSE: highly accurate OTU sequences from microbial amplicon reads", **Nature Methods**, v. 10, n. 10, p. 996–998, 18 out. 2013. DOI: 10.1038/nmeth.2604. .

EK, M., GELLERSTEDT, G., HENRIKSSON, G. **Wood Chemistry and Wood Biotechnology**. [S.l.], De Gruyter, 2009. v. 1.

EPA. "Method 352.1: Nitrogen, Nitrate (Colorimetric , Brucine) by Spectrophotometer", p. 5, 1971. .

FERRIMAN, A. "BMJ readers choose the “sanitary revolution” as greatest medical advance since 1840", **BMJ**, v. 334, n. 7585, p. 111.2-111, 20 jan. 2007. DOI: 10.1136/bmj.39097.611806.DB. .

FERRO, L., COLOMBO, M., POSADAS, E., *et al.* "Elucidating the symbiotic interactions between a locally isolated microalga *Chlorella vulgaris* and its co-occurring bacterium *Rhizobium* sp. in synthetic municipal wastewater", **Journal of Applied Phycology**, v. 31, n. 4, p. 2299–2310, 2 ago. 2019. DOI: 10.1007/s10811-019-1741-1. .

FIROUZSALARI, N. Z., SHAKERKHATIBI, M., POURAKBAR, M., *et al.* "Pyrethroid pesticide residues in a municipal wastewater treatment plant: Occurrence, removal efficiency, and risk assessment using a modified index", **Journal of Water Process Engineering**, v. 29, n. March, p. 100793, jun. 2019. DOI: 10.1016/j.jwpe.2019.100793. .

FUNASA. **Manual de Saneamento**. 3rd. ed. Brasília, Brasil, Fundação Nacional de Saúde, 2004.

GAIOTO, F. C. **Tratamento de Efluentes da Indústria Química pela Combinação de Processos Biológicos e Físico-Químicos visando ao Reúso**. 2019. Federal University of Rio de Janeiro, 2019.

GAO, Z.-M., XU, X., RUAN, L.-W. "Enrichment and characterization of an anaerobic cellulolytic microbial consortium SQD-1.1 from mangrove soil", **Applied Microbiology and Biotechnology**, v. 98, n. 1, p. 465–474, 26 jan. 2014. DOI: 10.1007/s00253-013-4857-2. .

GARCÍA-MANCHA, N., MONSALVO, V. M., PUYOL, D., *et al.* "Enhanced anaerobic degradability of highly polluted pesticides-bearing wastewater under thermophilic conditions", **Journal of Hazardous Materials**, v. 339, p. 320–329, out. 2017. DOI: 10.1016/j.jhazmat.2017.06.032. .

GOTELLI, N. J., CHAO, A., "Measuring and Estimating Species Richness, Species Diversity, and Biotic Similarity from Sampling Data". **Encyclopedia of Biodiversity**, 2nd. ed. USA, Elsevier, 2013. v. 5. p. 195–211. DOI: 10.1016/B978-0-12-384719-5.00424-X.

GOYAL, H. **BLEACHING STAGES AND SEQUENCES**. 2020a. Paper on Web. Disponível em: <https://paperonweb.com/bleach.htm>. Acesso em: 5 set. 2020.

GOYAL, H. **RAW MATERIALS FOR PAPERMAKING**. 2020b. Paper on Web. Disponível em: <https://paperonweb.com/RawMaterial.htm>. Acesso em: 18 ago. 2020.

GRADY, C. P. L., DAIGGER, G. T., LOVE, N. G., *et al.* **Biological Wastewater Treatment**. 3rd. ed. [S.l.], CRC Press, 2011.

GRAY, N. F. **Biology of Wastewater Treatment**. 2nd. ed. [S.l.], Imperial College Press, 2004.

GREENACRE, M., PRIMICERIO, R. **Multivariate Analysis of Ecological Data**. 1st. ed. Spain, Fundación BBVA, 2013.

HARREMOËS, P. "Criteria for Nitrification in Fixed Film Reactors", **Water Science and Technology**, v. 14, n. 1–2, p. 167–187, 1 jan. 1982. DOI: 10.2166/wst.1982.0056. .

HEM, L. J., RUSTEN, B., ØDEGAARD, H. "Nitrification in a moving bed biofilm reactor", **Water Research**, v. 28, n. 6, p. 1425–1433, jun. 1994. DOI: 10.1016/0043-1354(94)90310-7. .

HENZE, M., VAN LOOSDRECHT, M. C. M., EKAMA, G. A., *et al.* **Biological Wastewater Treatment - Principles, Modelling and Design**. 1st. ed. London, UK, IWA Publishing, 2008.

HOA, P., NAIR, L., VISVANATHAN, C. "The effect of nutrients on extracellular polymeric substance production and its influence on sludge properties", **Water SA**, v. 29, n. 4, p. 437–442, 3 ago. 2004. DOI: 10.4314/wsa.v29i4.5050. .

HOCKENBURY, M. R., GRADY, C. P. L. "Inhibition of Nitrification-Effects of Selected Organic Compounds", **Journal (Water Pollution Control Federation)**, v. 49, n. 5, p. 768–777, 1977. .

HOSSEINY, S. H., BORGHEI, S. M. "Modeling of Organic Removal in a Moving Bed Biofilm Reactor (MBBR)", **Scientia Iranica**, v. 9, n. 1, p. 53–58, 2002. .

INEA. **DZ-205.R-6 - Diretriz de Controle de Carga Orgânica em Efluentes Líquidos de Origem Industrial**. . Rio de Janeiro, [s.n.], 2007

INEA. **NT-202.R-10- Critérios e Padrões para Lançamento de Efluentes Líquidos**. . [S.l: s.n.], 1986

JAHREN, S., RINTALA, J., ØDEGAARD, H. "Aerobic moving bed biofilm reactor treating thermomechanical pulping whitewater under thermophilic conditions", **Water Research**, v. 36, p. 1067–1075, 2002. .

JARPA, M., POZO, G., BAEZA, R., *et al.* "Polyhydroxyalkanoate biosynthesis from paper mill wastewater treated by a moving bed biofilm reactor", **Journal of Environmental Science and Health, Part A**, v. 47, n. 13, p. 2052–2059, nov. 2012. DOI: 10.1080/10934529.2012.695699. .

JAYATHILAKE, P. G., JANA, S., RUSHTON, S., *et al.* "Extracellular Polymeric Substance Production and Aggregated Bacteria Colonization Influence the Competition of Microbes in Biofilms", **Frontiers in Microbiology**, v. 8, n. September, p. 1–14, 27 set. 2017. DOI: 10.3389/fmicb.2017.01865. .

JENKINS, D., RICHARD, M. G., DAIGGER, G. T. **Manual on the causes and control of activated sludge bulking, foaming, and other solids separation problems**. 3rd. ed. [S.l.], Lewis Publishers, 2004.

JIN, Z., PAN, Z., YU, S., *et al.* "Experimental study on pressurized activated sludge process for high concentration pesticide wastewater", **Journal of Environmental Sciences**, v. 22, n. 9, p. 1342–1347, set. 2010. DOI: 10.1016/S1001-0742(09)60260-6. .

JURETSCHKO, S., TIMMERMANN, G., SCHMID, M., *et al.* "Combined Molecular and Conventional Analyses of Nitrifying Bacterium Diversity in Activated Sludge : Nitrosococcus mobilis and Nitrospira -Like Bacteria as Dominant Populations", v. 64, n.

8, p. 3042–3051, 1998. .

KALLNER, A. **Laboratory Statistics - Handbook of Formulas and Terms**. 1st. ed. USA, Elsevier, 2014.

KAMALI, M., ALAVI-BORAZJANI, S. A., KHODAPARAST, Z., *et al.* "Additive and additive-free treatment technologies for pulp and paper mill effluents: Advances, challenges and opportunities", **Water Resources and Industry**, v. 21, n. June 2017, p. 100109, jun. 2019. DOI: 10.1016/j.wri.2019.100109. .

KAMPSCHREUR, M. J., TEMMINK, H., KLEEREBEZEM, R., *et al.* "Nitrous oxide emission during wastewater treatment", **Water Research**, v. 43, n. 17, p. 4093–4103, set. 2009. DOI: 10.1016/j.watres.2009.03.001. .

KARRASCH, B., PARRA, O., CID, H., *et al.* "Effects of pulp and paper mill effluents on the microplankton and microbial self-purification capabilities of the Biobío River, Chile", **Science of The Total Environment**, v. 359, n. 1–3, p. 194–208, abr. 2006. DOI: 10.1016/j.scitotenv.2005.03.029. .

KIM, B.-H., RAMANAN, R., CHO, D.-H., *et al.* "Role of Rhizobium, a plant growth promoting bacterium, in enhancing algal biomass through mutualistic interaction", **Biomass and Bioenergy**, v. 69, p. 95–105, out. 2014. DOI: 10.1016/j.biombioe.2014.07.015. .

KUTNER, M. H., NACHTSHEIM, C. J., NETER, J., *et al.* **Applied Linear Statistical Models**. 5th. ed. USA, McGraw-Hill, 2005.

LAFI, W. K., AL-QODAH, Z. "Combined advanced oxidation and biological treatment processes for the removal of pesticides from aqueous solutions", **Journal of Hazardous Materials**, v. 137, n. 1, p. 489–497, set. 2006. DOI: 10.1016/j.jhazmat.2006.02.027. .

LEWANDOWSKI, Z., BOLTZ, J. P., "Biofilms in Water and Wastewater Treatment". **Treatise on Water Science**, 1st. ed. [S.l.], Elsevier, 2011. p. 529–570. DOI: 10.1016/B978-0-444-53199-5.00095-6.

LIMA, P. S., DEZOTTI, M., BASSIN, J. P. "Interpreting the effect of increasing COD loading rates on the performance of a pre-anoxic MBBR system: implications on the attached and suspended biomass dynamics and nitrification–denitrification activity",

**Bioprocess and Biosystems Engineering**, v. 39, n. 6, p. 945–957, 3 jun. 2016. DOI: 10.1007/s00449-016-1574-0. .

LIN, C.-Y. "Aerobic treatment of pesticide-plant wastewater", **Biological Wastes**, v. 34, n. 1, p. 301–311, 1990a. DOI: 10.1007/BF00156600. .

LIN, C.-Y. "Anaerobic digestion of pesticide-plant wastewater", **Biological Wastes**, v. 34, n. 3, p. 215–226, jan. 1990b. DOI: 10.1016/0269-7483(90)90023-L. .

LIU, J., LI, J., TAO, Y., *et al.* "Analysis of bacterial, fungal and archaeal populations from a municipal wastewater treatment plant developing an innovative aerobic granular sludge process", **World Journal of Microbiology and Biotechnology**, v. 33, n. 1, p. 14, 24 jan. 2017. DOI: 10.1007/s11274-016-2179-0. .

LIU, ZHAO, G., PANG, Y., *et al.* "Integrated Biological and Electrochemical Oxidation Treatment for High Toxicity Pesticide Pollutant", **Industrial & Engineering Chemistry Research**, v. 49, n. 12, p. 5496–5503, 2010. DOI: 10.1021/ie100333v. .

LUO, Y., GUO, W., NGO, H. H., *et al.* "A review on the occurrence of micropollutants in the aquatic environment and their fate and removal during wastewater treatment", **Science of The Total Environment**, v. 473–474, p. 619–641, mar. 2014. DOI: 10.1016/j.scitotenv.2013.12.065. .

MAGOC, T., SALZBERG, S. L. "FLASH: fast length adjustment of short reads to improve genome assemblies", **Bioinformatics**, v. 27, n. 21, p. 2957–2963, 1 nov. 2011. DOI: 10.1093/bioinformatics/btr507. .

MALATO, S., BLANCO, J., MALDONADO, M. I., *et al.* "Optimising solar photocatalytic mineralisation of pesticides by adding inorganic oxidising species; application to the recycling of pesticide containers", **Applied Catalysis B: Environmental**, v. 28, n. 3–4, p. 163–174, dez. 2000. DOI: 10.1016/S0926-3373(00)00175-2. .

MALMQVIST, Å., BERGGREN, B., SJÖLIN, C., *et al.* "Full scale implementation of the nutrient limited BAS process at Södra Cell Värö", **Water Science and Technology**, v. 50, n. 3, p. 123–130, 1 ago. 2004. DOI: 10.2166/wst.2004.0177. .

MALMQVIST, Å., WELANDER, T., OLSSON, L. E. "Long term experience with the

nutrient limited BAS process for treatment of forest industry wastewaters", **Water Science and Technology**, v. 55, n. 6, p. 89–97, 1 mar. 2007. DOI: 10.2166/wst.2007.216.

MARA, D., HORAN, N. **The Handbook of Water and Wastewater Microbiology**. 1st. ed. UK, Academic Press - Elsevier, 2003.

MAŠIĆ, A., EBERL, H. J. "A Modeling and Simulation Study of the Role of Suspended Microbial Populations in Nitrification in a Biofilm Reactor", **Bulletin of Mathematical Biology**, v. 76, n. 1, p. 27–58, 5 jan. 2014. DOI: 10.1007/s11538-013-9898-2. .

MAYER, M., SMEETS, W., BRAUN, R., *et al.* "Enhanced ammonium removal from liquid anaerobic digestion residuals in an advanced sequencing batch reactor system", **Water Science and Technology**, v. 60, n. 7, p. 1649–1660, 1 out. 2009. DOI: 10.2166/wst.2009.546. .

MCILROY, S. J., KIRKEGAARD, R. H., MCILROY, B., *et al.* "MiDAS 2.0: an ecosystem-specific taxonomy and online database for the organisms of wastewater treatment systems expanded for anaerobic digester groups", **Database**, v. 2017, n. 1, p. 1–9, 1 jan. 2017. DOI: 10.1093/database/bax016. .

METCALF & EDDY, TCHOBANOGLOUS, G., BURTON, F. L., *et al.* **Wastewater Engineering: Treatment and Reuse**. 4th. ed. [S.l.], McGraw-Hill, 2003.

METCALF & EDDY, TCHOBANOGLOUS, G., STENSEL, H. D., *et al.* **Wastewater Engineering: Treatment and Resource Recovery**. 5th. ed. USA, McGraw-Hill, 2014.

MOBARRY, B. K., WAGNER, M., URBAIN, V., *et al.* "Phylogenetic probes for analyzing abundance and spatial organization of nitrifying bacteria.", **Applied and environmental microbiology**, v. 62, n. 6, p. 2156–2162, 1996. DOI: 10.1128/AEM.62.6.2156-2162.1996. .

MOREIRA, F. C., VILAR, V. J. P., FERREIRA, A. C. C., *et al.* "Treatment of a pesticide-containing wastewater using combined biological and solar-driven AOPs at pilot scale", **Chemical Engineering Journal**, v. 209, p. 429–441, out. 2012. DOI: 10.1016/j.cej.2012.08.009. .

MORGAN-SAGASTUME, F. "Biofilm development, activity and the modification of

carrier material surface properties in moving-bed biofilm reactors (MBBRs) for wastewater treatment", **Critical Reviews in Environmental Science and Technology**, v. 48, n. 5, p. 439–470, 4 mar. 2018. DOI: 10.1080/10643389.2018.1465759. .

MORGAN-SAGASTUME, F., ALLEN, D. G. "Effects of temperature transient conditions on aerobic biological treatment of wastewater", **Water Research**, v. 37, n. 15, p. 3590–3601, set. 2003. DOI: 10.1016/S0043-1354(03)00270-7. .

MULDER, C. De. **Impact of intrinsic and extrinsic parameters on the oxygen kinetic parameters of Ammonia and Nitrite Oxidizing Bacteria**. 2014. Universiteit Gent, 2014. DOI: 10.13140/RG.2.2.11347.17444.

NATIONAL RESEARCH COUNCIL (Org.). **The Future Role of Pesticides in US Agriculture**. Washington, D.C., USA, National Academic Press, 2000.

NIELSEN, P. H., KRAGELUND, C., SEVIOUR, R. J., *et al.* "Identity and ecophysiology of filamentous bacteria in activated sludge", **FEMS Microbiology Reviews**, v. 33, n. 6, p. 969–998, nov. 2009. DOI: 10.1111/j.1574-6976.2009.00186.x. .

NIELSEN, P. H., LEMMER, H., DAIMS, H. (Org.). **FISH Handbook for Biological Wastewater Treatment**. 1st. ed. UK, IWA Publishing, 2009.

NOUHA, K., KUMAR, R. S., BALASUBRAMANIAN, S., *et al.* "Critical review of EPS production, synthesis and composition for sludge flocculation", **Journal of Environmental Sciences**, v. 66, n. August, p. 225–245, abr. 2018. DOI: 10.1016/j.jes.2017.05.020. .

ØDEGAARD, H. "Innovations in wastewater treatment: the moving bed biofilm process", **Water Science and Technology**, v. 53, n. 9, p. 17–33, 1 maio 2006. DOI: 10.2166/wst.2006.284. .

ØDEGAARD, H., "MBBR and IFAS systems". **Advances in Wastewater Treatment**, 1st. ed. [S.l.], IWA Publishing, 2019. . DOI: 10.2166/9781780409719\_0101.

ØDEGAARD, H., RUSTEN, B., WESTRUM, T. "A New Moving Bed Biofilm Reactor - Applications and Results", **Water Science and Technology**, v. 29, n. 10–11, p. 157–165, 1994. .

OERKE, E.-C., DEHNE, H.-W. "Safeguarding production—losses in major crops and

the role of crop protection", **Crop Protection**, v. 23, n. 4, p. 275–285, abr. 2004. DOI: 10.1016/j.cropro.2003.10.001. .

OLIVEIRA, D. V. M. de. "Evaluation of a MBBR (Moving Bed Biofilm Reactor) Pilot Plant for Treatment of Pulp and Paper Mill Wastewater", **International Journal of Environmental Monitoring and Analysis**, v. 2, n. 4, p. 220, 2014. DOI: 10.11648/j.ijema.20140204.15. .

ORDAZ-DÍAZ, L. A., ROJAS-CONTRERAS, J. A., RUTIAGA-QUIÑONES, O. M., *et al.* "Microorganism Degradation Efficiency in BOD Analysis Formulating a Specific Microbial Consortium in a Pulp and Paper Mill Effluent", **BioResources**, v. 9, n. 4, p. 7189–7197, 14 out. 2014. DOI: 10.15376/biores.9.4.7189-7197. .

PAPADIMITRIOU, C., PALASKA, G., LAZARIDOU, M., *et al.* "The effects of toxic substances on the activated sludge microfauna", **Desalination**, v. 211, n. 1–3, p. 177–191, jun. 2007. DOI: 10.1016/j.desal.2006.03.594. .

PICULELL, M. **New Dimensions of Moving Bed Biofilm Carriers. Influence of biofilm thickness and control possibilities.** 2016. 78 f. 2016.

PICULELL, M., WELANDER, T., JÖNSSON, K. "Organic removal activity in biofilm and suspended biomass fractions of MBBR systems", **Water Science and Technology**, v. 69, n. 1, p. 55–61, 1 jan. 2014. DOI: 10.2166/wst.2013.552. .

PLIEGO, G., ZAZO, J. A., PARIENTE, M. I., *et al.* "Treatment of a wastewater from a pesticide manufacture by combined coagulation and Fenton oxidation", **Environmental Science and Pollution Research**, v. 21, n. 21, p. 12129–12134, 26 nov. 2014. DOI: 10.1007/s11356-014-2880-1. .

POKHREL, D., VIRARAGHAVAN, T. "Treatment of pulp and paper mill wastewater—a review", **Science of The Total Environment**, v. 333, n. 1–3, p. 37–58, out. 2004. DOI: 10.1016/j.scitotenv.2004.05.017. .

POMMERENING-RÖSER, A., RATH, G., KOOPS, H.-P. "Phylogenetic Diversity within the Genus *Nitrosomonas*", **Systematic and Applied Microbiology**, v. 19, n. 3, p. 344–351, out. 1996. DOI: 10.1016/S0723-2020(96)80061-0. .

QUAST, C., PRUESSE, E., YILMAZ, P., *et al.* "The SILVA ribosomal RNA gene

database project: improved data processing and web-based tools", **Nucleic Acids Research**, v. 41, n. D1, p. D590–D596, 27 nov. 2012. DOI: 10.1093/nar/gks1219. .

RAMETTE, A. "Multivariate analyses in microbial ecology", **FEMS Microbiology Ecology**, v. 62, n. 2, p. 142–160, nov. 2007. DOI: 10.1111/j.1574-6941.2007.00375.x. .

RANKIN, A., AERT, M. V. A. N., WELANDER, T. "Low sludge yield biofilm activated sludge (BAS) upgrade – Quesnel River Pulp", **Tappi Journal**, v. 6, n. 5, p. 17–22, 2007.

REVILLA, M., GALÁN, B., VIGURI, J. R. "An integrated mathematical model for chemical oxygen demand (COD) removal in moving bed biofilm reactors (MBBR) including predation and hydrolysis", **Water Research**, v. 98, p. 84–97, jul. 2016. DOI: 10.1016/j.watres.2016.04.003. .

REVILLA, M., GALÁN, B., VIGURI, J. R. "Analysis of simulation tools and optimization of the operational conditions for biofilm activated sludge industrial process", **International Journal of Environmental Science and Technology**, v. 15, n. 12, p. 2499–2510, 4 dez. 2018a. DOI: 10.1007/s13762-017-1626-2. .

REVILLA, M., GALÁN, B., VIGURI, J. R. "Optimization Methodology for High COD Nutrient-Limited Wastewaters Treatment Using BAS Process", **Water, Air, & Soil Pollution**, v. 229, n. 6, p. 191, jun. 2018b. DOI: 10.1007/s11270-018-3835-9. .

REVILLA, M., VIGURI, J. R., GALÁN, B. "Simulation and Optimization of Biofilm Activated Sludge Process for the Biological Treatment of Effluents from Cellulose and Viscose Industry", **24 European Symposium on Computer Aided Process Engineering**, v. 33, p. 1117–1122, 2014. DOI: 10.1016/B978-0-444-63455-9.50021-0. .

REZENDE, N. R. De, MOUNTEER, A. H., MOZER, G. C., *et al.* "Comparison of COD and Toxicity Removal during Activated Sludge and MBBR Treatment of Kraft Pulp Mill Effluent". 2012. **Anais [...]** [S.l.: s.n.], 2012.

RITTMANN, B. E., MCCARTY, P. L. **Environmental Biotechnology: Principles and Applications**. 1st. ed. US, McGraw-Hill, 2001. v. 7.

RUSTEN, B., EIKEBROKK, B., ULGENES, Y., *et al.* "Design and operations of the Kaldnes moving bed biofilm reactors", **Aquacultural Engineering**, - Esclarecimento

sobre carga orgânica superficial., v. 34, n. 3, p. 322–331, maio 2006. DOI: 10.1016/j.aquaeng.2005.04.002. .

RUSTEN, B., HEM, L. J., ØDEGAARD, H. "Nitrification of municipal wastewater in moving-bed biofilm reactors", **Water Environment Research**, v. 67, n. 1, p. 75–86, jan. 1995. DOI: 10.2175/106143095X131213. .

RUSTEN, B., MATTSSON, E., BROCH-DUE, A., *et al.* "TREATMENT OF PULP AND PAPER INDUSTRY WASTEWATERS IN NOVEL MOVING BED BIOFILM REACTORS", **Water Science and Technology**, v. 30, n. 3, p. 161–171, 1 ago. 1994. DOI: 10.2166/wst.1994.0091. .

SCIENTIFIC, T. F. **Fast and Accurate Thermo Scientific Gallery Discrete Industrial Analyzers - Automated Nutrient Analysis and Water Quality Monitoring**. [S.l.: s.n.], 2018.

SHAWAQFEH, A. T. "Removal of Pesticides from Water Using Anaerobic-Aerobic Biological Treatment", **Chinese Journal of Chemical Engineering**, v. 18, n. 4, p. 672–680, ago. 2010. DOI: 10.1016/S1004-9541(10)60274-1. .

SHORE, J. L., M'COY, W. S., GUNSCH, C. K., *et al.* "Application of a moving bed biofilm reactor for tertiary ammonia treatment in high temperature industrial wastewater", **Bioresource Technology**, v. 112, p. 51–60, maio 2012. DOI: 10.1016/j.biortech.2012.02.045. .

SILVA, M. F. de O., COSTA, L. M. da. "A indústria de defensivos agrícolas", **BNDES Setorial**, v. 35, p. 233–276, 2012. .

SLADE, A., ELLIS, R. "Nutrient minimisation in the pulp and paper industry: an overview", **Water Science and Technology**, n. August, p. 111–122, 2004. .

SÖDRA. **Our mill in Värö**. 2020. Disponível em: <https://www.sodra.com/en/global/pulp/production/sodra-cell-varo/>. Acesso em: 6 set. 2020.

SOINTIO, J., RANKIN, A., VAN AERT, M. "Biofilm Activated Sludge process at Quesnel River Pulp installation", **Environmental Science & Engineering Magazine**, p. 22–24, 2006. .

SOROKIN, D. Y., TOUROVA, T. P., SPIRIDONOVA, E. M., *et al.* "Thioclava pacifica gen. nov., sp. nov., a novel facultatively autotrophic, marine, sulfur-oxidizing bacterium from a near-shore sulfidic hydrothermal area", **International Journal of Systematic and Evolutionary Microbiology**, v. 55, n. 3, p. 1069–1075, 2005. DOI: 10.1099/ijs.0.63415-0. .

STAN, C. D., CRETESCU, I., PASTRAVANU, C., *et al.* "Treatment of Pesticides in Wastewater by Heterogeneous and Homogeneous Photocatalysis", **International Journal of Photoenergy**, v. 2012, p. 1–6, 2012. DOI: 10.1155/2012/194823. .

STOUTHAMER, A. H. (Org.). **Quantitative Aspects of Growth and Metabolism of Microorganisms**. 1st. ed. Amsterdam, The Netherlands, Springer, 1992.

SUN, S.-P., NÀCHER, C. P. i, MERKEY, B., *et al.* "Effective Biological Nitrogen Removal Treatment Processes for Domestic Wastewaters with Low C/N Ratios: A Review", **Environmental Engineering Science**, v. 27, n. 2, p. 111–126, fev. 2010. DOI: 10.1089/ees.2009.0100. .

TAKÁCS-GYÖRGY, K., TAKÁCS, I. "Use of Agrochemicals – Environmental , Social and Economic Impacts of Alternative Farming Strategies : Precision Weed Management", **World Sustainability Forum**, p. 1–16, 2011. .

THOMPSON, G., SWAIN, J., KAY, M., *et al.* "The treatment of pulp and paper mill effluent: a review", **Bioresource Technology**, v. 77, n. 3, p. 275–286, maio 2001. DOI: 10.1016/S0960-8524(00)00060-2. .

UN. **UN Sustainable Development Goals - Goal 6: Ensure access to water and sanitation for all**. 2016. Disponível em: <https://www.un.org/sustainabledevelopment/water-and-sanitation/>. Acesso em: 18 jul. 2020.

URIOC, S. **Market Outlook: Calculating the Value of Industrial Wastewater**. 2015. Disponível em: <https://www.waterworld.com/industrial/wastewater/article/16211380/market-outlook-calculating-the-value-of-industrial-wastewater>. Acesso em: 20 maio 2019.

VAN HAANDEL, A. C., VAN DER LUBBE, J. G. M. **Handbook of Biological Wastewater Treatment - Design and Optimisation of Activated Sludge Systems**. 2nd.

ed. London, UK, IWA Publishing, 2012.

VENTURA, M. "Linking biochemical and elemental composition in freshwater and marine crustacean zooplankton", **Marine Ecology Progress Series**, v. 327, n. June, p. 233–246, 7 dez. 2006. DOI: 10.3354/meps327233. .

VILLAMAR, C. A., JARPA, M., DECAP, J., *et al.* "Aerobic moving bed bioreactor performance: a comparative study of removal efficiencies of kraft mill effluents from *Pinus radiata* and *Eucalyptus globulus* as raw material", **Water Science and Technology**, v. 59, n. 3, p. 507–514, 1 fev. 2009. DOI: 10.2166/wst.2009.002. .

VIRKUTYTE, J., "Aerobic Treatment of Effluents From Pulp and Paper Industries". **Current Developments in Biotechnology and Bioengineering**, 1st. ed. [S.l.], Elsevier, 2017. p. 103–130. DOI: 10.1016/B978-0-444-63665-2.00004-7.

VISHNIAC, W., SANTER, M. "The thiobacilli.", **Bacteriological reviews**, v. 21, n. 3, p. 195–213, set. 1957. .

VON SPERLING, M. **Biological Wastewater Treatment (Volume 1: Wastewater Characteristics, Treatment and Disposal)**. 1st. ed. UK, IWA Publishing, 2007a.

VON SPERLING, M. **Biological Wastewater Treatment (Volume 2: Basic Principles of Wastewater Treatment)**. 1st. ed. UK, IWA Publishing, 2007b.

VON SPERLING, M. **Biological Wastewater Treatment (Volume 5: Activated Sludge and Aerobic Biofilm Reactors)**. 1st. ed. UK, IWA Publishing, 2007c.

WAGNER, M., RATH, G., AMANN, R., *et al.* "In situ Identification of Ammonia-oxidizing Bacteria", **Systematic and Applied Microbiology**, v. 18, n. 2, p. 251–264, jan. 1995. DOI: 10.1016/S0723-2020(11)80396-6. .

WAGNER, M., RATH, G., KOOPS, H.-P., *et al.* "In Situ Analysis of Nitrifying Bacteria in Sewage Treatment Plants", **Water Science and Technology**, v. 34, n. 1–2, p. 237–244, 1996. .

WANG, Q., GARRITY, G. M., TIEDJE, J. M., *et al.* "Naïve Bayesian Classifier for Rapid Assignment of rRNA Sequences into the New Bacterial Taxonomy", **Applied and Environmental Microbiology**, v. 73, n. 16, p. 5261–5267, 15 ago. 2007. DOI: 10.1128/AEM.00062-07. .

WANG, YUNG-TSE, H., HOWARD, H. Lo, *et al.* **Handbook of Industrial and Hazardous Wastes Treatment**. 2nd. ed. [S.l.], CRC Press, 2004.

WANG, YUNG-TSE, H., HOWARD, H. Lo, *et al.* **Waste Treatment in the Process Industries**. 1st. ed. USA, CRC Press, 2006.

WARD, D. V., GEVERS, D., GIANNOUKOS, G., *et al.* "Evaluation of 16S rDNA-Based Community Profiling for Human Microbiome Research", **PLoS ONE**, v. 7, n. 6, p. e39315, 13 jun. 2012. DOI: 10.1371/journal.pone.0039315. .

WEF. "Biofilm Reactors - WEF Manual of Practice No.35", **WEF manual of practice**, 2010. .

WELANDER, T., OLSSON, L., FASTH, C. "Nutrient-limited biofilm pretreatment: an efficient way to upgrade activated sludge plants", **Tappi Journal**, v. i, p. 20–26, 2002. .

WIESMANN, U., CHOI, I. S., DOMBROWSKI, E.-M. **Fundamentals of Biological Wastewater Treatment**. 1st. ed. Germany, Wiley, 2007. v. 2.

WOOD, A. **Compendium of Pesticide Common Names - Classified Lists of Pesticides**. 2017. Disponível em: [http://www.alanwood.net/pesticides/class\\_pesticides.html](http://www.alanwood.net/pesticides/class_pesticides.html).

WORLD HEALTH ORGANIZATION. "The Who Recommended Classification of Pesticides By Hazard and Guidelines To Classification 2009", **World Health Organization**, p. 1–60, 2010. DOI: ISBN 978 92 4 154796 3. .

WORLD HEALTH ORGANIZATION. **Water sanitation hygiene - Diseases and risks**. 2014. Disponível em: [https://www.who.int/water\\_sanitation\\_health/diseases-risks/en/](https://www.who.int/water_sanitation_health/diseases-risks/en/). Acesso em: 17 jul. 2020.

XAVIER, J. B., FOSTER, K. R. "Cooperation and conflict in microbial biofilms", **Proceedings of the National Academy of Sciences**, v. 104, n. 3, p. 876–881, 16 jan. 2007. DOI: 10.1073/pnas.0607651104. .

XAVIER, J. B., PICIOREANU, C., ALMEIDA, J. S., *et al.* "Monitorização e modelação da estrutura de biofilmes", **Boletim de Biotecnologia**, v. 76, p. 2–13, 2003. .

XIONG, Z., CHENG, X., SUN, D. "Pretreatment of heterocyclic pesticide wastewater

using ultrasonic/ozone combined process", **Journal of Environmental Sciences**, v. 23, n. 5, p. 725–730, maio 2011. DOI: 10.1016/S1001-0742(10)60465-2. .

ZAPATA, A., OLLER, I., SIRTORI, C., *et al.* "Decontamination of industrial wastewater containing pesticides by combining large-scale homogeneous solar photocatalysis and biological treatment", **Chemical Engineering Journal**, v. 160, n. 2, p. 447–456, jun. 2010. DOI: 10.1016/j.cej.2010.03.042. .

ZAPATA, A., VELEGRAKI, T., SÁNCHEZ-PÉREZ, J. A., *et al.* "Solar photo-Fenton treatment of pesticides in water: Effect of iron concentration on degradation and assessment of ecotoxicity and biodegradability", **Applied Catalysis B: Environmental**, v. 88, n. 3–4, p. 448–454, maio 2009. DOI: 10.1016/j.apcatb.2008.10.024. .

ZENG, Q., HAO, T., MACKAY, H. R., *et al.* "Alkaline textile wastewater biotreatment: A sulfate-reducing granular sludge based lab-scale study", **Journal of Hazardous Materials**, v. 332, p. 104–111, jun. 2017. DOI: 10.1016/j.jhazmat.2017.03.005. .

ZHANG, Y., PAGILLA, K. "Treatment of malathion pesticide wastewater with nanofiltration and photo-Fenton oxidation", **Desalination**, v. 263, n. 1–3, p. 36–44, nov. 2010. DOI: 10.1016/j.desal.2010.06.031. .

ZHAO, C., GAO, Z., QIN, Q., *et al.* "Mangroviflexus xiamenensis gen. nov., sp. nov., a member of the family Marinilabiliaceae isolated from mangrove sediment", **International Journal of Systematic and Evolutionary Microbiology**, v. 62, n. Pt\_8, p. 1819–1824, 1 ago. 2012. DOI: 10.1099/ijs.0.036137-0. .

ZHU, G., PENG, Y., WANG, S., *et al.* "Effect of influent flow rate distribution on the performance of step-feed biological nitrogen removal process", **Chemical Engineering Journal**, v. 131, n. 1–3, p. 319–328, jul. 2007. DOI: 10.1016/j.cej.2006.12.023. .

ZODI, S., LOUVET, J.-N., MICHON, C., *et al.* "Electrocoagulation as a tertiary treatment for paper mill wastewater: Removal of non-biodegradable organic pollution and arsenic", **Separation and Purification Technology**, v. 81, n. 1, p. 62–68, set. 2011. DOI: 10.1016/j.seppur.2011.07.002. .

## **A. APPENDIX: ANALYTICAL METHODS**

In this appendix, the analytical methods employed for each analyzed parameter are presented and explained. These were considered not crucial for a smooth reading experience of the thesis but are essential for further understanding and for reproducibility reasons. For a reader that is used to the methods, this appendix may be considered as optional reading. Table A.1 summarizes the analytical standard method, reagent kit or instrument utilized for each parameter and study (the pesticide or P&P research), and the respective subsection.

Table A.1 – Methods employed for each analysis performed during the experimental investigations.

Analysis	Research	Analytical Method, Instrument or Reaction Kit	Section
COD	<i>Pesticide</i>	5220 D	A.1
	<i>P&amp;P</i>	5220 D (Hach LCK 114)	
DOC	<i>Pesticide</i>	TOC-V <sub>CPN</sub>	A.2
TN	<i>Pesticide</i>	TOC-V <sub>CPN</sub> (TNM-1)	A.3
	<i>P&amp;P</i>	Hach LCK 138/238	
TAN	<i>Pesticide</i>	NBR 10560 – Nesslerization	A.4
	<i>P&amp;P</i>	Gallery™ Plus Discrete Analyzer	
Nitrite	<i>Pesticide</i>	Hach Nitriver 2 / 4500-NO <sub>2</sub> <sup>-</sup>	A.5
	<i>P&amp;P</i>	Gallery™ Plus Discrete Analyzer	
Nitrate	<i>Pesticide</i>	Hach Nitriver 5 / brucine (colorimetric)	A.6
	<i>P&amp;P</i>	Gallery™ Plus Discrete Analyzer	
N <sub>2</sub> O <sub>(g)</sub>	<i>Pesticide</i>	GC-ECD	A.7
Phosphate	<i>P&amp;P</i>	Gallery™ Plus Discrete Analyzer	A.8
Suspended Solids	<i>Pesticide</i>	2540 D and 2540 E	A.9
	<i>P&amp;P</i>		
Attached Solids	<i>Pesticide</i>	2540 B and 2540 E	A.10
	<i>P&amp;P</i>		
Turbidity	<i>Pesticide</i>	2130 B (PoliControl AP-2000)	A.11
pH	<i>Pesticide</i>	4500-H <sup>+</sup> B (various pHmeters)	A.12
	<i>P&amp;P</i>		
Temperature	<i>Pesticide</i>	Temperature probes within pHmeters	A.13
	<i>P&amp;P</i>		
Dissolved Oxygen	<i>Pesticide</i>	Oximeter (WTW Oxi 7310)	A.14
	<i>P&amp;P</i>	Oximeter (Hach HQ40d)	
Optical Microscopy	<i>Pesticide</i>	Boeco Germany BM – 800	A.15
	<i>P&amp;P</i>	Nikon Eclipse Ni	
Optical Stereomicroscopy	<i>Pesticide</i>	Nikon SMZ1270	A.16
	<i>P&amp;P</i>		
FISH	<i>Pesticide</i>	Refer to section	A.17
DNA	<i>P&amp;P</i>	Refer to section	A.18
Microtoxicity	<i>Pesticide</i>	NBR 15411-3:2012	A.19

The sections below give the detailed description of the methodologies and equipment used to perform each analysis. Whenever there are considerable differences between the methods applied for a certain analyte for the two studies that compose this work, subsections “a) Pesticide Research” and “b) P&P Research” specify the respective approaches.

Overall, most analytical procedures were performed by the author of this work with the assistance of undergraduate interns for the study with the pesticide wastewater,

whilst most analysis from the P&P research were executed by technicians from AnoxKaldnes's accredited laboratory. Exceptions are described in each subsection below, if applicable.

### **A.1. Chemical Oxygen Demand (COD)**

#### *a) Pesticide Research*

The COD of the samples, expressed as mgO<sub>2</sub>/L (or simply mg/L), was quantified using the closed reflux colorimetric method (5220 D) (APHA, AWWA, *et al.*, 2017). The substances liable to oxidation in the sample, either organic or inorganic, react with the oxidant potassium dichromate (K<sub>2</sub>Cr<sub>2</sub>O<sub>7</sub>), in acid medium (H<sub>2</sub>SO<sub>4</sub>), in a closed vessel at high temperature (150°C) for 2 hours. Prior to digestion, 2 mL of the sample (or its dilution) was mixed with two solutions: 1.2 mL of digestion solution, containing the dichromate, sulfuric acid and mercury II sulphate diluted in water; and 2.8 mL of catalytic solution, containing sulfuric acid and silver (I) sulphate.

After digestion and cooling down, COD was quantified by linearly relating it with the color change of the medium proportional to chromium reduction (Cr<sup>6+</sup> to Cr<sup>3+</sup>). The color was measured by absorbance at a specified wavelength in a spectrophotometer (Hach DR/2800) and related to COD content by comparison with a calibration curve constructed with various known COD of potassium biphthalate standards solutions.

Analysis were conducted in triplicates and two COD fractions were usually quantified: the total COD (tCOD) from the raw samples; and the soluble COD (sCOD) from the filtered samples (0.45 µm nominal pore, nitrate cellulose membrane). As described in section B.2, the difference between total and soluble COD corresponds to particulate COD (pCOD).

#### *b) P&P Research*

Despite following the same method/principle described above, during the research with the P&P wastewater Hach LCK 114 reagents kits were used instead of preparing reagent solutions in the lab. Most of the times the samples were handed to technicians from AnoxKaldnes accredited laboratory to perform this analysis. Hach DR 3900

spectrophotometer was used for absorbance measurement and COD calculation against calibration curve.

### **A.2. Dissolved Organic Carbon (DOC)**

The dissolved organic carbon (DOC) corresponds to the soluble portion of the total organic carbon (TOC) present in the sample. Therefore, the analysis was performed after filtration of the samples through nitrate cellulose membrane with 0.45  $\mu\text{m}$  nominal pore. It is expressed in mgC/L (milligrams of carbon per liter).

DOC analysis was performed in an organic carbon analyzer Shimadzu TOC-V<sub>CPN</sub>. Its working principle involves the soluble total carbon (TC) and inorganic carbon (IC) quantifications. The former is determined by combustion of the sample at 680°C, generating carbon dioxide that is detected by an infrared analyzer proportionally to the TC contained in the sample. In turn, IC is quantified by acidifying the sample to pH lower than 3, converting all the carbonates to carbon dioxide. Then, the difference between the TC and IC corresponds to the TOC. Calibration curves for TC and IC were made, respectively, with standard solution of potassium biphthalate and sodium bicarbonate.

### **A.3. Total Nitrogen (TN)**

#### *a) Pesticide Research*

TN was assessed by the total nitrogen analyzer Shimadzu TNM-1, coupled to the TOC-V<sub>CPN</sub> equipment. The analysis occurs by combusting the sample at 720°C, making the totality of the nitrogen in the sample to transform to nitrogen monoxide (NO), which is detected by a chemiluminescence gas analyzer. Calibration curve of the method was built with potassium nitrate standard solutions. Results, in mgN/L (milligram of nitrogen per liter), were always related the dissolved total nitrogen, as samples were prefiltered (0.45  $\mu\text{m}$  nominal pore membranes).

#### *b) P&P Research*

Samples were handed to AnoxKaldnes accredited lab staff, that performed the total nitrogen analysis using the colorimetric reagents kits Hach LCK 138 and LCK 238. In both kits, organic and inorganic nitrogen are oxidized to nitrate by digestion with

peroxodisulphate. Then nitrophenol is formed by the reaction of nitrate ions with 2,6-dimethylphenol in a solution of sulphuric and phosphoric acids. Results are expressed in mgN/L and both unfiltered and filtered samples (through glass fiber membranes, pore size  $\leq 2 \mu\text{m}$ ) were considered for assessing particulate and soluble fractions of total nitrogen. Spectrophotometer Hach DR 3900 was used for measuring absorbance and calculating TN concentration by comparison with a calibration curve.

#### **A.4. Total Ammoniacal Nitrogen (TAN)**

##### *a) Pesticide Research*

Quantification of the total ammoniacal nitrogen in the samples was done using the Nessler colorimetric method, or Nesslerization, adapted from the norm NBR 10560 and the method 4500-NH<sub>3</sub>X (Standard Methods, 19<sup>th</sup> edition). The principle of this method involves the formation of a yellow-brownish colloidal dispersion from the reaction of ammonia with the iodide contained in the Nessler reactive, in highly alkaline medium (which virtually converts all the ammonium to ammonia, see section B.6). The color intensity of the resulting solution is linearly proportional to the amount of TAN present in the sample. Nessler reactive consists of a solution holding 0.100 g/L of mercury (II) iodide (HgI<sub>2</sub>), 0.070 g/L of potassium iodide (KI) and 0.160 g/L of sodium hydroxide (NaOH). This solution is prepared in reagent-grade water and left decanting for a few days before utilization.

Analysis were done in triplicate by mixing 0.1 mL of the Nessler reagent with 5 mL of the sample (or aliquot diluted to 5 mL) prefiltered in nitrate cellulose membrane with 0.45  $\mu\text{m}$  pore size. After 10 minutes of the reagent addition, color intensity was determined by absorption at 425 nm wavelength in a spectrophotometer Hach DR/2800 and compared with the calibration curve constructed with NH<sub>4</sub>Cl standard solutions.

##### *b) P&P Research*

Photometric method from the Thermo Fisher Scientific™ Gallery™ Plus Discrete Analyzer was used by staff from the accredited lab of AnoxKaldnes to analyze the TAN concentration from filtered samples (glass fiber membranes, pore size  $\leq 2 \mu\text{m}$ ). Sodium dichloroisocyanurate, sodium salicylate and sodium nitroprusside are the chemical compounds used in the instrument's method for TAN. Further details and references may

be found in the equipment's manufacturer e-book "Fast and Accurate Thermo Scientific Gallery Discrete Industrial Analyzers - Automated Nutrient Analysis and Water Quality Monitoring" (THERMO FISHER SCIENTIFIC, 2018).

#### **A.5. Nitrite (NO<sub>2</sub><sup>-</sup>)**

##### *a) Pesticide Research*

Two colorimetric methods were employed for assessing nitrite concentration in prefiltered samples (0.45 µm membranes). Standard solutions prepared with NaNO<sub>2</sub> were used for calibrating the methods. Results are expressed in mg NO<sub>2</sub><sup>-</sup>-N/L, unless specified otherwise.

The first procedure made use of the kit Nitriver 2 Nitrite Reagent (Hach), based on ferrous sulphate as reducing agent. Nitrous oxide is then formed and couples with ferrous ions, resulting in solution color ranging from green to brown. Samples were added (5 mL) in Hach test tubes followed by the reagent kit and mixing. After 10 minutes reaction, a spectrophotometer (Hach DR/2800) was used to read the absorbance at 585 nm. By comparison of the obtained absorbance with a calibration curve, the nitrite concentration was then determined.

The second method for nitrite was the standard colorimetric method 4500-NO<sub>2</sub><sup>-</sup> with sulfanilamide and NED (N-(1-Naphthyl) ethylenediamine) (APHA, AWWA, *et al.*, 2017). Diazotized sulfanilamide couples with NED, resulting in a reddish-purple solution. Analysis was performed in duplicate by mixing 5 mL of the sample with 0.20 mL of the sulfanilamide/NED solution (1% m/v NED, 0.1% m/v sulfanilamide, 10% v/v of H<sub>3</sub>PO<sub>4</sub> reagent grade solution). After letting the mixture sitting for 10 minutes, absorbance at 543 nm was read. The absorbance was then compared with a calibration curve made with NaNO<sub>2</sub> concentrated solutions to calculate the nitrite concentration.

##### *b) P&P Research*

Nitrite measurement from filtered samples (through glass fiber membranes, pore size ≤ 2 µm) was conducted by the accredited lab personnel from AnoxKaldnes, using photometric method of the Thermo Fisher Scientific™ Gallery™ Plus Discrete Analyzer. Chemical reagents and principle are the same as the second method employed during the study with pesticide wastewater. Further details and references may be found in the

equipment's manufacturer e-book "Fast and Accurate Thermo Scientific Gallery Discrete Industrial Analyzers - Automated Nutrient Analysis and Water Quality Monitoring" (SCIENTIFIC, 2018).

#### **A.6. Nitrate (NO<sub>3</sub><sup>-</sup>)**

##### *a) Pesticide Research*

Alike the nitrite analysis, two colorimetric methods were used for nitrate evaluation in samples filtered through 0.45 µm nominal pore membranes. For both methods, the calibration curves were prepared with standard KNO<sub>3</sub> solutions. Nitrate concentrations, unless otherwise specified, are always expressed as mg NO<sub>3</sub><sup>-</sup>-N/L.

Initially, the Hach kit Nitraver 5 Nitrate Reagent was used. This method is based on the consecutive reduction of nitrate to nitrite by cadmium, then the nitrite to diazonium salt by sulfanilic acid. Then the salt reacts with gentisic acid, producing an amber colored solution. 5 mL sample and the reagent kit were added together in test tube and mixed for 1 minute. 5 minutes later the absorbance at 500 nm was read in a spectrophotometer (Hach DR/2800). A calibration curve was compared with the absorbance value to obtain the nitrate concentration of the sample.

The second method used for nitrate measurement was the colorimetric with brucine (EPA, 1971). The sample (1.25 mL), processed in duplicate, was mixed with 0.25 mL brucine solution (1% m/v brucine, 0.1% m/v sulfanilic acid, 0.35 M HCl) and 2.5 mL of H<sub>2</sub>SO<sub>4</sub> solution (14.5 M) and let sitting in the dark for 10 minutes. Then 2.5 mL of distilled water was added and another 20 minutes in the dark passed before reading the absorbance at 410 nm in a spectrophotometer (Hach DR/2800).

##### *b) P&P Research*

Measurement of nitrate concentration was performed in samples filtered through glass fiber membranes samples (pore size ≤ 2 µm) by the accredited lab team from AnoxKaldnes, using the Thermo Fisher Scientific™ Gallery™ Plus Discrete Analyzer photometric method. Nitrate was measured indirectly by analyzing both nitrite and total oxidized nitrogen (nitrate + nitrite) and subtracting the former from the latter. Hydrazine is the chemical reagent used for total oxidized nitrogen analysis. More details and references may be found in the equipment's manufacturer e-book "Fast and Accurate

Thermo Scientific Gallery Discrete Industrial Analyzers - Automated Nutrient Analysis and Water Quality Monitoring” (SCIENTIFIC, 2018).

#### **A.7. Nitrous Oxide Gas (N<sub>2</sub>O)**

Gas samples were collected with a syringe from a glassware connected to a funnel partially submerged upside down into the liquid surface of the reactor, after letting the apparatus standing overnight, so it was homogenously filled with the offgas coming from the reactor. With a needle, the offgas was injected into an ampoule filled with saline solution that minimizes nitrous oxide dissolution into the liquid. Ampoules were kept upside down in a refrigerator (4°C) and later sent to nitrous oxide measurement.

The two measurements of nitrous oxide gas concentration in the MBBR offgas, during the pesticide research, were outsourced to laboratories of the Federal Fluminense University (UFF, Niterói, RJ). Gas chromatography coupled to electron capture detector (ECD) was used as the measuring method.

#### **A.8. Phosphate (PO<sub>4</sub><sup>3-</sup>)**

Phosphate was determined in samples filtered through glass fiber membranes (pore size  $\leq 2 \mu\text{m}$ ) by the accredited lab staff from AnoxKaldnes, using the Thermo Fisher Scientific™ Gallery™ Plus Discrete Analyzer photometric method. Chemistry of the method for phosphate analysis include the chemicals antimony potassium tartrate, ammonium molybdate and ascorbic acid. Further details and references may be found in the instrument’s manufacturer e-book “Fast and Accurate Thermo Scientific Gallery Discrete Industrial Analyzers - Automated Nutrient Analysis and Water Quality Monitoring” (SCIENTIFIC, 2018).

#### **A.9. Suspended Solids (TSS, VSS and FSS)**

Measurement of total, volatile and fixed suspended solids (TSS, VSS and FSS) followed the adaptation of the standard methods 2540 D and 2540 E in duplicates or single analysis of each sample (APHA, AWWA, *et al.*, 2017). The procedure starts by washing a glass fiber filter (pore size  $\leq 2 \mu\text{m}$ ) with reagent-grade water, drying it at 550°C in a muffle for 1 h, then weighing the set in an analytical balance. In sequence, a known

volume of sample (20 to 200 mL) is filtered through the same glass fiber membrane and the set (with the solids residues) is dried at 103-105°C for 24 h or until constant mass is obtained. Mass increase in the filter set divided by the sample volume gives the TSS concentration. Then the set is taken to ignition at 550°C for 1 h and the mass reduction, in relation to the previous step, is associated with the volatile fraction of the suspended solids. By subtracting the volatile suspended solids from the total ones, the fixed portion is obtained.

#### A.10. Attached Solids (TAS, VAS and FAS)

The total, volatile and fixed attached solids (TAS, VAS, FAS) were quantified by adapted standard methods 2540 B and 2540 E, for total and volatile/fixed solids (APHA, AWWA, *et al.*, 2017). A known number of carriers were taken from the MBBR and had the biofilm entirely scraped off - using interdental brushes and distilled water (Figure A.1) – into a pre-weighed dish, and then dried at 103-105°C for 24 h or until constant mass. Increase of the dish mass divided by the number of carriers was the TAS concentration, expressed as mg/carrier. Next, the dish was taken to the muffle at 550°C for 1 h and the mass reduction, related to the previous step, divided by the number of carriers, was the VAS concentration, in mg/carrier. The calculations necessary for expressing TAS and VAS per unit of reactional volume or surface area, as well as for calculating the total amount of attached solids in the reactor are given in section B.9, below.

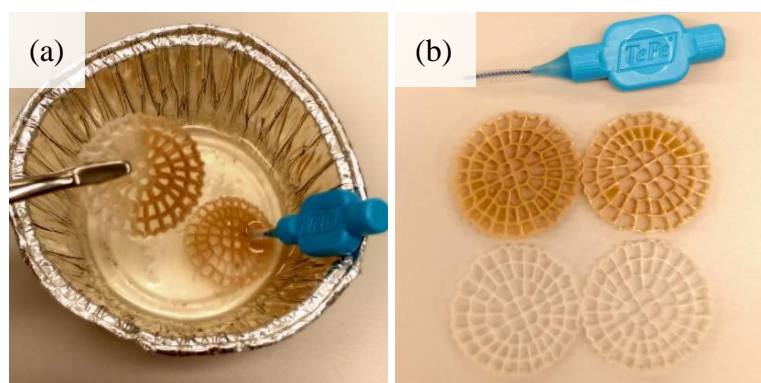


Figure A.1 – Biofilm extraction (a) and biofilm carriers after (bottom) and before (middle) cleaning with the interdental brush (top).

It is important to state that the same number of carriers taken for analysis was replaced by clean carriers in the MBBR. Those were marked to avoid using them later for biomolecular or attached solids analysis.

### **A.11. Turbidity**

The nephelometric standard method 2130 B (APHA, AWWA, *et al.*, 2017) was applied for turbidity assessment by means of a turbidimeter PoliControl AP-2000, calibrated with standard formazin suspensions supplied by the manufacturer. Recently collected samples were homogenized, transferred to clean glass vials compatible with the turbidimeter, and left standing for just enough time so that no more gas bubbles were visible, then the turbidity was read and registered in NTU (Nephelometric Turbidity Units).

### **A.12. pH**

#### *a) Pesticide Research*

The power of hydrogen was measured by the potentiometric standard method, 4500-H<sup>+</sup> B (APHA, AWWA, *et al.*, 2017), using a Hanna Instruments HI 2221 bench top pHmeter, equipped with selective glass electrode. Previous calibration with standard pH buffer solutions was performed. The electrode measures the electric potential difference in relation to the hydrogen ion diffusion potential, resulting from the gradient of hydrogen concentration from the sample to the interior of the electrode. A temperature probe connected to the equipment reads the temperature of the sample, correcting the pH reading.

#### *b) P&P Research*

Based on the same principle, a portable pHmeter Hanna HI 991001 was employed for tracking the pH in the reactors and other solutions. On the same way, temperature corrections were provided by simultaneously measuring it with the integrated temperature probe.

### **A.13. Temperature**

For both research projects, temperature in the reactors were always registered, in °C, during pH measurements using the temperature probes that accompanied the pH sensors.

### **A.14. Dissolved Oxygen (DO)**

#### *a) Pesticide Research*

For measuring dissolved oxygen, a bench top oximeter WTW Oxi 7310 was used directly in the MBBR. The instrument was equipped with a temperature probe for temperature correction of the DO concentration. Results were registered in mgO<sub>2</sub>/L.

#### *b) P&P Research*

A portable DO meter Hach HQ40d was used for monitoring the dissolved oxygen concentration inside the reactors. A temperature sensor is included along the DO probe, so corrections regarding the temperature were automatic. Results were registered in mgO<sub>2</sub>/L.

### **A.15. Optical Microscopy (Biomass)**

After collecting the biomass (whether suspended or attached), it was immediately placed (one or two drops) in glass microscope slides for observation. Biomass attached to the carriers was collected as described in section A.10. Suspended biomass was collected from the reactors effluent and decanted by gravity for sludge concentration prior to observation.

During the pesticide study, an optical microscope Boeco Germany BM – 800, coupled to a camera HDCE – X5, was used for biomass observation under magnification of 100 or 400 times. Same procedure was followed for the P&P study but using the Nikon Eclipse Ni optical microscope instead. Optical zoom range was 100 or 200 times.

### **A.16. Optical Stereomicroscopy (Carriers)**

For observing the biofilm morphology, carriers were taken and carefully rinsed with tap water for getting rid of suspended flocs that might have adhered to the carrier while sampling. Next, carriers were placed in petri dishes and observed in a stereomicroscope Nikon SMZ1270. Eventually, carriers were also observed after removing excess water absorbed into the biofilm by gently placing them over a paper towel and then in a dry dish under the stereomicroscope lens. Optical image amplification of 1, 2, 3, 4, 6 and 8 times were used.

### **A.17. Fluorescence *in situ* hybridization (FISH)**

Fluorescence *in situ* hybridization (FISH) technique, including microscopy and image processing, was performed to determine the relative abundance of the nitrifying bacteria, AOB and NOB (see section 2.2.4.1), with regards to the total bacterial community. This biomolecular technique was employed for the biofilm of the study with the pesticide wastewater. The procedure was performed by one scientific internship student, advised by professors.

The FISH principle consists of fixing biomass samples and hybridizing them with DNA oligonucleotide probes that attach specifically to rRNA sequences of target organisms. The probes are fluorescently labeled and may, consequently, be visualized by microscopy and analyzed by image processing software for quantification of the targeted groups in relation to the total bacterial community (which is hybridized with universal bacterial probe labeled with another color). Overall, the procedure consists of fixing the biomass sample - for cell inactivation and permeabilization for probes penetration -, sample immobilization, hybridization, washing of excess probe, microscope examination and image analysis. Further explanations about the working principle of this technique are given in the literature (BASSIN, DEZOTTI, *et al.*, 2018, NIELSEN, LEMMER, *et al.*, 2009).

Biofilm samples were extracted from the carriers (as done for attached solids analysis, section A.10) at the end of each operational phase and immediately fixed in Eppendorf vials with paraformaldehyde 4% m/v. The fixation procedure started by macerating the extracted biomass, letting it decant and removing the excess supernatant water. The resulting biomass slurry was transferred to a 2 mL Eppendorf vial and

centrifuged for 2 minutes at 1400 rpm, followed by removal of the supernatant liquid. Then, i) 2 mL of PBS (Phosphate Buffered Saline) was added, ii) the biomass was resuspended and homogenized, iii) and centrifuged (2 min, 1400 rpm) for supernatant removal. PBS addition and subsequent steps were repeated another 2 times. After that, around threefold the biomass volume of paraformaldehyde (4 % m/v) was added and the biomass resuspended. After resting in the fridge for 1 to 3 h, the mixture was centrifuged (2 min, 1400 rpm) and the supernatant taken away. Steps i) to iii) were repeated for another three times. Finally, the Eppendorf volume was completed with equal parts of ethanol (98% v/v) and PBS solution, and stored in the freezer at -20°C until utilization.

For preparing the slides for sample immobilization, they were dipped in gelatin solution at 70°C for 5 minutes, then air-dried in the oven at 48°C. Gelatin solution was previously prepared by mixing, at 70°C, 100 mL of distilled water, 0.1 g of microbiological gelatin and 0.01 g of  $\text{KCr}(\text{SO}_4)_2$ , then stored at 4°C. For each sample, triplicates were added in equal sized wells contained in the plate (0.2  $\mu\text{L}$ ). The slides were dried at 48°C for 15-30 minutes with posterior dehydration with growing concentrations of ethanol (50, 70 and 98 % v/v) by sequentially submerging the plate in each ethanol solution for 3 minutes. Figure A.2 illustrates the samples setup for hybridization, with triplicates for each operational phase performed in three wells of the prepared slides.

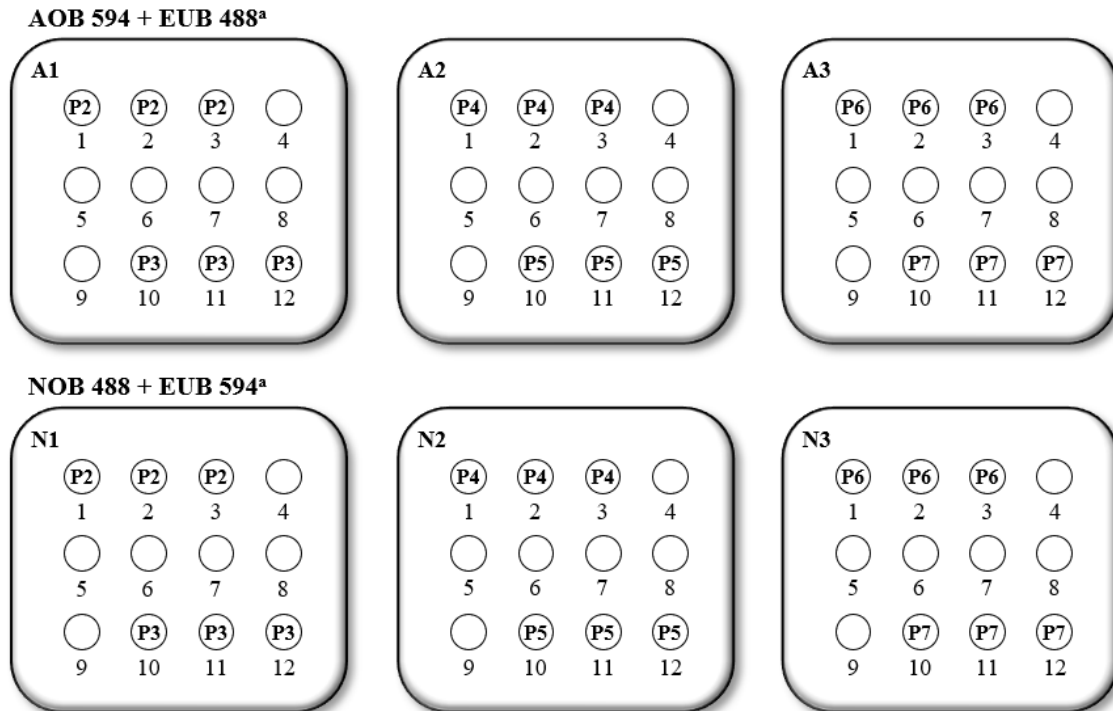


Figure A.2 – Immobilized samples in each slide during FISH procedure, showing triplicates for each phase (P2 to P7), for each combination of probes targeting AOB and NOB. <sup>a</sup> AOB, NOB and EUB stands for the oligonucleotide hybridization probe blends (Table A.2), while the fluorescent labels are denoted by 488 (Alexa Fluor 488 - green) and 594 (Alexa Fluor 594 - red).

After air-drying the slides, 10  $\mu\text{L}$  of hybridization buffer (NaCl 5 M, Na<sub>2</sub>EDTA 0.5 M, Tris/HCl 1 M, sodium dodecyl sulfate (SDS) 10% v/v) was blended with 1  $\mu\text{L}$  of different fluorescent labeled oligonucleotide probe blends (green, Alexa Fluor 488, and red, Alexa Fluor 594), leading to final probe concentrations in each well of 5 ng probe/ $\mu\text{L}$ . Table A.2 describes the hybridization probe blends employed for the AOB, NOB and total bacteria (EUB). More details regarding the probes and target groups are given elsewhere (NIELSEN, LEMMER, *et al.*, 2009).

Table A.2 – Oligonucleotide probes utilized and target microbial groups.

Blend	Probe	Sequence (5'-3')	Target Groups	Ref. <sup>a</sup>
EUB	EUB338 I	GCTGCCTCCCGTAGGAGT	(Most bacteria)	[1]
	EUB338 II	GCAGCCACCCGTAGGTGT	<i>Planctomycetales</i> order	[2]
	EUB338 III	GCTGCCACCCGTAGGTGT	<i>Verrucomicrobiales</i> order	[2]
AOB	NEU	CCCCTCTGCTGCACTCTA	Most halophilic and halotolerant <i>Nitrosomonas</i> spp.	[3]
	S*Nse1472	ACCCCAGTCATGACCCCC	<i>Nitrosomonas europaea</i> -lineage	[4]
	Nso1225	CGCCATTGTATTACGTGTGA	Ammonia oxidizing $\beta$ -proteobacteria	[5]
	NmV	CCGCGTAGTCTCTGAGGA	<i>Nitrosococcus mobilis</i> -lineage	[6]
	Nso190	CGATCCCCTGCTTTTCTCC	Ammonia oxidizing $\beta$ -proteobacteria	[5]
NOB	NIT3(1035)	CCTGTGCTCCATGCTCCG	<i>Nitrobacter</i> spp.	[7]
	SGNtspa662	GGAATCCGCGCTCCTCT	<i>Nitrospira</i> spp.	[8]

<sup>a</sup> [1] (AMANN, BINDER, et al., 1990); [2] (DAIMS, BRÜHL, et al., 1999); [3] (WAGNER, RATH, et al., 1995); [4] (JURETSCHKO, TIMMERMANN, et al., 1998); [5] (MOBARRY, WAGNER, et al., 1996); [6] (POMMERENING-RÖSER, RATH, et al., 1996); [7] (WAGNER, RATH, et al., 1996); [8] (DAIMS, NIELSEN, et al., 2001).

Hybridization was carried out for 16 h after the addition of the marking probes in a dark chamber saturated with the hybridization buffer at 46°C. Next, the slide was submerged in the washing buffer for removal of excess probe (that did not hybridize) for 15 minutes at 48°C. Finally, it was washed with distilled water and air-dried again. Finished the hybridization, the slide was embedded with Vectashield (Vector Laboratories) with DAPI at 1 µg/L for 15 minutes at 4°C, then stored at -20°C until microscope visualization.

Confocal laser scanning microscope (Zeiss LSM 710) was used to evaluate the samples triplicates on the slides. Six images of each well were obtained by the Black Zeiss software as .czi extension files that were exported to the Python Jupyter software to avoid loss of information. Figure A.3 shows examples of images taken during NOB evaluation. Then, quantification was performed by image analysis for each specific probe in relation to the total bacterial quantified. Results were expressed in % as biovolume fraction which was calculated by the ratio of the area of the target group to the area of the universal probe (EUB).

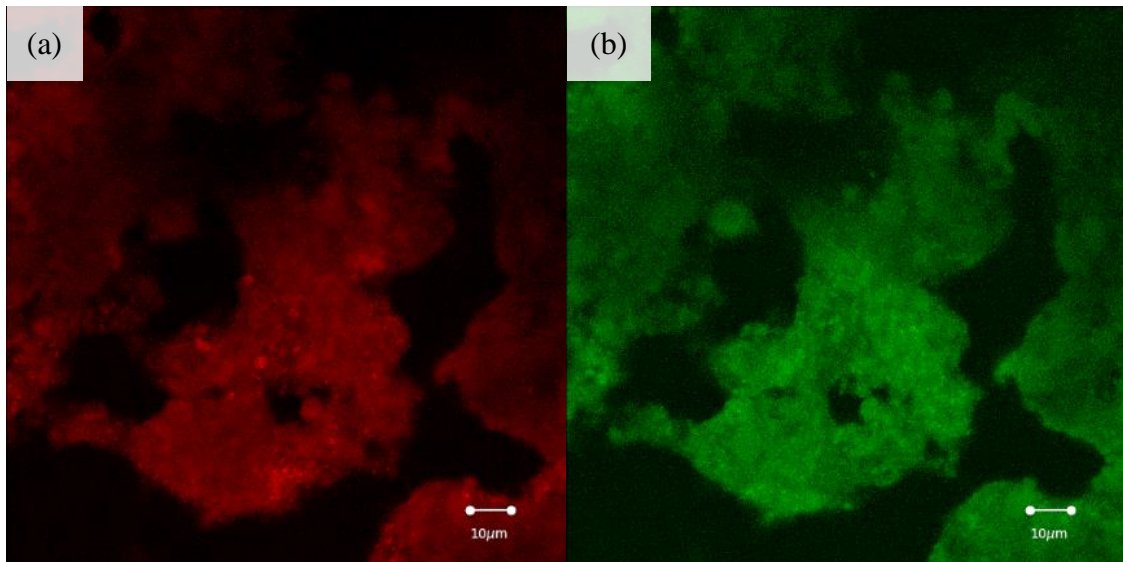


Figure A.3 – Example of images taken during NOB evaluation where (a) is the area of the red labeled hybridized total bacteria (EUB), (b) is the area of the green labeled NOB.

#### A.18. DNA Screening

For the study with P&P wastewater, analysis of the microbial community in biofilm samples at the end of each operational phase - and also from BioChip P carriers taken at the full-scale MBBR – was done by DNA extraction followed by PCR and 16S rRNA gene amplicon sequencing (with PCR) targeting the bacterial variable regions V1-V3. Biofilm was extracted from 1-2 carriers from each MBBR with interdental brushes and distilled water (Figure A.4a), similar as for attached solids analysis (section A.10). The content was transferred to 15 mL Falcon tubes for settling during 15 to 30 minutes (Figure A.4b), then 2 to 2.5 mL of the concentrated sludge was pipetted to Eppendorf tubes (Figure A.4c) that were immediately stored at -20°C.

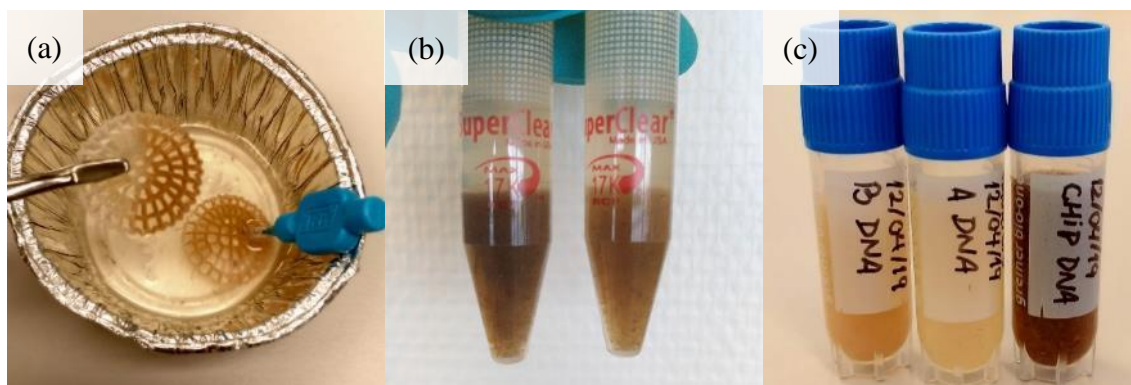


Figure A.4 – Biofilm extraction (a), settling (b), and storage (c) for subsequent DNA screening.

DNA extraction, sequencing and raw data processing were outsourced to the company DNASense, based in Aalborg, Denmark. Latest research standards for sample preparation and sequencing were followed by the company. The following methods were written based on the information contained in the final report sent by the DNASense, shown in Annex I.

Standard protocol for FastDNA Spin kit for Soil (MP Biomedicals, USA) was used for performing DNA extraction. In a Lysing Matrix E tube were added 500  $\mu$ L of sample, 480  $\mu$ L of sodium phosphate buffer and 120  $\mu$ L of MT Buffer. Bead beating was done at 6 m/s for 4x40 s (ALBERTSEN, KARST, *et al.*, 2015). Validation of product size and purity of a subset of DNA extracts was accomplished by gel electrophoresis utilizing Tapestation 2200 and Genomic DNA screentapes (Agilent, USA). DNA concentration was obtained using Qubit dsDNA HS/BR Assay kit (Thermo Fisher Scientific, USA).

Preparation of gene sequencing libraries of bacteria 16S V1-V3 rRNA followed a custom protocol based on the literature (CAPORASO, LAUBER, *et al.*, 2012). For PCR amplification of the bacteria 16S V1-V3 rRNA gene amplicons, as much as 10 ng of extracted DNA was used. Every PCR reaction (25  $\mu$ L) included dNTPs (100  $\mu$ M of each),  $MgSO_4$  (1.5 mM), Platinum Taq DNA polymerase HF (0.5 U/reaction), Platinum High Fidelity buffer (1X) (Thermo Fisher Scientific, USA) and barcoded library adaptors (400 nM of each forward and reverse). The following steps were followed for performing PCR: initial denaturation at 95°C for 2 min, 30 cycles of amplification (95°C for 20 s, 56°C for 30 s, 72°C for 60 s), and a final elongation at 72°C for 5 min. For each sample, duplicate PCR was promoted with posterior pooling of the duplicates. The 16S V1-3 specific primers contained in the adaptors were [27F] AGA GTTT GAT CCT GGC TCA G and

[534R] ATT ACC GCG GCT GCT GG (WARD, GEVERS, *et al.*, 2012). Obtained amplicon libraries were purified using standard protocol for Agencourt Ampure XP Beads (Beckman Coulter, USA) with a 4:5 bead to sample ratio. DNA was eluted in 25  $\mu$ L of nuclease free water (Qiagen, Germany). Concentration of DNA was quantified using Qubit dsDNA HS Assay kit (Thermo Fisher Scientific, USA). Gel electrophoresis using TapeStation 2200 and D1000/High sensitivity D1000 screentapes (Agilent, USA) was utilized to validate purity and product size of a subset of sequencing libraries.

The purified sequencing libraries were pooled in equimolar concentrations and diluted to 6 nM. On a MiSeq (Illumina, USA), samples were paired-end sequenced (2x300 bp) using a MiSeq Reagent kit v3 (Illumina, USA) and following the standard guidelines for preparing and loading samples on the MiSeq. Control library was spiked in (>10 % PhiX) to avoid low complexity issues frequently noticed with amplicon samples.

Trimmomatic v. 0.32 software – with settings SLIDINGWINDOW:5:3 and MINLEN:275 – was used for trimming forward and reverse reads (BOLGER, LOHSE, *et al.*, 2014). Once trimmed, the forward and reverse reads were first merged using FLASH v.1.2.7 (MAGOC, SALZBERG, 2011), configured for -m 10 -M 200, and then dereplicated and formatted for use in the UPARSE workflow (EDGAR, 2013). The dereplicated reads were clustered making use of the usearch v. 7.0.1090 -cluster\_otus command with default settings. Operational taxonomic unit (OTU) relative abundances were estimated using the usearch v. 7.0.1090 -usearch\_global command with -id 0.97 -maxaccepts 0 -maxrejects 0. The abundance is influenced by DNA extraction, gene copy number and primer biases and does not necessarily represent the true in situ abundance. Taxonomy was assigned by means of the RDP classifier (WANG, GARRITY, *et al.*, 2007) as implemented in the parallel\_assign\_taxonomy\_rdo.py script in QIIME (CAPORASO, KUCZYNSKI, *et al.*, 2010), using -confidence 0.8 and the MiDAS database v. 1.23 (MCILROY, KIRKEGAARD, *et al.*, 2017), that is a curated database founded on the SILVA database, release 123 (QUAST, PRUESSE, *et al.*, 2012). The statistical environment R v. 3.5.1 was used for analyzing the results through the Rstudio IDE, using the ampvis package v 2.5.8 (ALBERTSEN, KARST, *et al.*, 2015).

Access to the data was provided via the online application of DNASense for results visualization, processing, and interpretation. This environment was used for generating tables, heatmaps and plots for most abundant OTUs at different taxonomic

levels, richness and alpha diversity metrics (both calculated in a basis of 10000 reads per sample for fair samples comparison), and ordination plots for beta diversity analysis.

#### **A.19. Microtoxicity to *Vibrio fischeri***

Final sample from the PAC adsorption (section 3.1.2) was handed to the accredited laboratory from the pesticide formulation industry for analyzing the inhibitory effect to the bioluminescence of *Vibrio fischeri* bacteria. The procedure is described by the technical norm NBR 15411-3:2012, from the Brazilian Association of Technical Norms (ABNT).

## B. APPENDIX: CALCULATION PROCEDURES

Just like the analytical methods, most calculation procedures were considered not essential for the thesis reading if the reader is already familiarized with the calculated parameters. However, the description of the calculation procedures is crucial for further understanding of the discussed concepts and for reproducibility of the studies.

Subsections below indicate the equations and procedures used for calculating parameters derived from results of analysis or design parameters. For every equation, dimensional consistency should be observed for its correct application. The list of symbols and acronyms, given before the summary of this document, contains all the notations included in the equations.

### B.1. Removal Efficiencies

According to Equation (B.1) the efficiency of removal ( $\eta$ ) of a certain parameter in relation to the influent concentration is given as function of the influent ( $C_i$ ) and effluent ( $C_e$ ) concentrations of such parameter.

$$\eta = \left( \frac{C_i - C_e}{C_i} \right) 100\% \quad (\text{B.1})$$

### B.2. Total, Particulate and Soluble Concentrations

Considering that a certain component is distributed in solution in soluble and particulate fractions, then the total concentration ( $tC$ ) equals the sum of the soluble ( $sC$ ) and particulate ( $pC$ ) ones, as in Equation (B.2).

$$tC = sC + pC \quad (\text{B.2})$$

Usually, total and soluble portions are directly analyzed, allowing the calculation of the particulate portion. In this work, the following parameters are distributed in suspended solids and dissolved fractions: COD, TN, TP.

### B.3. Hydraulic Retention Time (HRT)

The hydraulic retention time obtained as a function of the flow rate ( $Q$ ) and the reactional volume ( $V$ ) is shown in Equation (B.3). This parameter corresponds to the effective average contact time between the microorganisms and the substrates.

$$HRT = \frac{V}{Q} \quad (\text{B.3})$$

### B.4. Theoretical Chemical Oxygen Demand

The theoretical chemical oxygen demand of a substance is indicated by the stoichiometry of its complete oxidation with oxygen. In other words, the COD is the amount of oxygen that would be necessary to fully oxidize chemically a certain sample. For instance, Equation (B.4) shows that the oxidation of 46 g of ethanol requires 96 g of oxygen, so that the theoretical COD of ethanol corresponds to  $96/46 = 2.09 \text{ gO}_2/\text{g ethanol}$ . Hence, a liquid sample containing 100 g ethanol/L would have COD of 209 gO<sub>2</sub>/L (HENZE, VAN LOOSDRECHT, *et al.*, 2008).



Calculations of theoretical oxygen demand were employed in this work for assessing the required quantity of organic substrates in a synthetic feed to achieve certain COD.

### B.5. Nitrogen Mass Balance in Liquid Phase

Equation (B.5) demonstrates the nitrogen mass balance used to calculate the organic nitrogen content ( $[N_{org}]$ ) as function of the concentration of the analyzed nitrogen species, namely total nitrogen ( $[TN]$ ); total ammoniacal nitrogen ( $[TAN]$ ); nitrite ( $[N_{NO_2^-}]$ ); and nitrate ( $[N_{NO_3^-}]$ ).

$$[N_{org}] = [TN] - [TAN] - [N_{NO_2^-}] - [N_{NO_3^-}] \quad (B.5)$$

The nitrogen fraction that may theoretically be oxidized via nitrification is the sum of the organic and ammoniacal nitrogen, known as total kjeldahl nitrogen (TKN), as Equation (B.6).

$$[TKN] = [N_{org}] + [TAN] \quad (B.6)$$

It should be regarded that organic species containing nitrogen might appear in as solids, being, thus, important to clarify regarding soluble or particulate forms of organic or total nitrogen.

### B.6. Ammoniacal Nitrogen Distribution

Ammoniacal nitrogen is found in soluble form whether as free ammonia (NH<sub>3</sub>) or ammonium (NH<sub>4</sub><sup>+</sup>), according to the equilibrium shown in Equation (B.7) (METCALF & EDDY, TCHOBANOGLOUS, et al., 2003).



According to the Le Chatelier principle, in acid mediums the equilibrium is shifted in the direction of ammonium. Therefore, free ammonia predominates in alkaline medium. Equation (B.8) allows the calculation of the ratio of free ammonia-nitrogen to total ammoniacal nitrogen (TAN) as a function of pH (within 6.0 and 10.0) and temperature in °C (within 0 to 50°C) (VON SPERLING, 2007a).

$$\frac{[N_{NH_3}]}{[TAN]} = \left\{ 1 + 10^{0.09018 + [2729.92/(T+273.20)] - pH} \right\}^{-1} \times 100\% \quad (B.8)$$

### B.7. Fraction of Nitrogen Assimilated

Nitrogen present in the wastewater may be assimilated by bacteria via anabolic pathways. For estimating the fraction of nitrogen anabolized in relation to the total

removed nitrogen, first it may be considered that the volatile fraction of cell material is typically constituted by 12.4% of nitrogen, considering the cell composition as  $C_5H_7O_2N$  (HENZE, VAN LOOSDRECHT, *et al.*, 2008). If assuming that the volatile biomass production corresponds to the outlet VSS concentration ( $[VSS]_e$ ), then Equation (B.9) relates to the amount of assimilated nitrogen, in mg/L.

$$\text{Assimilated } N = 0.124 \cdot [VSS]_e \quad (\text{B.9})$$

Other implied assumptions are that the incoming solids are in low concentration and are completely metabolized, and that the EPS content has similar N percentage than the cell material. Thus, the fraction of assimilated nitrogen in relation to the overall nitrogen removal was calculated by Equation (B.10).

$$\text{Fraction of Assimilated } N = \frac{\text{Assimilated } N}{[TN]_i - [TN]_e} \quad (\text{B.10})$$

Where  $[TN]_i$  and  $[TN]_e$  are the influent and effluent total nitrogen concentration. If organic nitrogen is negligible, then total nitrogen concentrations may be substituted by total ammoniacal nitrogen concentrations.

### B.8. Volumetric and Surface Loading Rates (VLR and SLR)

Volumetric loading rates (VLR) are important parameters for designing biological reactors, particularly in terms of organic or nitrogenated matter. It is calculated as in Equation (B.11), where ( $C_i$ ) is the influent concentration of the parameter to be expressed as volumetric loading rate; ( $Q$ ) is the flow rate; and ( $V$ ) is the reactional volume.

$$VLR = \frac{Q \cdot C_i}{V} = \frac{C_i}{HRT} \quad (\text{B.11})$$

For bioreactors with attached growth, the surface loading rates (SLR) is a design parameter, as it considers the total area available for biofilm development ( $A$ ), given by the product of the carrier specific protected surface area ( $a$ ) – specified by the carrier

manufacturer –, the reactional volume ( $V$ ), and the carrier filling ratio ( $f$ ). Hence, the SLR is calculated as seen in Equation (B.12).

$$SLR = \frac{Q \cdot C_i}{V \cdot a \cdot f} = \frac{C_i}{HRT \cdot a \cdot f} = \frac{Q \cdot C_i}{A} \quad (\text{B.12})$$

Overall, organic VLR and SLR as expressed in kg COD/(m<sup>3</sup>·d) and g COD/(m<sup>2</sup>·d). These quantities may also be expressed as soluble, particulate or total portions, according to the respective fraction of the substrate used in the calculation.

### B.9. Quantity and Concentration of Attached Biomass

The concentration of total biomass per carrier unit ( $TAS$ ) is measured by the attached solids analysis, described in section A.10. Therefore, the total amount of attached biomass contained in the reactor ( $TAS_T$ ) is the product of ( $TAS$ ) by the number of carriers in the reactor ( $n$ ), as in Equation (B.13).

$$TAS_T = TAS \cdot n \quad (\text{B.13})$$

By dividing ( $TAS_T$ ) by the reactional volume ( $V$ ), the volumetric concentration of total attached solids ( $TAS_V$ ) can be obtained, as seen in Equation (B.14).

$$TAS_V = \frac{TAS_T}{V} = \frac{TAS \cdot n}{V} \quad (\text{B.14})$$

It is also possible to calculate the surface concentration of total attached solids ( $TAS_S$ ) using Equation (B.15).

$$TAS_S = \frac{TAS_T}{V \cdot a \cdot f} = \frac{TAS \cdot n}{V \cdot a \cdot f} \quad (\text{B.15})$$

Naturally,  $TAS$  assumes the form of  $VAS$  or  $FAS$ , if assessing the volatile or fixed attached solids fractions.

### B.10. Heterotrophic Cell Yield

The heterotrophic cell yield is a parameter that allows the evaluation of the sludge production per amount of consumed substrate. It was calculated by Equation (B.16), and expressed as g VSS/g COD.

$$Y_{Hv} = \frac{[VSS]_e}{C_i - C_e} \quad (\text{B.16})$$

Above,  $[VSS]_e$  is the volumetric concentration of volatile suspended solids, and the difference between influent and effluent concentrations ( $C_i - C_e$ ) expresses the amount of removed substrate.

The calculation considers the biofilm has reached equilibrium, so the amount of formed biofilm is equal to the amount sloughed off. Beyond that, assumption is made that the suspended solids entering the reactor are completely metabolized and do not contribute to the effluent solids concentration. At last, it is considered that the autotrophic biomass fraction is much lower than the heterotrophic one.

It is also usual to show heterotrophic yield in terms of  $gCOD_{VSS}/gCOD$ , ( $Y_H$ ), as in Equation (B.17). In this case, it is considered the conversion factor of 1.42  $gCOD_{VSS}/gVSS$  (HENZE, VAN LOOSDRECHT, *et al.*, 2008).

$$Y_H = 1.42 \cdot \frac{[VSS]_e}{C_i - C_e} = 1.42 \cdot Y_{Hv} \quad (\text{B.17})$$

### B.11. Apparent and Maximum Substrate Removal Rates

From one operating biological system, substrate removal rates may be calculated. Let ( $r$ ) be the volumetric removal rate, ( $s$ ) the surface removal rate, and ( $q$ ) the specific removal rate – usually expressed as  $kg/(m^3 \cdot d)$ ,  $g/(m^2 \cdot d)$  and  $g/(gVS \cdot d)$ , respectively. If the amount of removed substrate – COD or TAN, in this case – corresponds to the difference between influent and effluent concentrations ( $C_i - C_e$ ), then the apparent substrate removal rates of continuous operation are calculated according to Equations (B.18), (B.19) e (B.20).

$$r = \frac{(C_i - C_e)}{HRT} \quad (\text{B.18})$$

$$s = \frac{(C_i - C_e)}{HRT \cdot a \cdot f} = \frac{r}{a \cdot f} \quad (\text{B.19})$$

$$q = \frac{(C_i - C_e)}{HRT \cdot (VAS_V + [VSS])} = \frac{r}{(VAS_V + [VSS])} \quad (\text{B.20})$$

Where  $HRT$  is the hydraulic retention time;  $a$  is the specific surface area of the carrier;  $f$  is the carrier filling degree in the MBBR;  $VAS_V$  and  $[VSS]$  are, respectively, the volumetric concentrations of volatile attached and suspended solids. With regards to the specific removal rate, it should be noticed that for MBBRs,  $VAS_V \gg [VSS]$ , normally. Thus, as  $VAS_V$  was analyzed much less often than  $[VSS]$  due to practical issues, there are few dates (close to VAS measurement) where  $q$  is quantitatively reliable.

Now, let  $r^*$ ,  $s^*$  and  $q^*$  be the respective maximum substrate utilization rates. Considering that the batch trials were performed in presence of excess substrates and oxygen and that the biodegradation followed zero-order kinetics, the substrate removal rate tends to be constant and equal to the maximum removal rate as long as the substrates persisted in excess through the trial (HENZE, VAN LOOSDRECHT, *et al.*, 2008). This means that the substrate concentration decays linearly with time for the first data points and that the maximum removal rate can be obtained as the initial slope of the linear regression ( $C \times t$ ). Equation (B.21) shows this relation.

$$r^* = -\frac{dC}{dt} \quad (\text{B.21})$$

To acquire  $s^*$  and  $q^*$ , each data point must have the substrate concentration ( $C$ ) expressed either as surface concentration or specific concentration, respectively, as in Equations (B.22) and (B.23), before performing the linear regression. As the total area and biofilm quantity stays the same during the trial, for every instant that surface or specific concentrations are calculated correction regarding the total volume sampled should be done to the concentrations of substrate and suspended biomass. This is the reason why it is inappropriate to simply convert the volumetric maximum removal rate to the surface and specific ones by dividing the former by total area ( $A$ ) and biomass,

respectively, especially if the sampled volume is significant compared to the total volume of the batch trial (which is not unusual in lab-scale trials).

$$C_{surface}(t) = \frac{C \cdot (V - V_{sampled}(t))}{A} \quad (B.22)$$

$$C_{specific}(t) = \frac{C \cdot (V - V_{sampled}(t))}{VAS_T + [VSS] \cdot (V - V_{sampled}(t))} \quad (B.23)$$

$V_{sampled}(t)$  is the total sampled volume up to the instant  $t$  of the trial duration. Observation should be done that biofilm trials were performed with negligible amount of suspended solids (see section 3.1.7), thus  $C_{specific}$  was calculated only based on total volatile attached solids ( $VAS_T$ ), disregarding  $[VSS]$ . In turn, suspended biomass batch assays had no biofilm, so that the  $VAS_T$  was zero.

Therefore,  $s^*$  and  $q^*$  are calculated via the linear regression of the respective concentrations as a function of time, as shown in Equations (B.24) and (B.25).

$$s^* = -\frac{dC_{surface}}{dt} \quad (B.24)$$

$$q^* = -\frac{dC_{specific}}{dt} \quad (B.25)$$

Decision on which data points should be included in the linear regression and which should be excluded as outliers was made by using the statistical concept of Cook's Distance, further explained in section B.12.

## B.12. Statistical Methods

Standard deviations of parameters were calculated as square root of the variance and are shown next to average values, whenever applicable. For propagating experimental errors for the parameters calculated using mathematical functions, general formula based on partial derivatives and individual standard deviations was used. The Shapiro-Wilk test for normality was employed whenever some dataset was required to be normal (or normal-like) distributed for performing other statistics, as the one-way analysis of

variance (ANOVA). Detailed description of the aforementioned statistical concepts are given elsewhere (DODGE, 2008, KALLNER, 2014).

The ANOVA test was used for checking if there was statistically significant difference between two or more independent data sets, being the associated statistics F and p values always registered. The lower the F and higher the p values, the safer it is to assume the null hypothesis of ANOVA (the groups' averages are equal) as correct. Confidence level of 95% is considered for assuming the hypothesis as true ( $p > 0.05$ ), denying it otherwise ( $p < 0.05$ ).

The statistical concept of Cook's Distance was used to remove the data points that fit the least to linear regressions, using as decision factor three times the average Cook's Distance of all points. This parameter indicates how much each data point impacts the least-squares linear regression by weighting the leverage and residual values of each observation (KUTNER, NACHTSHEIM, *et al.*, 2005).

Multivariate analysis was performed for reducing the dimensionality of the dataset resulting from the DNA screening of the biofilm samples and facilitating the evaluation of similarity or disparity of the microbiome between samples (beta diversity). Non-metric multidimensional scaling (NMDS), based on Bray-Curtis (also known as Odum) distance between samples, was applied within the DNASense online application for data and results visualization. This method is usually one of the most suitable and efficient for assessing the relative abundance data of species within samples (RAMETTE, 2007). Further details about NMDS analysis and the Bray-Curtis distance are found in the literature (GREENACRE, PRIMICERIO, 2013).

## I. ANNEX: DNASENSE REPORT

### CP638 Microbial community analysis

Mie Bech Lukassen & Mads Albertsen, DNASense ApS

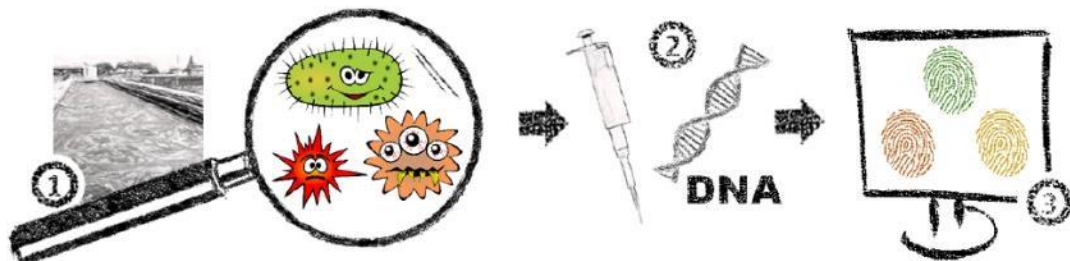
19-05-2020, Aalborg, Denmark

#### Project scope

This project concerns the analysis of microbial communities in DNA samples from Maria Piculell at **Veolia**. DNASense received a total of 13 samples of biomass, where DNA was extracted and analysed with 16S rRNA gene amplicon sequencing targeting the bacterial variable regions V1-V3. The project deals with biofilms on MMBR from a laboratory experiment with pulp and paper water.

#### Microbial community analysis through DNASense ApS

The general microbial community analysis workflow, from raw sample to a final report is outlined in the figure below. First, the incoming samples are registered in the laboratory and DNA is extracted from all organisms in the sample. Afterwards, the extracted community DNA is taken through a complex molecular process, which ends with DNA sequencing on state-of-the-art equipment at Aalborg University. DNA from each microbe in the community has specific “fingerprint” genes, that can be used to identify the organisms. Examples of fingerprint genes is the 16S ribosomal RNA gene for Bacteria and Archaea and the ITS for fungi. DNA sequencing is used to count the number of fingerprint genes from each microbe in the sample, which is then used as an estimate of the relative abundance of the microbe in the community. Around 10,000 fingerprints are measured from each sample to provide a high resolution of the community structure. The fingerprint genes can be matched with a database of known references and thereby the microbes in the community can be identified.



**Workflow figure:** Overview of the general workflow from sample to results.

Sample preparation and DNA sequencing for the fingerprint genes were conducted in agreement with the latest research standards. The raw sequencing data was processed using the research standard [UPARSE workflow](#) and data analysed through Rstudio using the [ampvis2 package](#) developed at Aalborg University.

The abundances of the species presented in the analysis represent the count of each bacterial 16S rRNA gene in the sample. The abundance is influenced by DNA extraction, gene copy number and primer biases and does not necessarily represent the true *in situ* abundance.

## Results

### Data availability

The data is available from the following dropbox folder /CP638 with the password [REDACTED]. The file `raw.zip` contains the raw unprocessed sequencing data. The file `otutable.xlsx` contains the different OTUs that were identified in all samples, their abundances and taxonomic assignment. Each OTU is identified by a name e.g. OTU\_1 and the corresponding DNA sequence of the specific OTU can be found in the file `otus.fa`. Data can also be explored, filtered and visualized in heatmaps and ordination plots, such as PCA, in the DNASense app using the link <https://dnasense.shinyapps.io/dnasense/> with the username CP638 and the same password as above.

### DNA extraction, library preparation and sequencing

DNA extraction was successful for all samples, yielding  $>5$  ng/ $\mu$ L and based on gel electrophoresis the majority of the DNA was  $>5000$  bp, which is recommended for amplicon sequencing. Library preparation for bacterial sequencing (V1-V3) was successful for all samples and yielded between 24743 and 32187 reads after QC and bioinformatic processing (Table 1).

### Microbial community composition

In Table 2 an overview of the 25 most abundant genera is provided across all samples. All unassigned bacteria in the OTU table is removed prior to analysis. In addition, we have included information on each microorganism from the MiDAS database if available. The samples share many of the same microorganisms but at varying abundances. The most abundant organisms in the A and the C samples are *Mangroviflexus* and *Rhizobium*. In the B samples the most abundant microorganisms are *Mangroviflexus*, the chemoautotroph *Acetobacterium* and the aerobic heterotroph *Proteiniphilum*.

In Figure 1 we have used multivariate statistics (PCA) to compare the overall microbial composition in all samples and it supports the groups from the heatmap. To illustrate the variation in the microbial community a trajectory is added for the A and B samples.

## Figures and Tables

**Table 1: Sequencing statistics**

Information about sample characteristics. **SeqID** is the name of the sequencing data files. **Sample Name** was the name on the sample tubes. **Extraction Conc.** is the concentration of the extracted DNA (ng/ $\mu$ L). **Library Conc.** is the concentration of the sequencing library (ng/ $\mu$ L). **Reads** is the number of reads after sequencing, QC and bioinformatic processing. **Observed OTUs** is the number of observed OTUs in each sample, in order to compare between samples it is calculated based on 10,000 reads pr. sample. **Shannon Index** a commonly used alpha-diversity index, in order to compare between samples it is calculated based on 10,000 reads pr. sample.

Sequencing ID	Sample Name	Extraction Conc. [ng/uL]	Library Conc. [ng/uL]	Reads	Observed OTUs	Shannon Index
MQ200507-222	A_1	481.9	39.5	27748	188	3.9
MQ200507-223	B_1	239.4	37.8	24743	207	4.1
MQ200507-224	A_2	154.6	41.7	30274	170	3.1
MQ200507-225	B_2	338.6	43.2	30794	128	2.8
MQ200507-226	A_3	449.1	44.1	25678	290	4.0
MQ200507-227	B_3	491.6	43.4	25586	201	3.4
MQ200507-228	A_4	420.5	42.3	25771	323	4.3
MQ200507-229	B_4	394.1	37.3	29884	277	3.7
MQ200507-230	A_5	657.5	25	32187	261	2.7
MQ200507-231	B_5	231.5	37.9	31093	294	3.4
MQ200507-232	A_6	769.2	33.1	29319	351	4.2
MQ200507-233	B_6	594.3	31.4	26836	268	4.1
MQ200507-234	CHIP	241.7	32.6	29207	280	4.1

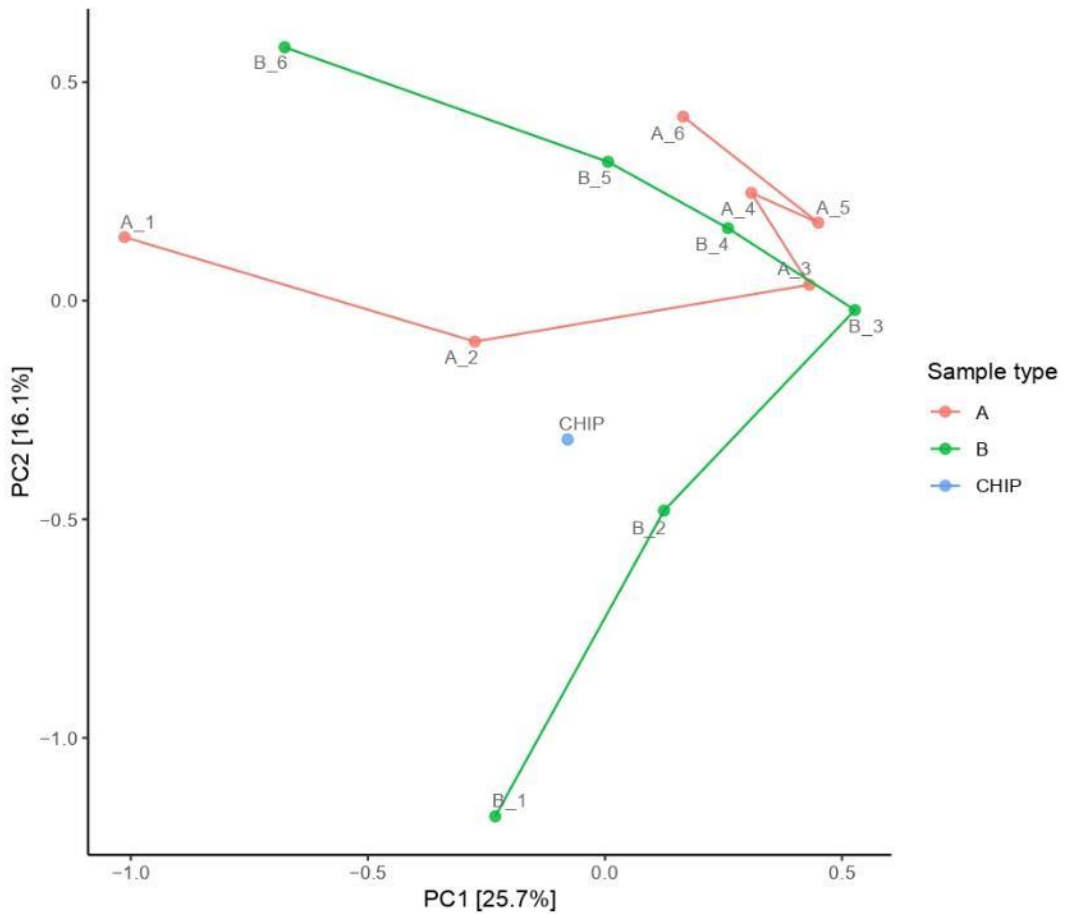
**Table 2: The 25 most abundant genera**

The most abundant genera across all samples. If no genus level classification could be obtained, the lowest assigned taxonomic classification is given. In addition, the phylum level classification is given (Proteobacteria at class level).

	A						B						C
Bacteroidetes; Mangroviflexus -	0.3	18	28.3	14.4	5.1	20.9	0.3	27.7	21.1	3.4	29.9	3.3	10.9
Alphaproteobacteria; Rhizobium -	21.3	19	1.5	4.4	0.5	2.1	7.8	1.8	0.1	2.9	4.5	4.7	6.8
Firmicutes; Acetobacterium -	0	0	0.4	0.5	0.1	0.1	0	0	38.6	30.9	0.2	0.1	0
Alphaproteobacteria; Thioclava -	0	3.8	0.6	1.3	1.2	0.8	5.9	4.7	5.7	4.6	5.1	0.4	5.9
Bacteroidetes; Proteiniphilum -	1.3	0.2	0.7	1.1	1	2.1	2.8	23.3	1.8	1.9	0.5	0.5	0.7
Deltaproteobacteria; Desulfostipes -	0	0	4.1	7.7	4.8	6.6	0	0	2.7	6.8	0.2	0.1	0
Firmicutes; Christensenellaceae R-7 group -	0	0	4.1	6.7	3.7	5.3	0.4	0.7	6	4.3	0.4	0.2	0.8
Alphaproteobacteria; Caenispirillum -	0	13.1	1.4	0.3	0.8	0.5	1.3	9.7	0.4	0.3	2.9	0.4	0
Chloroflexi; f__Anaerolineaceae_OTU_2 -	0	0	0	0.6	0.9	4.3	0	0.8	2.6	6.8	8.9	5.5	0.6
Chloroflexi; f__Anaerolineaceae_OTU_12 -	0	14.8	3.7	2.3	1.7	1.1	0	0.3	0.1	0.6	2.9	1.1	0.4
Alphaproteobacteria; Pleomorphomonas -	0	0.4	4.9	3.8	1.5	1.2	2.6	7.1	3.4	1.1	0.1	0	1.3
Firmicutes; Dehalobacter -	0	0	6.1	5.3	1.8	1.7	4.4	0	3.9	1.9	0.3	0.2	0.6
Alphaproteobacteria; Devosia -	15.8	0.7	0.1	0.1	0	3.4	0	0	0	0.1	0.2	2.5	0
Deltaproteobacteria; Desulfovibrio -	0	0	5.1	5.4	1	1.1	0.5	1.1	1.7	1.4	0.2	0.2	1
Alphaproteobacteria; f__Rhodospirillaceae_OTU_13 -	0	0.1	2.3	1.7	0.9	2.5	0.4	2.4	0.1	1.1	0.4	0.2	4.1
Betaproteobacteria; Propionivibrio -	0.1	0	4.3	0.6	2.5	0.7	0.9	1.8	3.3	0.4	0.3	0.1	1
Firmicutes; Erysipelothrix -	0	0	5.7	1.7	0.6	0.7	0.9	1.8	2.6	0.8	0.2	0.1	0
Alphaproteobacteria; Hyphomicrobium -	1.4	1.5	0.5	1.1	0.2	0.7	0	0	0	0.3	1.6	4.4	2.2
Alphaproteobacteria; Rhodobacter -	0.1	0.1	0.2	2.1	0.2	0.9	0	0	0	6.2	3.2	0.4	0.1
Chloroflexi; Anaerolinea -	0	0.1	1.2	2.8	1.7	4.2	0	0	0	0	0	0.1	3
Betaproteobacteria; f__Comamonadaceae_OTU_26 -	3.2	0	0	0.1	0	0	0	0	0	0	0	9.4	0
Betaproteobacteria; Azoarcus -	1.1	0.4	1.4	0.3	2.1	0.6	0	0.2	0.2	0.2	4.4	0.3	1.2
Bacteroidetes; Flavobacterium -	0.8	0.5	0.5	0.4	1.1	0.8	0.7	0.4	0.9	0.3	3.3	1.2	0.2
Betaproteobacteria; Xenophilus -	7.3	0	0	0	0	1.1	0	0	0.1	0.4	0	1.3	0
Alphaproteobacteria; Starkeya -	1.7	0.2	0.1	1.5	0	1.1	0	0	0	0.2	0.9	4.3	0.2
	A_1 -	A_2 -	A_3 -	A_4 -	A_5 -	A_6 -	B_1 -	B_2 -	B_3 -	B_4 -	B_5 -	B_6 -	CHIP -

**Figure 1: Principal component analysis**

Identification of samples with similar microbial communities using multivariate statistics (PCA). Each point represent the microbial community in a specific sample. Distance between the sample dots signifies similarity; the closer the samples are, the more similar microbial composition they have.



## Materials and methods

### DNA extraction

#### FastDNA SPIN Kit for Soil

DNA extraction was performed using the standard protocol for FastDNA Spin kit for Soil (MP Biomedicals, USA) with the following exceptions. 500 µL of sample, 480 µL Sodium Phosphate Buffer and 120 µL MT Buffer were added to a Lysing Matrix E tube. Bead beating was performed at 6 m/s for 4x40s (Albertsen et al., 2015). Gel electrophoresis using Tapestation 2200 and Genomic DNA screentapes (Agilent, USA) was used to validate product size and purity of a subset of DNA extracts. DNA concentration was measured using Qubit dsDNA HS/BR Assay kit (Thermo Fisher Scientific, USA).

### Bacterial community analysis targeting 16S V1-V3 rRNA

#### Library preparation

Bacteria 16S V1-3 rRNA gene sequencing libraries were prepared by a custom protocol based on Caporaso et al. (2012). Up to 10 ng of extracted DNA was used as template for PCR amplification of the the bacteria 16S V1-3 rRNA gene amplicons. Each PCR reaction (25 µL) contained dNTPs (100 µM of each), MgSO<sub>4</sub> (1.5 mM), Platinum Taq DNA polymerase HF (0.5 U/reaction), Platinum High Fidelity buffer (1X) (Thermo Fisher Scientific, USA) and barcoded library adaptors (400 nM of each forward and reverse). PCR was conducted with the following program: Initial denaturation at 95 °C for 2 min, 30 cycles of amplification (95 °C for 20 s, 56 °C for 30 s, 72 °C for 60 s) and a final elongation at 72 °C for 5 min. Duplicate PCR reactions were performed for each sample and the duplicates were pooled after PCR. The adaptors contain 16S V1-3 specific primers: [27F] AGAGTTTGGATCCTGGCTCAG and [534R] ATTACCGCGGCTGCTGG (Ward et al., 2012). The resulting amplicon libraries were purified using the standard protocol for Agencourt Ampure XP Beads (Beckman Coulter, USA) with a bead to sample ratio of 4:5. DNA was eluted in 25 µL of nuclease free water (Qiagen, Germany). DNA concentration was measured using Qubit dsDNA HS Assay kit (Thermo Fisher Scientific, USA). Gel electrophoresis using Tapestation 2200 and D1000/High sensitivity D1000 screentapes (Agilent, USA) was used to validate product size and purity of a subset of sequencing libraries.

#### DNA sequencing

The purified sequencing libraries were pooled in equimolar concentrations and diluted to 6 nM. The samples were paired-end sequenced (2x300 bp) on a MiSeq (Illumina, USA) using a MiSeq Reagent kit v3 (Illumina, USA) following the standard guidelines for preparing and loading samples on the MiSeq. >10% PhiX control library was spiked in to overcome low complexity issues often observed with amplicon samples.

#### Bioinformatic processing

Forward and reverse reads were trimmed for quality using Trimmomatic v. 0.32 (Bolger et al., 2014) with the settings SLIDINGWINDOW:5:3 and MINLEN:275. The trimmed forward and reverse reads were merged using FLASH v. 1.2.7 (Magoč and Salzberg, 2011) with the settings -m 10 -M 200. The trimmed reads were dereplicated and formatted for use in the UPARSE workflow (Edgar, 2013). The dereplicated reads were clustered, using the usearch v. 7.0.1090 -cluster\_otus command with default settings. OTU abundances were estimated using the usearch v. 7.0.1090 -usearch\_global command with -id 0.97 -maxaccepts 0 -maxrejects 0. Taxonomy was assigned using the RDP classifier (Wang et al., 2007) as implemented in the parallel\_assign\_taxonomy\_rdp.py script in QIIME (Caporaso et al., 2010), using -confidence 0.8 and the MiDAS database v. 1.23 (McIlroy et al., 2017), which is a curated database based on the SILVA database, release 123 (Quast et al., 2013). The results were analysed in R v. 3.5.1 (R Core Team, 2017) through the Rstudio IDE using the ampvis package v.2.5.8 (Albertsen et al., 2015).

## References

- Albertsen, M., Karst, S.M., Ziegler, A.S., Kirkegaard, R.H., and Nielsen, P.H. (2015) Back to Basics – The Influence of DNA Extraction and Primer Choice on Phylogenetic Analysis of Activated Sludge Communities. *PLOS ONE* **10**: e0132783.
- Bolger, A.M., Lohse, M., and Usadel, B. (2014) Trimmomatic: A flexible trimmer for Illumina sequence data. *Bioinformatics* **30**: 2114–2120.
- Caporaso, J.G., Kuczynski, J., Stombaugh, J., Bittinger, K., Bushman, F.D., Costello, E.K., et al. (2010) QIIME allows analysis of high-throughput community sequencing data. **7**: 335–336.
- Caporaso, J.G., Lauber, C.L., Walters, W. a, Berg-Lyons, D., Huntley, J., Fierer, N., et al. (2012) Ultra-high-throughput microbial community analysis on the Illumina HiSeq and MiSeq platforms. *The ISME journal* **6**: 1621–4.
- Edgar, R.C. (2013) UPARSE: highly accurate OTU sequences from microbial amplicon reads. *Nature methods* **10**: 996–8.
- Magoč, T. and Salzberg, S.L. (2011) FLASH: fast length adjustment of short reads to improve genome assemblies. *Bioinformatics (Oxford, England)* **27**: 2957–63.
- McIlroy, S.J., Kirkegaard, R.H., McIlroy, B., Nierychlo, M., Kristensen, J.M., Karst, S.M., et al. (2017) MiDAS 2.0: An ecosystem-specific taxonomy and online database for the organisms of wastewater treatment systems expanded for anaerobic digester groups. *Database* **2017**:
- Quast, C., Pruesse, E., Yilmaz, P., Gerken, J., Schweer, T., Yarza, P., et al. (2013) The silva ribosomal rna gene database project: Improved data processing and web-based tools. *Nucl. Acids Res.* **41**: D590–D596.
- R Core Team (2017) R: A language and environment for statistical computing.
- Wang, Q., Garrity, G.M., Tiedje, J.M., and Cole, J.R. (2007) Naive Bayesian classifier for rapid assignment of rRNA sequences into the new bacterial taxonomy. *Applied and environmental microbiology* **73**: 5261–7.
- Ward, D.V., Gevers, D., Giannoukos, G., Earl, A.M., Methé, B.A., Sodergren, E., et al. (2012) Evaluation of 16s rDNA-based community profiling for human microbiome research. *PLoS ONE* **7**: e39315.